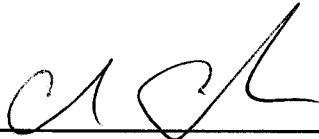
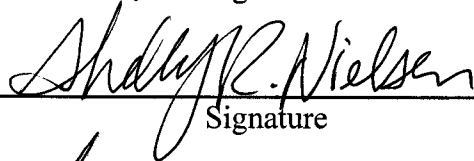
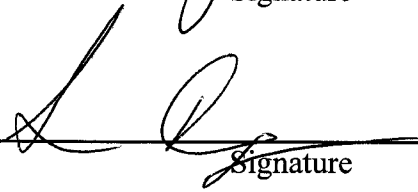


559980

**Sandia National Laboratories  
Waste Isolation Pilot Plant**

**Analysis Package for Salado Flow Modeling Done in  
the 2014 Compliance Recertification Application Performance  
Assessment (CRA-2014 PA)**

**Revision 0**

Author:	Chris Camphouse		4/30/13
	Print	Signature	Date
Technical Review:	Daniel Clayton	<i>Full Zett for Dan Clayton</i>	4/30/2013
	Print	Signature	Date
QA Review:	Shelly Nielsen		4-30-13
	Print	Signature	Date
Management Review:	Sean Dunagan		4/30/13
	Print	Signature	Date

WIPP:1.2.5:PA:QA-L:559199

## Table of Contents

1	Executive Summary.....	7
2	Introduction .....	8
2.1	Changes since the PABC-2009 .....	9
2.1.1	Replacement of Option D with ROMPCS.....	9
2.1.2	Inclusion of Additional Mined Volume in the Experimental Region.....	16
2.1.3	Refinement to the Corrosion Rate of Steel .....	16
2.1.4	Waste Inventory Parameter Updates.....	17
2.1.5	Refinement to Repository Water Balance.....	18
3	Conceptual Approach for the CRA-2014 PA.....	18
3.1	Repository Representation in BRAGFLO.....	18
4	Salado Flow Modeling Methodology .....	26
4.1	Initial Conditions.....	30
4.2	Boundary Conditions.....	31
5	CRA-2014 PA Cases and Run Control .....	31
6	Results .....	33
6.1	Results for an Undisturbed Repository (Scenario S1-BF) .....	34
6.2	Results for an E1 Intrusion at 350 Years (Scenario S2-BF) .....	77
6.3	Results for an E2 Intrusion at 350 Years (Scenario S4-BF) .....	95
6.4	Results for an E2 Intrusion at 1000 Years Followed by a E1 Intrusion at 2000 Years (Scenario S6-BF).....	114
7	Summary.....	117
8	References .....	119

## List of Figures

Figure 2-1: A Schematic of the “Option D” Panel Closure.....	10
Figure 2-2: Schematic Diagram of the ROMPCS.....	10
Figure 3-1: PABC-2009 BRAGFLO Grid and Material Map ( $\Delta x$ , $\Delta y$ , and $\Delta z$ dimensions in meters).....	20
Figure 3-2: CRA-2014 PA BRAGFLO Grid and Material Map, Years 0 to 100.....	21
Figure 3-3: CRA-2014 PA BRAGFLO Grid and Material Map, Years 100 to 200.....	22
Figure 3-4: CRA-2014 PA BRAGFLO Grid and Material Map, Years 200 to Time of Intrusion.....	23
Figure 3-5: CRA-2014 PA BRAGFLO Grid and Material Map for an E1 Intrusion.....	24
Figure 3-6: CRA-2014 PA BRAGFLO Grid and Material Map for an E2 Intrusion.....	25
Figure 6-1: Horsetail Plot of Waste Panel Pressure for Case CRA14-BL, Scenario SI-BF.....	40
Figure 6-2: Replicate 1 Means of Waste Panel Pressure, Scenario SI-BF.....	40
Figure 6-3: Horsetail Plot of Waste Panel Pressure for Case CRA14-0, Scenario SI-BF.....	41
Figure 6-4: Replicate Means of Waste Panel Pressure for Case CRA14-0, Scenario SI-BF.....	41
Figure 6-5: Overall Means of Waste Panel Pressure, Scenario SI-BF.....	42
Figure 6-6: Horsetail Plot of SRoR Pressure for Case CRA14-BL, Scenario SI-BF.....	42
Figure 6-7: Replicate 1 Means of SRoR Pressure, Scenario SI-BF.....	43
Figure 6-8: Horsetail Plot of SRoR Pressure for Case CRA14-0, Scenario SI-BF.....	43
Figure 6-9: Replicate Means of SRoR Pressure for Case CRA14-0, Scenario SI-BF.....	44
Figure 6-10: Overall Means of SRoR Pressure, Scenario SI-BF.....	44
Figure 6-11: Horsetail Plot of NRoR Pressure for Case CRA14-BL, Scenario SI-BF.....	45
Figure 6-12: Replicate 1 Means of NRoR Pressure, Scenario SI-BF.....	45
Figure 6-13: Horsetail Plot of NRoR Pressure for Case CRA14-0, Scenario SI-BF.....	46
Figure 6-14: Replicate Means of NRoR Pressure for Case CRA14-0, Scenario SI-BF.....	46
Figure 6-15: Overall Means of NRoR Pressure, Scenario SI-BF.....	47
Figure 6-16: Horsetail Plot of Experimental Region Pressure for Case CRA14-BL, Scenario SI-BF.....	47
Figure 6-17: Replicate 1 Means of Experimental Region Pressure, Scenario SI-BF.....	48
Figure 6-18: Horsetail Plot of Experimental Region Pressure for Case CRA14-0, Scenario SI-BF.....	48
Figure 6-19: Replicate Means of Experimental Region Pressure, Case CRA14-0, Scenario SI-BF.....	49
Figure 6-20: Overall Means of Experimental Region Pressure, Scenario SI-BF.....	49
Figure 6-21: Horsetail Plot of Molar Gas Generation for Case CRA14-BL, Scenario SI-BF.....	50
Figure 6-22: Replicate 1 Means of Molar Gas Generation for Case CRA14-BL, Scenario SI-BF.....	50
Figure 6-23: Horsetail Plot of Molar Gas Generation for Case CRA14-0, Scenario SI-BF.....	51
Figure 6-24: Means of Molar Gas Generation for Case CRA14-0, Scenario SI-BF (Replicate 1 Means – Solid, Overall Means – Dotted).....	51
Figure 6-25: Fraction of Iron Remaining, Case CRA14-BL, Scenario SI-BF (Mean in Red).....	52
Figure 6-26: Fraction of Iron Remaining, Case CRA14-0, Scenario SI-BF (Mean in Red).....	52
Figure 6-27: Fraction of Cellulose Remaining, Case CRA14-BL, Scenario SI-BF (Mean in Red).....	53
Figure 6-28: Fraction of Cellulose Remaining, Case CRA14-0, Scenario SI-BF (Mean in Red).....	53
Figure 6-29: Horsetail Plot of Cumulative Brine Inflow to the Waste Panel, Case CRA14-BL, Scenario SI-BF.....	54
Figure 6-30: Replicate 1 Means of Cumulative Brine Inflow to the Waste Panel, Scenario SI-BF.....	54
Figure 6-31: Horsetail Plot of Cumulative Brine Inflow to the Waste Panel, Case CRA14-0, Scenario SI-BF.....	55
Figure 6-32: Replicate Means of Cumulative Brine Inflow to the Waste Panel, Case CRA14-0, Scenario SI-BF.....	55
Figure 6-33: Overall Means of Cumulative Brine Inflow to the Waste Panel, Scenario SI-BF.....	56
Figure 6-34: Horsetail Plot of Cumulative Brine Inflow to the SRoR, Case CRA14-BL, Scenario SI-BF.....	56
Figure 6-35: Replicate 1 Means of Cumulative Brine Inflow to the SRoR, Scenario SI-BF.....	57
Figure 6-36: Horsetail Plot of Cumulative Brine Inflow to the SRoR, Case CRA14-0, Scenario SI-BF.....	57

Figure 6-37: Replicate Means of Cumulative Brine Inflow to the SRoR, Case CRA14-0, Scenario S1-BF.....	58
Figure 6-38: Overall Means of Cumulative Brine Inflow to the SRoR, Scenario S1-BF.....	58
Figure 6-39: Horsetail Plot of Cumulative Brine Inflow to the NRoR, Case CRA14-BL, Scenario S1-BF.....	59
Figure 6-40: Replicate 1 Means of Cumulative Brine Inflow to the NRoR, Scenario S1-BF.....	59
Figure 6-41: Horsetail Plot of Cumulative Brine Inflow to the NRoR, Case CRA14-0, Scenario S1-BF.....	60
Figure 6-42: Replicate Means of Cumulative Brine Inflow to the NRoR, Case CRA14-0, Scenario S1-BF.....	60
Figure 6-43: Overall Means of Cumulative Brine Inflow to the NRoR, Scenario S1-BF.....	61
Figure 6-44: Horsetail Plot of Cumulative Brine Inflow to the Repository, Case CRA14-BL, Scenario S1-BF.....	61
Figure 6-45: Replicate 1 Means of Cumulative Brine Inflow to the Repository, Scenario S1-BF.....	62
Figure 6-46: Horsetail Plot of Cumulative Brine Inflow to the Repository, Case CRA14-0, Scenario S1-BF.....	62
Figure 6-47: Replicate Means of Cumulative Brine Inflow to the Repository, Case CRA14-0, Scenario S1-BF.....	63
Figure 6-48: Overall Means of Cumulative Brine Inflow to the Repository, Scenario S1-BF.....	63
Figure 6-49: Horsetail Plot of Brine Flow up the Shaft, Case CRA14-BL, Scenario S1-BF.....	64
Figure 6-50: Replicate 1 Means of Brine Flow up the Shaft, Scenario S1-BF.....	64
Figure 6-51: Horsetail Plot of Brine Flow up the Shaft, Case CRA14-0, Scenario S1-BF.....	65
Figure 6-52: Replicate Means of Brine Flow up the Shaft, Case CRA14-0, Scenario S1-BF.....	65
Figure 6-53: Overall Means of Brine Flow up the Shaft, Scenario S1-BF.....	66
Figure 6-54: Horsetail Plot of Waste Panel Brine Saturation, Case CRA14-BL, Scenario S1-BF.....	66
Figure 6-55: Replicate 1 Means of Waste Panel Brine Saturation, Scenario S1-BF.....	67
Figure 6-56: Horsetail Plot of Waste Panel Brine Saturation, Case CRA14-0, Scenario S1-BF.....	67
Figure 6-57: Replicate Means of Waste Panel Brine Saturation, Case CRA14-0, Scenario S1-BF.....	68
Figure 6-58: Overall Means of Waste Panel Brine Saturation, Scenario S1-BF.....	68
Figure 6-59: Horsetail Plot of SRoR Saturation, Case CRA14-BL, Scenario S1-BF.....	69
Figure 6-60: Replicate 1 Means of SRoR Saturation, Scenario S1-BF.....	69
Figure 6-61: Horsetail Plot of SRoR Saturation, Case CRA14-0, Scenario S1-BF.....	70
Figure 6-62: Replicate Means of SRoR Saturation, Case CRA14-0, Scenario S1-BF.....	70
Figure 6-63: Overall Means of SRoR Saturation, Scenario S1-BF.....	71
Figure 6-64: Horsetail Plot of NRoR Saturation, Case CRA14-BL, Scenario S1-BF.....	71
Figure 6-65: Replicate 1 Means of NRoR Saturation, Scenario S1-BF.....	72
Figure 6-66: Horsetail Plot of NRoR Saturation, Case CRA14-0, Scenario S1-BF.....	72
Figure 6-67: Replicate Means of NRoR Saturation, Case CRA14-0, Scenario S1-BF.....	73
Figure 6-68: Overall Means of NRoR Saturation, Scenario S1-BF.....	73
Figure 6-69: Horsetail Plot of Waste Panel Porosity, Case CRA14-BL, Scenario S1-BF.....	74
Figure 6-70: Replicate 1 Means of Waste Panel Porosity, Scenario S1-BF.....	74
Figure 6-71: Horsetail Plot of Waste Panel Porosity, Case CRA14-0, Scenario S1-BF.....	75
Figure 6-72: Replicate Means of Waste Panel Porosity, Case CRA14-0, Scenario S1-BF.....	75
Figure 6-73: Overall Means of Waste Panel Porosity, Scenario S1-BF.....	76
Figure 6-74: Horsetail Plot of Waste Panel Pressure for Case CRA14-BL, Scenario S2-BF.....	80
Figure 6-75: Replicate 1 Means of Waste Panel Pressure, Scenario S2-BF.....	80
Figure 6-76: Horsetail Plot of Waste Panel Pressure for Case CRA14-0, Scenario S2-BF.....	81
Figure 6-77: Replicate Means of Waste Panel Pressure for Case CRA14-0, Scenario S2-BF.....	81
Figure 6-78: Overall Means of Waste Panel Pressure, Scenario S2-BF.....	82
Figure 6-79: Horsetail Plot of Molar Waste Panel Gas Generation for Case CRA14-BL, Scenario S2-BF.....	82
Figure 6-80: Replicate 1 Means of Molar Waste Panel Gas Generation for Case CRA14-BL, Scenario S2-BF.....	83
Figure 6-81: Horsetail Plot of Molar Waste Panel Gas Generation for Case CRA14-0, Scenario S2-BF.....	83
Figure 6-82: Means of Molar Waste Panel Gas Generation for Case CRA14-0, Scenario S2-BF (Replicate 1 Means – Solid, Overall Means – Dotted).....	84
Figure 6-83: Horsetail Plot of Cumulative Brine Inflow to the Waste Panel, Case CRA14-BL, Scenario S2-BF.....	84

Figure 6-84: Replicate 1 Means of Cumulative Brine Inflow to the Waste Panel, Scenario S2-BF..... 85

Figure 6-85: Horsetail Plot of Cumulative Brine Inflow to the Waste Panel, Case CRA14-0, Scenario S2-BF..... 85

Figure 6-86: Replicate Means of Cumulative Brine Inflow to the Waste Panel, Case CRA14-0, Scenario S2-BF..... 86

Figure 6-87: Overall Means of Cumulative Brine Inflow to the Waste Panel, Scenario S2-BF..... 86

Figure 6-88: Horsetail Plot of Cumulative Brine Inflow to the Repository, Case CRA14-BL, Scenario S2-BF..... 87

Figure 6-89: Replicate 1 Means of Cumulative Brine Inflow to the Repository, Scenario S2-BF..... 87

Figure 6-90: Horsetail Plot of Cumulative Brine Inflow to the Repository, Case CRA14-0, Scenario S2-BF..... 88

Figure 6-91: Replicate Means of Cumulative Brine Inflow to the Repository, Case CRA14-0, Scenario S2-BF..... 88

Figure 6-92: Overall Means of Cumulative Brine Inflow to the Repository, Scenario S2-BF..... 89

Figure 6-93: Horsetail Plot of Brine Flow up the Borehole, Case CRA14-BL, Scenario S2-BF..... 89

Figure 6-94: Replicate 1 Means of Brine Flow up the Borehole, Scenario S2-BF..... 90

Figure 6-95: Horsetail Plot of Cumulative Brine Inflow to the Repository, Case CRA14-0, Scenario S2-BF..... 90

Figure 6-96: Replicate Means of Brine Flow up the Borehole, Case CRA14-0, Scenario S2-BF..... 91

Figure 6-97: Overall Means of Brine Flow up the Borehole, Scenario S2-BF..... 91

Figure 6-98: Horsetail Plot of Waste Panel Brine Saturation, Case CRA14-BL, Scenario S2-BF..... 92

Figure 6-99: Replicate 1 Means of Waste Panel Brine Saturation, Scenario S2-BF..... 92

Figure 6-100: Horsetail Plot of Waste Panel Brine Saturation, Case CRA14-0, Scenario S2-BF..... 93

Figure 6-101: Replicate Means of Waste Panel Brine Saturation, Case CRA14-0, Scenario S2-BF..... 93

Figure 6-102: Overall Means of Waste Panel Brine Saturation, Scenario S2-BF..... 94

Figure 6-103: Horsetail Plot of Waste Panel Pressure for Case CRA14-BL, Scenario S4-BF..... 99

Figure 6-104: Replicate 1 Means of Waste Panel Pressure, Scenario S4-BF..... 99

Figure 6-105: Horsetail Plot of Waste Panel Pressure for Case CRA14-0, Scenario S4-BF..... 100

Figure 6-106: Replicate Means of Waste Panel Pressure for Case CRA14-0, Scenario S4-BF..... 100

Figure 6-107: Overall Means of Waste Panel Pressure, Scenario S4-BF..... 101

Figure 6-108: Horsetail Plot of Molar Waste Panel Gas Generation for Case CRA14-BL, Scenario S4-BF..... 101

Figure 6-109: Replicate 1 Means of Molar Waste Panel Gas Generation for Case CRA14-BL, Scenario S4-BF... 102

Figure 6-110: Horsetail Plot of Molar Waste Panel Gas Generation for Case CRA14-0, Scenario S4-BF..... 102

Figure 6-111: Means of Molar Waste Panel Gas Generation for Case CRA14-0, Scenario S4-BF (Replicate 1 Means – Solid, Overall Means – Dotted)..... 103

Figure 6-112: Horsetail Plot of Cumulative Brine Inflow to the Waste Panel, Case CRA14-BL, Scenario S4-BF. 103

Figure 6-113: Replicate 1 Means of Cumulative Brine Inflow to the Waste Panel, Scenario S4-BF..... 104

Figure 6-114: Horsetail Plot of Cumulative Brine Inflow to the Waste Panel, Case CRA14-0, Scenario S4-BF..... 104

Figure 6-115: Replicate Means of Cumulative Brine Inflow to the Waste Panel, Case CRA14-0, Scenario S4-BF. 105

Figure 6-116: Overall Means of Cumulative Brine Inflow to the Waste Panel, Scenario S4-BF..... 105

Figure 6-117: Horsetail Plot of Cumulative Brine Inflow to the Repository, Case CRA14-BL, Scenario S4-BF. .... 106

Figure 6-118: Replicate 1 Means of Cumulative Brine Inflow to the Repository, Scenario S4-BF..... 106

Figure 6-119: Horsetail Plot of Cumulative Brine Inflow to the Repository, Case CRA14-0, Scenario S4-BF..... 107

Figure 6-120: Replicate Means of Cumulative Brine Inflow to the Repository, Case CRA14-0, Scenario S4-BF.... 107

Figure 6-121: Overall Means of Cumulative Brine Inflow to the Repository, Scenario S4-BF..... 108

Figure 6-122: Horsetail Plot of Brine Flow up the Borehole, Case CRA14-BL, Scenario S4-BF..... 108

Figure 6-123: Replicate 1 Means of Brine Flow up the Borehole, Scenario S4-BF..... 109

Figure 6-124: Horsetail Plot of Brine Flow up the Borehole, Case CRA14-0, Scenario S4-BF..... 109

Figure 6-125: Replicate Means of Brine Flow up the Borehole, Case CRA14-0, Scenario S4-BF..... 110

Figure 6-126: Overall Means of Brine Flow up the Borehole, Scenario S4-BF..... 110

Figure 6-127: Horsetail Plot of Waste Panel Brine Saturation, Case CRA14-BL, Scenario S4-BF..... 111

Figure 6-128: Replicate 1 Means of Waste Panel Brine Saturation, Scenario S4-BF..... 111

Figure 6-129: Horsetail Plot of Waste Panel Brine Saturation, Case CRA14-0, Scenario S4-BF..... 112

Figure 6-130: Replicate Means of Waste Panel Brine Saturation, Case CRA14-0, Scenario S4-BF..... 112

Figure 6-131: Overall Means of Waste Panel Brine Saturation, Scenario S4-BF..... 113  
 Figure 6-132: Horsetail Plot of Brine Flow up the Borehole, Case CRA14-BL, Scenario S6-BF..... 115  
 Figure 6-133: Replicate 1 Means of Brine Flow up the Borehole, Scenario S6-BF..... 115  
 Figure 6-134: Horsetail Plot of Brine Flow up the Borehole, Case CRA14-0, Scenario S6-BF..... 116  
 Figure 6-135: Replicate Means of Brine Flow up the Borehole, Case CRA14-0, Scenario S6-BF..... 116  
 Figure 6-136: Overall Means of Brine Flow up the Borehole, Scenario S6-BF..... 117

### List of Tables

Table 2-1: Sampled ROMPCS Parameters for the CRA-2014 PA..... 12  
 Table 2-2: Constant Panel Closure Parameters for the CRA-2014 PA..... 14  
 Table 2-3: DRZ\_1 and DRZ\_PCS Porosities and Permeabilities..... 15  
 Table 2-4: STEEL:CORRMCO2 Distribution in the CRA-2014 PA..... 16  
 Table 2-5: STEEL:CORRMCO2 Distribution in the PABC-2009..... 17  
 Table 2-6: Iron and CPR Inventories in the PABC-2009 and the CRA-2014 PA..... 17  
 Table 2-7: Nitrate and Sulfate Inventories in the PABC-2009 and the CRA-2014 PA..... 17  
 Table 4-1: BRAGFLO Modeling Scenarios..... 27  
 Table 5-1: Cases Considered in the CRA-2014 PA..... 32  
 Table 6-1: Summary Statistics for Scenario S1-BF..... 39  
 Table 6-2: Summary Statistics for Scenario S2-BF..... 79  
 Table 6-3: Summary Statistics for Scenario S4-BF..... 98  
 Table 6-4: Summary Statistics for Scenario S6-BF..... 114

## 1 EXECUTIVE SUMMARY

The Land Withdrawal Act requires that the U.S. Department of Energy (DOE) apply for recertification of the Waste Isolation Pilot Plant (WIPP) every five years following the initial 1999 waste shipment. The 2014 Compliance Recertification Application (CRA-2014) is the third WIPP recertification application submitted for approval by the U.S. Environmental Protection Agency. A performance assessment (PA) has been executed by Sandia National Laboratories in support of the DOE submittal of the CRA-2014. Results found in the CRA-2014 PA are compared to those obtained in the 2009 Performance Assessment Baseline Calculation (PABC-2009) in order to assess repository performance in terms of the current regulatory baseline. This package documents the Salado flow analysis component of the CRA-2014 PA. Changes incorporated into the CRA-2014 PA include planned changes as well as parameter and implementation changes. Changes included in the CRA-2014 PA that potentially affect Salado flow results as compared to the PABC-2009 are:

- Replacement of the Option D Panel Closure System (PCS) with a newly designed Run-of-Mine Panel Closure System (ROMPCS)
- Additional excavation in the WIPP experimental area
- Updated waste inventory parameters
- Refinement to the iron corrosion rate parameter STEEL:CORRMCO2
- Implementation of a water balance that includes MgO hydration

For undisturbed repository conditions, these changes yield a reduction in the mean pressure calculated for repository waste areas as compared to the PABC-2009. Waste areas at higher elevation have lower mean brine saturations in the CRA-2014 PA results as compared to the PABC-2009 due to water sequestration in the refined water budget implementation. Waste panels at lowest elevation have a lower mean brine saturation at early times as compared to the PABC-2009. However, the brine saturation for these panels gradually increases until it becomes greater than that seen in the PABC-2009. The sequestration of brine in the refined water budget implementation yields a repository that tends to be drier overall for undisturbed conditions as compared to the PABC-2009.

For E1 intrusion scenarios, the ROMPCS effectively isolates impacts associated with borehole intrusion to the intruded panel. Changes included in the CRA-2014 PA yield an increase to the mean pressure in the intruded panel for a period of time after the intrusion as compared to results from the PABC-2009, but the mean waste panel pressure eventually falls below that seen in the PABC-2009. The mean brine saturation of the intruded panel is increased in the CRA-2014 PA as compared to the PABC-2009.

For E2 intrusion scenarios, the ROMPCS effectively isolates impacts associated with borehole intrusion to the intruded panel. Changes included in the CRA-2014 PA yield a decrease to the mean pressure in the intruded panel as compared to results from the PABC-2009 with a corresponding increase to the mean brine saturation.

## 2 INTRODUCTION

The Waste Isolation Pilot Plant (WIPP), located in southeastern New Mexico, has been developed by the U.S. Department of Energy (DOE) for the geologic (deep underground) disposal of transuranic (TRU) waste. Containment of TRU waste at the WIPP is regulated by the U.S. Environmental Protection Agency (EPA) according to the regulations set forth in Title 40 of the Code of Federal Regulations (CFR), Part 191. The DOE demonstrates compliance with the containment requirements according to the Certification Criteria in Title 40 CFR Part 194 by means of performance assessment (PA) calculations performed by Sandia National Laboratories (SNL). WIPP PA calculations estimate the probability and consequence of potential radionuclide releases from the repository to the accessible environment for a regulatory period of 10,000 years after facility closure. The models used in PA are maintained and updated with new information as part of an ongoing process. Improved information regarding important WIPP features, events, and processes typically results in refinements and modifications to PA models and the parameters used in them. Planned changes to the repository and/or the components therein also result in updates to WIPP PA models. WIPP PA models are used to support the repository recertification process that occurs at five-year intervals following the receipt of the first waste shipment at the site in 1999.

PA calculations were included in the 1996 Compliance Certification Application (CCA) (U.S. DOE 1996), and in a subsequent Performance Assessment Verification Test (PAVT) (MacKinnon and Freeze 1997a, 1997b and 1997c). Based in part on the CCA and PAVT PA calculations, the EPA certified that the WIPP met the regulatory containment criteria. The facility was approved for disposal of transuranic waste in May 1998 (U.S. EPA 1998). PA calculations were an integral part of the 2004 Compliance Recertification Application (CRA-2004) (U.S. DOE 2004). During their review of the CRA-2004, the EPA requested an additional PA calculation, referred to as the CRA-2004 Performance Assessment Baseline Calculation (PABC) (Leigh et al. 2005), be conducted with modified assumptions and parameter values (Cotsworth 2005). Following review of the CRA-2004 and the CRA-2004 PABC, the EPA recertified the WIPP in March 2006 (U.S. EPA 2006).

PA calculations were completed for the second WIPP recertification and documented in the 2009 Compliance Recertification Application (CRA-2009). The CRA-2009 PA resulted from continued review of the CRA-2004 PABC, including a number of technical changes and corrections, as well as updates to parameters and improvements to the PA computer codes (Clayton et al. 2008). To incorporate additional information which was received after the CRA-2009 PA was completed, but before the submittal of the CRA-2009, the EPA requested an additional PA calculation, referred to as the 2009 Compliance Recertification Application Performance Assessment Baseline Calculation (PABC-2009) (Clayton et al. 2010), be undertaken which included updated information (Cotsworth 2009). Following the completion and submission of the PABC-2009, the WIPP was recertified in 2010 (U.S. EPA 2010a).

The Land Withdrawal Act (U.S. Congress 1992) requires that the DOE apply for WIPP recertification every five years following the initial 1999 waste shipment. The 2014 Compliance Recertification Application (CRA-2014) is the third WIPP recertification application submitted by the DOE for EPA approval. The PA executed by SNL in support of the CRA-2014 is detailed



in AP-164 (Camphouse 2013). The CRA-2014 PA includes a number of technical changes and parameter refinements, as well as a redesigned WIPP panel closure system. Results found in the CRA-2014 PA are compared to those obtained in the PABC-2009 in order to assess repository performance in terms of the current regulatory baseline. This package documents the Salado flow analysis component of the CRA-2014 PA.

## **2.1 Changes since the PABC-2009**

Several changes are incorporated in the CRA-2014 PA relative to the PABC-2009 that potentially impact Salado flow results. The changes are:

- Replacement of the “Option D” WIPP panel closure with the newly designed ROMPCS.
- Inclusion of additional mined volume in the repository experimental area.
- Refinement to the corrosion rate of steel.
- Updates to WIPP waste inventory parameters.
- Implementation of a more detailed repository water balance that includes MgO hydration.

Changes listed above are discussed in more detail in the sections that follow.

### ***2.1.1 Replacement of Option D with ROMPCS***

Among the changes included in the CRA-2014 PA is the replacement of the Option D WIPP panel closure system (PCS) with a newly designed Run-of-Mine Panel Closure System (ROMPCS). The DOE has submitted a planned change request (PCR) to the EPA requesting that EPA modify Condition 1 of the Final Certification Rulemaking for 40 CFR Part 194 (U. S. EPA, 1998) for the WIPP, and that the ROMPCS be approved for use in all waste panels (U.S. DOE, 2011a). Regulatory compliance impacts associated with the implementation of the ROMPCS in the WIPP were assessed in a PA named PCS-2012. Results of the PCS-2012 PA are documented in Camphouse et al. (2012b), with Salado flow results documented in Camphouse (2012a). Total normalized releases calculated in the PCS-2012 PA remained below their regulatory limits. Replacement of the Option D panel closure with the ROMPCS design does not result in WIPP non-compliance with the containment requirements of 40 CFR Part 191.

The Option D PCS consists of three primary components, namely, a concrete explosion isolation wall, an open drift section, and a concrete monolith. The dimensions of the individual Option D components are shown in Figure 2-1.

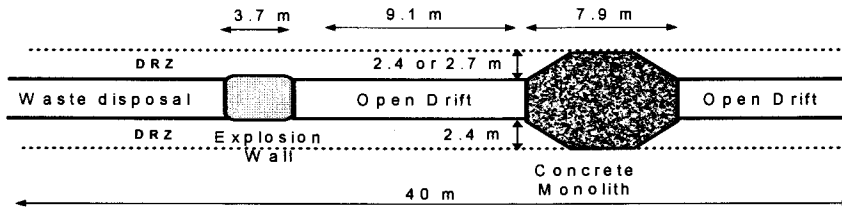
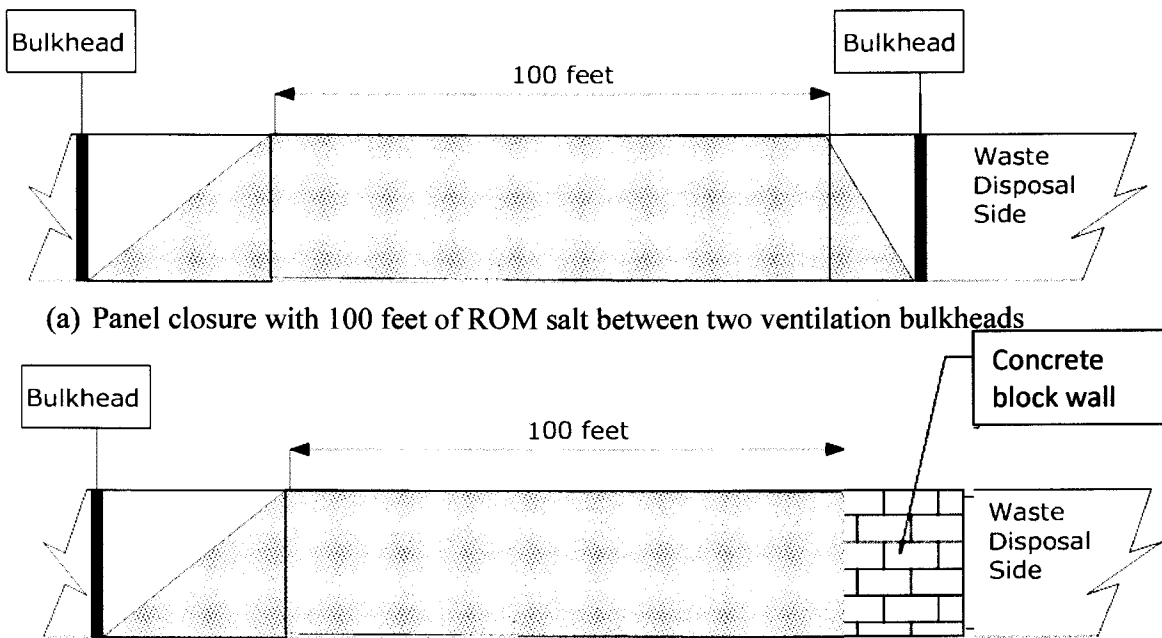


Figure 2-1: A Schematic of the "Option D" Panel Closure

The ROMPCS design (Figure 2-2) is comprised of 100 feet of run-of-mine (ROM) salt with barriers at each end. The ROM salt is generated from ongoing mining operations at the WIPP while the barriers consist of ventilation bulkheads, similar to those currently used in the panels as room closures.



(a) Panel closure with 100 feet of ROM salt between two ventilation bulkheads

(b) Panel closure with 100 feet of ROM salt between a ventilation bulkhead & explosion wall

Figure 2-2: Schematic Diagram of the ROMPCS

ROMPCS properties used in the CRA-2014 PA are almost identical to those prescribed in the PCS-2012 PA. The ROM salt comprising the ROMPCS is represented by three materials, denoted as PCS\_T1 for the first 100 years after facility closure, PCS\_T2 from 100 to 200 years,

and PCS\_T3 for 200 to 10,000 years. For the first 200 years post-closure, the disturbed rock zone (DRZ) above and below the ROMPCS maintains the same properties as specified to the DRZ surrounding the disposal rooms (PA material DRZ\_1). After 200 years, the DRZ above and below the ROMPCS is modeled as having healed, and is represented by material DRZ\_PCS.

In the PCS-2012 PA, the permeabilities of material PCS\_T1 were assigned a uniform distribution having a minimum value of  $1 \times 10^{-21} \text{ m}^2$ . The permeability for material PCS\_T2 was calculated as a function of its sampled porosity value. The lowest obtainable calculated value for the permeability of PCS\_T2 in the X, Y, and Z directions was  $1.44 \times 10^{-21} \text{ m}^2$ , which is slightly greater than the minimum possible sampled value during the first 100 years. A lower ROMPCS permeability could be obtained during the first 100 years than was feasible for years 100 to 200, depending on the sampled PCS\_T1 permeability value. As creep closure reconsolidates the ROMPCS over time, the expectation is that ROMPCS permeability will not increase as time increases. As a result, the permeability distribution of ROMPCS material PCS\_T1 is modified slightly in the CRA-2014 PA, and is assigned a uniform distribution with a minimum value of  $1 \times 10^{-20.84} \text{ m}^2$  and the same maximum value as in the PCS-2012 PA. This parameter change is cosmetic in nature, and is implemented to improve consistency between the modeled ROMPCS temporal evolution and the mechanics of ROM salt reconsolidation. As was done in the PCS-2012 PA (Camphouse et al. 2012b), a conditional relationship is enforced in the CRA-2014 PA so that the permeability of material PCS\_T2 is never greater than the permeability of material PCS\_T1. Likewise, the permeability of material PCS\_T3 is never greater than the permeability of material PCS\_T2.

For similar reasons, the permeability of material DRZ\_PCS is modified slightly in the CRA-2014 PA as compared to the PCS-2012 PA and the PABC-2009. It is expected that healing of the DRZ region above and below the PCS will not yield an increase in permeability when compared to the damaged DRZ. A relationship is implemented in the CRA-2014 PA to enforce that the permeability of material DRZ\_PCS is never greater than the permeability of material DRZ\_1. Using the MATERIAL:PROPERTY parameter naming convention used in WIPP PA, the constraint placed on the permeability for DRZ\_PCS is that  $\text{DRZ\_PCS:PRMX} \leq \text{DRZ\_1:PRMX}$ , and likewise in the y and z directions. If the sampled permeability for DRZ\_PCS is greater than that obtained for DRZ\_1, then DRZ\_PCS retains the DRZ\_1 permeability. The uncertainty distributions specified for the permeabilities of materials DRZ\_1 and DRZ\_PCS in the CRA-2014 PA are identical to those used in the PCS-2012 PA and the PABC-2009.

Finally, in the CRA-2014 PA, the initial brine saturation of the ROMPCS is set equal to the sampled residual brine saturation value for material PCS\_T1 in each vector. This modification ensures that the initial brine saturation of the PCS is never lower than the PCS residual brine saturation in a given vector. A consequence of this change is that PCS-2012 PA parameter PCS\_T1:SAT\_IBRN is not used in the CRA-2014 PA. The full set of sampled and constant parameters used to represent the ROMPCS in the CRA-2014 PA is shown in Table 2-1 and Table 2-2. Select parameters associated with the damaged and healed DRZ are shown in Table 2-3.

Table 2-1: Sampled ROMPCS Parameters for the CRA-2014 PA

Parameter	Units	Description	Distribution Type	Distribution Parameters	Default Value	Source
PCS_T1:POROSITY	none	Porosity of run-of-mine panel closure, years 0 to 100	Uniform	Min = 0.066 Max = 0.187 Mean = 0.1265	0.1265	Camphouse et al. (2012a) Table 2 and page 15
PCS_T2:POROSITY <sup>1</sup>	none	Porosity of run-of-mine panel closure, years 100 to 200	Uniform	Min = 0.025 Max = 0.075 Mean = 0.05	0.05	Camphouse et al. (2012a) Table 2 and page 15
PCS_T3:POROSITY <sup>2</sup>	none	Porosity of run-of-mine panel closure, years 200 to 10,000	Uniform	Min = 0.001 Max = 0.0519 Mean = 0.0265	0.0265	Camphouse et al. (2012a) Table 2 and page 15
PCS_T1:PRMX_LOG <sup>3</sup> PCS_T1:PRMY_LOG PCS_T1:PRMZ_LOG	log(m <sup>2</sup> )	log <sub>10</sub> of intrinsic permeability, X, Y, and Z directions.	Uniform	Min = -20.84 Max = -12.0 Mean = -16.42	-16.42	Camphouse (2013) Table 2-1
PCS_T2:POR2PERM <sup>4</sup> PCS_T3:POR2PERM	none	Distribution used to calculate permeability from sampled porosity values	Normal	Min = -1.72 Max = 1.72 Mean = 0.0 SD = 0.86	0.0	Camphouse et al. (2012a) Page 15 (sampled $\alpha$ value)
PCS_T1:SAT_RBRN <sup>5</sup> PCS_T2:SAT_RBRN PCS_T3:SAT_RBRN	none	Residual Brine Saturation	Cumulative	(Prob,Value): (0,0) (0.5,0.2) (1.0,0.6)	0.2	Camphouse et al. (2012a) Table 6

<sup>1</sup> PCS\_T2:POROSITY is constrained such that PCS\_T2:POROSITY ≤ PCS\_T1:POROSITY for a given vector in order to avoid non-physical instantaneous increases in ROMPCS porosity at 100 years.

<sup>2</sup> PCS\_T3:POROSITY is constrained such that PCS\_T3:POROSITY ≤ PCS\_T2:POROSITY for a given vector in order to avoid non-physical instantaneous increases in ROMPCS porosity at 200 years.

<sup>3</sup> Parameter values are sampled for PCS\_T1:PRMX\_LOG. PCS\_T1:PRMY\_LOG and PCS\_T1:PRMZ\_LOG inherit the sampled value obtained for PCS\_T1:PRMX\_LOG for each vector.

<sup>4</sup> Parameter values are sampled for PCS\_T2:POR2PERM. PCS\_T3:POR2PERM inherits the sampled value obtained for PCS\_T2:POR2PERM for each vector.

<sup>5</sup> Parameter values are sampled for PCS\_T1:SAT\_RBRN. PCS\_T2: SAT\_RBRN and PCS\_T3: SAT\_RBRN inherit the sampled value obtained for PCS\_T1:SAT\_RBRN for each vector.

Table 2-1 (cont): Sampled Panel Closure Parameters for the CRA-2014 PA

PCS_T1:SAT_RGAS <sup>6</sup> PCS_T2:SAT_RGAS PCS_T3:SAT_RGAS	none	Residual Gas Saturation	Uniform	Min = 0.0 Max = 0.4 Mean = 0.2	0.2	Camphouse et al. (2012a) Table 6
PCS_T1:PORE_DIS <sup>7</sup> PCS_T2:PORE_DIS PCS_T3:PORE_DIS	none	Brooks-Corey pore distribution parameter	Cumulative	(Prob,Value): (0,0.11) (0.5,0.94) (1.0,8.1)	0.94	Camphouse et al. (2012a) Table 8

<sup>6</sup> Parameter values are sampled for PCS\_T1:SAT\_RGAS. PCS\_T2: SAT\_RGAS and PCS\_T3: SAT\_RGAS inherit the sampled value obtained for PCS\_T1:SAT\_RGAS for each vector.

<sup>7</sup> Parameter values are sampled for PCS\_T1:PORE\_DIS. PCS\_T2: PORE\_DIS and PCS\_T3: PORE\_DIS inherit the sampled value obtained for PCS\_T1: PORE\_DIS for each vector.

Table 2-2: Constant Panel Closure Parameters for the CRA-2014 PA

Parameter	Units	Description	Value	Source
PCS_T2:PRMX_LOG <sup>8</sup> PCS_T2:PRMY_LOG PCS_T2:PRMZ_LOG	log(m <sup>2</sup> )	log <sub>10</sub> of intrinsic permeability, X, Y, and Z directions.	-18.6	See Footnote
PCS_T3:PRMX_LOG <sup>9</sup> PCS_T3:PRMY_LOG PCS_T3:PRMZ_LOG	log(m <sup>2</sup> )	log <sub>10</sub> of intrinsic permeability, X, Y, and Z directions.	-19.1	See Footnote
PCS_T1:RELP_MOD PCS_T2:RELP_MOD PCS_T3:RELP_MOD	none	Relative Permeability Model Number	4	Camphouse et al. (2012a) Table 7
PCS_T1:CAP_MOD PCS_T2:CAP_MOD PCS_T3:CAP_MOD	none	Capillary Pressure Model Number	1	Camphouse (2012b) Camphouse (2012c)
PCS_T1:KPT PCS_T2:KPT PCS_T3:KPT	none	Flag to Enable Dynamic Updating of Threshold Capillary Pressure as a Function of Permeability	0.0	Camphouse et al. (2012a) Table 8
PCS_T1:PCT_A PCS_T2:PCT_A PCS_T3:PCT_A	Pa	Threshold Capillary Pressure Linear Parameter	0.0	Camphouse (2012b) Camphouse (2012c)
PCS_T1:PCT_EXP PCS_T2:PCT_EXP PCS_T3:PCT_EXP	none	Threshold Capillary Pressure Exponential Parameter	0.0	Camphouse (2012b) Camphouse (2012c)
PCS_T1:PC_MAX PCS_T2:PC_MAX PCS_T3:PC_MAX	Pa	Maximum Allowable Capillary Pressure	1 x 10 <sup>8</sup>	Camphouse et al. (2012a) Table 8

<sup>8</sup> Permeabilities of PCS\_T2 in the X, Y, and Z directions are calculated from the sampled PCS\_T2:POROSITY values as described in Camphouse et al. (2012a). A constant default log-permeability is specified, however, to allow for parameter traceability in CRA-2014 PA input files as compared to those used in the PABC-2009. The specified default value is the average of the minimum and maximum values listed in Table 5 of Camphouse et al. (2012a).

<sup>9</sup> Permeabilities of PCS\_T3 in the X, Y, and Z directions are calculated from the sampled PCS\_T3:POROSITY values as described in Camphouse et al. (2012a). The specified constant default value is the average of the minimum and maximum values listed in Table 5 of Camphouse et al. (2012a).

Table 2-2 (cont): Constant Panel Closure Parameters for the CRA-2014 PA				
PCS_T1:P0_MIN PCS_T2:P0_MIN PCS_T3:P0_MIN	Pa	Minimum Brine Pressure for Capillary Model 3 (CAP_MOD = 3 has never been used in PA)	$1.01325 \times 10^5$	Camphouse et al. (2012a) Table 8
PCS_T1:COMP_RCK PCS_T2:COMP_RCK PCS_T3:COMP_RCK	$\text{Pa}^{-1}$	Bulk Compressibility	$8.0 \times 10^{-11}$	Camphouse et al. (2012a) Table 8

Table 2-3: DRZ\_1 and DRZ\_PCS Porosities and Permeabilities

Parameter	Units	Description	Distribution Type	Distribution Parameters	Default Value	Source
DRZ_1:POROSITY	none	Porosity of the DRZ after facility closure	Cumulative	Min = 0.0039 Median = 0.0129 Max = 0.0548	0.0129	Ismail (2007a)
DRZ_1:PRMX_LOG DRZ_1:PRMY_LOG DRZ_1:PRMZ_LOG	$\log(\text{m}^2)$	$\log_{10}$ of intrinsic permeability, X, Y, and Z directions	Uniform	Min = -19.4 Mean = -16.0 Max = -12.5	-16.0	Hansen (2002)
DRZ_PCS:POROSITY	none	Porosity of the healed DRZ above and below the PCS	Cumulative	Min = 0.0039 Median = 0.0129 Max = 0.0548	0.0129	Ismail (2007b)
DRZ_PCS:PRMX_LOG <sup>10</sup> DRZ_PCS:PRMY_LOG DRZ_PCS:PRMZ_LOG	$\log(\text{m}^2)$	$\log_{10}$ of intrinsic permeability, X, Y, and Z directions	Triangular	Min = -20.699 Mode = -18.7496 Max = -17.0	-18.7496	Stein (2002)

<sup>10</sup>In the CRA-2014 PA, the sampled permeability value of material DRZ\_PCS is compared to the sampled permeability value for DRZ\_1. If the sampled value for DRZ\_PCS is greater than that sampled for DRZ\_1, then DRZ\_PCS retains the sampled DRZ\_1 value.

### 2.1.2 Inclusion of Additional Mined Volume in the Experimental Region

Following the recertification of the WIPP in November of 2010 (U.S. EPA 2010a), the DOE submitted a planned change notice (PCN) to the EPA that justified additional excavation in the WIPP experimental area (U.S. DOE, 2011b). A PA was undertaken to determine the impact of the additional excavation on the long-term performance of the facility, and is documented in Camphouse et al. (2011). Total normalized releases remained below regulatory release limits when the additional excavated volume was added to the repository. Moreover, total normalized releases calculated with the additional excavation were indistinguishable from those obtained in the PABC-2009. The additional excavation in the WIPP experimental area does not result in WIPP non-compliance with the containment requirements of 40 CFR Part 191.

The same approach used in Camphouse et al. (2011) is used in the CRA-2014 PA to include additional mined volume in the WIPP experimental area. The volume of the experimental region implemented in the PABC-2009 was 87,675 m<sup>3</sup>. The added volume that results from additional excavation in the experimental area is 60,335 m<sup>3</sup>. As a result, the target volume of the experimental region implemented in the CRA-2014 PA is 87,675 m<sup>3</sup> + 60,335 m<sup>3</sup> = 148,010 m<sup>3</sup>. To achieve this value, the experimental region in the CRA-2014 PA is modified as in Camphouse et al. (2011) to yield an experimental region with a volume of 148,011 m<sup>3</sup>, one cubic meter greater than the target value.

### 2.1.3 Refinement to the Corrosion Rate of Steel

WIPP PA parameter STEEL:CORRMCO2 represents the anoxic steel corrosion rate for brine-inundated steel in the absence of microbially produced CO<sub>2</sub>. A series of steel and lead corrosion experiments have recently been conducted under Test Plan TP 06-02, *Iron and Lead Corrosion in WIPP-Relevant Conditions* (Wall and Enos, 2006). The object of these experiments has been to directly determine steel and lead corrosion rates under WIPP-relevant conditions. A description of the new experiments and the use of their results to determine an updated steel corrosion rate are presented in Roselle (2013). Based on the newly obtained experimental corrosion data and its subsequent analysis, Roselle (2013) recommends that both the distribution type and values for parameter STEEL:CORRMCO2 be changed. The revised steel corrosion parameter is shown in Table 2-4. The steel corrosion parameter used in the PABC-2009 is shown in Table 2-5 for reference.

Table 2-4: STEEL:CORRMCO2 Distribution in the CRA-2014 PA

Parameter	Units	Description	Distribution Type	Distribution Parameters	Default Value
STEEL:CORRMCO2	m/s	Inundated corrosion rate for steel in the absence of CO <sub>2</sub>	Student-t (n = 64)	Min=3.287e-16 Mean = 6.059e-15 Max=1.835e-14	6.059e-15



Table 2-5: STEEL:CORRMCO2 Distribution in the PABC-2009

Parameter	Units	Description	Distribution Type	Distribution Parameters	Default Value
STEEL: CORRMCO2	m/s	Inundated corrosion rate for steel in the absence of CO <sub>2</sub>	Uniform	Min=0.0 Mean = 1.585e-14 Max=3.17e-14	1.585e-14

### 2.1.4 Waste Inventory Parameter Updates

The Performance Assessment Inventory Report (PAIR) – 2012 (Van Soest 2012) was released on November 29, 2012. The PAIR – 2012 contains updated estimates to the radionuclide content and waste material parameters, scaled to a full repository, based on inventory information collected up to December 31, 2011. The waste inventory detailed in the PAIR - 2012 is used in the CRA-2014 PA.

Waste inventory changes in the PAIR – 2012 potentially impact gas generation results of Salado flow calculations. Specifically, changes to iron and CPR (carbon, plastic, and rubber) content in the waste inventory can alter the gas production that occurs when these materials comingle with brine. The PAIR – 2012 contains updated information for iron and CPR content in the repository. Inventory masses of these materials are compared to their PABC-2009 counterparts in Table 2-6. Values shown in that table are calculated using Table 6-3 and Table 6-4 of the PAIR – 2012. Iron and CPR mass values given in the PAIR – 2012 for CH (contact-handled) and RH (remote-handled) waste and packaging materials are added to the corresponding emplacement material masses, yielding the values shown in Table 2-6.

Table 2-6: Iron and CPR Inventories in the PABC-2009 and the CRA-2014 PA

Material	PABC-2009 Inventory (kg)	CRA-2014 PA Inventory (kg)
Iron	5.08 x 10 <sup>7</sup>	4.91 x 10 <sup>7</sup>
Cellulose	7.92 x 10 <sup>6</sup>	4.65 x 10 <sup>6</sup>
Plastics	1.05 x 10 <sup>7</sup>	9.51 x 10 <sup>6</sup>
Rubber	9.92 x 10 <sup>5</sup>	1.25 x 10 <sup>6</sup>
Total CPR	1.94 x 10 <sup>7</sup>	1.54 x 10 <sup>7</sup>

Microbial degradation of CPR consumes nitrate (NO<sub>3</sub><sup>-</sup>) and sulfate (SO<sub>4</sub><sup>2-</sup>) in the repository. Emplacements of these ions are updated in the CRA-2014 PA, with values shown in Table 2-7. Values shown in that table for the PABC-2009 are taken from Table C-5 of Fox, Clayton and Kirchner (2009). Table C-5 of Kicker and Zeitler (2013) provides values for the CRA-2014 PA.

Table 2-7: Nitrate and Sulfate Inventories in the PABC-2009 and the CRA-2014 PA

Ion	PABC-2009 Inventory (moles)	CRA-2014 PA Inventory (moles)
Nitrate	2.79 x 10 <sup>7</sup>	2.74 x 10 <sup>7</sup>
Sulfate	6.15 x 10 <sup>6</sup>	4.91 x 10 <sup>6</sup>

### ***2.1.5 Refinement to Repository Water Balance***

The saturation and pressure history of the repository are used throughout PA. Along with flow in and out of the repository, the saturation and pressure are influenced by the reaction of materials placed in the repository with the surrounding environment. As part of the review of the CRA-2009, EPA noted several issues for possible additional investigation, including the potential implementation of a more detailed repository water balance (U.S. EPA 2010b). The main objective of refining the repository water balance in the CRA-2014 PA is to include the major gas and brine producing and consuming reactions in the existing conceptual model. As described in the Chemical Conditions Conceptual Model, the major reactions in the repository include CPR, iron, and MgO (U.S. DOE 2004, sections PEER-2004 1.1.3, PEER-2004 1.1.4 and PEER-2004 1.1.5). The reaction chemistry and associated parameters used in the water balance refinement implemented in the CRA-2014 PA are developed in Clayton (2013).

## **3 CONCEPTUAL APPROACH FOR THE CRA-2014 PA**

The conceptual models implemented in the BRAGFLO simulations for the CRA-2014 PA are unchanged from those used in the PABC-2009. The computational grid, particularly the material map used by BRAGFLO, is altered slightly for the CRA-2014 PA in order to incorporate the ROMPCS and the additional mined volume in the repository experimental region. These changes are discussed below. The same porosity surface is used in the CRA-2014 PA BRAGFLO calculation as was used in the PCS-2012 PA and the PABC-2009.

### **3.1 Repository Representation in BRAGFLO**

The BRAGFLO grid and material map used in the PABC-2009 represented the Option D PCS, and is shown in Figure 3-1. Note that a minor error has been corrected in the material map schematic shown in Figure 3-1. That figure depicts an E1 intrusion into the repository. The BRAGFLO schematic included with the PABC-2009 Salado flow analysis package (Nemer 2010) depicts the lower borehole extending only to the bottom horizon of the lower DRZ. In actuality, the lower borehole extends to the floor of the intruded waste panel. The PABC-2009 BRAGFLO grid and material map shown in Figure 3-1 has been modified so that it represents the correct extent of the lower borehole in an E1 intrusion.

The ROMPCS was modeled as consisting of 100 feet of ROM salt in the PCS-2012 PA (Camphouse 2012a). The same ROMPCS representation is used in the CRA-2014 PA. The temporal evolution of the ROMPCS in BRAGFLO for the CRA-2014 PA is illustrated in Figure 3-2 to Figure 3-4. As seen in Figure 3-2 and Figure 3-3, the only change in the BRAGFLO grid and material map for time periods 0 to 100 years and 100 to 200 years is the material used to represent the panel closure. Material PCS\_T1 is used to represent the ROMPCS for years 0 to 100 while material PCS\_T2 represents the panel closure for years 100 to 200. As discussed previously, the ROMPCS is modeled as having no impact on the DRZ above and below the closure for the first 200 years after emplacement. For the first 200 years, the DRZ material above and below the closure in the BRAGFLO material map is the same as the material above and below other repository regions. After 200 years, the material used to represent the ROMPCS changes to PCS\_T3, and the regions of healed DRZ above and below the closure are modeled by

material DRZ\_PCS, as shown in Figure 3-4. The repository representation shown in Figure 3-4 is used for times between 200 years and the time of intrusion. The BRAGFLO grid and element maps corresponding to particular intrusion types are shown in Figure 3-5 and Figure 3-6.

The Option D panel closure implemented in the PABC-2009 is 40 meters long, while the ROMPCS implemented in the CRA-2014 PA is 100 feet (30.48 meters) long. Consequently, the panel closure length is reduced to a value of 30.48 meters in the CRA-2014 PA (identical to what was done in the PCS-2012 PA), with panel closures represented by two elements in the x-direction, each 15.24 meters long. As was done in Camphouse et al. (2011), elements corresponding to the experimental area are lengthened in the z-direction to account for the additional mined volume in that region. Two elements with lengths of 30.61 meters in the z-direction were used in the PABC-2009 to represent the experimental area. These two lengths are increased to 51.67 meters and 51.68 meters in the CRA-2014 PA, resulting in an experimental region volume of 148,011 m<sup>3</sup>, one cubic meter greater than the target value.

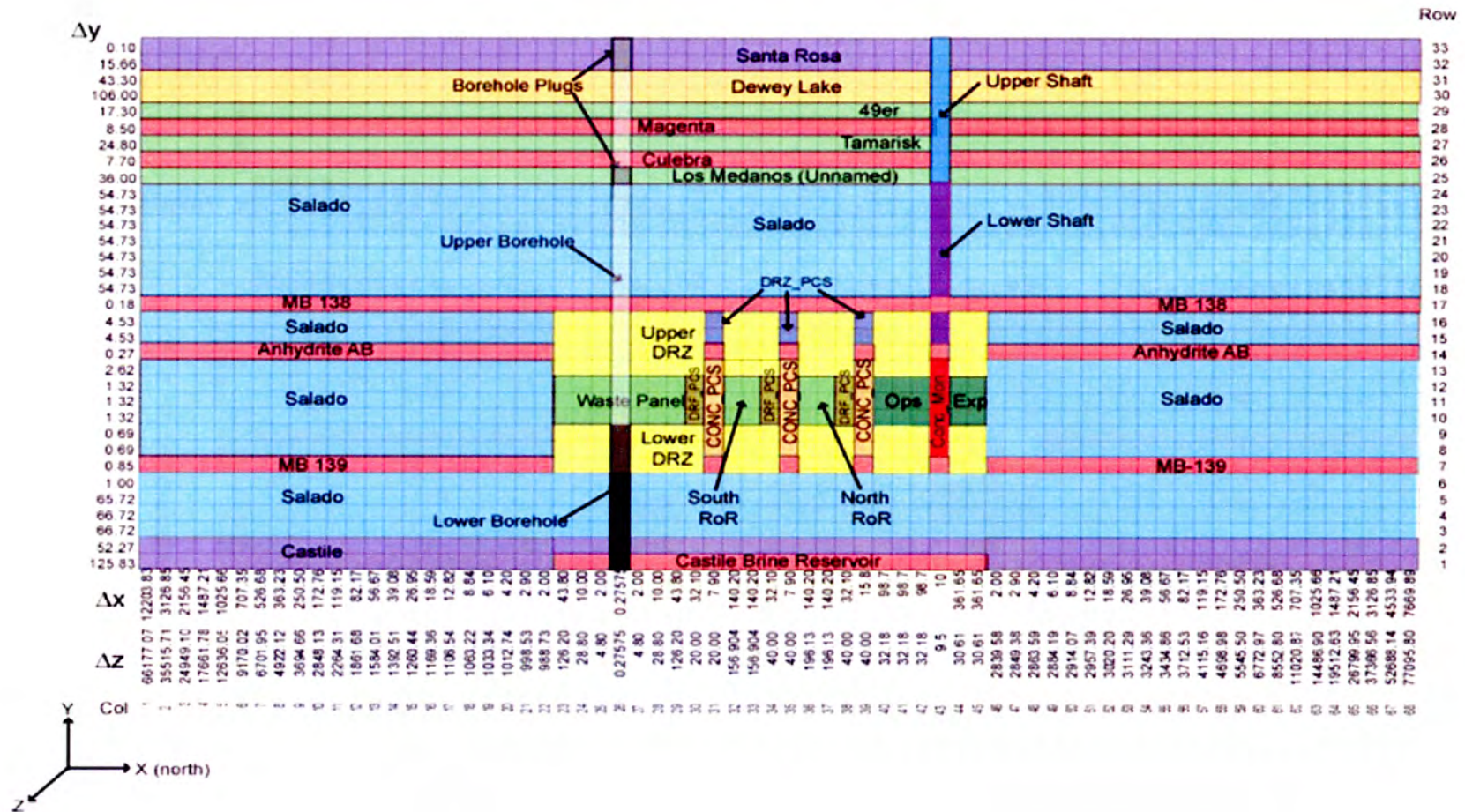


Figure 3-1: PABC-2009 BRAGFLO Grid and Material Map ( $\Delta x$ ,  $\Delta y$ , and  $\Delta z$  dimensions in meters).

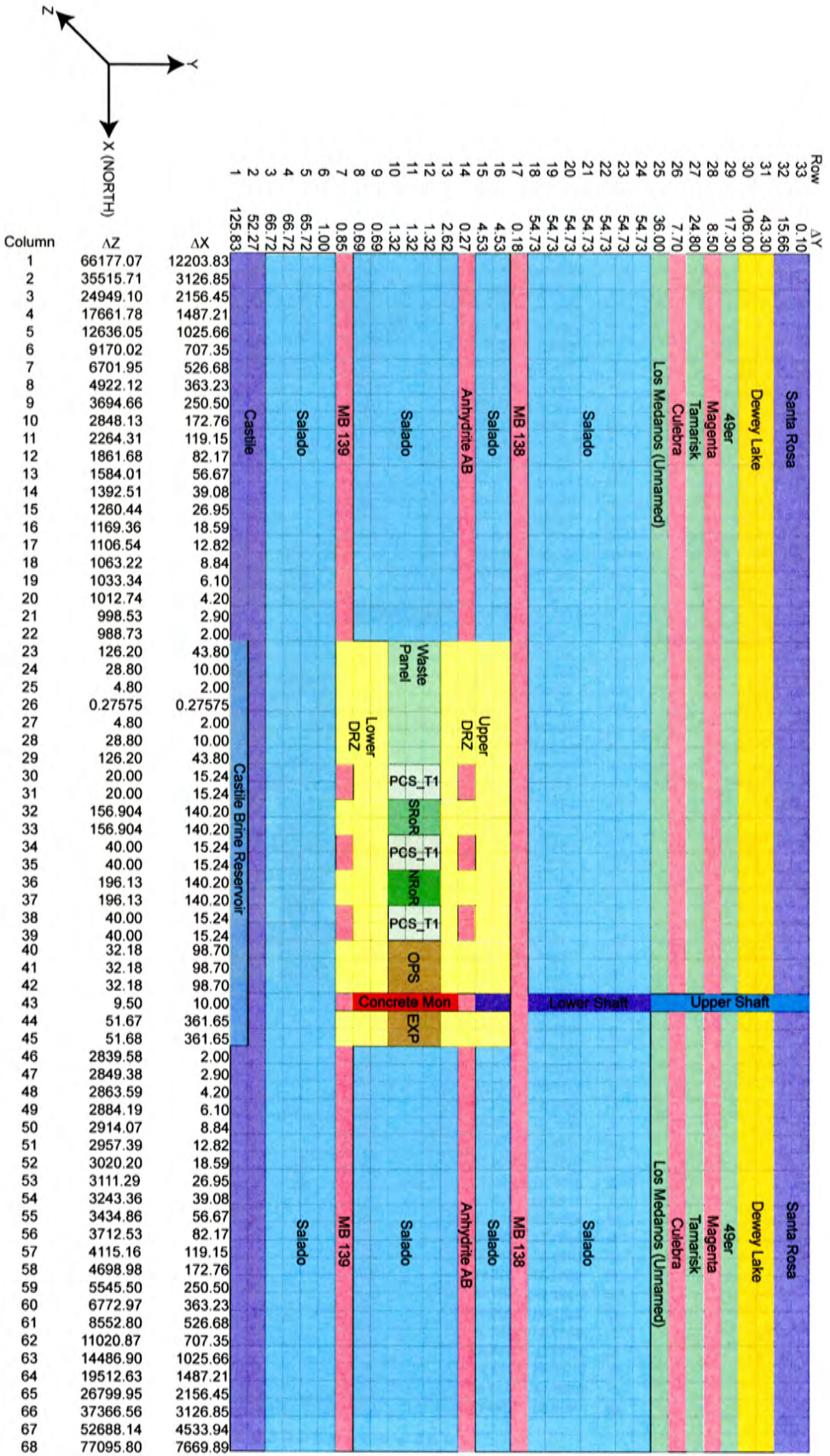


Figure 3-2: CRA-2014 PA BRAGFLO Grid and Material Map, Years 0 to 100

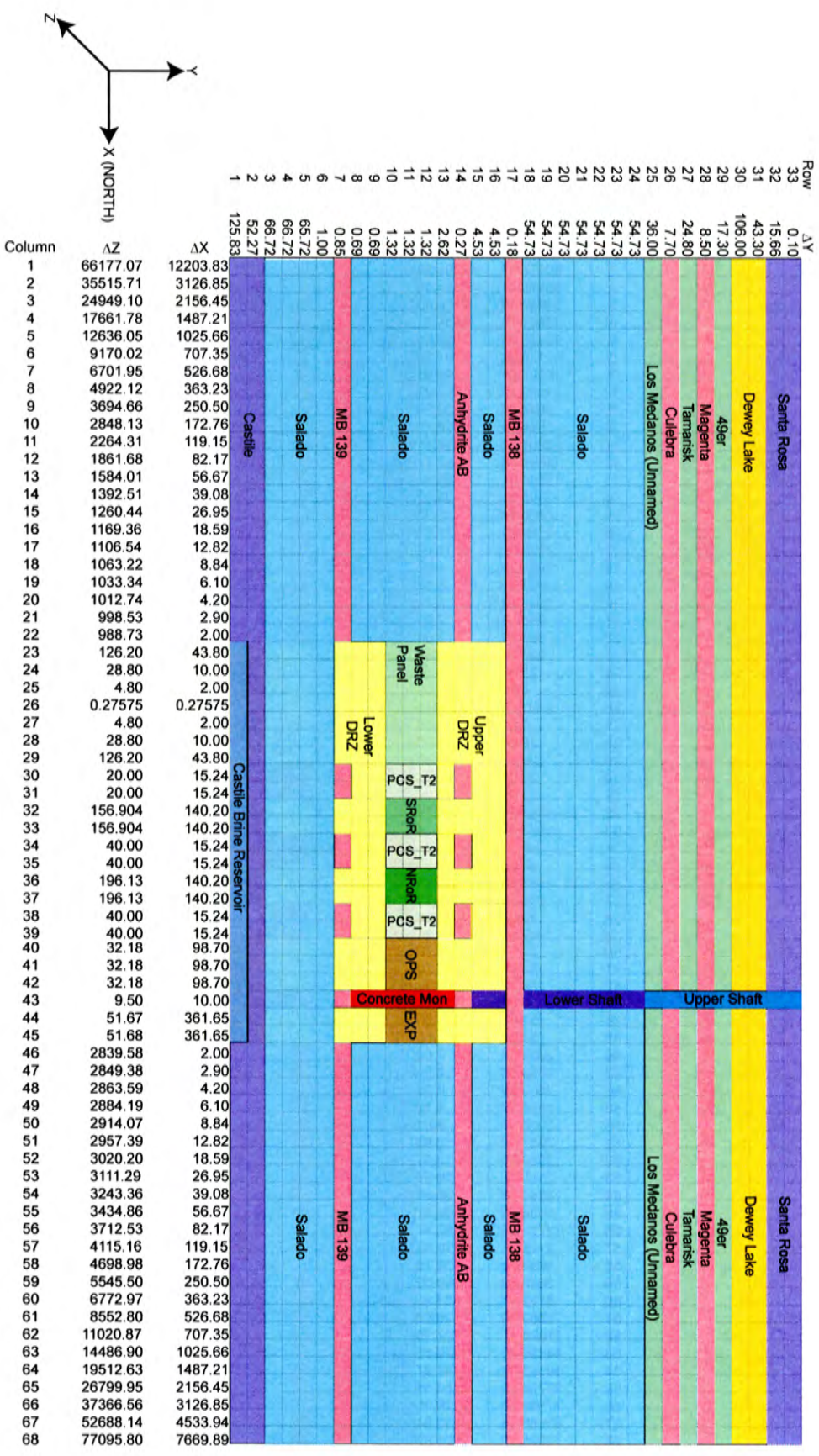


Figure 3-3: CRA-2014 PA BRAGFLO Grid and Material Map, Years 100 to 200

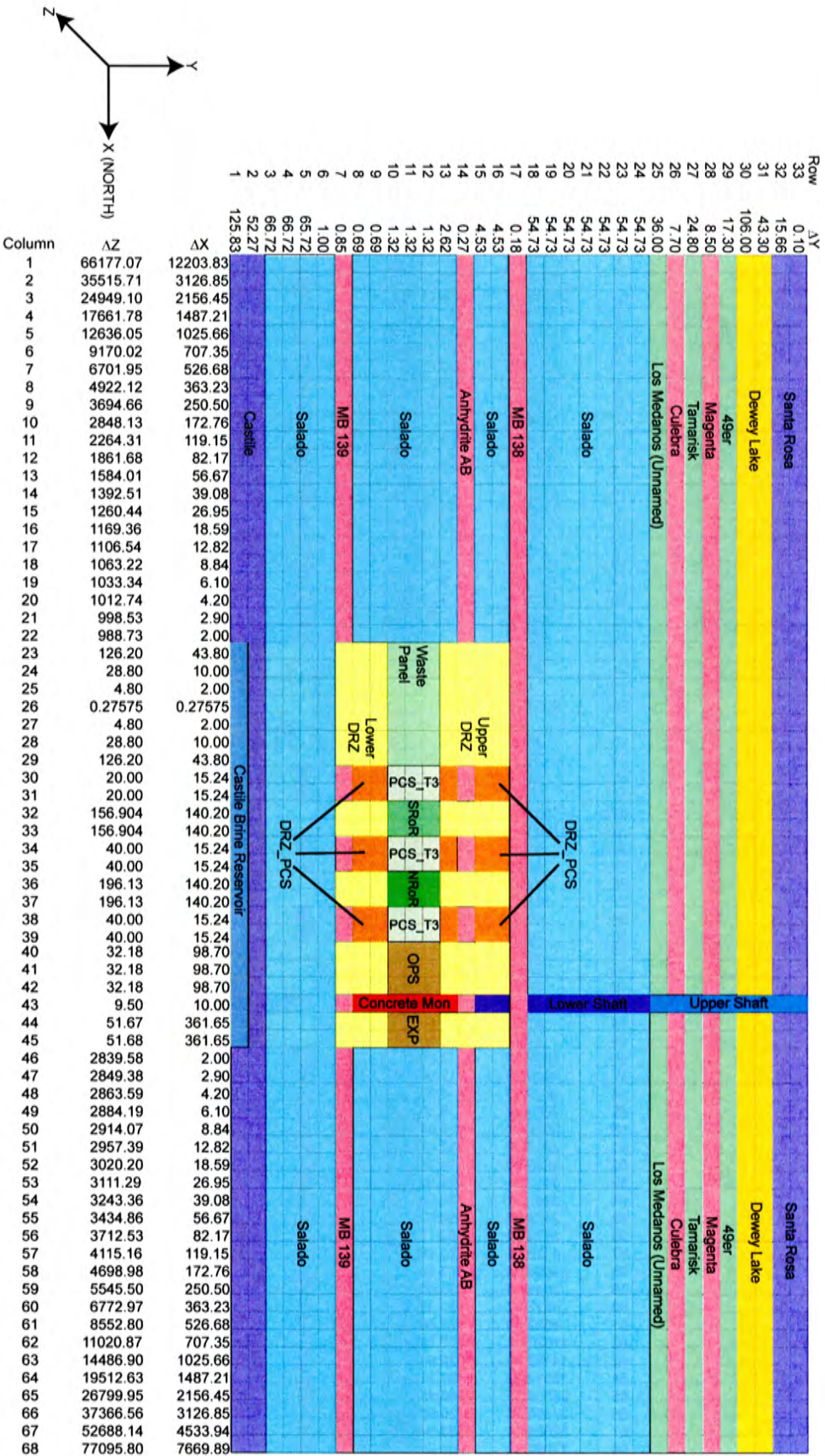


Figure 3-4: CRA-2014 PA BRAGFLO Grid and Material Map, Years 200 to Time of Intrusion

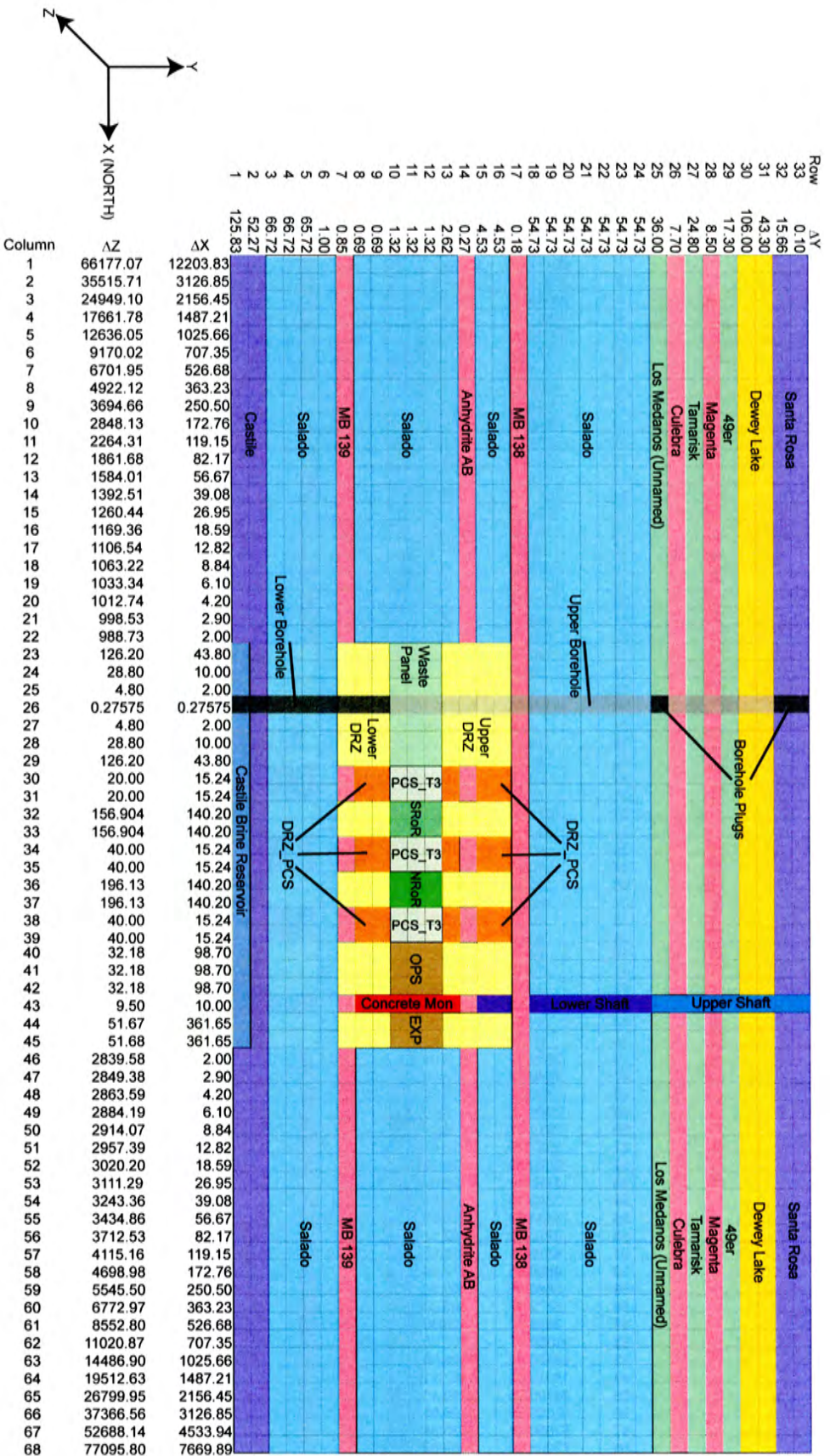
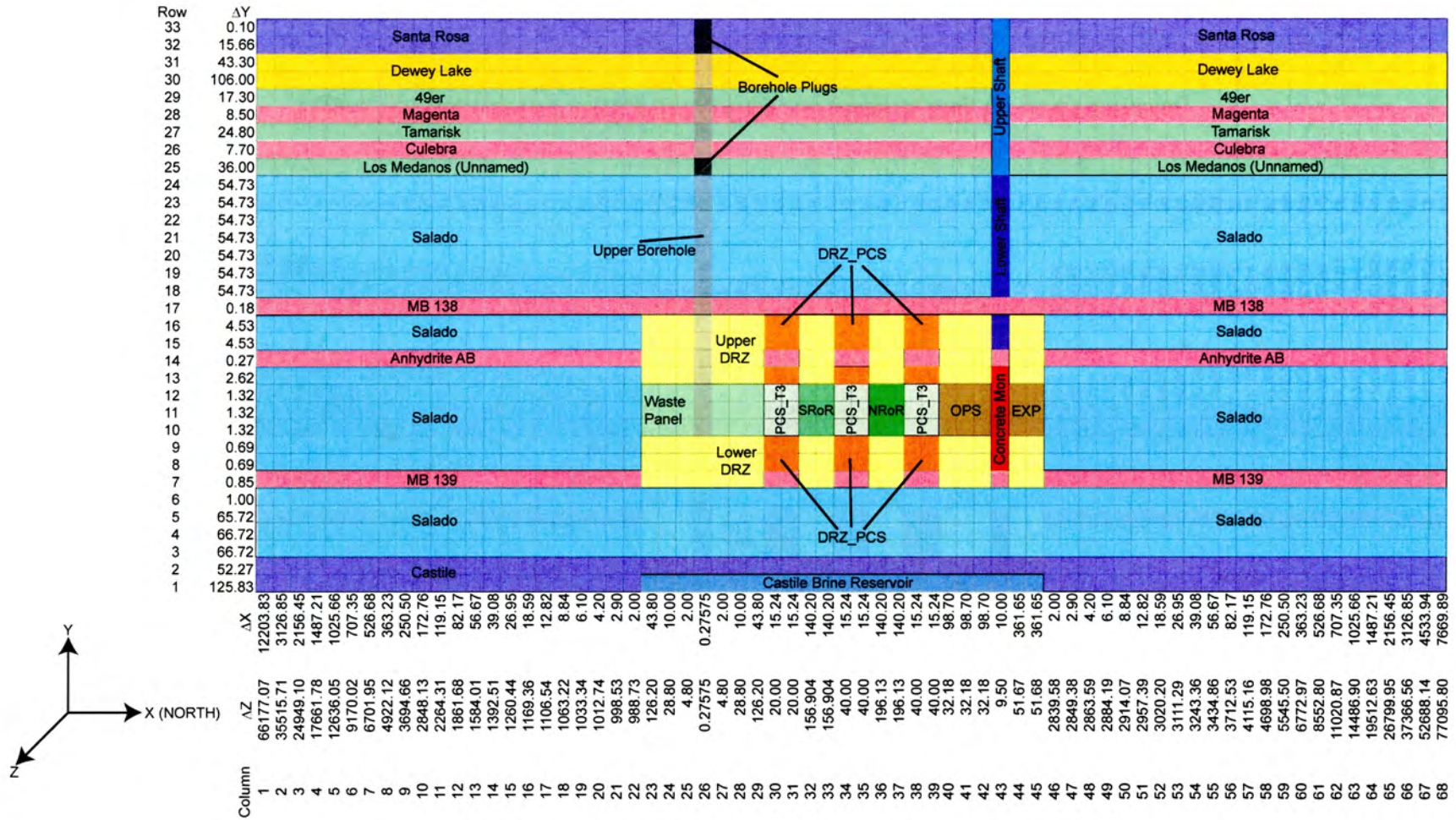


Figure 3-5: CRA-2014 PA BRAGFLO Grid and Material Map for an E1 Intrusion





## 4 SALADO FLOW MODELING METHODOLOGY

The BRAGFLO numerical code calculates the flow of brine and gas in the vicinity of the WIPP repository over a 10,000-year regulatory compliance period. The results of these calculations are used by other codes to calculate potential radionuclide releases to the accessible environment. Some of the specific processes included in the BRAGFLO calculations include:

- Brine and gas flow.
- Pressure generation as a function of time and space.
- Creep closure of the waste filled regions within the repository.
- Physical changes (e.g. permeability and porosity) in the modeling domain over time.
- Cumulative brine flow into and out of the repository and its subregions.

There is significant uncertainty associated with characterizing the physical properties of geologic materials that influence these processes. WIPP PA addresses these uncertainties in two ways. Properties such as permeability and porosity are usually measured indirectly and vary significantly depending upon location. The uncertainty in particular physical property values is called subjective (epistemic) uncertainty. Subjective uncertainty can, in theory, be reduced by further study of the system. Subjective uncertainty is addressed within Salado flow modeling by the use of probability distributions for subjectively uncertain parameters. Multiple flow realizations are performed in which the values of uncertain parameters are sampled from their respective distributions. For subjectively uncertain, spatially distributed quantities, e.g. the permeability of the DRZ, one sampled value is used to specify a particular parameter value over its entire spatial extent in a single realization. To reduce the number of realizations required and to ensure that low probability (and possibly high consequence) combinations are represented, Latin Hypercube Sampling (LHS) is used to create the realizations. For the WIPP PA, the LHS software (Vugrin 2005) is used to create a “replicate” of 100 distinct parameter sets (“vectors”) that are sampled from the full range of parameter uncertainty. To ensure that the Latin Hypercube replicates are representative, a total of three replicates are run for a total of 300 separate vectors.

Another type of uncertainty encountered in WIPP PA is that of stochastic (aleatory) uncertainty associated with incomplete knowledge of future events. Unlike subjective uncertainty, stochastic uncertainty cannot be reduced by further study. WIPP PA addresses stochastic uncertainty by employing a Monte Carlo sampling technique on random futures. In this context, a future is defined as one possible sequence of events. During BRAGFLO calculations, stochastic uncertainty is addressed by defining a set of six scenarios for which brine and gas flow is calculated for each of the vectors generated by the LHS software. The total number of BRAGFLO simulations that have to be run for a WIPP PA calculation is 300 vectors times 6 scenarios equaling 1,800 BRAGFLO simulations.

The six scenarios used in the CRA-2014 PA are unchanged from those used for the 1996 CCA and the PABC-2009. Results obtained in the six scenarios from BRAGFLO are used to initialize flow and material properties in subsequent codes in the PA computational suite, e.g. in the calculation of direct brine releases. The intrusion types specified in PA code calculations

subsequent to BRAGFLO are the same as those implemented in BRAGFLO. The intrusion times, however, are not always equal. To avoid confusion resulting from the use of identical scenario notation for scenarios with unequal intrusion times in the various PA codes, the scenarios in BRAGFLO are denoted as S1-BF to S6-BF. The scenarios include one undisturbed scenario (S1-BF), four scenarios that include a single inadvertent future drilling intrusion into the repository during the 10,000 year regulatory period (S2-BF to S5-BF), and one scenario investigating the effect of two intrusions into a single waste panel (S6-BF). Two types of intrusions, denoted as E1 and E2, are considered. An E1 intrusion assumes the borehole passes through a waste-filled panel and into a region of pressurized brine that may exist under the repository in the Castile formation. An E2 intrusion assumes that the borehole passes through the repository but does not encounter pressurized brine. Scenarios S2-BF and S3-BF model the effect of an E1 intrusion occurring at 350 years and 1000 years, respectively, after the repository is closed. Scenarios S4-BF and S5-BF model the effect of an E2 intrusion at 350 and 1000 years. Scenario S6-BF models an E2 intrusion occurring at 1000 years, followed by an E1 intrusion into the same panel at 2000 years. BRAGFLO results obtained in Scenario S6-BF are used to calculate transport releases to the Culebra. Table 4-1 summarizes the six scenarios used in WIPP PA Salado flow analyses.

Table 4-1: BRAGFLO Modeling Scenarios

Scenario	Description
S1-BF	Undisturbed Repository
S2-BF	E1 intrusion at 350 years
S3-BF	E1 intrusion at 1,000 years
S4-BF	E2 intrusion at 350 years
S5-BF	E2 intrusion at 1,000 years
S6-BF	E2 intrusion at 1,000 years; E1 intrusion at 2,000 years.

The particular mechanics of each scenario are shown below. Note that the ROMPCS implemented in the CRA-2014 PA, as well as materials used to represent the shaft, attain their long-term permeability values at 200 years, well before the occurrence of any of the waste panel intrusions in scenarios S2-BF to S6-BF.

**Scenario S1-BF (Undisturbed Conditions)**

**0 years:** ROMPCS represented by material PCS\_T1 with no healing of the DRZ above and below the panel closure.

**100 years:** ROMPCS material transitions from PCS\_T1 to PCS\_T2 with no healing of the DRZ above and below the panel closure.

**200 years:** ROMPCS material transitions from PCS\_T2 to PCS\_T3 with healed regions of DRZ above and below the panel closure represented by material DRZ\_PCS. Lower shaft material properties are changed.

**Scenario S2-BF (E1 intrusion at 350 years)**

**0 years:** ROMPCS represented by material PCS\_T1 with no healing of the DRZ above and below the panel closure.

**100 years:** ROMPCS material transitions from PCS\_T1 to PCS\_T2 with no healing of the DRZ above and below the panel closure.

**200 years:** ROMPCS material transitions from PCS\_T2 to PCS\_T3 with healed regions of DRZ above and below the panel closure represented by material DRZ\_PCS. Lower shaft material properties are changed.

**350 years:** Borehole intrusion through the Waste Panel and into a hypothetical pressurized brine region in the underlying Castile Formation, with the borehole represented by material BH\_OPEN. Concrete borehole plugs, represented by material CONC\_PLG, immediately emplaced in the borehole below the Culebra and at the surface.

**550 years:** Borehole plugs fail, and the entire borehole is modeled as having properties equivalent to sand. The borehole, bottom to top, is represented by material BH\_SAND.

**1550 years:** The permeability of the borehole between the repository and the Castile brine region decreases due to creep closure of the salt. The lower borehole is represented by material BH\_CREEP as a result.

Scenario S3-BF (E1 intrusion at 1000 years)

**0 years:** ROMPCS represented by material PCS\_T1 with no healing of the DRZ above and below the panel closure.

**100 years:** ROMPCS material transitions from PCS\_T1 to PCS\_T2 with no healing of the DRZ above and below the panel closure.

**200 years:** ROMPCS material transitions from PCS\_T2 to PCS\_T3 with healed regions of DRZ above and below the panel closure represented by material DRZ\_PCS. Lower shaft material properties are changed.

**1000 years:** Borehole intrusion through the Waste Panel and into a hypothetical pressurized brine region in the underlying Castile Formation, with the borehole represented by material BH\_OPEN. Concrete borehole plugs, represented by material CONC\_PLG, immediately emplaced in the borehole below the Culebra and at the surface.

**1200 years:** Borehole plugs fail, and the entire borehole is modeled as having properties equivalent to sand. The borehole, bottom to top, is represented by material BH\_SAND.

**2200 years:** The permeability of the borehole between the repository and the Castile brine reservoir decreases due to creep closure of the salt. The lower borehole is represented by material BH\_CREEP as a result.

Scenario S4-BF (E2 intrusion at 350 years)

**0 years:** ROMPCS represented by material PCS\_T1 with no healing of the DRZ above and below the panel closure.

**100 years:** ROMPCS material transitions from PCS\_T1 to PCS\_T2 with no healing of the DRZ above and below the panel closure.

**200 years:** ROMPCS material transitions from PCS\_T2 to PCS\_T3 with healed regions of DRZ above and below the panel closure represented by material DRZ\_PCS. Lower shaft material properties are changed.

**350 years:** Borehole intrusion terminating at the floor of the Waste Panel, with the borehole represented by material BH\_OPEN. Concrete borehole plugs, represented by

material CONC\_PLG, immediately emplaced in the borehole below the Culebra and at the surface.

**550 years:** Borehole plugs fail, and the entire borehole is modeled as having properties equivalent to sand. The borehole, bottom to top, is represented by material BH\_SAND.

Scenario S5-BF (E2 intrusion at 1000 years)

**0 years:** ROMPCS represented by material PCS\_T1 with no healing of the DRZ above and below the panel closure.

**100 years:** ROMPCS material transitions from PCS\_T1 to PCS\_T2 with no healing of the DRZ above and below the panel closure.

**200 years:** ROMPCS material transitions from PCS\_T2 to PCS\_T3 with healed regions of DRZ above and below the panel closure represented by material DRZ\_PCS. Lower shaft material properties are changed.

**1000 years:** Borehole intrusion terminating at the floor of the Waste Panel, with the borehole represented by material BH\_OPEN. Concrete borehole plugs, represented by material CONC\_PLG, immediately emplaced in the borehole below the Culebra and at the surface.

**1200 years:** Borehole plugs fail, and the entire borehole is modeled as having properties equivalent to sand. The borehole, bottom to top, is represented by material BH\_SAND.

Scenario S6-BF (E2 intrusion at 1000 years, E1 intrusion at 2000 years)

**0 years:** ROMPCS represented by material PCS\_T1 with no healing of the DRZ above and below the panel closure.

**100 years:** ROMPCS material transitions from PCS\_T1 to PCS\_T2 with no healing of the DRZ above and below the panel closure.

**200 years:** ROMPCS material transitions from PCS\_T2 to PCS\_T3 with healed regions of DRZ above and below the panel closure represented by material DRZ\_PCS. Lower shaft material properties are changed.

**1000 years:** Borehole intrusion terminating at the floor of the Waste Panel, with the borehole represented by material BH\_OPEN. Concrete borehole plugs, represented by material CONC\_PLG, immediately emplaced in the borehole below the Culebra and at the surface.

**1200 years:** Borehole plugs fail, and the entire borehole is modeled as having properties equivalent to sand. The borehole, bottom to top, is represented by material BH\_SAND.

**2000 years:** A second borehole intrusion connects the waste panel to a hypothetical pressurized brine region in the underlying Castile Formation. The lower borehole is represented by material BH\_OPEN.

**2200 years:** The lower borehole is modeled as having properties equivalent to sand, and is represented by material BH\_SAND.

**3200 years:** The permeability of the borehole between the repository and the Castile brine region decreases due to creep closure of the salt. The lower borehole is represented by material BH\_CREEP as a result.

## 4.1 Initial Conditions

BRAGFLO simulation of the six scenarios listed above requires the assignment of initial conditions including brine pressure, brine saturation, and concentrations of iron and biodegradable material. These initial conditions are provided to BRAGFLO through various pre-processing steps in which values are retrieved from the WIPP PA Performance Assessment Parameter Database or sampled as appropriate.

At the beginning of each BRAGFLO run (scenario-vector combination), the model simulates a short period of time representing disposal operations. This portion of the run is called the initialization period and lasts for 5 years (from  $t = -5$  to 0 years), corresponding to the time a typical waste panel is expected to be open during disposal operations. All grid blocks require initial pressure and saturation at the beginning of the run ( $t = -5$  years). At the beginning of the regulatory period (0 to 10,000 years), BRAGFLO resets initial conditions within the excavated regions and in the shaft.

The initial conditions specified for BRAGFLO modeling are listed below:

- Brine pressure in all non-excavated regions is equal to lithostatic pressure. This pressure is sampled at a single location and assumed hydrostatic at all other locations.
- Pressure within excavated regions is set to one atmosphere ( $1.01325 \times 10^5$  Pa) at  $t = -5$  years.
- At  $t = 0$  years, pressure in the excavated waste regions is increased to  $1.28039 \times 10^5$  Pa in order to account for the pressure increase ( $0.26714 \times 10^5$  Pa) associated with microbial gas produced at short times (see Subsection 4.2.1 of Nemer et al. 2005).
- Brine saturation within the non-excavated regions is set to 1.0.
- Brine saturation within the excavated regions is set to a value of 0 at  $t = -5$  years.
- Brine saturation in the excavated regions at  $t = 0$  is prescribed the following values:
  - 0.015 for the excavated waste regions, which was chosen to be conservative with respect to the WIPP Waste Acceptance Criteria which allows waste to come to WIPP with no more than 1 % liquids by volume (see Subsection 3.4.1 of DOE 2007).
  - 0.0 for the operations and experimental areas
  - 0.9999999 for the concrete portion of the shaft.
  - For each vector, the initial brine saturation of the ROMPCS is set to the sampled residual brine saturation value for material PCS\_T1, obtained from a cumulative distribution with a minimum of 0.0, a mean of 0.25, and a maximum of 0.6.

During the initialization period brine tends to flow into the excavated areas and the shaft, resulting in decreased pressure and saturation in the rock immediately adjacent to the excavations. At time  $t = 0$  the pressure and saturation in all the excavations is reset to initial conditions for the materials used to represent these regions for the regulatory period. This practice is intended to capture the effect of evaporation of brine inflow during the operational period and the transport of this brine up the shaft ventilation system, as well as the depressurization of the surrounding rock formations due to excavation.

## 4.2 Boundary Conditions

The boundary conditions assigned for the BRAGFLO calculations in the CRA-2014 PA are the same as those for the PABC-2009.

- Constant pressure at the north and south ends of the Culebra and Magenta dolomites.
- Constant pressure ( $1.01325 \times 10^5$  Pa) and saturation (0.08363) conditions at the land surface boundary of the grid, except at the shaft cell on the land surface boundary (Vaughn 1996). The saturation in this cell is set along with the rest of the shaft to the initial saturation prescribed in the WIPP parameter database (SAT\_IBRN) for each of the respective shaft materials.
- No-flow conditions at all other grid boundaries.

## 5 CRA-2014 PA CASES AND RUN CONTROL

Changes incorporated into the CRA-2014 PA include planned changes as well as parameter and implementation changes. As discussed in AP-164 (Camphouse 2013), the approach taken in the CRA-2014 PA is to reasonably isolate impacts associated with these changes, and then to assess the combined impact when all are included in the PA. To that end, four individual cases are investigated in the CRA-2014 PA. Each case is treated as a separate analysis during code execution to ensure that the sequential implementation of change described in AP-164 is done correctly. Two of the cases impact computed BRAGFLO results, and are described below.

The first case considered in the CRA-2014 PA is used to compare the impact of a baseline set of changes relative to the PABC-2009. The name given to this case is CRA14-BL (for CRA-2014 Baseline). A single replicate (Replicate 1) is executed for Case CRA14-BL and used to ascertain regulatory compliance impacts associated with a set of baseline changes. Changes included in Case CRA14-BL that impact BRAGFLO results as compared to the PABC-2009 are:

- Replacement of Option D with the ROMPCS
- Additional excavation in the WIPP experimental area
- Updated waste inventory parameters

Case CRA14-0 is the fourth case considered, and incorporates all changes included in the CRA-2014 PA. In terms of BRAGFLO, Case CRA14-0 includes the changes implemented in Case CRA14-BL listed above, as well as the refinement to the steel corrosion rate and the implementation of a water balance that includes MgO hydration. Three replicates are executed for case CRA14-0, and are used to determine regulatory compliance impacts associated with the full set of changes implemented in the CRA-2014 PA.

A summary of the four cases considered in the CRA-2014 PA is shown in Table 5-1, where changes that impact the Salado flow analysis are shown in bold red font. (BRAGFLO results obtained in Case CRA14-BL are also used in Case CRA14-TP and Case CRA14-BV.)

Table 5-1: Cases Considered in the CRA-2014 PA

<b>CRA-2014 PA Cases</b>				
	Case CRA14-BL	Case CRA14-TP	Case CRA14-BV	Case CRA14-0
CRA-2014 PA changes included	<b>Replacement of Option D PCS with the ROMPCS</b>	Replacement of Option D PCS with the ROMPCS	Replacement of Option D PCS with the ROMPCS	<b>Replacement of Option D PCS with the ROMPCS</b>
	<b>Inclusion of additional mined volume in the WIPP experimental area</b>	Inclusion of additional mined volume in the WIPP experimental area	Inclusion of additional mined volume in the WIPP experimental area	<b>Inclusion of additional mined volume in the WIPP experimental area</b>
	<b>Updated WIPP waste inventory parameters</b>	Updated WIPP waste inventory parameters	Updated WIPP waste inventory parameters	<b>Updated WIPP waste inventory parameters</b>
	Updated radionuclide solubilities and uncertainty, colloid parameters	Updated radionuclide solubilities and uncertainty, colloid parameters	Updated radionuclide solubilities and uncertainty, colloid parameters	Updated radionuclide solubilities and uncertainty, colloid parameters
	Updated drilling rate and plugging pattern parameters	Updated drilling rate and plugging pattern parameters	Updated drilling rate and plugging pattern parameters	Updated drilling rate and plugging pattern parameters
		BOREHOLE:TAUFAIL and GLOBAL:PBRINE parameter distribution refinements	BOREHOLE:TAUFAIL and GLOBAL:PBRINE parameter distribution refinements	BOREHOLE:TAUFAIL and GLOBAL:PBRINE parameter distribution refinements
			Variable Brine Volume Implementation	Variable Brine Volume Implementation
				<b>Update to parameter STEEL:CORRMC02</b>
				<b>Refinement to Repository Water Balance Implementation</b>
Number of replicates	1	1	1	3



Run control, including code versions used and descriptions of code sequencing used to obtain BRAGFLO results in the CRA-2014 PA, is documented in Long (2013).

Case CRA14-BL results obtained in the BRAGFLO post-processing step have file names ALG2\_BF\_CRA14BL\_R1\_Ss\_Vvvv.CDB, where s (the scenario number) equals 1,2,3,4,5, or 6, and vvv (the vector number) is between 001 and 100. These files are located in CMS library LIBCRA14\_BFRrSs in class CRA14-BL.

Case CRA14-0 results obtained in the BRAGFLO post-processing step have file names ALG2\_BF\_CRA14\_Rr\_Ss\_Vvvv.CDB, where r (the replicate number) equals 1,2, or 3, s (the scenario number) equals 1,2,3,4,5, or 6, and vvv (the vector number) is between 001 and 100. These files are located in CMS library LIBCRA14\_BFRrSs under class CRA14-0.

PCS-2012 PA results obtained in the BRAGFLO post-processing step have file names ALG2\_BF\_AP161\_Rr\_Ss\_Vvvv.CDB, where r (the replicate number) equals 1,2, or 3, s (the scenario number) equals 1,2,3,4,5, or 6, and vvv (the vector number) is between 001 and 100. These files are located in CMS library LIBAP161\_BFRrSs under class AP161-0.

PABC-2009 results obtained in the BRAGFLO post-processing step have file names ALG2\_BF\_PABC09\_Rr\_Ss\_Vvvv.CDB, and are located in CMS library LIBPABC09\_BFRrSs under class PABC09-0.

## 6 RESULTS

Computed results are now presented for the CRA-2014 PA and compared with those obtained in the PABC-2009. In the following sections, results are presented in terms of volume-averaged quantities. For example, volume-averaged pressure is obtained by forming the product of grid block pressure and grid block volume for each grid block in the region of concern, summing this product up over all grid blocks in the region, and dividing by the bulk volume of the region. All other volume-averaged quantities are computed in the same manner. Cumulative flow volumes are also presented. Cumulative flow into a region is defined as the time-dependent flow into a region integrated over time.

As previously discussed, the regulatory impacts associated with implementing the ROMPCS in WIPP were evaluated in the PCS-2012 PA. As the PCS-2012 PA was done after the PABC-2009 and prior to the CRA-2014 PA, BRAGFLO results obtained in the PCS-2012 PA are useful in that they provide an intermediate result between the PABC-2009 and the CRA-2014 PA. In terms of BRAGFLO, Case CRA14-BL is essentially a re-run of replicate 1 of the PCS-2012 PA with an updated waste inventory and additional volume added to the repository experimental region. The impact of these two changes can be determined by comparing results obtained in Case CRA14-BL to those obtained in the PABC-2009 and the PCS-2012 PA. Thus, BRAGFLO results presented for Case CRA14-BL are compared to their PABC-2009 and PCS-2012 PA counterparts. Impacts of the updated steel corrosion rate and the refined repository water balance implementation are then determined by comparing results of Case CRA14-0 to those found in the PABC-2009, with discussion of Case CRA14-BL and PCS-2012 PA results as appropriate. In the results that follow, the routine calculation of means and generation of plots were done with Matlab version R2008b, a Commercial off-the Shelf (COTS) software package.

## 6.1 Results for an Undisturbed Repository (Scenario S1-BF)

Results are now presented for undisturbed scenario S1-BF. Results for each quantity are presented first for Case CRA14-BL, followed by their Case CRA14-0 counterpart.

### Pressure

The horsetail plot of volume-averaged waste panel pressure, quantity WAS\_PRES, obtained in Case CRA14-BL is shown in Figure 6-1. The replicate 1 means of this quantity obtained in the PABC-2009, the PCS-2012 PA, and Case CRA14-BL are shown together in Figure 6-2. As seen in that figure, and discussed more fully in Camphouse (2012a), the replacement of the Option D PCS with the ROMPCS results in a slightly higher mean pressure in the waste panel for undisturbed conditions. The result is a mean waste panel pressure curve in the PCS-2012 PA that is slightly greater than that of the PABC-2009. Additional mined volume in the WIPP experimental area results in a slight reduction to the mean waste panel pressure, yielding a mean waste panel pressure curve in Case CRA14-BL that is slightly lower than that seen in the PABC-2009. This result is consistent with that found in Camphouse et al. (2011). Decreases in the iron and CPR inventory in the CRA-2014 PA also likely contribute to the reduction in mean waste panel pressure seen in Case CRA14-BL. The horsetail plot of waste panel pressure obtained for the 300 vector realizations of Case CRA14-0 is shown in Figure 6-3, with the three replicate means plotted together in Figure 6-4. As is evident in Figure 6-4, very close agreement is seen among the three replicate means. The revised steel corrosion rate and water balance implementation utilized in Case CRA14-0 result in even further reduction to the mean waste panel pressure as compared to that obtained in the PABC-2009. The overall means, calculated over all 300 vector realizations, for quantity WAS\_PRES in the PABC-2009 and Case CRA14-0 are shown together in Figure 6-5.

Pressure trends seen in the waste panel are also evident in the South Rest-of-Repository (SRoR) and North Rest-of-Repository (NRoR) waste regions. Pressure in these regions is denoted by SRR\_PRES and NRR\_PRES, respectively, and results for these quantities are shown in Figure 6-6 to Figure 6-15.

The increased permeability of the ROMPCS and surrounding DRZ for years 0 to 200, as compared to the Option D PCS, contributes to the reduction in mean pressure in repository waste regions by allowing for pressure release into the operational and experimental areas at early times (Camphouse 2012a). The increase in mined volume of the experimental area translates to a pressure reduction in that region, allowing for additional reductions to waste area mean pressures. The horsetail plot of volume averaged pressure in the experimental area, denoted by quantity EXP\_PRES, obtained in Case CRA14-BL is shown in Figure 6-16. The replicate 1 means of this quantity obtained in the PABC-2009, the PCS-2012 PA, and Case CRA14-BL are shown together in Figure 6-17. As seen in Figure 6-17, the long-term mean pressure in the experimental region is lowest for Case CRA14-BL, due to the additional mined volume in that region. The horsetail plot of experimental region pressure obtained for the 300 vector realizations of Case CRA14-0 is shown in Figure 6-18, with the three replicate means plotted together in Figure 6-19. The overall means, calculated over all 300 vector realizations, for quantity EXP\_PRES in the PABC-2009 and Case CRA14-0 are shown together in Figure 6-20. As is clear in that figure, the refined steel corrosion rate and water budget implementation

utilized in Case CRA14-0 yield further reductions to the mean pressure in the experimental region.

### Gas Generation

The reduction in waste region pressure from Case CRA14-BL to Case CRA14-0 is largely due to the revised iron corrosion rate implemented in the latter case. The horsetail plot of molar gas generation in all repository waste regions, quantity GASMOL\_T, for Case CRA14-BL is shown in Figure 6-21. The replicate 1 mean of quantity GASMOL\_T obtained in Case CRA14-BL is shown in Figure 6-22. Also seen in Figure 6-22 are the mean curves of gas generation due to iron corrosion (quantity FEMOL\_T) and microbial degradation of cellulose (quantity CELMOL\_T). As is clear from Figure 6-22, the majority of gas generated in repository waste regions in Case CRA14-BL is due to iron corrosion. The means shown in Figure 6-22 are similar, but slightly reduced in comparison, to those obtained in the PABC-2009 (see Figure 6-18 of Nemer (2010)). The slight decrease to mean gas generation seen in Case CRA14-BL is likely due to the decreased iron and CPR inventories used in the CRA-2014 PA. The horsetail plot of total molar gas generation obtained in Case CRA14-0 is shown in Figure 6-23. Means of total molar gas generation obtained in Case CRA14-0 are shown in Figure 6-24. (Figure 6-24 includes replicate 1 means as well as overall means to allow for direct comparison to results shown in Figure 6-22.) As is clear from Figure 6-24, gas generation due to iron corrosion is still the dominant gas production mechanism in Case CRA14-0. However, the moles of gas generated by iron corrosion in Case CRA14-0 are significantly reduced (on average) as compared to case CRA14-BL. The revised iron corrosion rate implemented in Case CRA14-0 results in a slower rate of gas production (on average).

The inclusion of MgO chemistry in the revised water balance implementation also contributes to the reduction in gas generation for Case CRA14-0. Gas production due to iron corrosion and CPR microbial degradation both require freely available brine in repository waste regions. The formation of brucite in the revised water balance implementation sequesters free water, making less available for gas production processes. The impact of the revised water balance implementation on gas production can be determined by comparing the mean curves for quantity CELMOL\_T in Figure 6-22 and Figure 6-24. Moles of gas produced by microbial degradation of cellulose is slightly reduced (on average) from Case CRA14-BL to Case CRA14-0. The revised iron corrosion rate and water balance implementation both contribute to the reduction in mean total molar gas generation. Most of the gas generation reduction seen in Case CRA14-0 is due to the revised iron corrosion rate, however.

The mass fraction of iron remaining in the repository, denoted by quantity FEREM\_T, is obviously impacted by the revised iron corrosion rate. The horsetail plot, with the mean overlaid in red, for quantity FEREM\_T obtained in Case CRA14-BL is shown in Figure 6-25. The analogous result obtained in Case CRA14-0 is shown in Figure 6-26. As is clearly seen by comparing these two figures, the reduction in the iron corrosion rate (on average) results in a higher fraction of iron remaining in the repository at later times. The rate of iron consumption by gas production processes is decreased with the remaining mass fraction increasing correspondingly, even though the total mass of emplaced iron is slightly reduced in the CRA-2014 PA as compared to the PABC-2009 (Table 2-6). A similar result is evident for the mass fraction of cellulose remaining, denoted by quantity CELREM\_T. As seen in Figure 6-27 and

Figure 6-28, the mass fraction of cellulose remaining in the repository is increased at later times (on average) in Case CRA14-0. The sequestration of free water as brucite forms results in less gas being produced by microbial degradation of cellulose, resulting in an increase to the mass fraction of cellulose remaining.

### Cumulative Brine Flow

The trend toward waste panel pressure reduction in the CRA14-0 result yields a corresponding increase (on average) in cumulative waste panel brine inflow, denoted by quantity BRNWASIC. The horsetail plot of this quantity obtained in Case CRA14-BL is shown in Figure 6-29. Replicate 1 means obtained for quantity BRNWASIC in the PABC-2009, the PCS-2012 PA, and Case CRA14-BL are shown together in Figure 6-30. As discussed in Camphouse (2012a), the replacement of the Option D panel closure with the ROMPCS results in an increase in the mean cumulative brine inflow to the waste panel as compared to the PABC-2009. Additional excavation in the repository experimental region results in a slight reduction to the mean waste panel pressure, with a corresponding increase to the mean waste panel cumulative brine inflow in the CRA14-BL result. Further pressure reduction, due to reduced gas generation, yields an additional increase to the waste panel brine inflow (on average) in the CRA14-0 result. The horsetail plot for quantity BRNWASIC obtained in Case CRA14-0 is shown in Figure 6-31, with the three replicate means plotted together in Figure 6-32. As is evident in Figure 6-32, there is close agreement among the three replicate means obtained in Case CRA14-0 for quantity BRNWASIC. The overall means of cumulative waste panel brine inflow, calculated over all 300 vector realizations, obtained in the PABC-2009 and Case CRA14-0 are plotted together in Figure 6-33.

Results obtained for the south and north rest-of-repository regions are similar to those seen for the waste panel. Cumulative brine inflows to these repository regions are denoted by BRNSRRIC and BRNNRRIC, respectively, and results for these quantities are shown in Figure 6-34 to Figure 6-43. As can be seen by comparing Figure 6-33, Figure 6-38, and Figure 6-43, the increase to the mean cumulative brine inflow relative to the PABC-2009 is more pronounced for panels at lower elevation. Mean brine inflow results obtained in the PABC-2009 and Case CRA14-0 are quite similar for the NRoR (Figure 6-43), while the difference seen between the PABC-2009 and Case CRA14-0 result is more pronounced for the SRoR (Figure 6-38) and the southernmost (lowest elevation) waste panel (Figure 6-33).

Trends seen in the waste panel for cumulative brine inflow are also apparent when investigated for the entire repository. Results obtained for cumulative brine inflow to the repository, denoted by quantity BRNREPIC, are shown in Figure 6-44 to Figure 6-48.

The horsetail plot of cumulative brine flow up the shaft, denoted by quantity BNSHUDRZ, obtained in case CRA14-BL is shown in Figure 6-49. Replicate 1 means for this quantity obtained in the PABC-2009, the PCS-2012 PA, and Case CRA14-BL are plotted together in Figure 6-50. The repository shaft is modeled in WIPP PA as being directly between the operations and experimental regions of the repository. Consequently, the pressure in these repository regions impacts the volume of brine moved up the shaft toward the ground surface. The trends seen for the mean cumulative brine flow up the shaft in Figure 6-50 correspond closely to the pressure trends shown in Figure 6-17 for the experimental region. The horsetail

plot for quantity BNSHUDRZ obtained in Case CRA14-0 is shown in Figure 6-51 with replicate means shown in Figure 6-52. As seen in Figure 6-52, there is good agreement seen among the three replicate means for this quantity in Case CRA14-0. The overall mean of quantity BNSHUDRZ obtained in Case CRA14-0 is compared to the PABC-2009 result in Figure 6-53. As seen in that figure, the mean cumulative brine flow up the shaft is reduced in the Case CRA14-0, with trends following those seen for mean pressure in the experimental region (Figure 6-20).

### Brine Saturation

The changes in brine inflow to repository waste regions have a direct impact on the brine saturations calculated for those areas. The horsetail plot of waste panel brine saturation, denoted by quantity WAS\_SATB, obtained in Case CRA14-BL is shown in Figure 6-54. Replicate 1 means obtained for this quantity in the PABC-2009, the PCS-2012 PA, and Case CRA14-BL are plotted together in Figure 6-55. The increases in the mean cumulative waste panel brine inflow from the PABC-2009 to Case CRA14-BL yield corresponding increases to the mean waste panel brine saturation. The horsetail plot for waste panel brine saturation calculated in Case CRA14-0 is shown in Figure 6-56, with the three replicate means plotted together in Figure 6-57. As seen in Figure 6-57, there is good agreement among the three replicate means. The overall means of waste panel brine saturation obtained in the PABC-2009 and the Case CRA14-0 are plotted together in Figure 6-58. The increase in cumulative waste panel brine inflow seen in the CRA14-0 result yields a corresponding increase in the waste panel brine saturation. The refined water budget implementation in Case CRA14-0 results in brine being sequestered at early times as brucite is formed, yielding a mean waste panel brine saturation curve that is lower than that seen in the PABC-2009 prior to roughly 750 years. As brucite is transformed to hydromagnesite and then magnesite, water is released to the repository, yielding a mean waste panel brine saturation curve with an upward trend as compared to the PABC-2009 result.

As seen in the results already discussed, increased mean cumulative brine inflows are seen in Case CRA14-0 for the SRoR and the NRoR as compared to the PABC-2009, but the increases are less pronounced than those seen in the waste panel due to its lower elevation. For the SRoR and NRoR, the refined water budget implementation utilized in Case CRA14-0 results in mean brine saturation curves that remain below those calculated in the PABC-2009 for the duration of the regulatory period. As the SRoR and NRoR together represent nine of the ten repository waste panels, the sequestration of brine in the refined water budget implementation yields a repository that tends to be drier overall for undisturbed conditions as compared to the PABC-2009. CRA-2014 PA results obtained for the SRoR and NRoR are shown in Figure 6-59 to Figure 6-68.

### Porosity

The trend toward lower mean pressure in repository waste areas for the CRA14-0 results yields a corresponding trend toward reduced mean porosity in those areas. The horsetail plot of waste panel porosity, denoted by quantity WAS\_POR, obtained for Case CRA14-BL is shown in Figure 6-69. Replicate 1 means obtained for this quantity in the PABC-2009, the PCS-2012 PA, and Case CRA14-BL are plotted together in Figure 6-70. As is clear from that figure, results obtained for mean waste panel porosity in the three analyses are nearly identical. The horsetail

plot of waste panel porosity calculated in Case CRA14-0 is shown in Figure 6-71, with the three replicate means plotted together in Figure 6-72. As seen in Figure 6-72, there is very good agreement among the three replicate means obtained in Case CRA14-0. The overall means of waste panel porosity obtained in the PABC-2009 and Case CRA14-0 are plotted together in Figure 6-73. The lower mean waste panel pressure seen in the CRA14-0 result translates to a lower mean waste panel porosity when compared to the PABC-2009. Porosity results for the SROr and NROr waste regions are virtually identical to those obtained for the waste panel.

#### Summary of Results for an Undisturbed Repository

Pressures and brine saturations in repository waste regions are important quantities relevant to direct release mechanisms considered in WIPP PA. Spallings releases depend directly on repository pressure. Direct brine releases (DBRs) depend on both repository pressure and brine saturation. Changes included in the CRA-2014 PA yield a reduction in the mean pressure calculated for undisturbed repository waste areas as compared to the PABC-2009. The expanded mined volume in the repository experimental area contributes somewhat to this reduction, but it is primarily due to reduced gas generation seen in the CRA14-0 results. The revised iron corrosion rate utilized in Case CRA14-0 results in slower gas production due to iron corrosion (on average). The addition of MgO chemistry in the revised water balance implementation also reduces the amount of free water available for gas production by iron corrosion and microbial degradation of cellulose. The sequestration of free water further reduces gas production, and consequently pressure, in repository waste areas.

Waste area brine saturation trends in the CRA14-0 results are a function of waste panel elevation. Mean cumulative brine inflows to repository waste areas are increased in the CRA14-0 results (as compared to the PABC-2009), but these increases are more pronounced for waste areas at lower elevation. As a result, waste areas at higher elevation, such as the SROr and the NROr, have lower mean brine saturations in the CRA14-0 results as compared to the PABC-2009 due to water sequestration in the refined water balance implementation. Waste panels at lowest elevation, such as the separately modeled waste panel in BRAGFLO, have a lower mean brine saturation at early times as compared to the PABC-2009. However, the mean waste panel brine saturation gradually increases until it becomes greater than that seen in the PABC-2009 at roughly 750 years. As the SROr and NROr together represent nine of the ten repository waste panels, the sequestration of brine in the refined water budget implementation yields a repository that tends to be drier overall for undisturbed conditions as compared to the PABC-2009.

Summary statistics for BRAGFLO scenario S1-BF are shown in Table 6-1. Results presented in that table are calculated over all 300 vector realizations (and all times) of the PABC-2009 and Case CRA14-0 of the CRA-2014 PA. Note that the maximum quantities of generated gas shown in Table 6-1 are not additive. That is, the maximum value given for quantity GASMOL\_T in Table 6-1 is not equal to the sum of maximum values given for quantities FEMOL\_T and CELMOL\_T. Maximum values for FEMOL\_T and CELMOL\_T can (and often do) occur in different vectors and at different times than those yielding a maximum value for GASMOL\_T. For example, vector 28 of replicate 1 in Case CRA14-0 attains the maximum value shown for quantity GASMOL\_T. This same vector also attains the maximum value listed for CELMOL\_T. However, the maximum value seen in this vector for quantity FEMOL\_T is  $474.03 \times 10^6$  moles, roughly 60% of the maximum value listed for this quantity in Table 6-1.

Table 6-1: Summary Statistics for Scenario S1-BF

Quantity (units)	Description	Mean Value		Maximum Value	
		PABC-2009	CRA14-0	PABC-2009	CRA14-0
WAS_PRES (MPa)	Volume-averaged pressure in the waste panel.	6.52	3.44	16.19	15.73
SRR_PRES (MPa)	Volume-averaged pressure in the SRoR.	6.37	2.93	16.17	15.85
NRR_PRES (MPa)	Volume-averaged pressure in the NRoR.	6.21	2.66	16.12	15.71
EXP_PRES (MPa)	Volume-averaged pressure in the experimental area.	4.46	1.79	15.65	14.27
GASMOL_T (x10 <sup>6</sup> moles)	Total moles of gas generated in repository waste areas.	231.35	84.44	1345.67	878.83
FEMOL_T (x10 <sup>6</sup> moles)	Total moles of gas generated by iron corrosion in repository waste areas.	189.20	67.60	920.94	796.25
CELMOL_T (x10 <sup>6</sup> moles)	Total moles of gas generated by microbial degradation of CPRs in repository waste areas.	42.15	16.85	494.01	404.80
BRNWASIC (x10 <sup>3</sup> m <sup>3</sup> )	Cumulative brine inflow to the waste panel.	1.78	2.80	12.46	16.40
BRNSRRIC (x10 <sup>3</sup> m <sup>3</sup> )	Cumulative brine inflow to the SRoR.	4.82	5.26	37.78	49.73
BRNNRRIC (x10 <sup>3</sup> m <sup>3</sup> )	Cumulative brine inflow to the NRoR.	6.04	6.18	48.02	39.27
BRNREPIC (x10 <sup>3</sup> m <sup>3</sup> )	Cumulative brine inflow to the entire repository.	17.83	21.68	118.86	140.04
WAS_SATB (none)	Brine saturation in the waste panel.	0.160	0.209	0.985	0.991
SRR_SATB (none)	Brine saturation in the SRoR.	0.120	0.085	0.938	0.936
NRR_SATB (none)	Brine saturation in the NRoR.	0.121	0.077	0.937	0.720
BNSHUDRZ (m <sup>3</sup> )	Cumulative brine flow up the repository shaft.	2.74	0.61	34.76	24.66
WAS_POR (none)	Porosity in the waste panel.	0.17	0.13	0.85	0.85

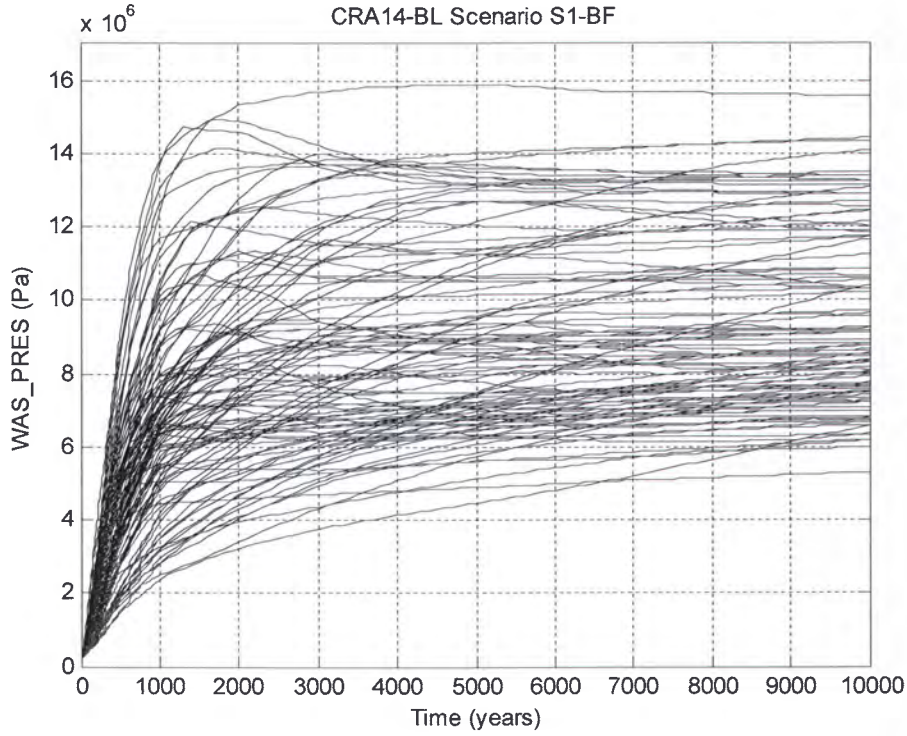


Figure 6-1: Horsetail Plot of Waste Panel Pressure for Case CRA14-BL, Scenario S1-BF

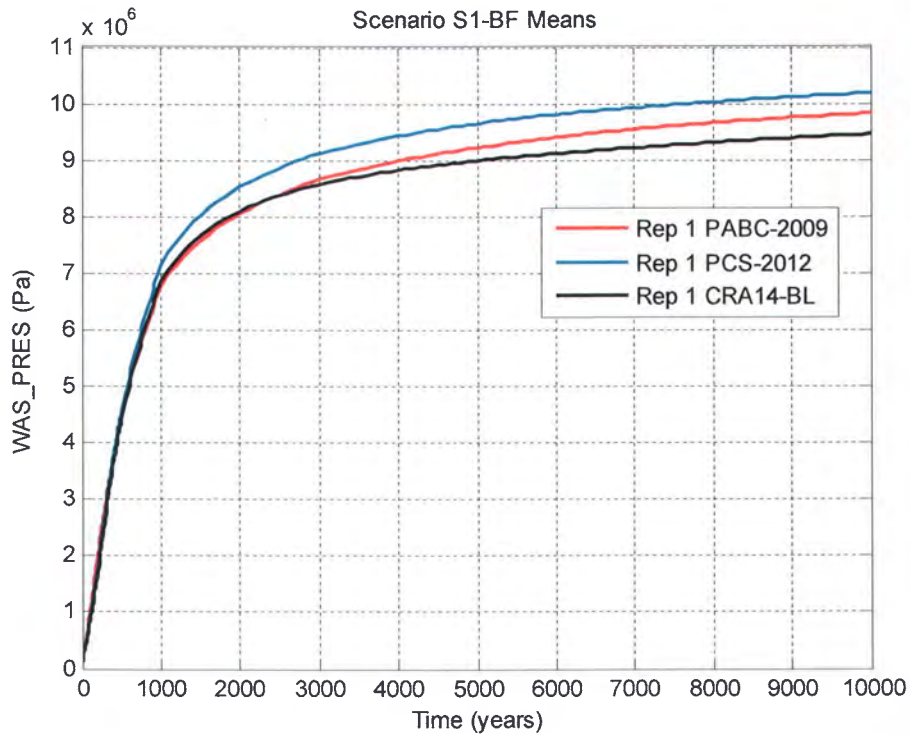


Figure 6-2: Replicate 1 Means of Waste Panel Pressure, Scenario S1-BF



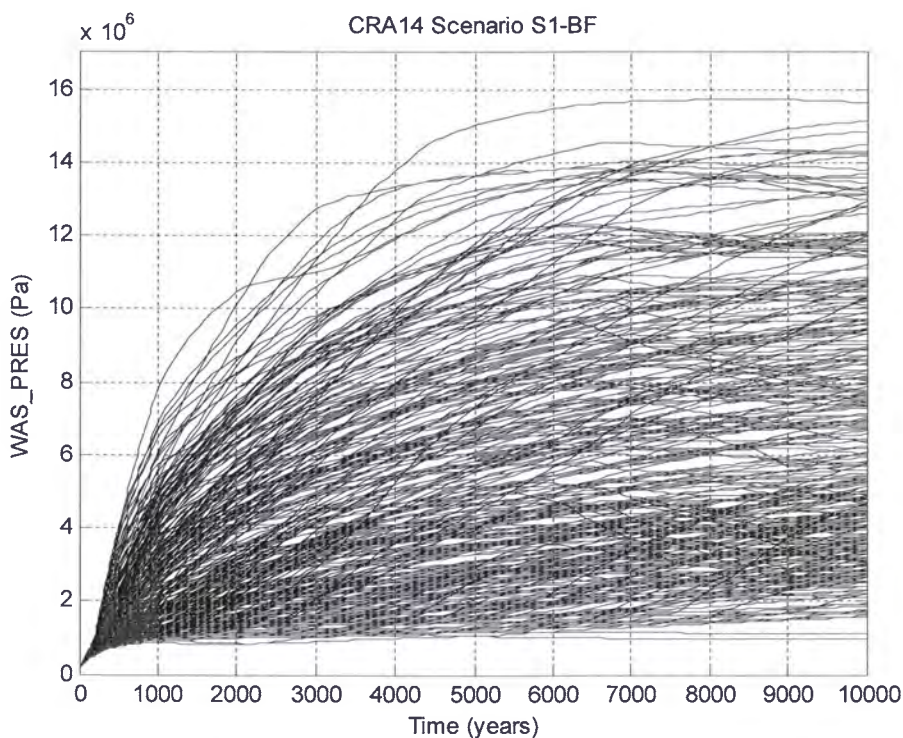


Figure 6-3: Horsetail Plot of Waste Panel Pressure for Case CRA14-0, Scenario S1-BF

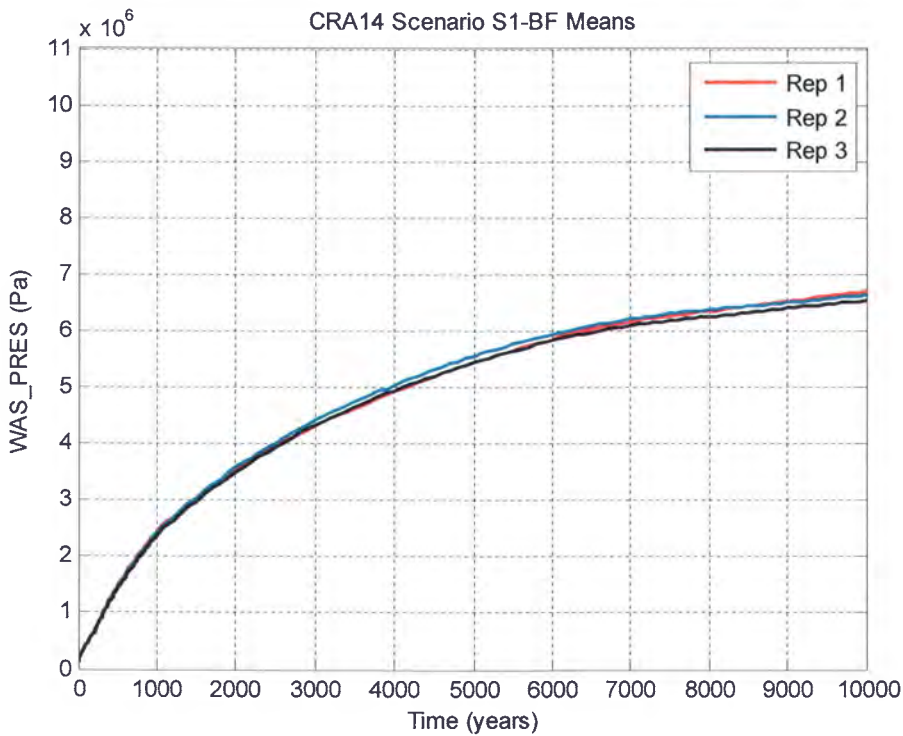


Figure 6-4: Replicate Means of Waste Panel Pressure for Case CRA14-0, Scenario S1-BF

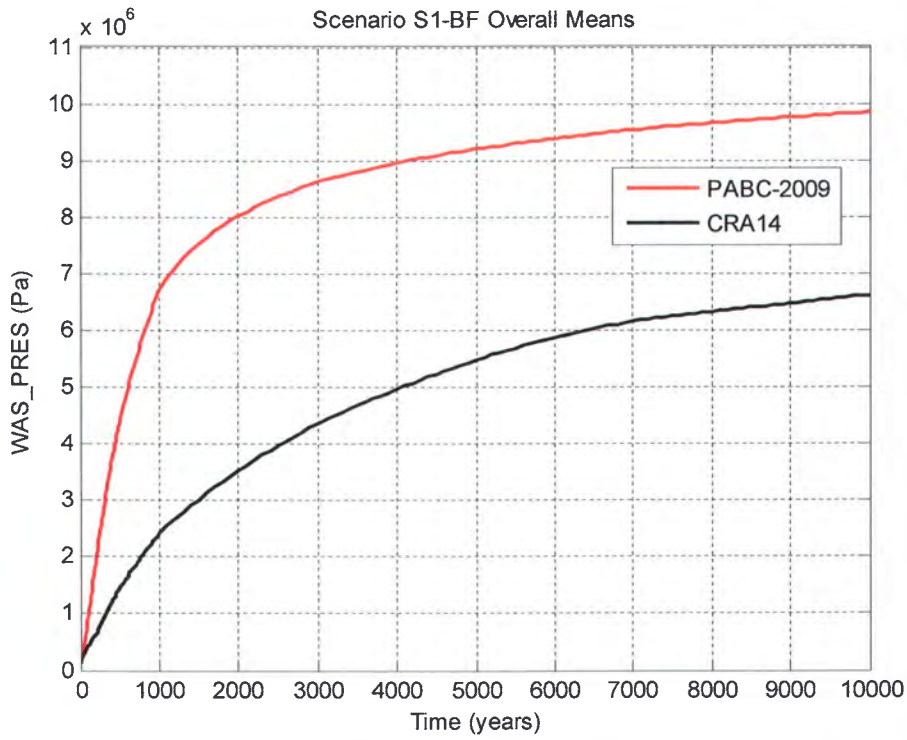


Figure 6-5: Overall Means of Waste Panel Pressure, Scenario S1-BF

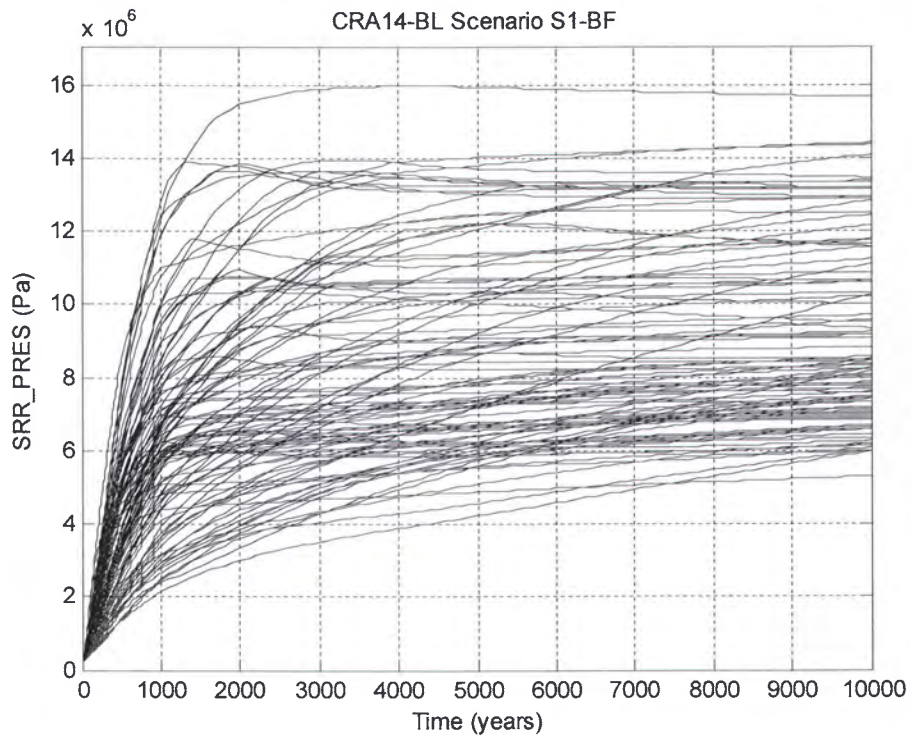


Figure 6-6: Horsetail Plot of SRoR Pressure for Case CRA14-BL, Scenario S1-BF

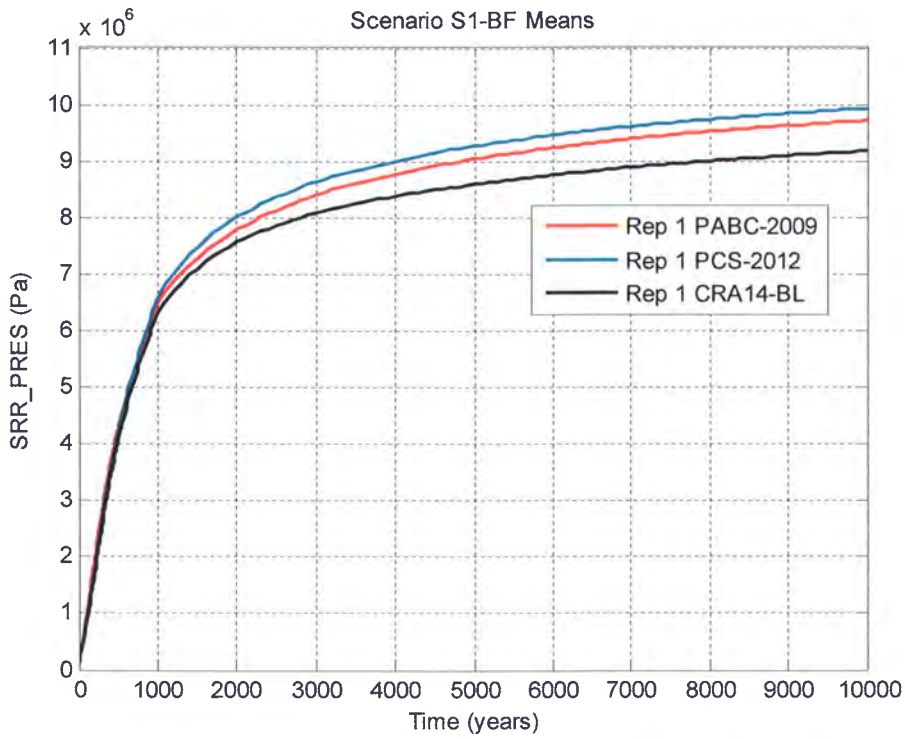


Figure 6-7: Replicate 1 Means of SRoR Pressure, Scenario S1-BF

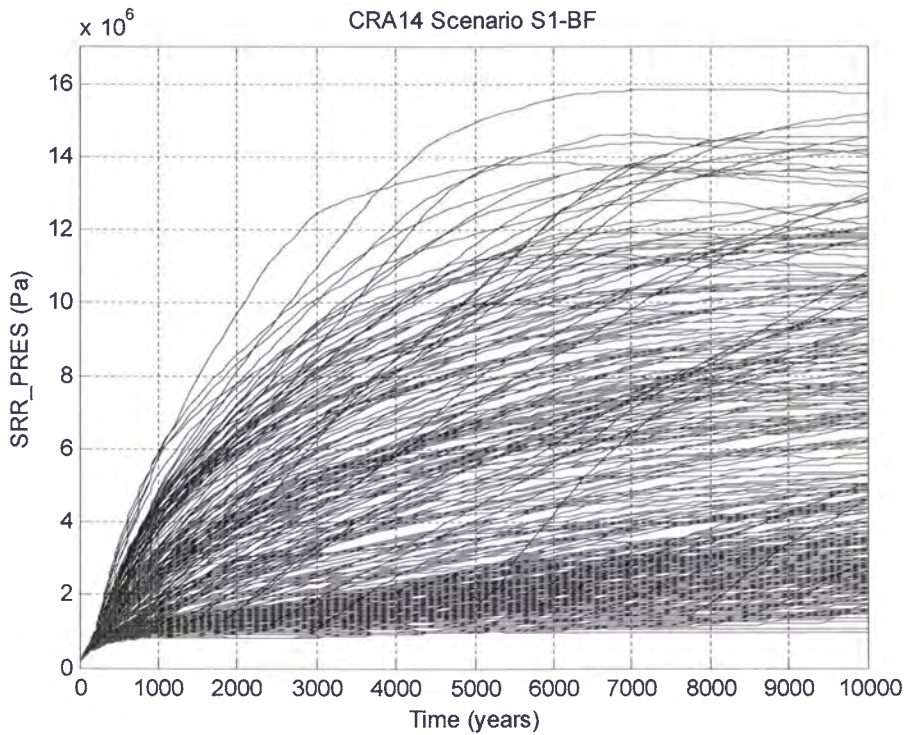


Figure 6-8: Horsetail Plot of SRoR Pressure for Case CRA14-0, Scenario S1-BF

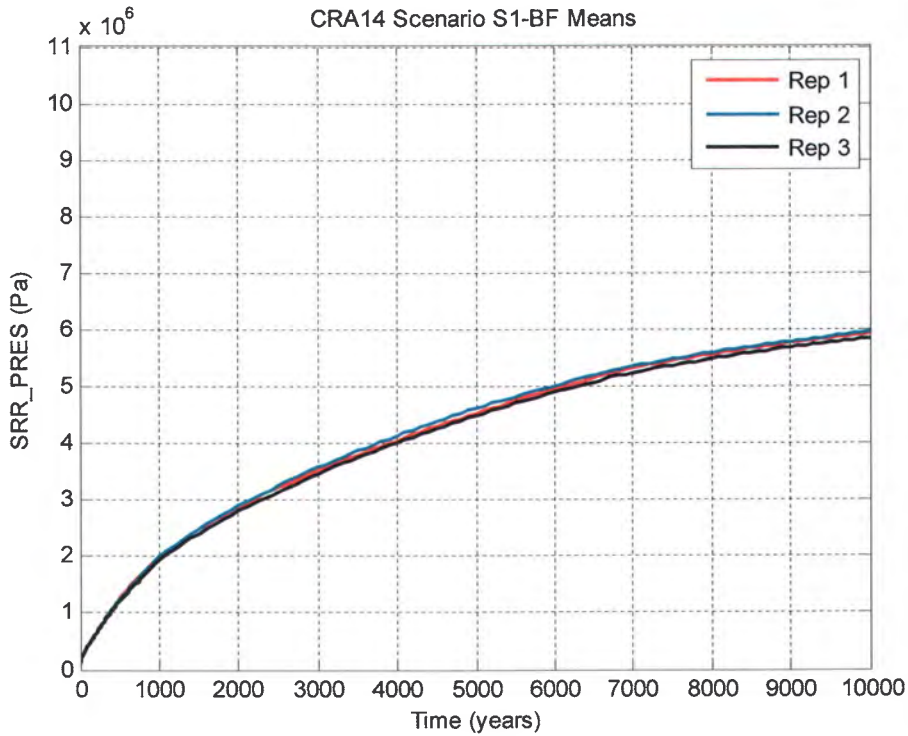


Figure 6-9: Replicate Means of SRoR Pressure for Case CRA14-0, Scenario S1-BF

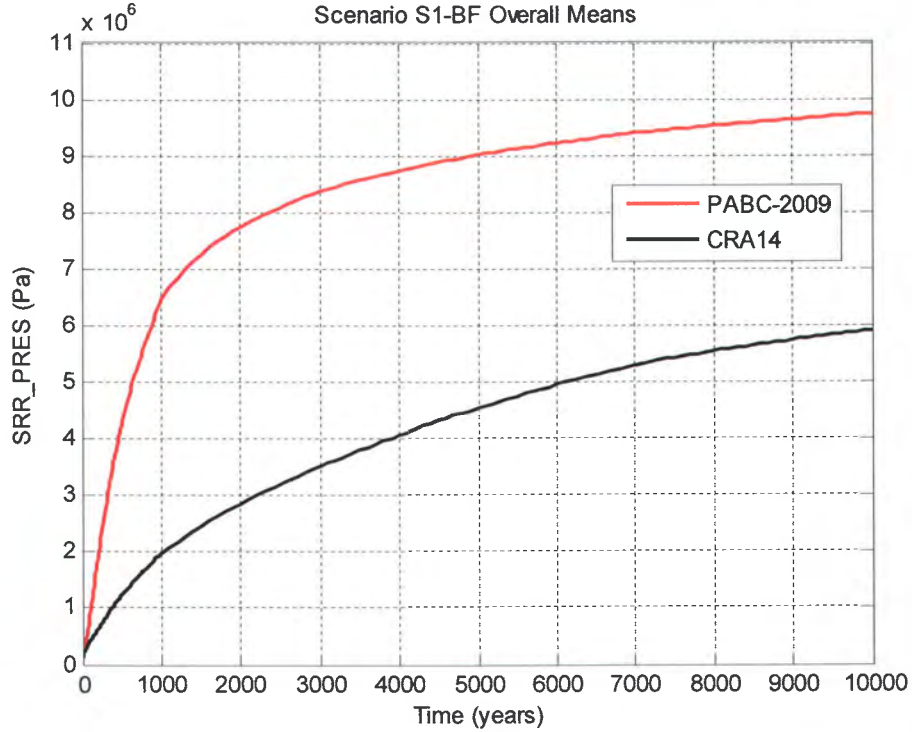


Figure 6-10: Overall Means of SRoR Pressure, Scenario S1-BF

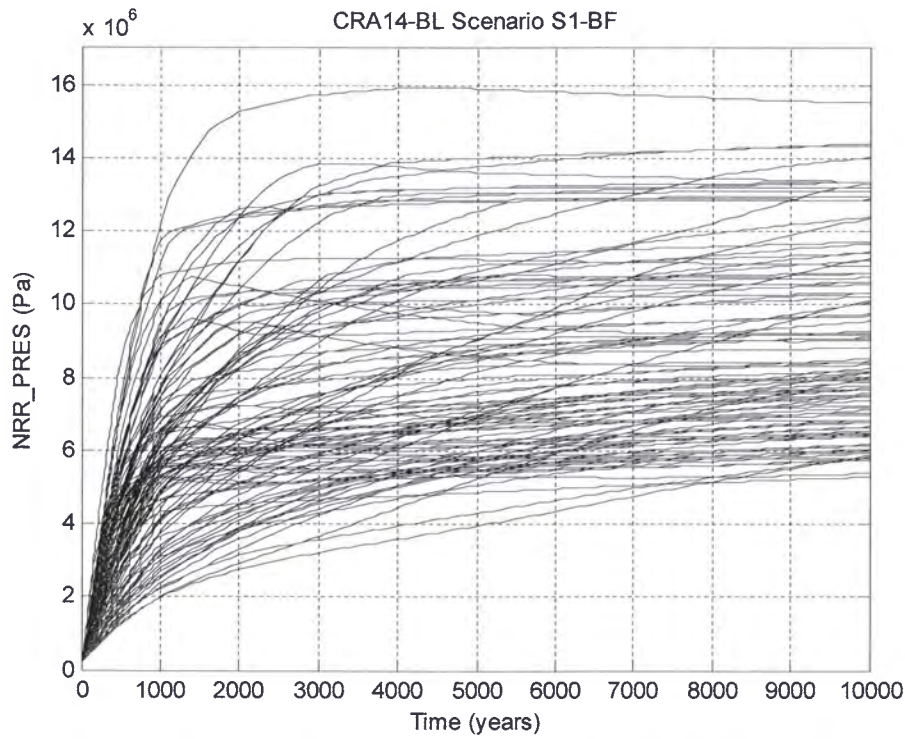


Figure 6-11: Horsetail Plot of NRR Pressure for Case CRA14-BL, Scenario S1-BF

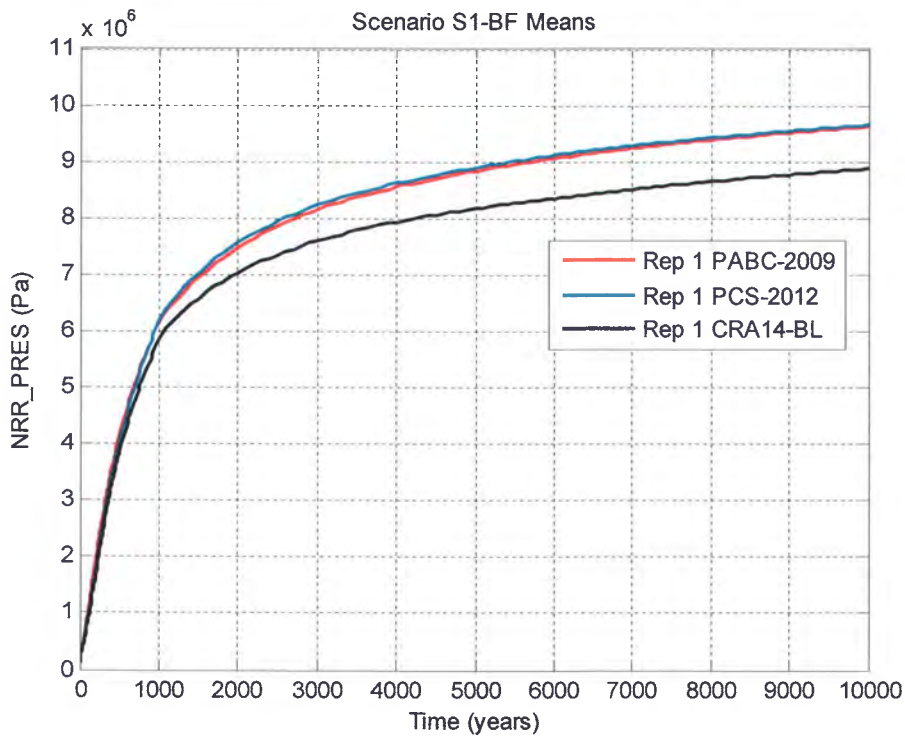


Figure 6-12: Replicate 1 Means of NRR Pressure, Scenario S1-BF

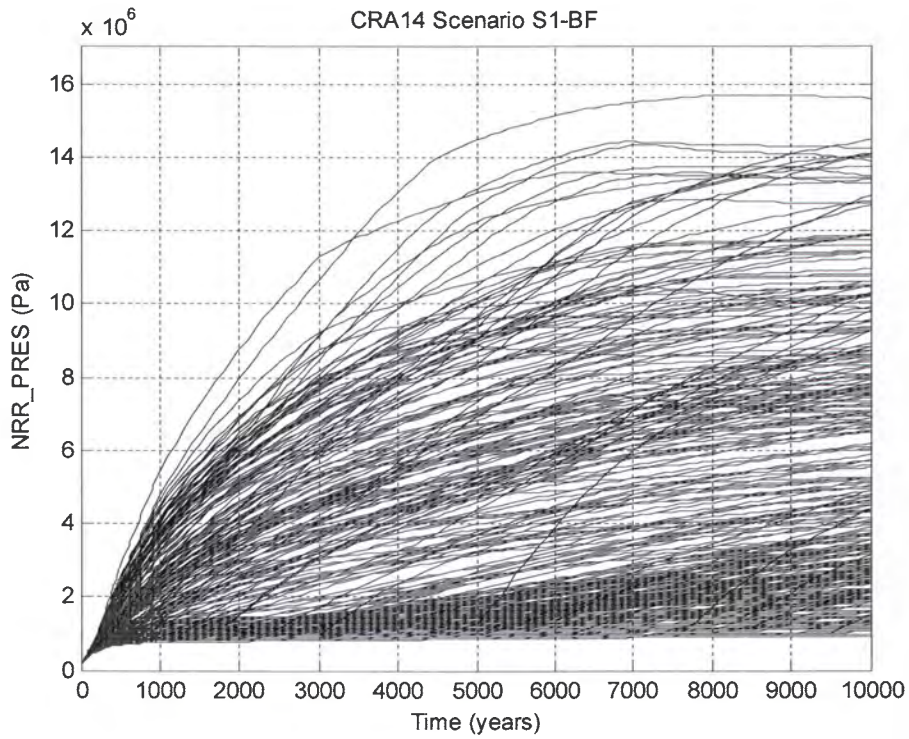


Figure 6-13: Horsetail Plot of NRoR Pressure for Case CRA14-0, Scenario S1-BF

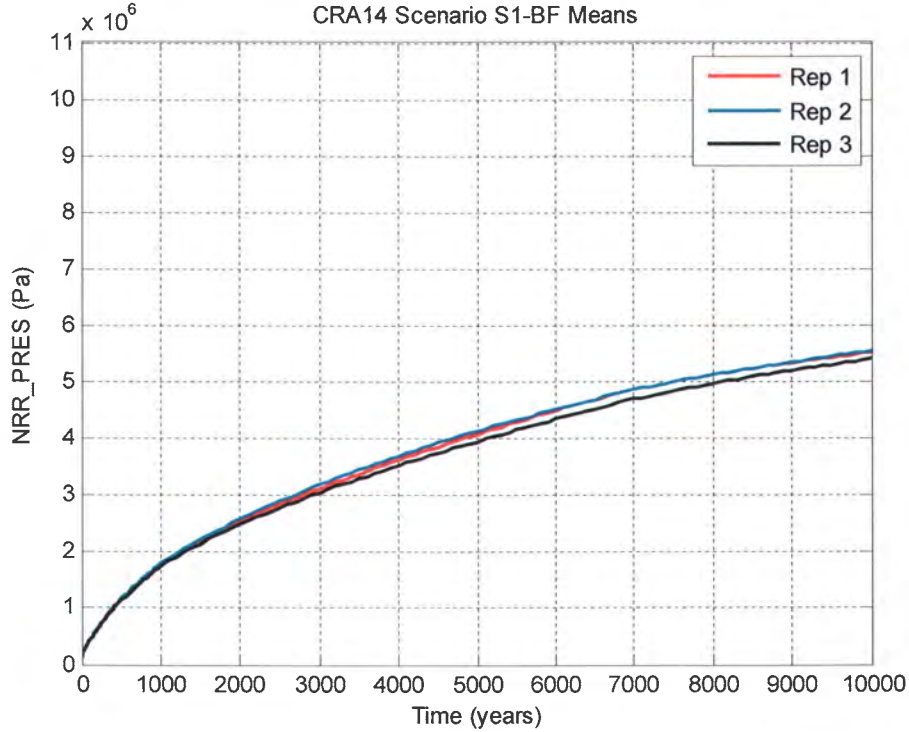


Figure 6-14: Replicate Means of NRoR Pressure for Case CRA14-0, Scenario S1-BF

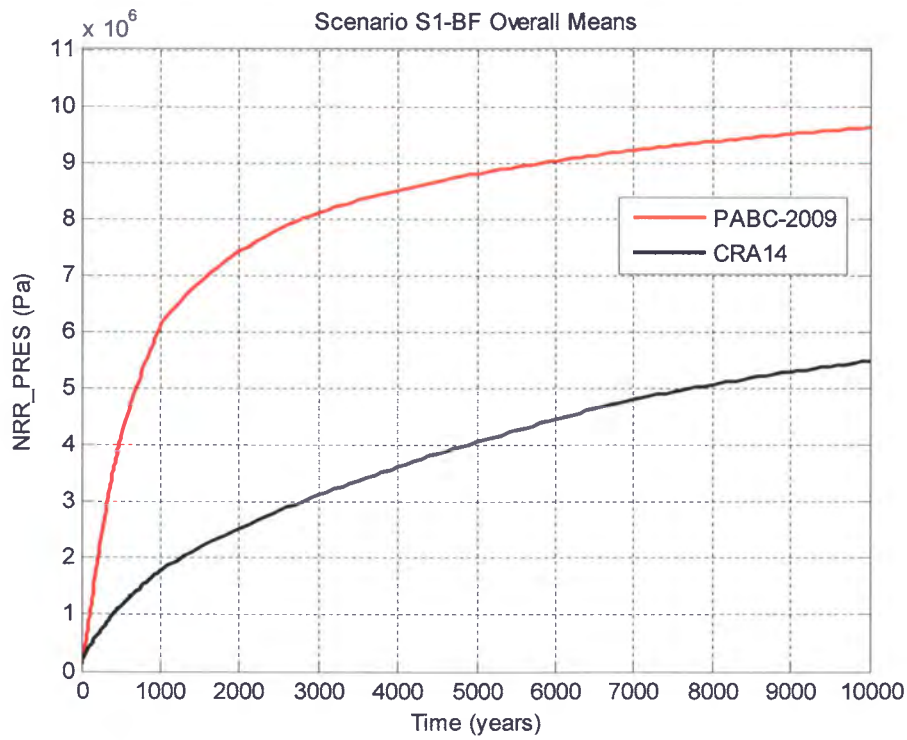


Figure 6-15: Overall Means of NRoR Pressure, Scenario S1-BF

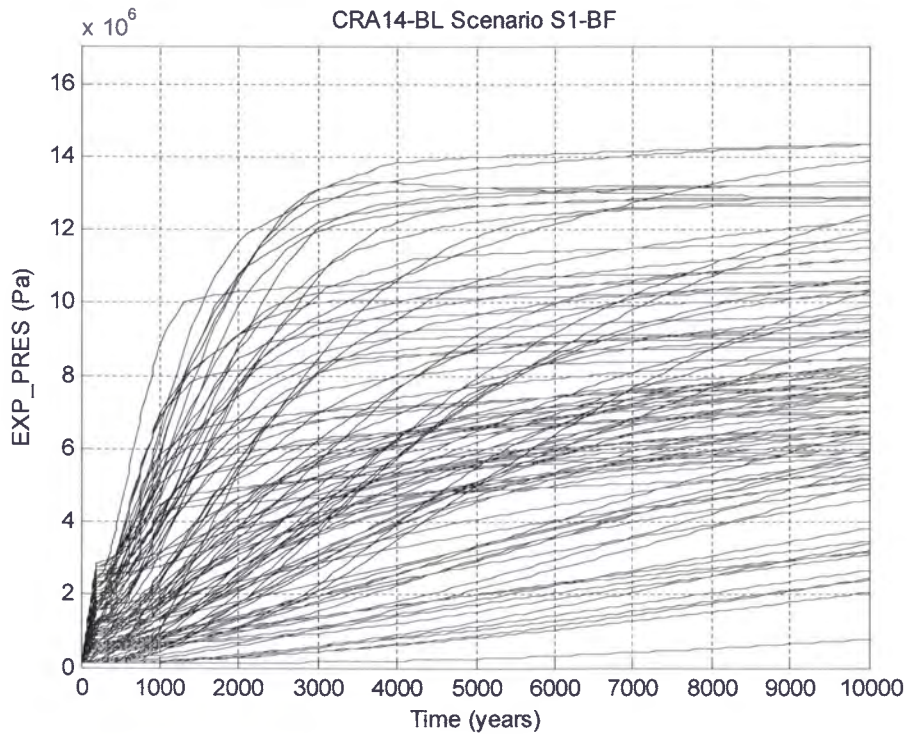


Figure 6-16: Horsetail Plot of Experimental Region Pressure for Case CRA14-BL, Scenario S1-BF

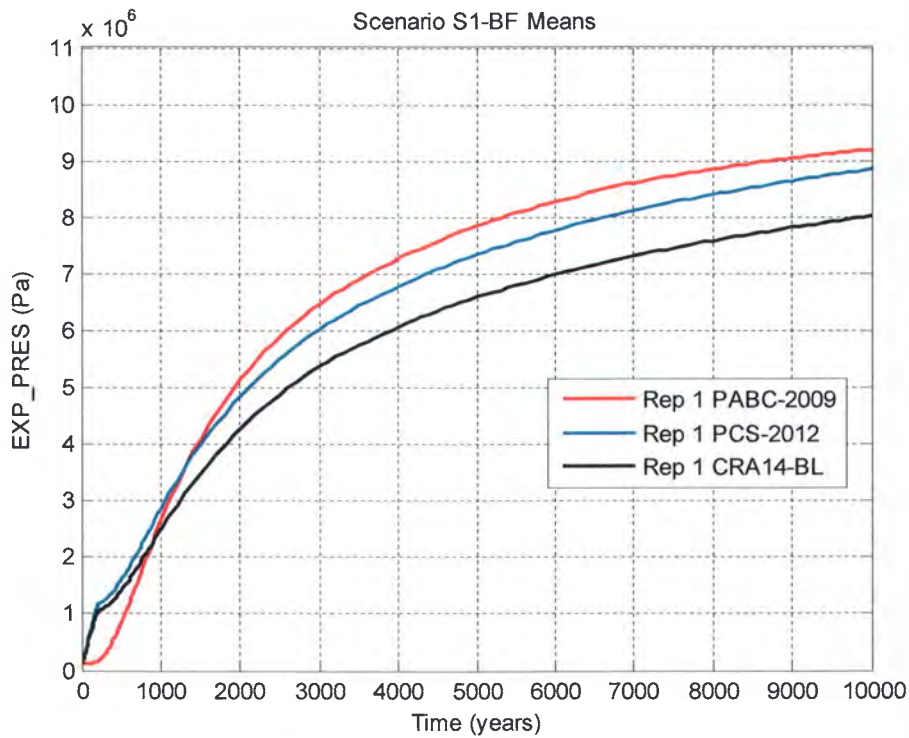


Figure 6-17: Replicate 1 Means of Experimental Region Pressure, Scenario S1-BF

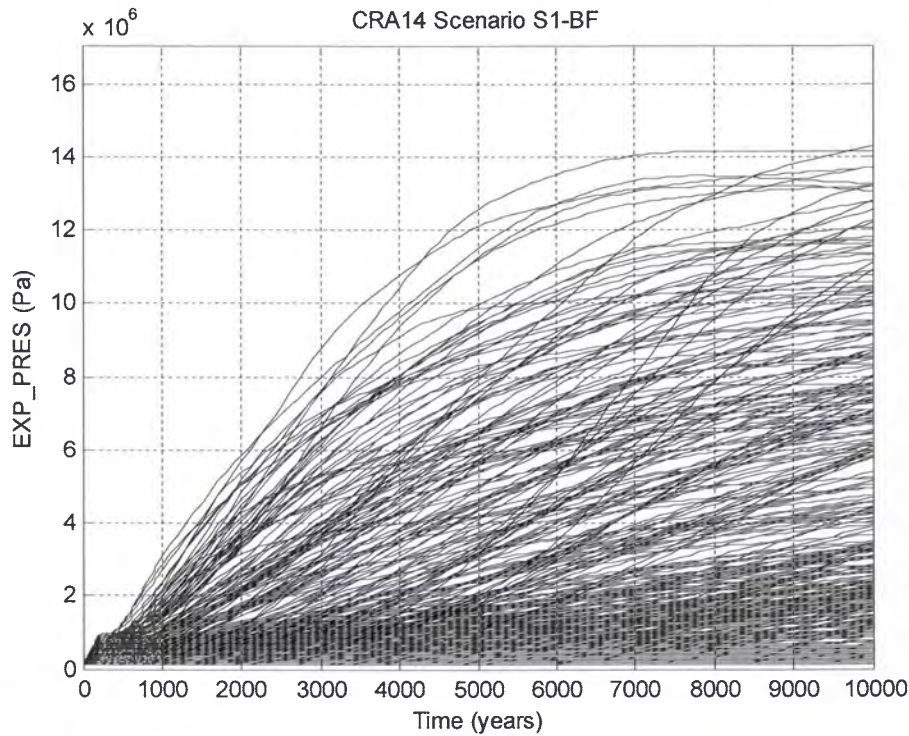


Figure 6-18: Horsetail Plot of Experimental Region Pressure for Case CRA14-0, Scenario S1-BF



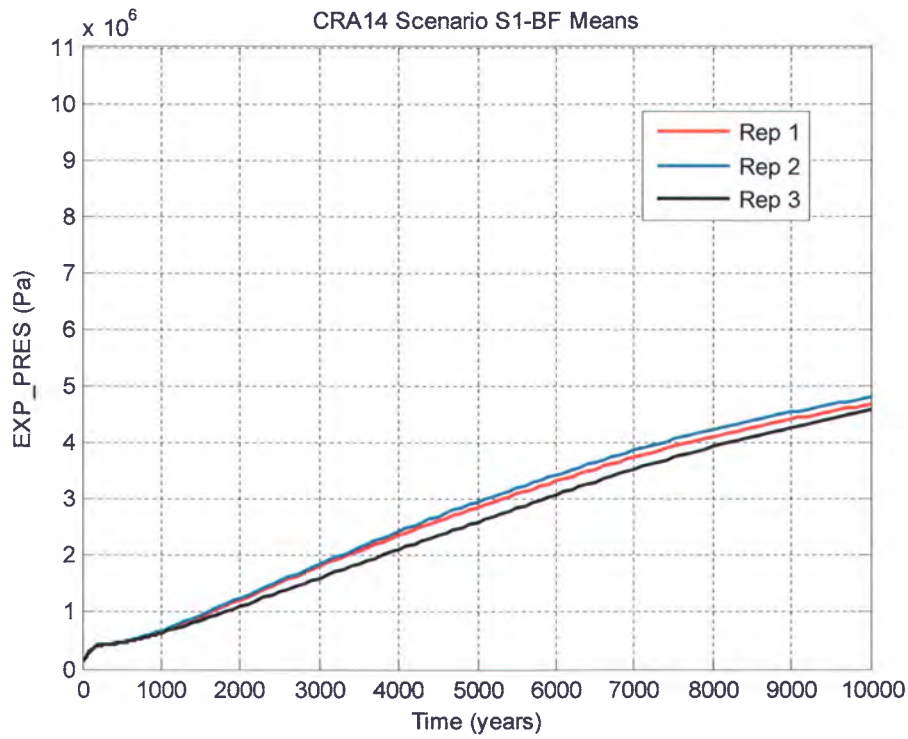


Figure 6-19: Replicate Means of Experimental Region Pressure, Case CRA14-0, Scenario S1-BF

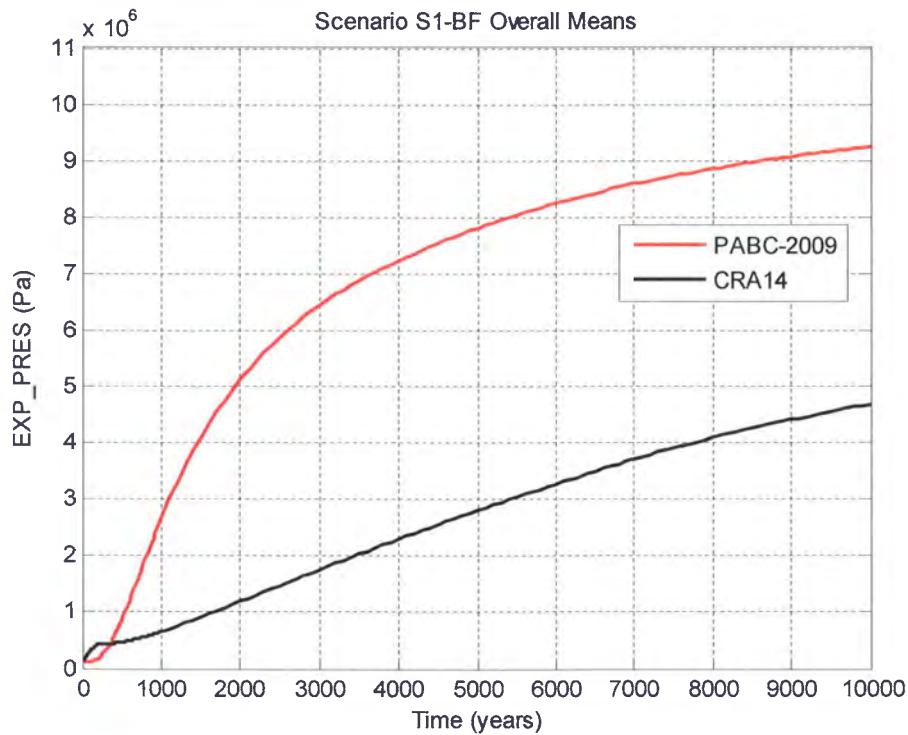


Figure 6-20: Overall Means of Experimental Region Pressure, Scenario S1-BF

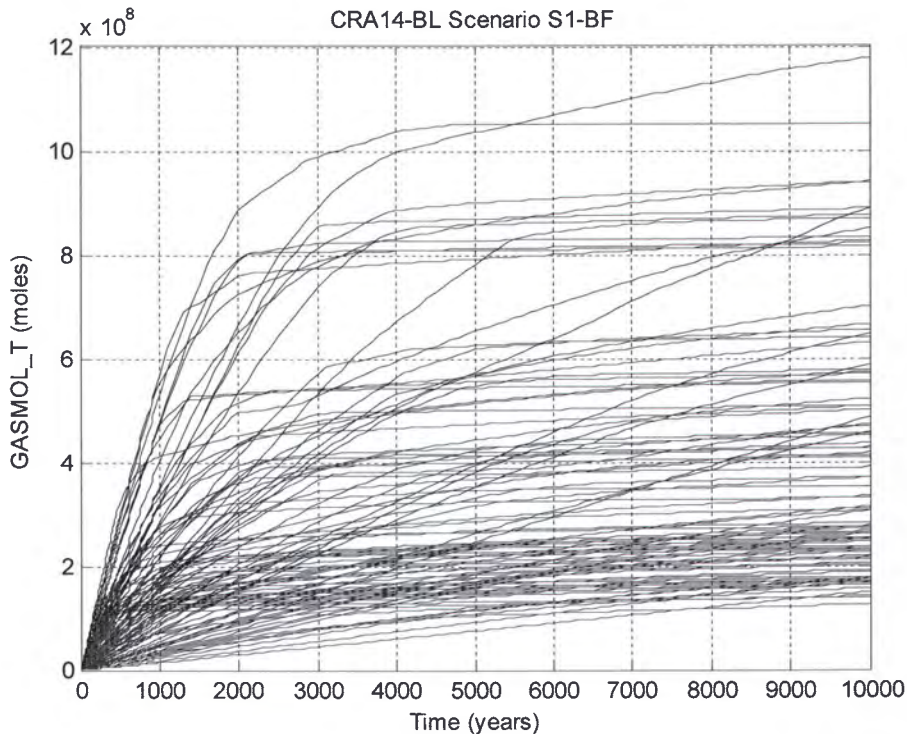


Figure 6-21: Horsetail Plot of Molar Gas Generation for Case CRA14-BL, Scenario S1-BF

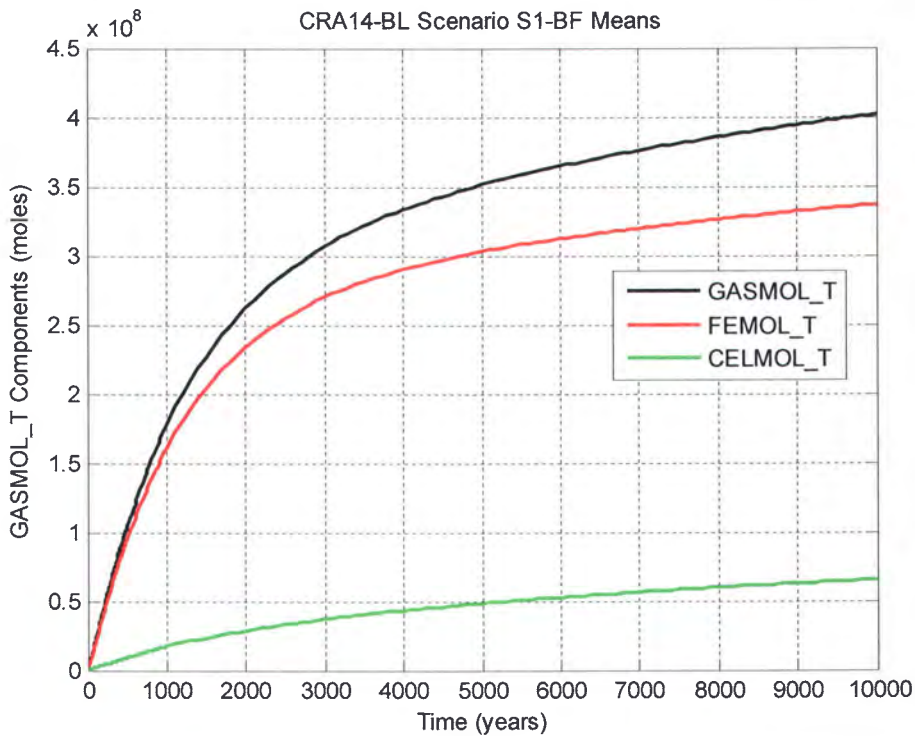


Figure 6-22: Replicate 1 Means of Molar Gas Generation for Case CRA14-BL, Scenario S1-BF

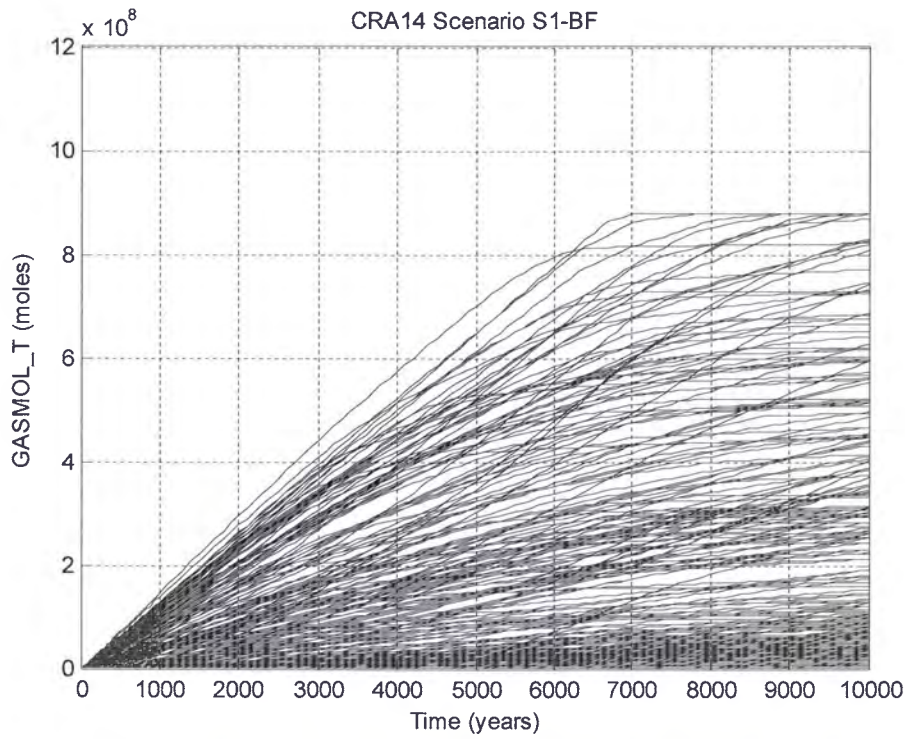


Figure 6-23: Horsetail Plot of Molar Gas Generation for Case CRA14-0, Scenario S1-BF

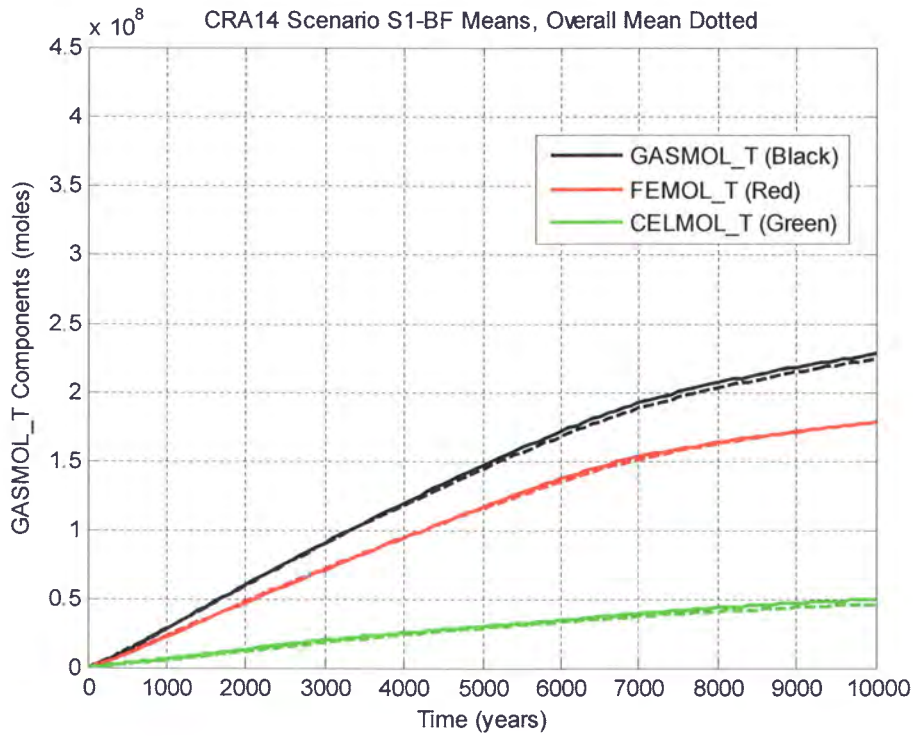


Figure 6-24: Means of Molar Gas Generation for Case CRA14-0, Scenario S1-BF (Replicate 1 Means – Solid, Overall Means – Dotted)

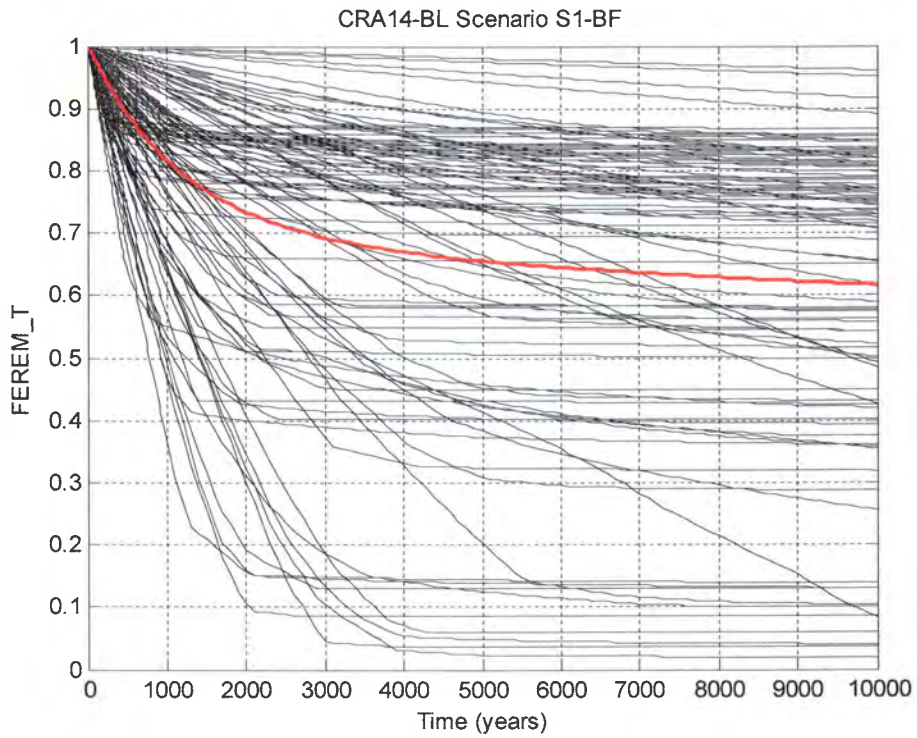


Figure 6-25: Fraction of Iron Remaining, Case CRA14-BL, Scenario S1-BF (Mean in Red)

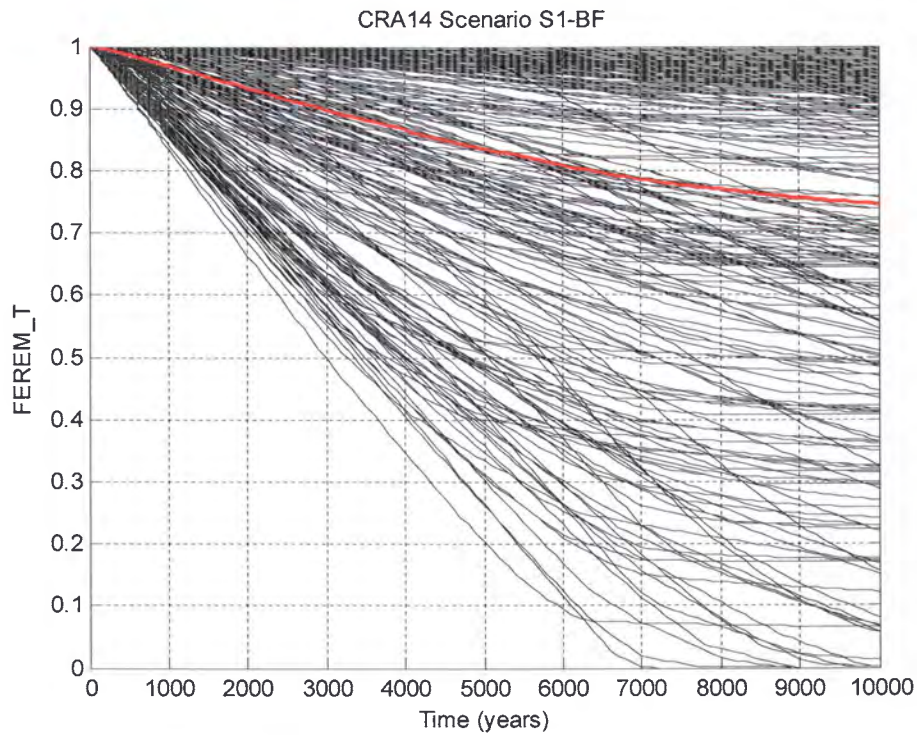


Figure 6-26: Fraction of Iron Remaining, Case CRA14-0, Scenario S1-BF (Mean in Red)

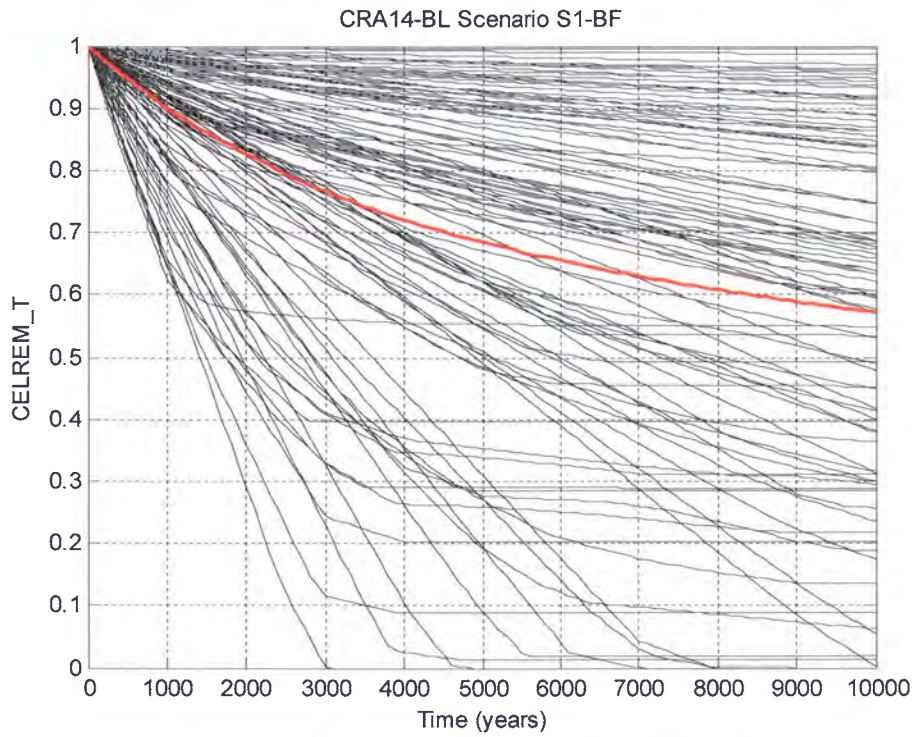


Figure 6-27: Fraction of Cellulose Remaining, Case CRA14-BL, Scenario S1-BF (Mean in Red)

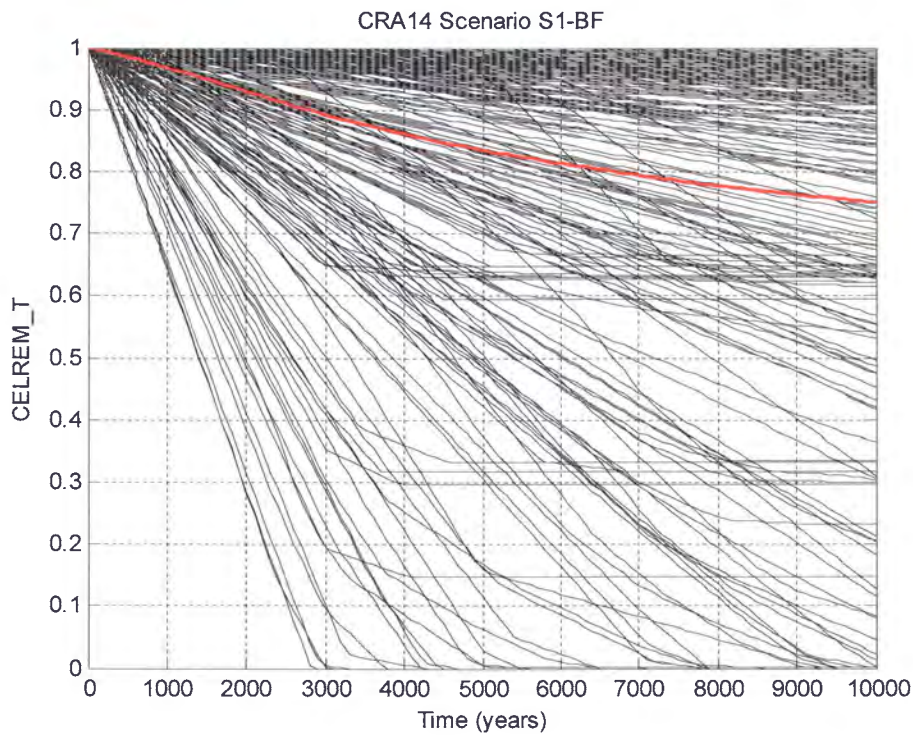


Figure 6-28: Fraction of Cellulose Remaining, Case CRA14-0, Scenario S1-BF (Mean in Red)

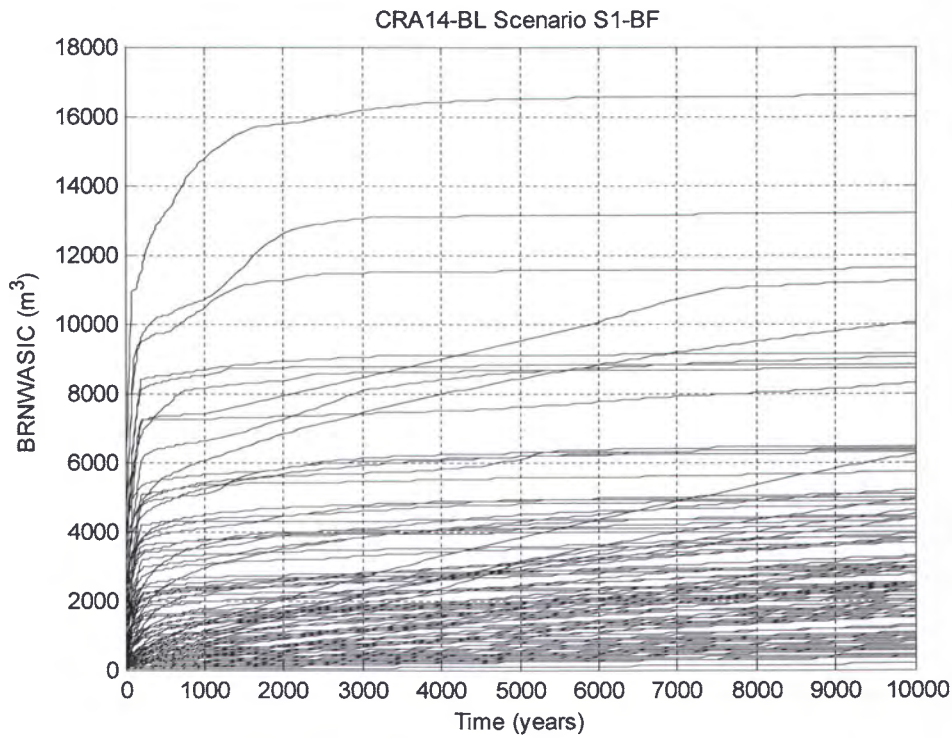


Figure 6-29: Horsetail Plot of Cumulative Brine Inflow to the Waste Panel, Case CRA14-BL, Scenario S1-BF.

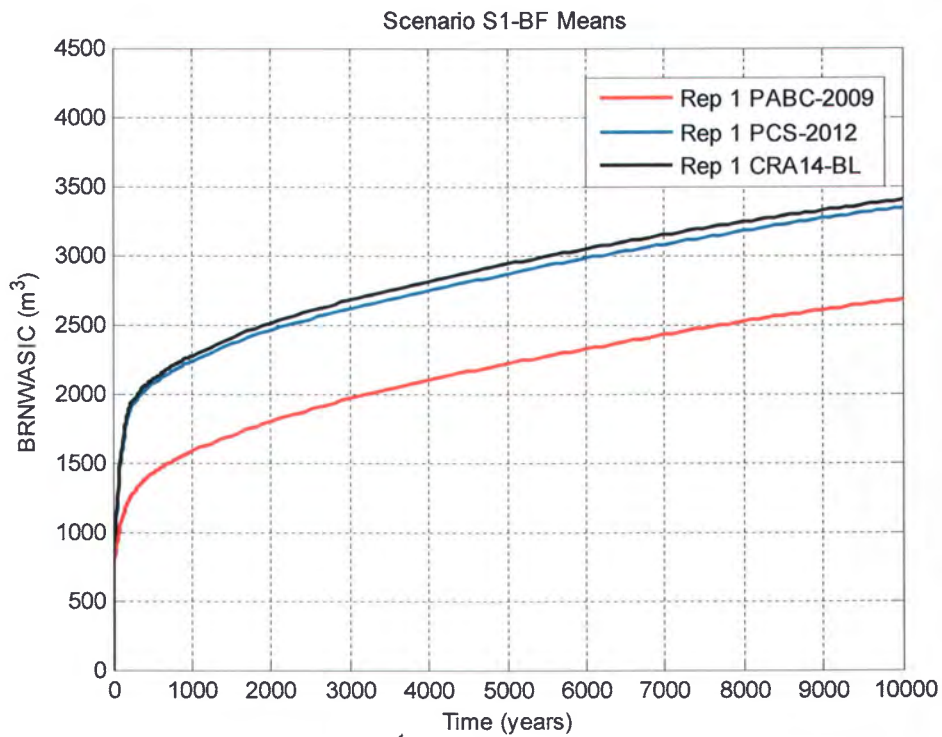


Figure 6-30: Replicate 1 Means of Cumulative Brine Inflow to the Waste Panel, Scenario S1-BF.

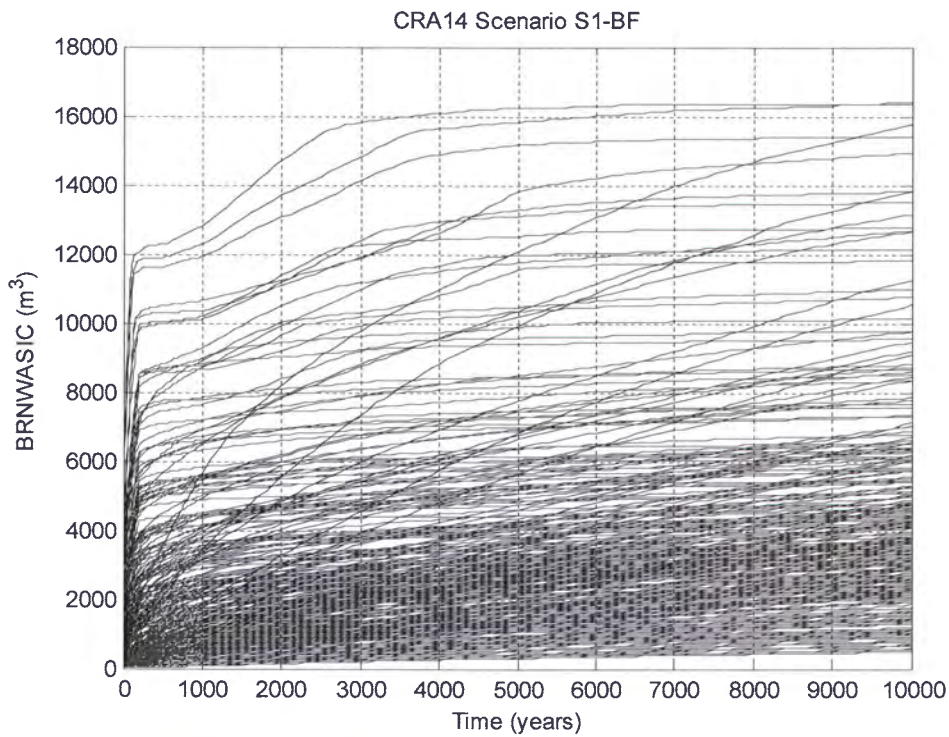


Figure 6-31: Horsetail Plot of Cumulative Brine Inflow to the Waste Panel, Case CRA14-0, Scenario S1-BF.

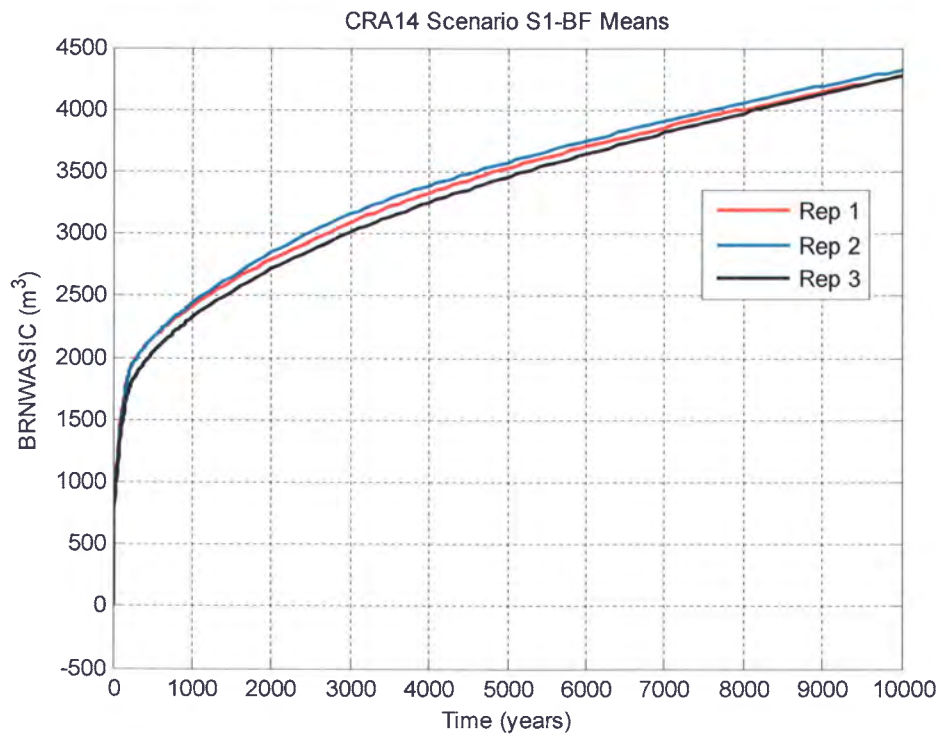


Figure 6-32: Replicate Means of Cumulative Brine Inflow to the Waste Panel, Case CRA14-0, Scenario S1-BF.

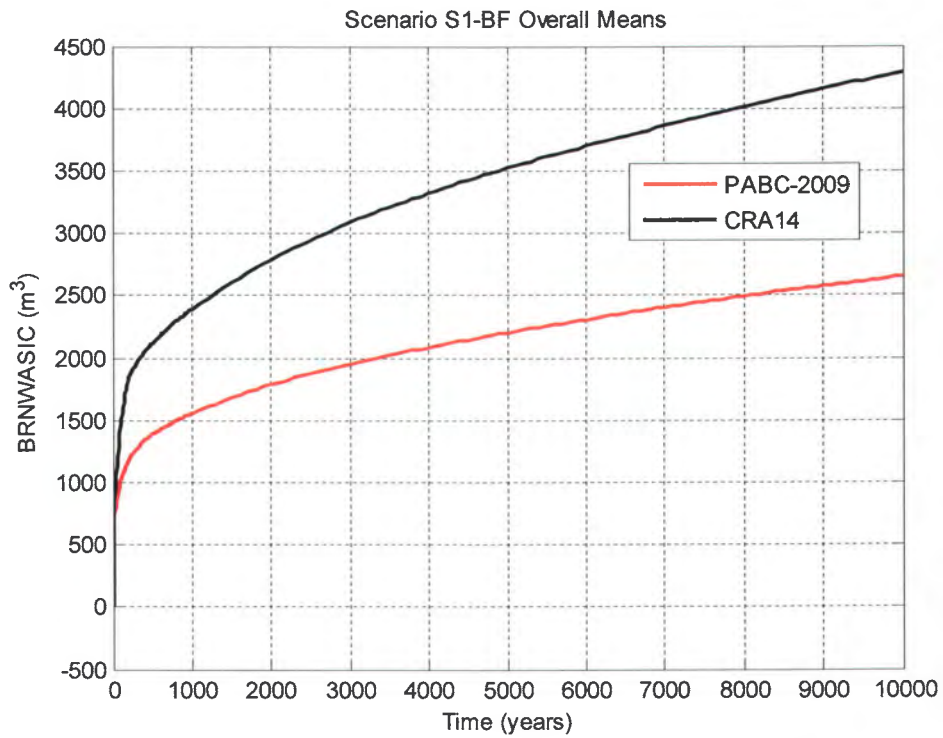


Figure 6-33: Overall Means of Cumulative Brine Inflow to the Waste Panel, Scenario S1-BF.

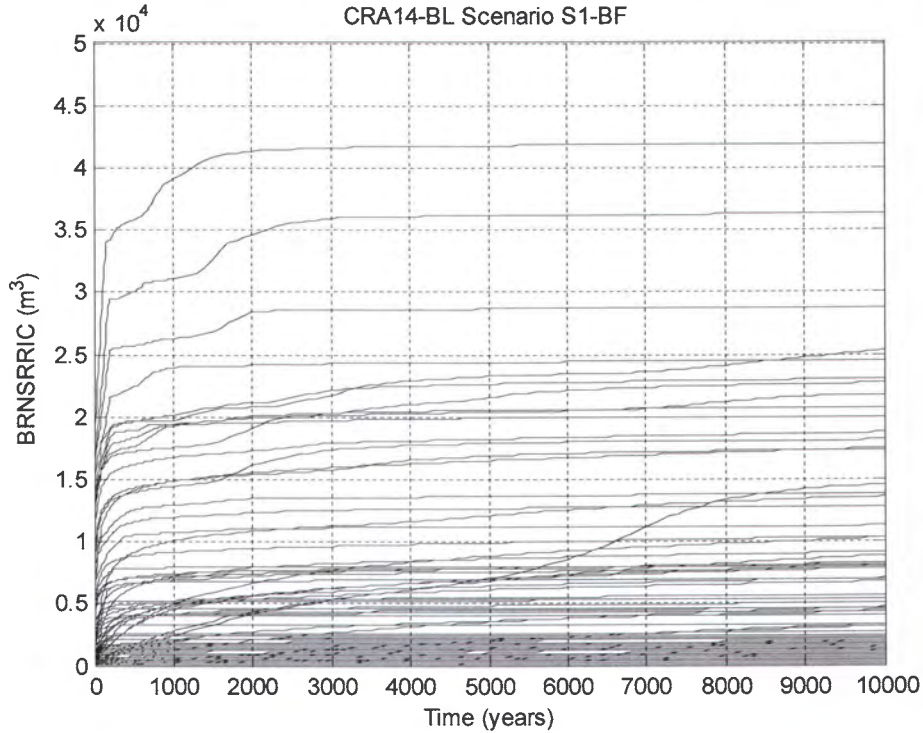


Figure 6-34: Horsetail Plot of Cumulative Brine Inflow to the SRoR, Case CRA14-BL, Scenario S1-BF.



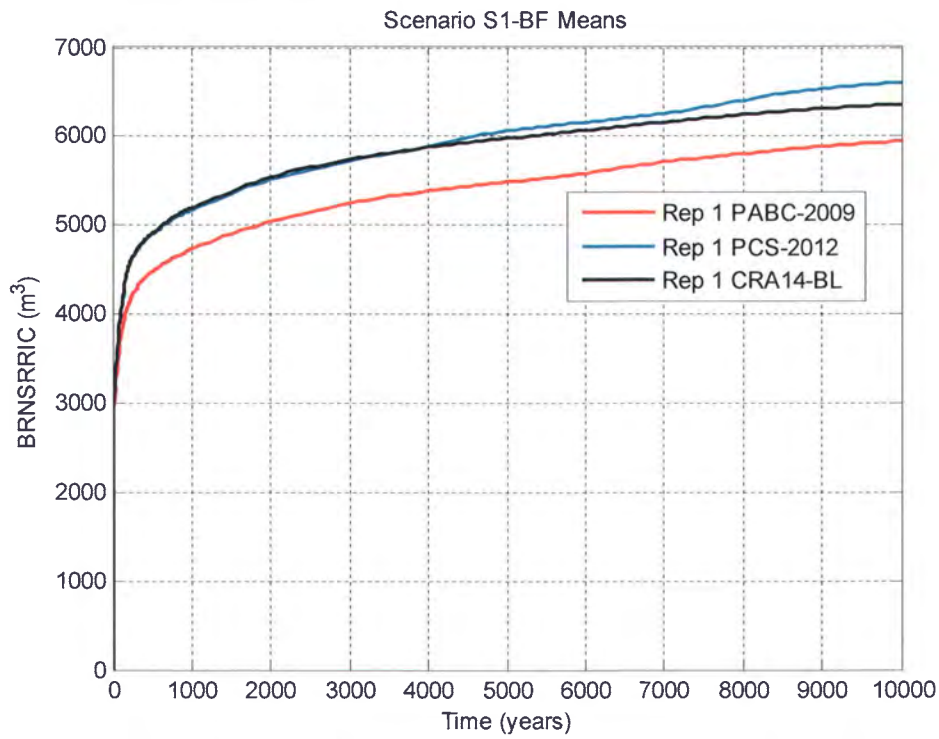


Figure 6-35: Replicate 1 Means of Cumulative Brine Inflow to the SRoR, Scenario S1-BF.

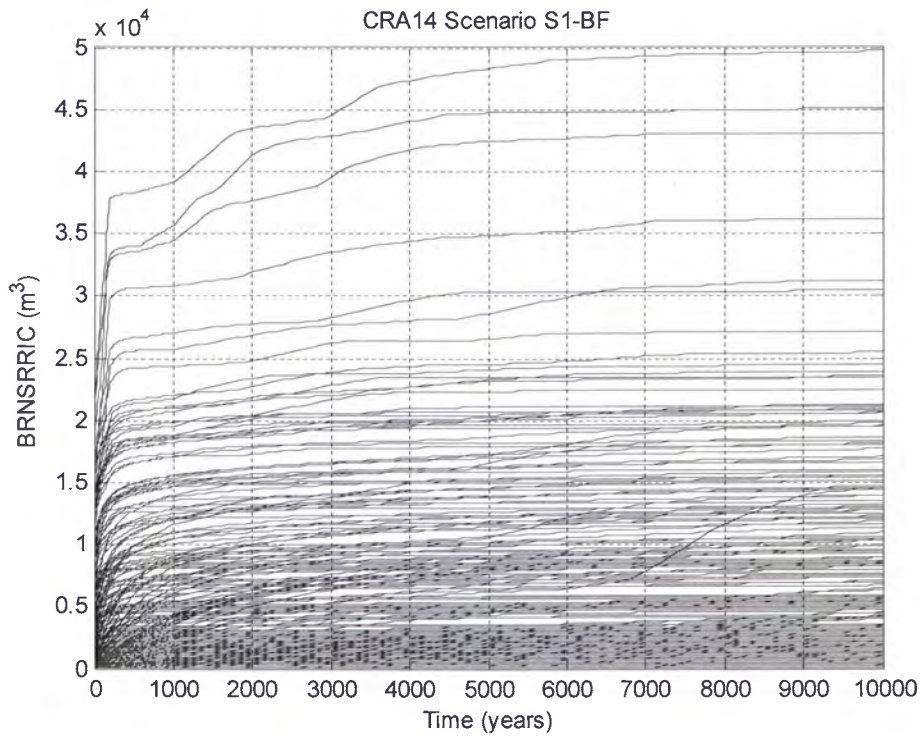


Figure 6-36: Horsetail Plot of Cumulative Brine Inflow to the SRoR, Case CRA14-0, Scenario S1-BF.

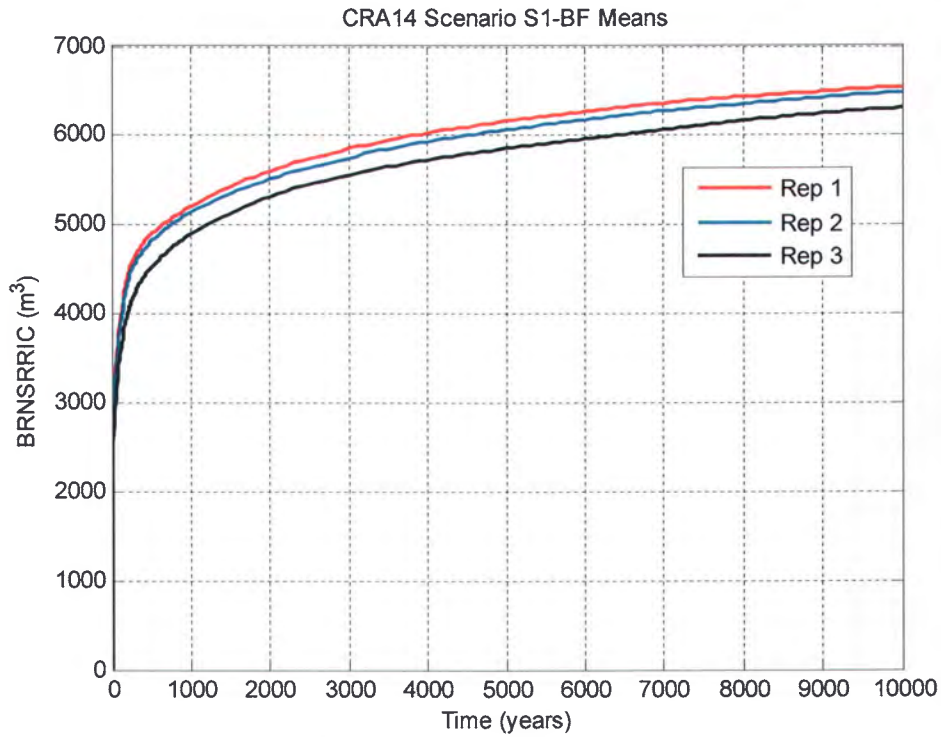


Figure 6-37: Replicate Means of Cumulative Brine Inflow to the SRoR, Case CRA14-0, Scenario S1-BF.

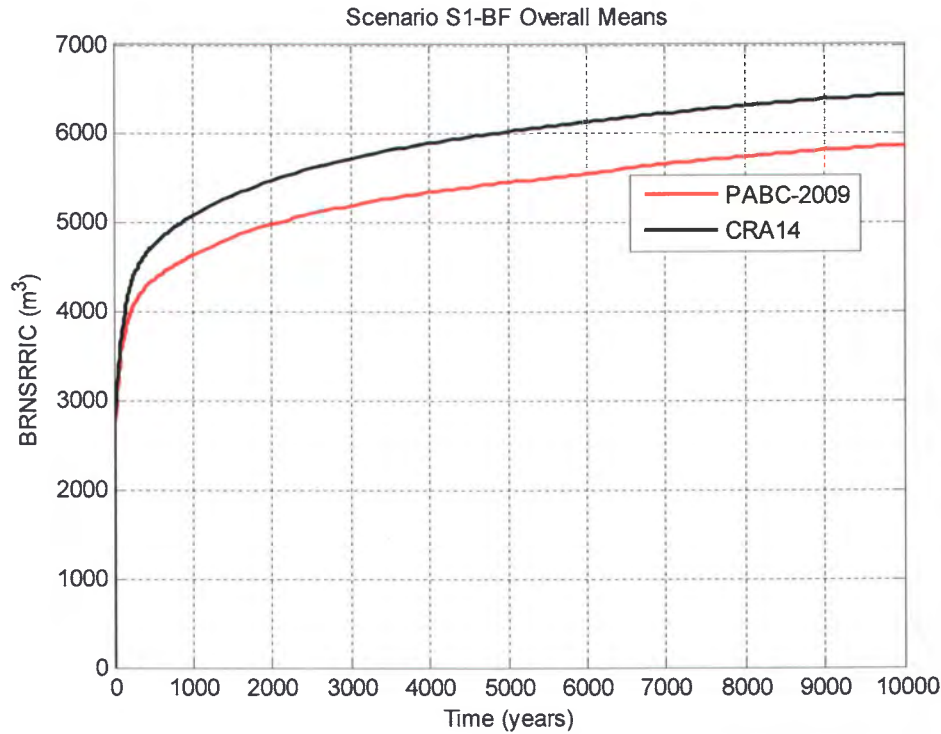


Figure 6-38: Overall Means of Cumulative Brine Inflow to the SRoR, Scenario S1-BF.

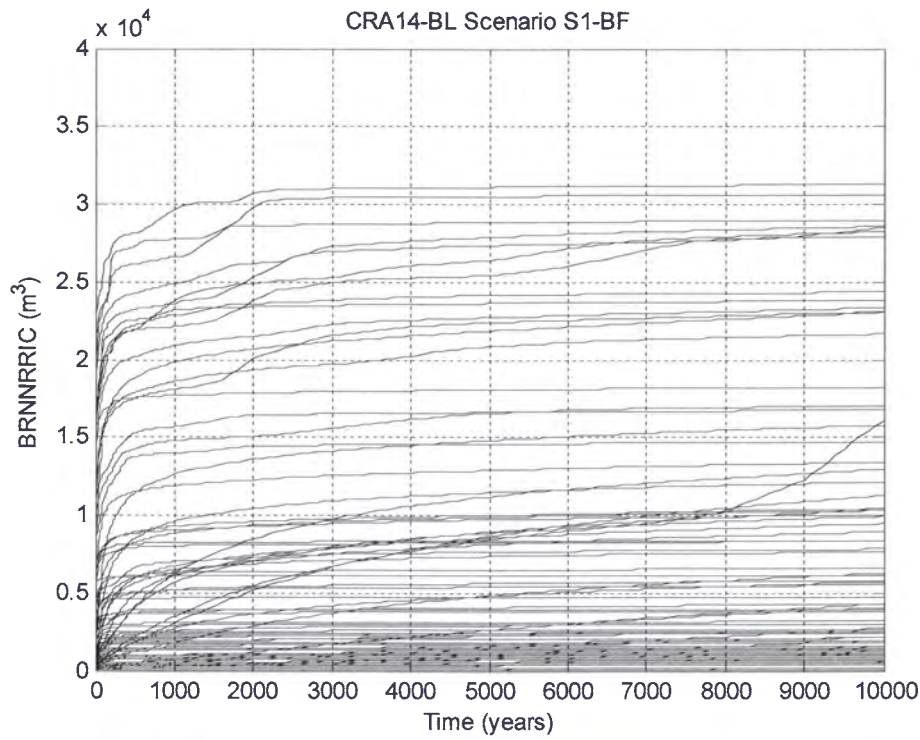


Figure 6-39: Horsetail Plot of Cumulative Brine Inflow to the NRoR, Case CRA14-BL, Scenario S1-BF.

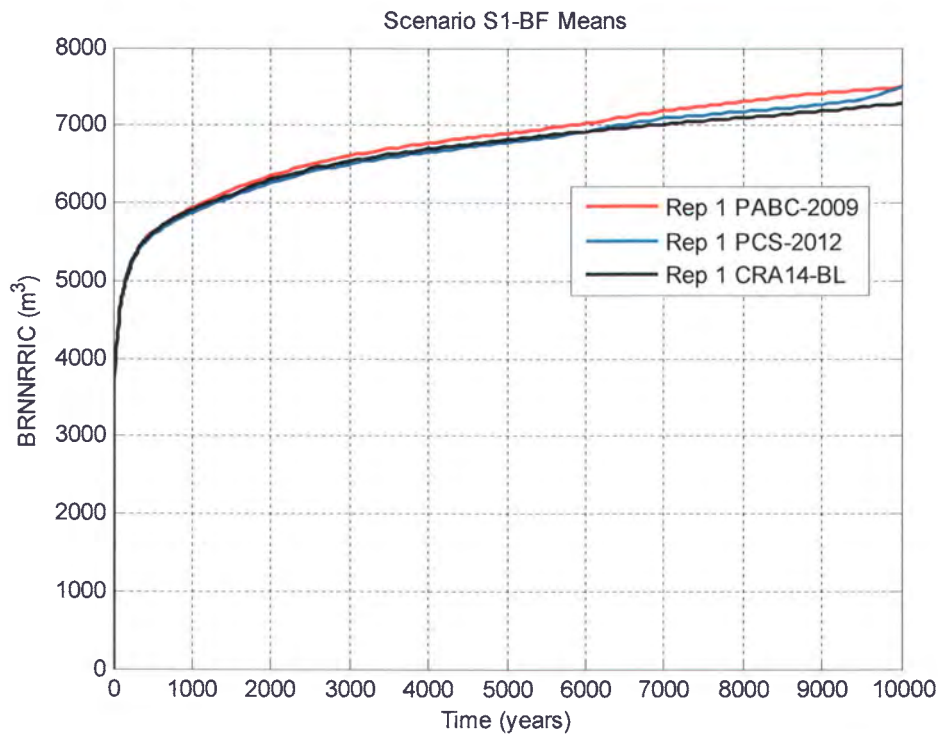


Figure 6-40: Replicate 1 Means of Cumulative Brine Inflow to the NRoR, Scenario S1-BF.

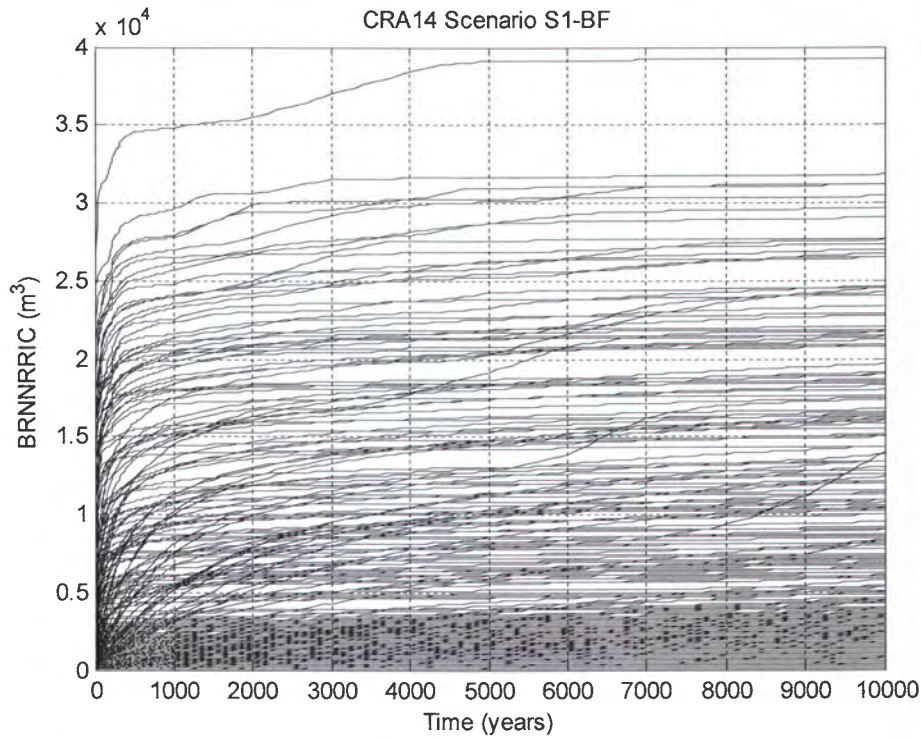


Figure 6-41: Horsetail Plot of Cumulative Brine Inflow to the NRoR, Case CRA14-0, Scenario S1-BF.

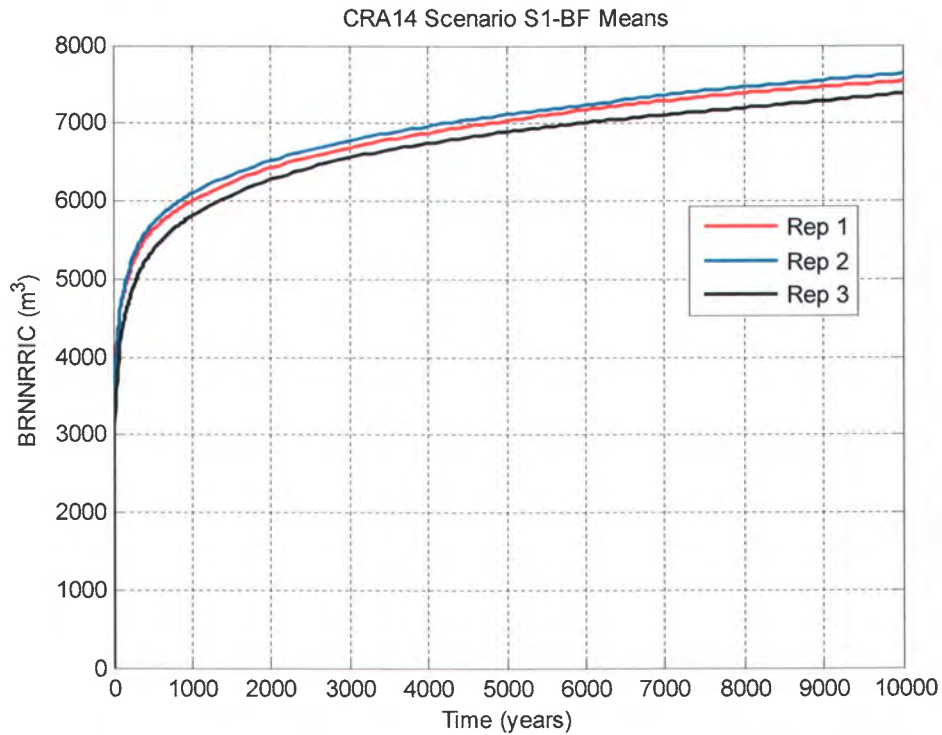


Figure 6-42: Replicate Means of Cumulative Brine Inflow to the NRoR, Case CRA14-0, Scenario S1-BF.

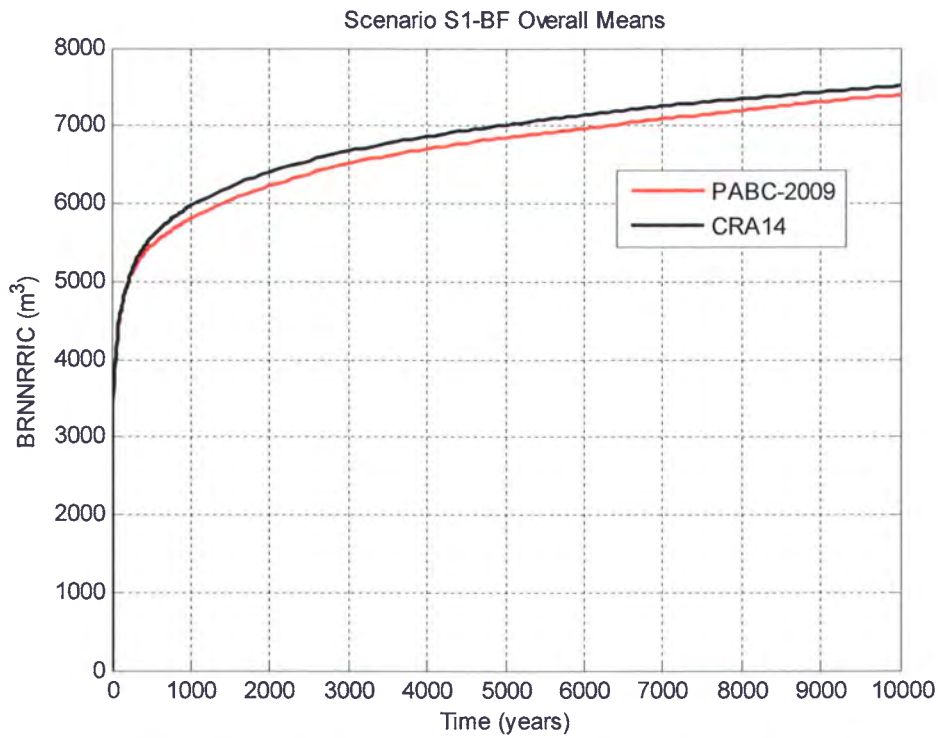


Figure 6-43: Overall Means of Cumulative Brine Inflow to the NRoR, Scenario S1-BF.

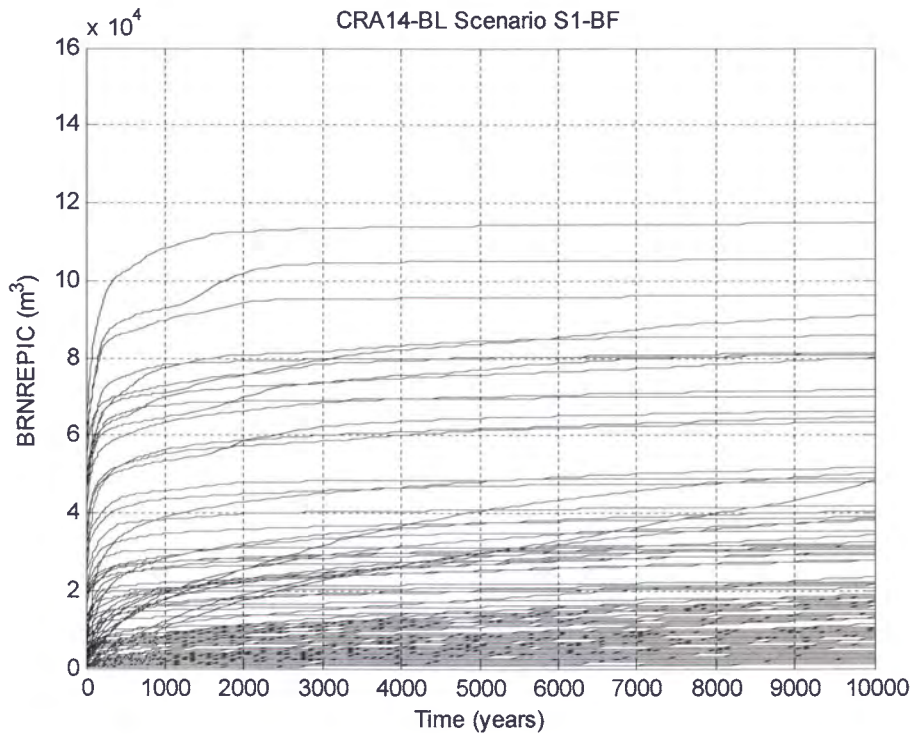


Figure 6-44: Horsetail Plot of Cumulative Brine Inflow to the Repository, Case CRA14-BL, Scenario S1-BF.

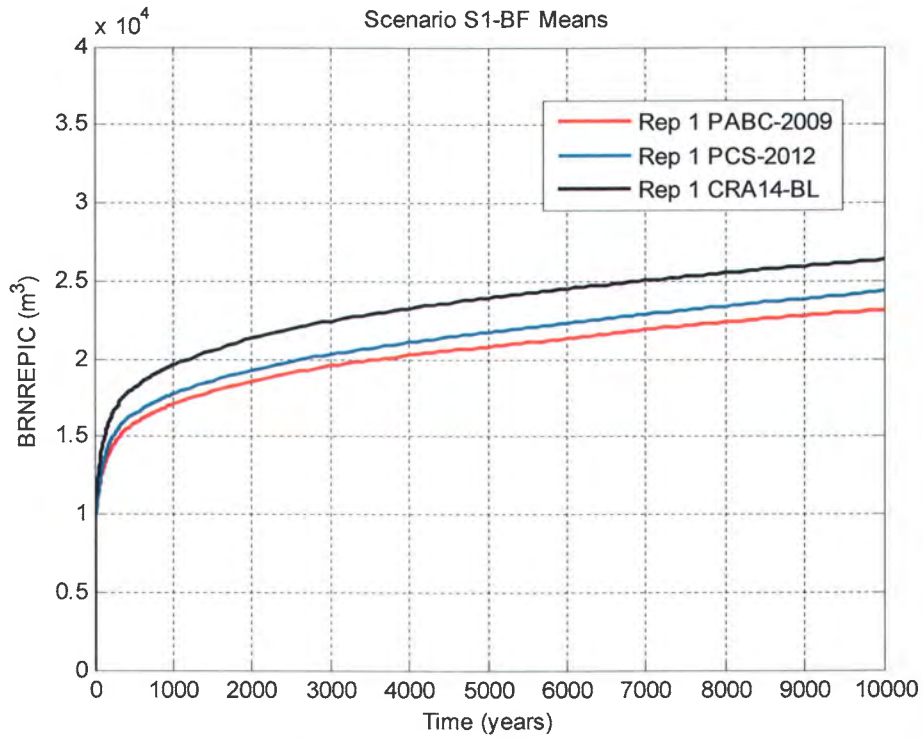


Figure 6-45: Replicate 1 Means of Cumulative Brine Inflow to the Repository, Scenario S1-BF.

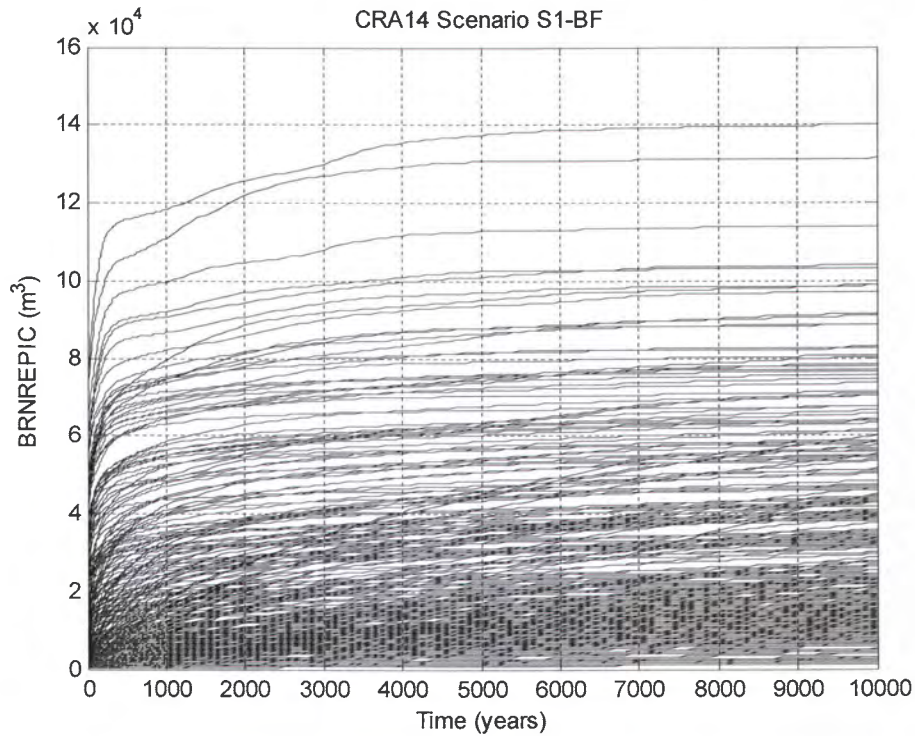


Figure 6-46: Horsetail Plot of Cumulative Brine Inflow to the Repository, Case CRA14-0, Scenario S1-BF.

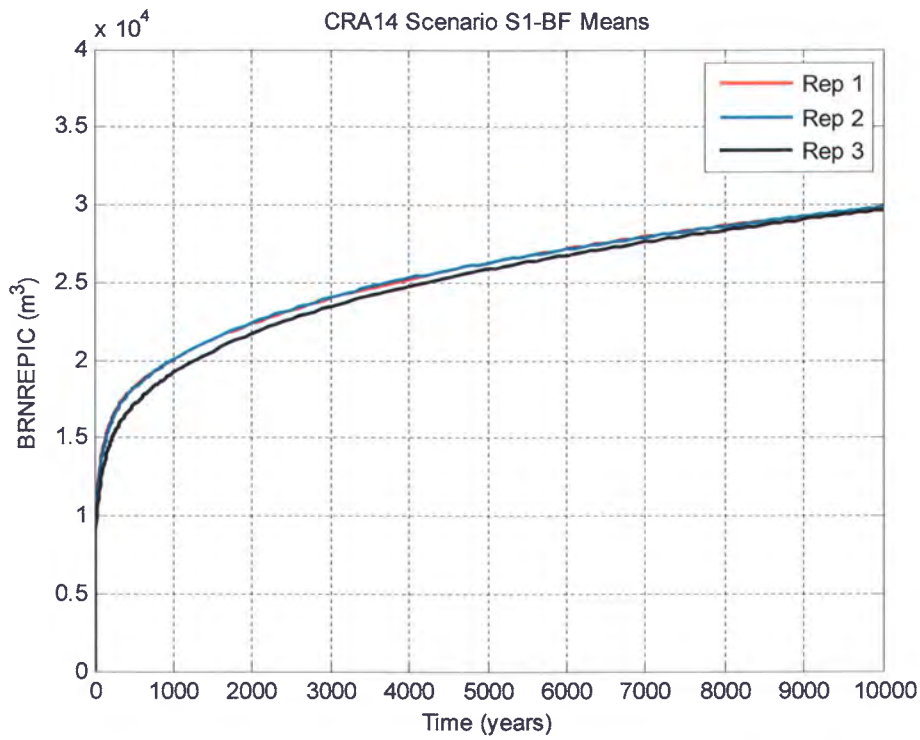


Figure 6-47: Replicate Means of Cumulative Brine Inflow to the Repository, Case CRA14-0, Scenario S1-BF.

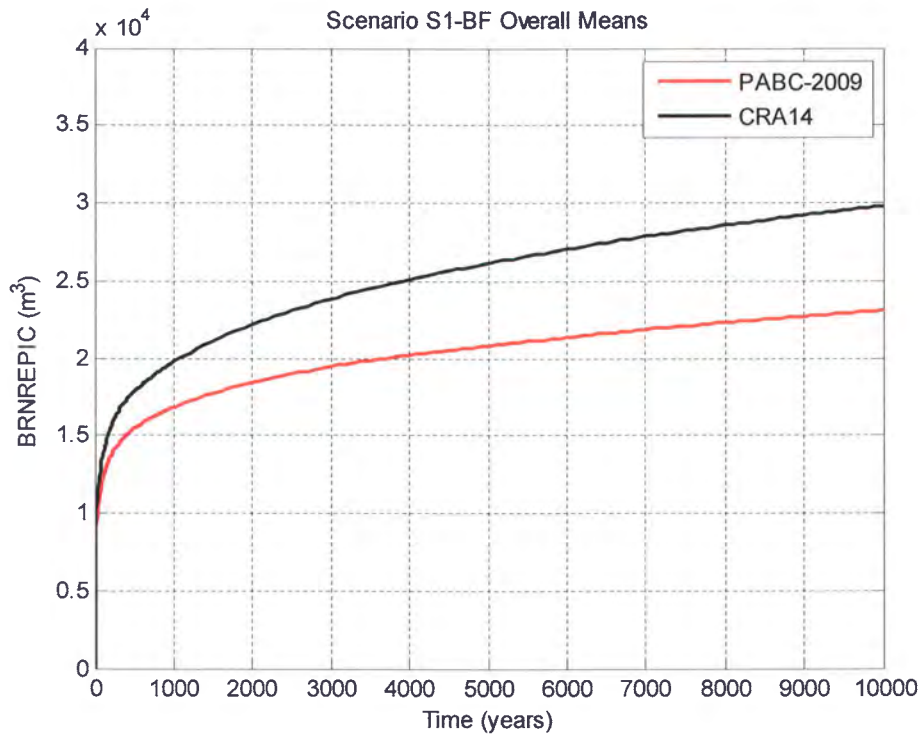


Figure 6-48: Overall Means of Cumulative Brine Inflow to the Repository, Scenario S1-BF.

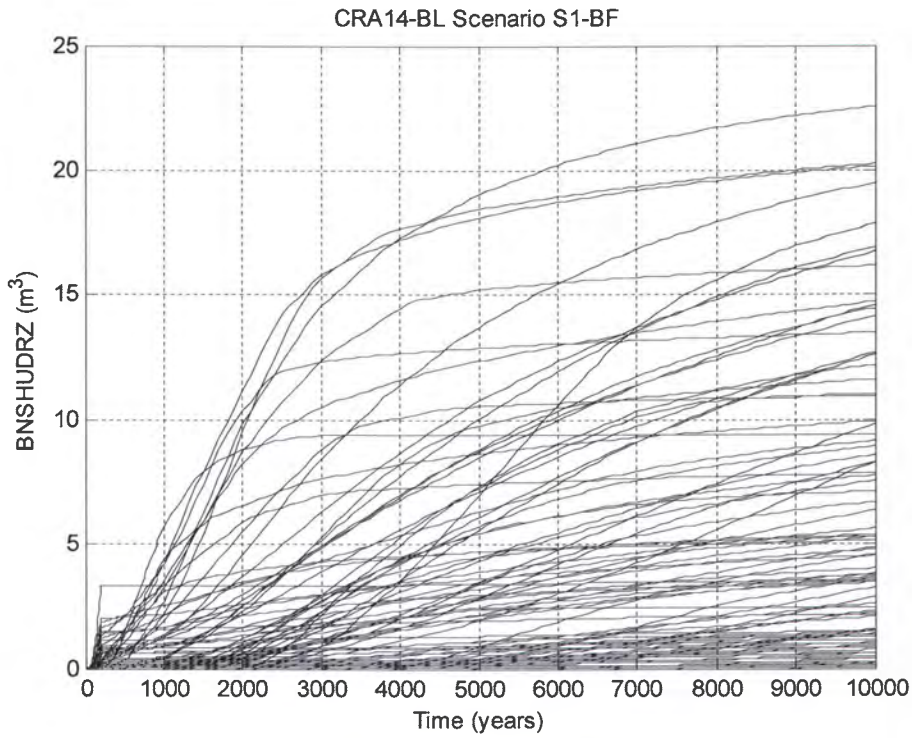


Figure 6-49: Horsetail Plot of Brine Flow up the Shaft, Case CRA14-BL, Scenario S1-BF.

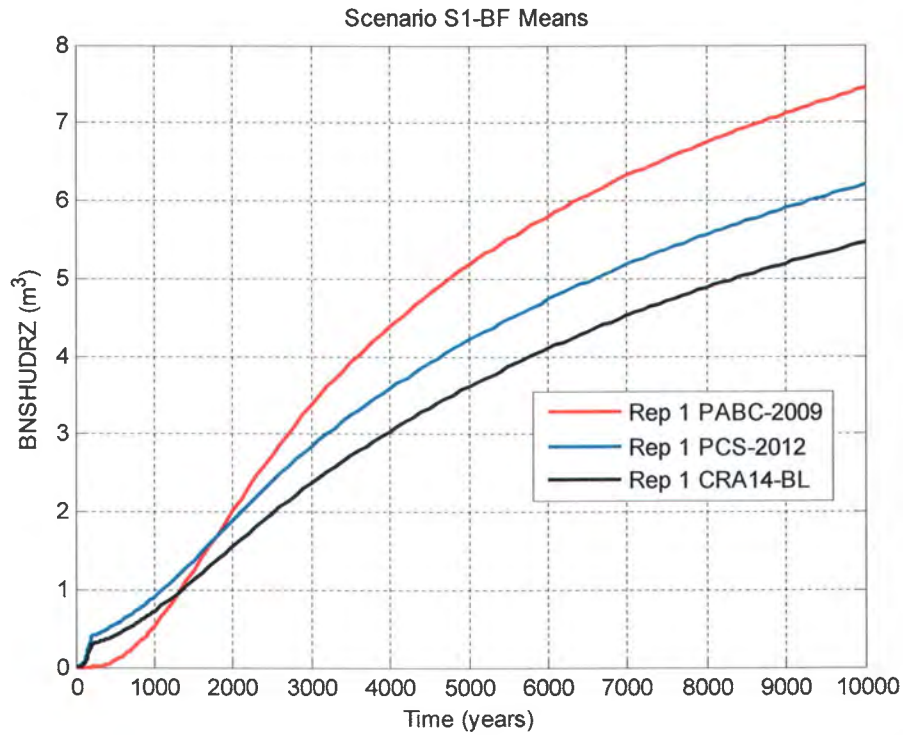


Figure 6-50: Replicate 1 Means of Brine Flow up the Shaft, Scenario S1-BF.



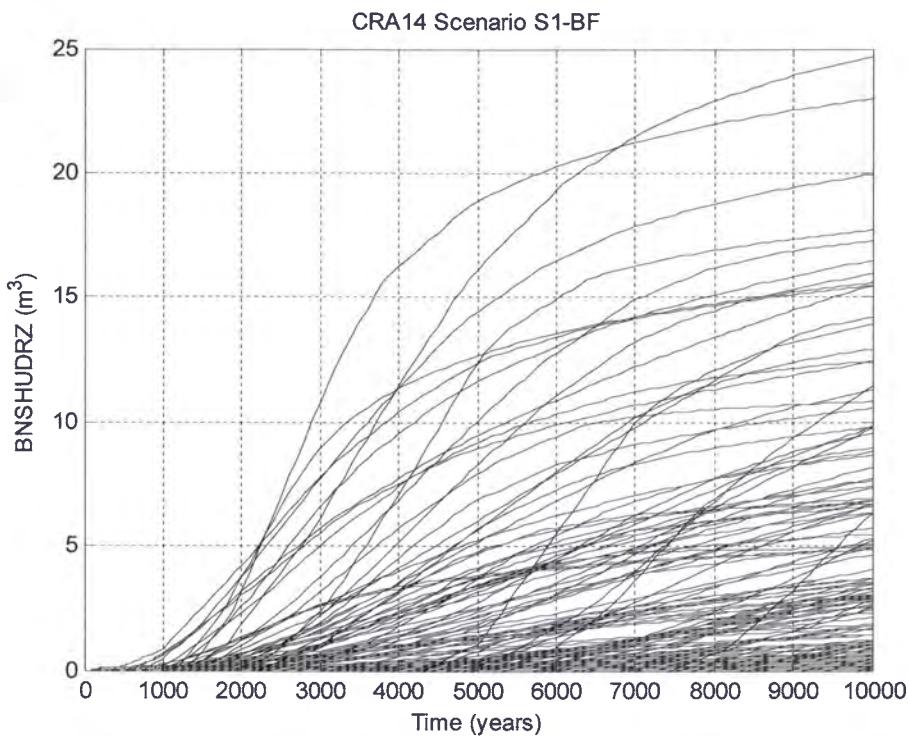


Figure 6-51: Horsetail Plot of Brine Flow up the Shaft, Case CRA14-0, Scenario S1-BF.

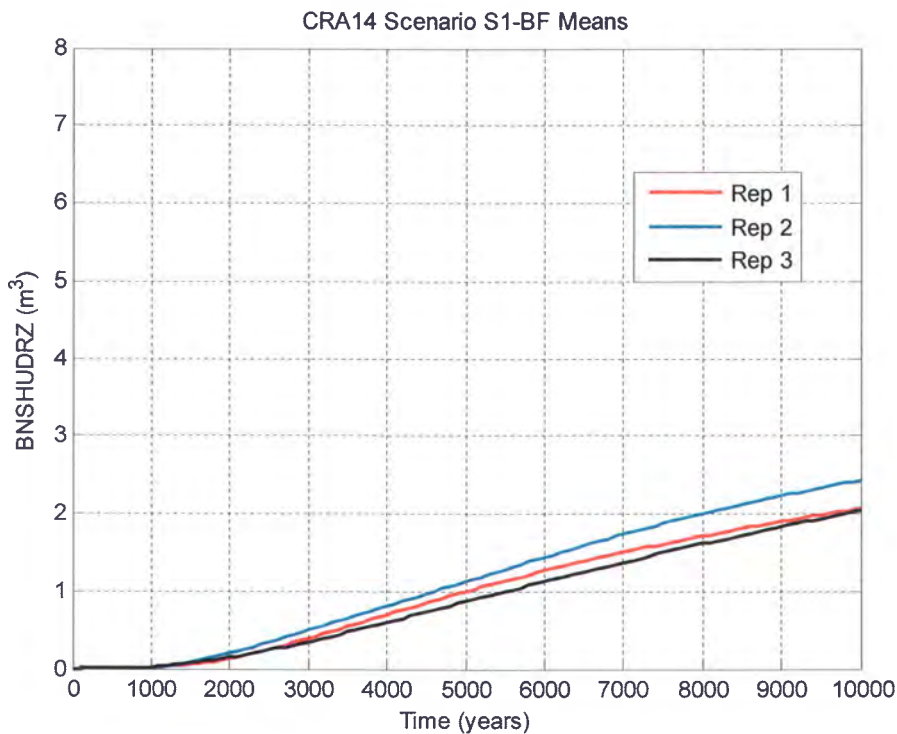


Figure 6-52: Replicate Means of Brine Flow up the Shaft, Case CRA14-0, Scenario S1-BF.

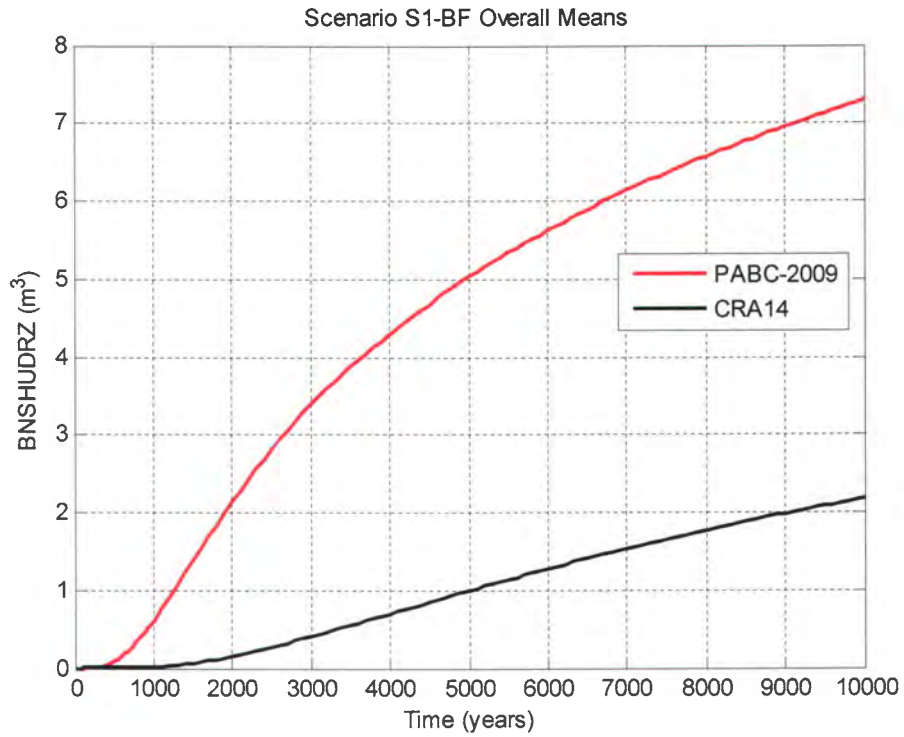


Figure 6-53: Overall Means of Brine Flow up the Shaft, Scenario S1-BF.

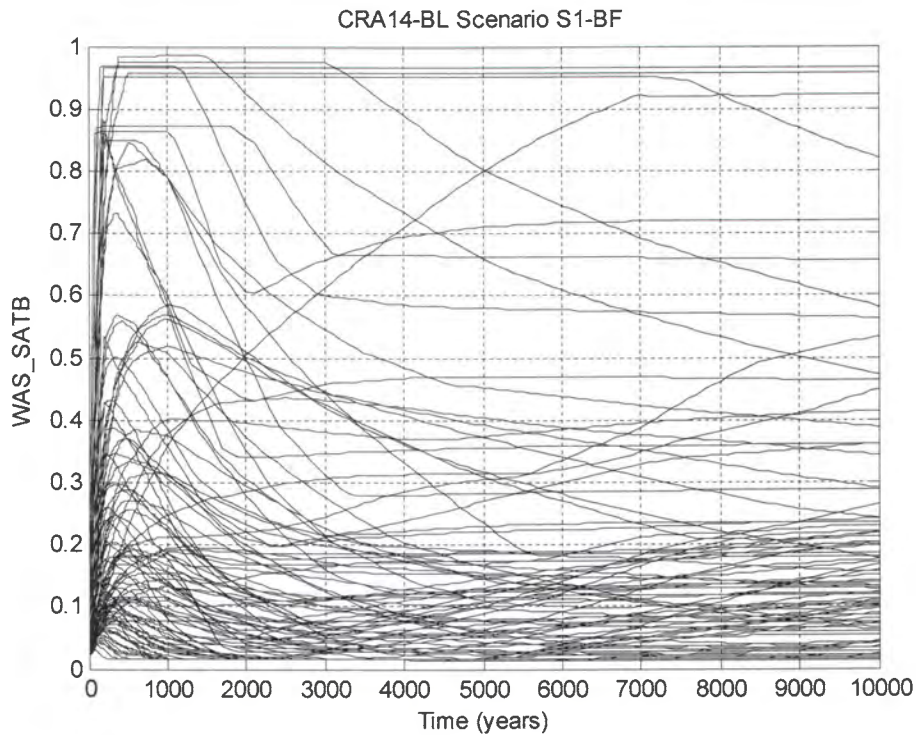


Figure 6-54: Horsetail Plot of Waste Panel Brine Saturation, Case CRA14-BL, Scenario S1-BF.

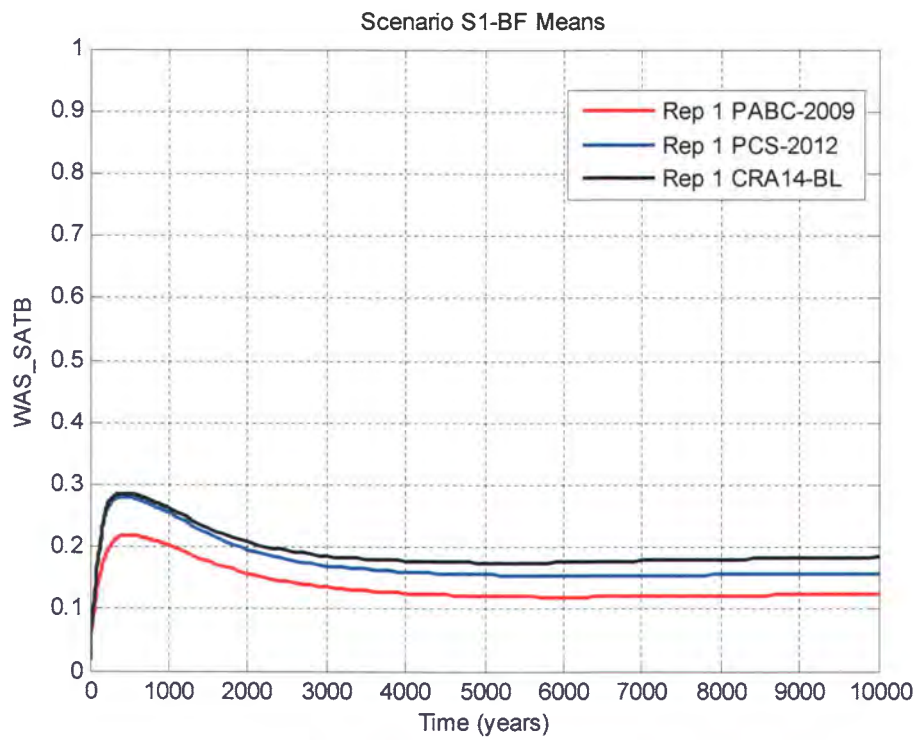


Figure 6-55: Replicate 1 Means of Waste Panel Brine Saturation, Scenario S1-BF.

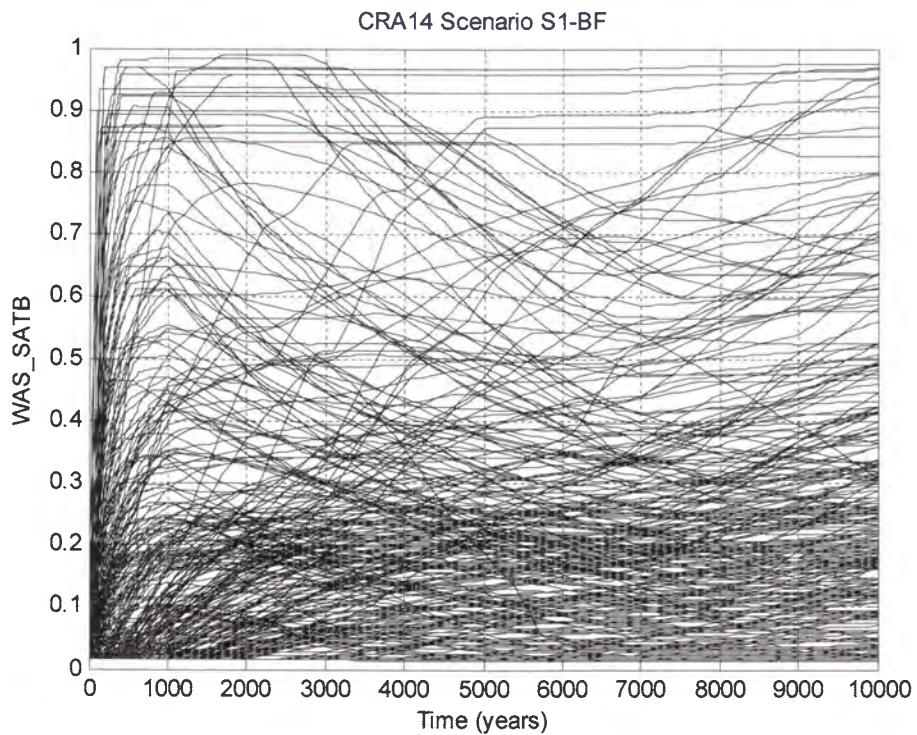


Figure 6-56: Horsetail Plot of Waste Panel Brine Saturation, Case CRA14-0, Scenario S1-BF.

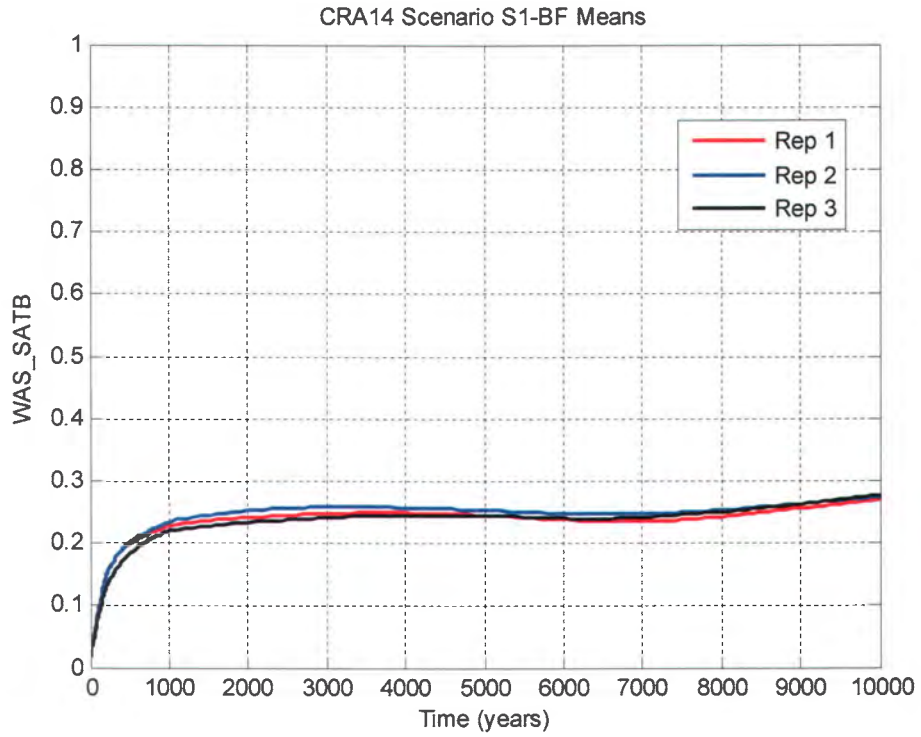


Figure 6-57: Replicate Means of Waste Panel Brine Saturation, Case CRA14-0, Scenario S1-BF.

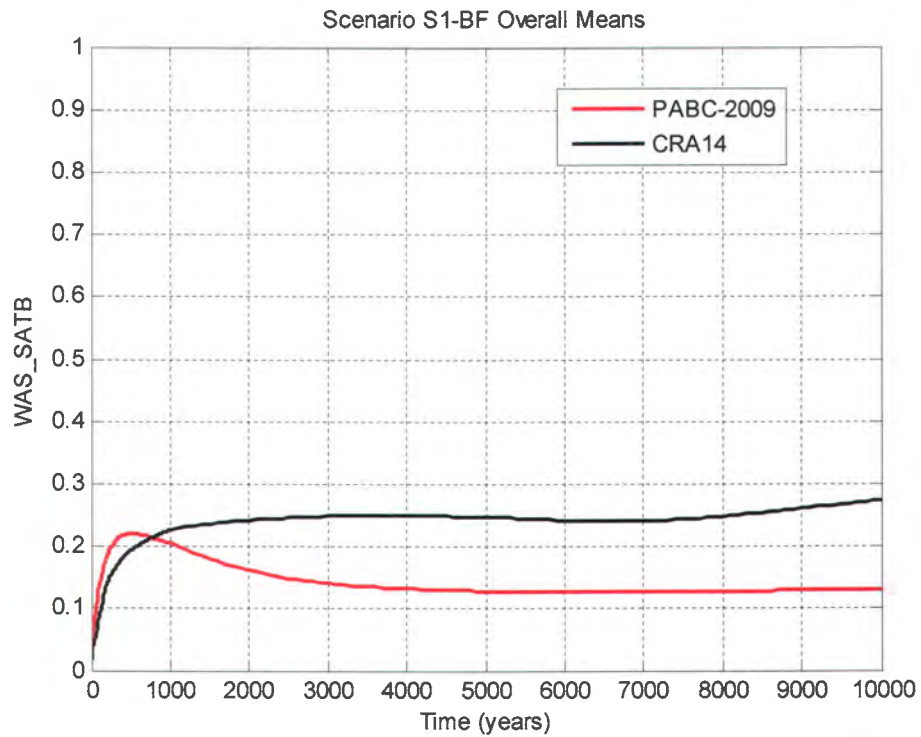


Figure 6-58: Overall Means of Waste Panel Brine Saturation, Scenario S1-BF.

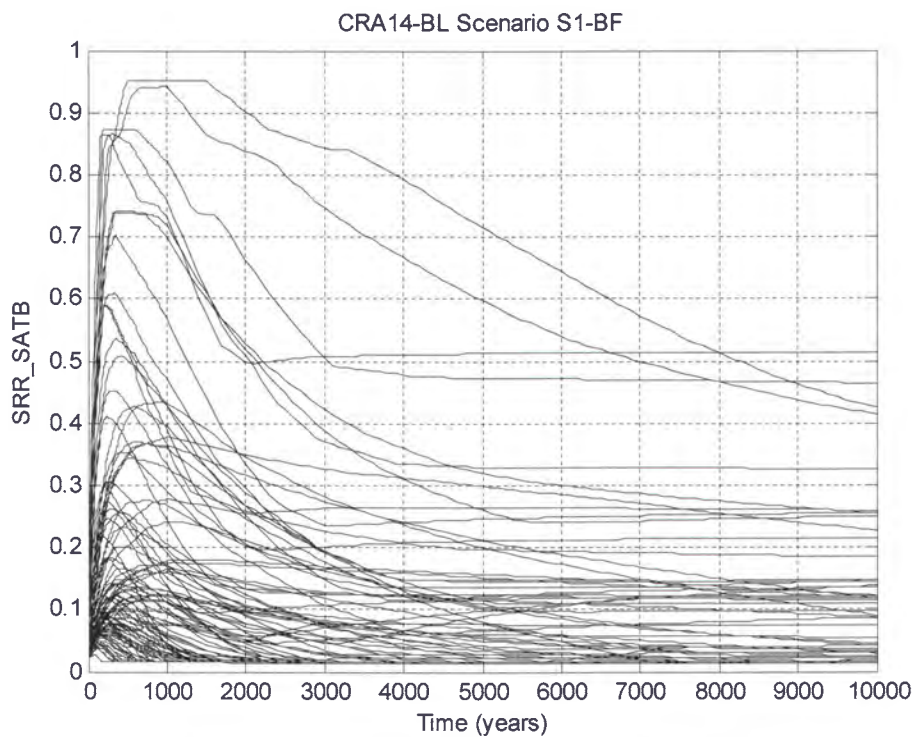


Figure 6-59: Horsetail Plot of SRoR Saturation, Case CRA14-BL, Scenario S1-BF.

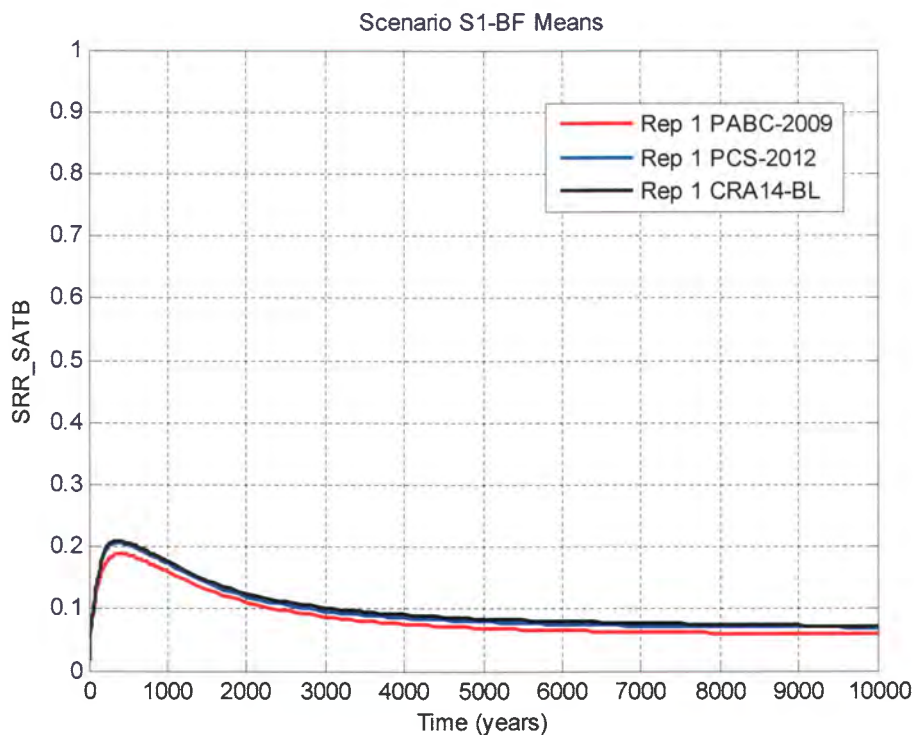


Figure 6-60: Replicate 1 Means of SRoR Saturation, Scenario S1-BF.

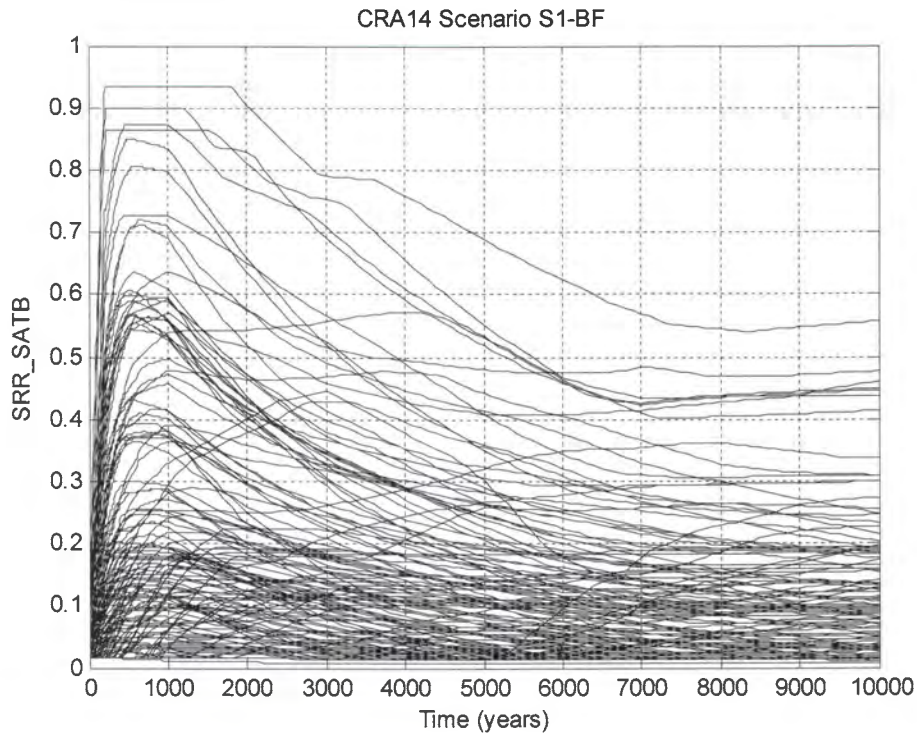


Figure 6-61: Horsetail Plot of SRoR Saturation, Case CRA14-0, Scenario S1-BF.

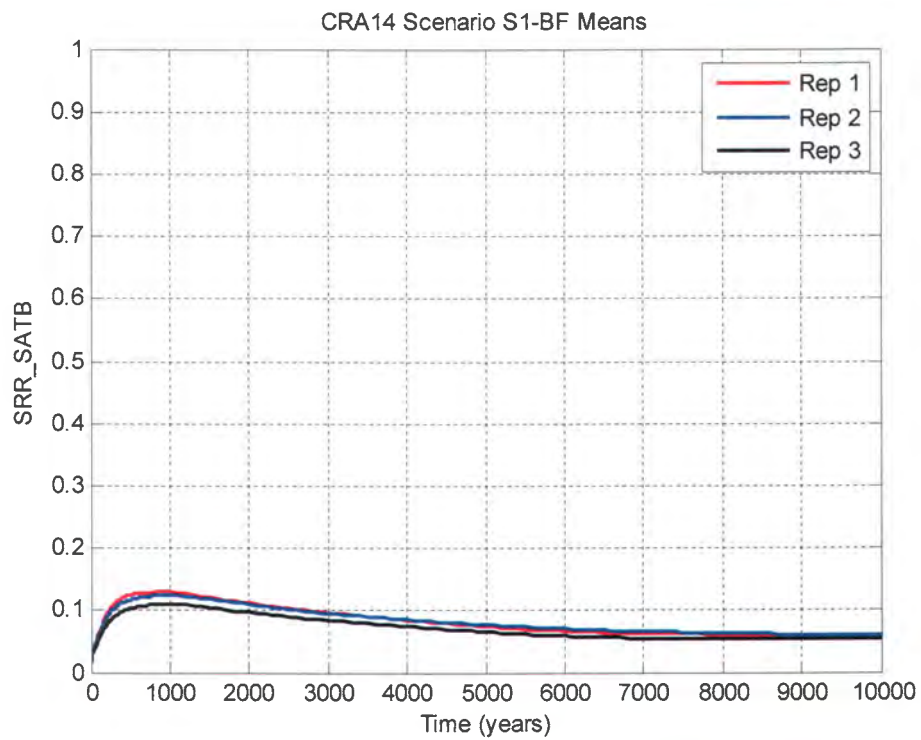


Figure 6-62: Replicate Means of SRoR Saturation, Case CRA14-0, Scenario S1-BF.

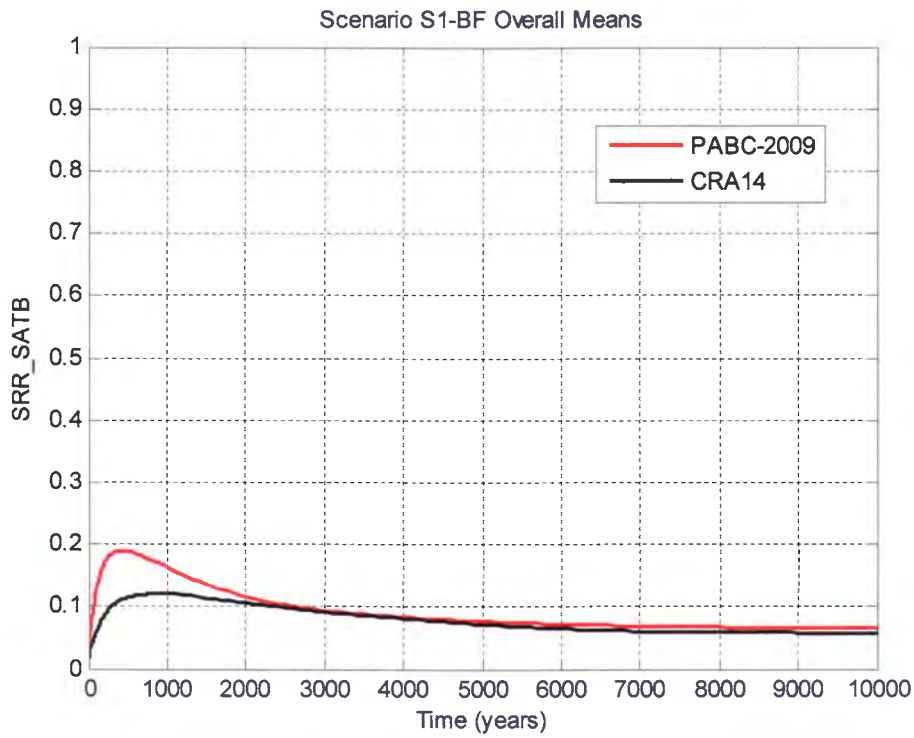


Figure 6-63: Overall Means of SRoR Saturation, Scenario S1-BF.

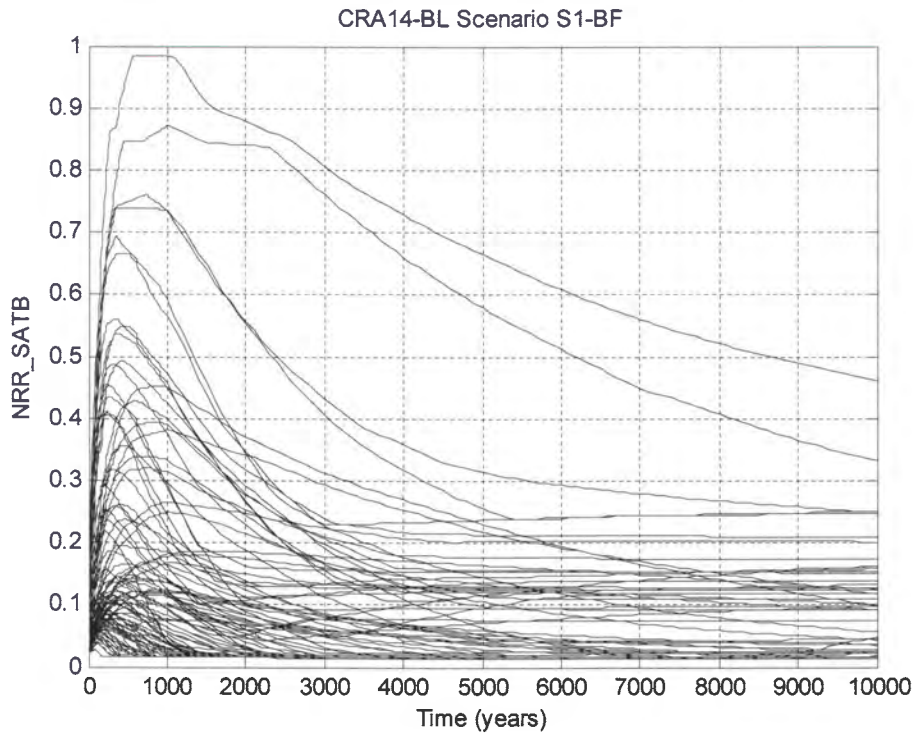


Figure 6-64: Horsetail Plot of NRoR Saturation, Case CRA14-BL, Scenario S1-BF.

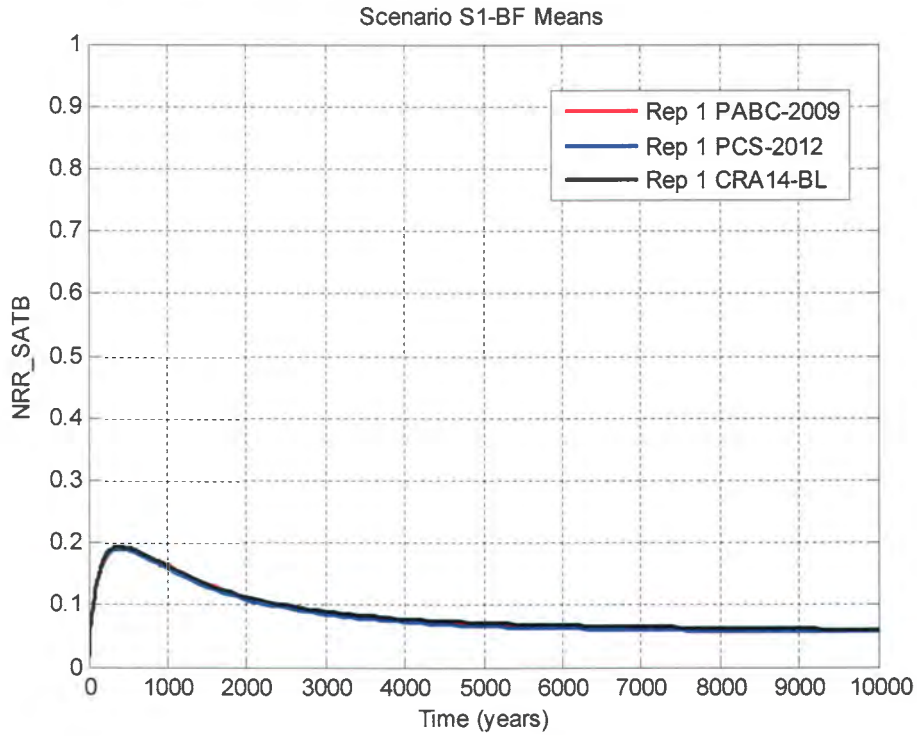


Figure 6-65: Replicate 1 Means of NRoR Saturation, Scenario S1-BF.

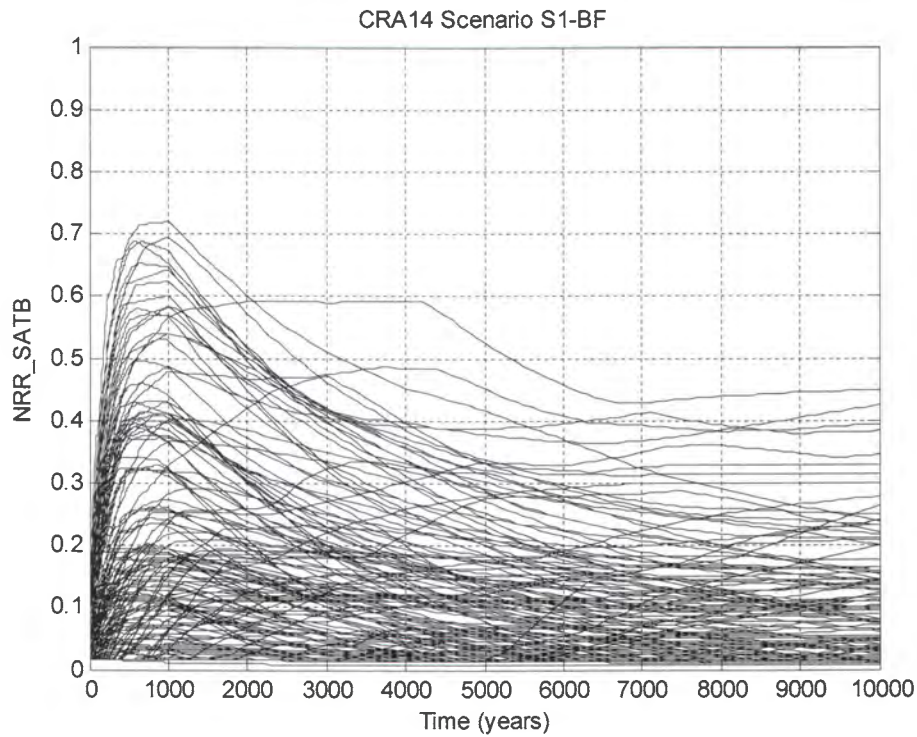


Figure 6-66: Horsetail Plot of NRoR Saturation, Case CRA14-0, Scenario S1-BF.



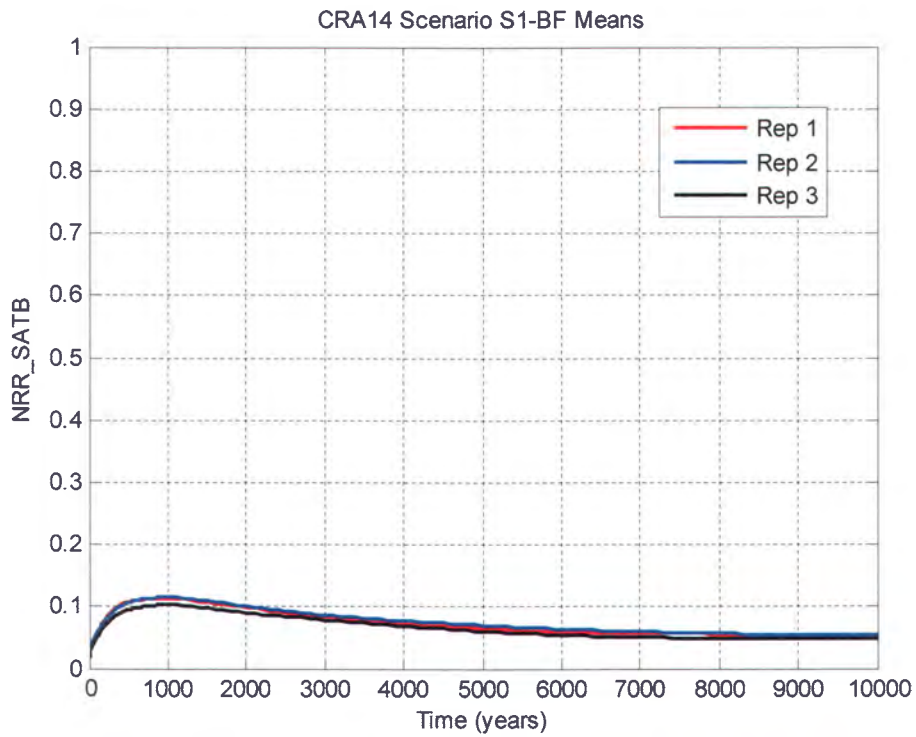


Figure 6-67: Replicate Means of NRoR Saturation, Case CRA14-0, Scenario S1-BF.

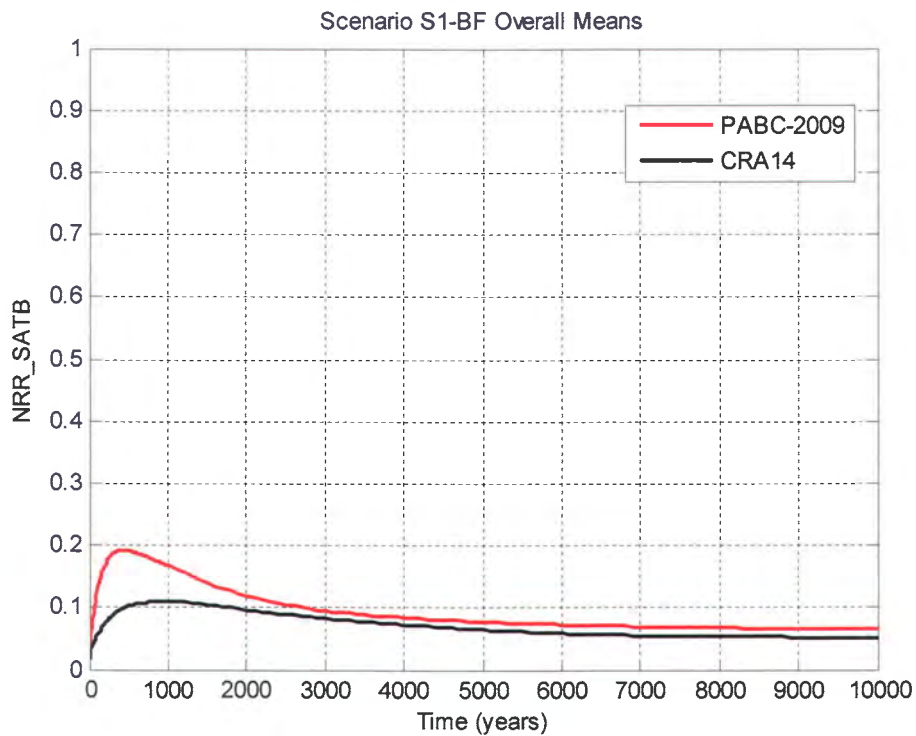


Figure 6-68: Overall Means of NRoR Saturation, Scenario S1-BF.

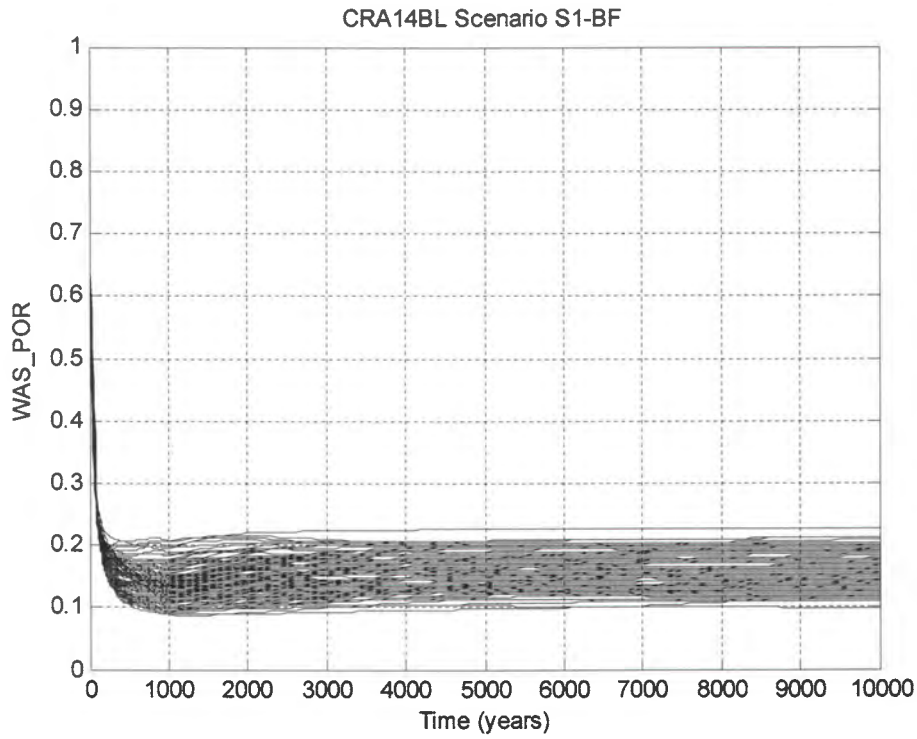


Figure 6-69: Horsetail Plot of Waste Panel Porosity, Case CRA14-BL, Scenario S1-BF.

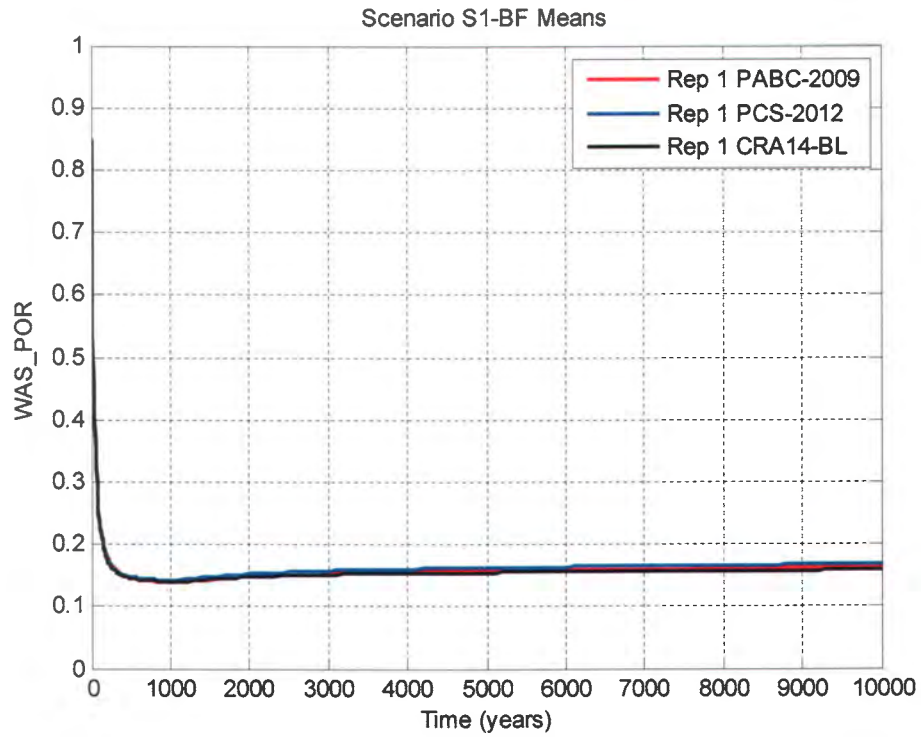


Figure 6-70: Replicate 1 Means of Waste Panel Porosity, Scenario S1-BF.

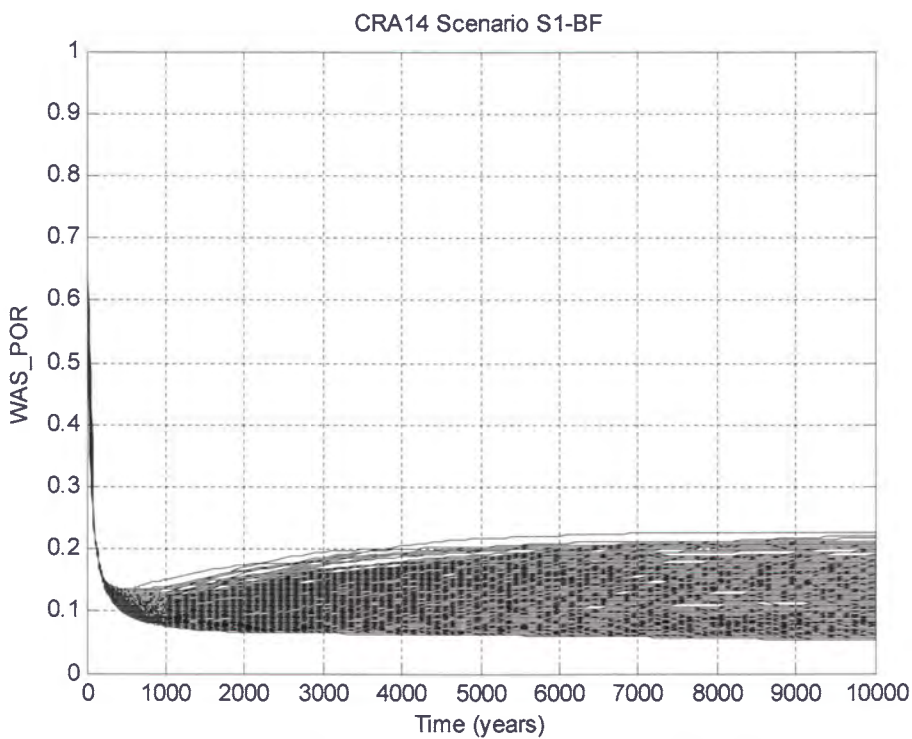


Figure 6-71: Horsetail Plot of Waste Panel Porosity, Case CRA14-0, Scenario S1-BF.

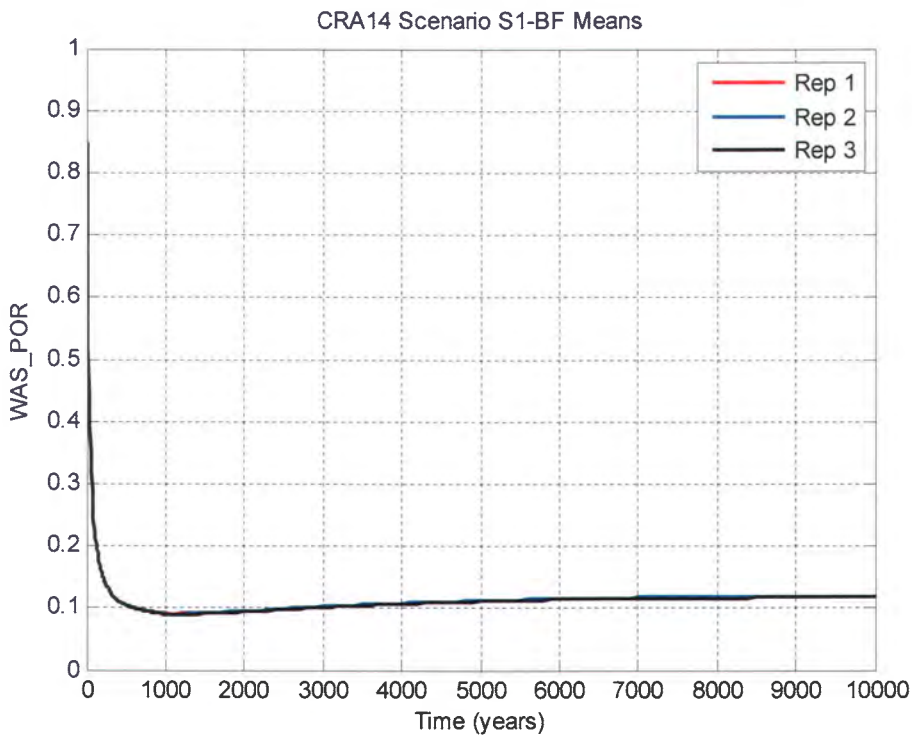


Figure 6-72: Replicate Means of Waste Panel Porosity, Case CRA14-0, Scenario S1-BF.

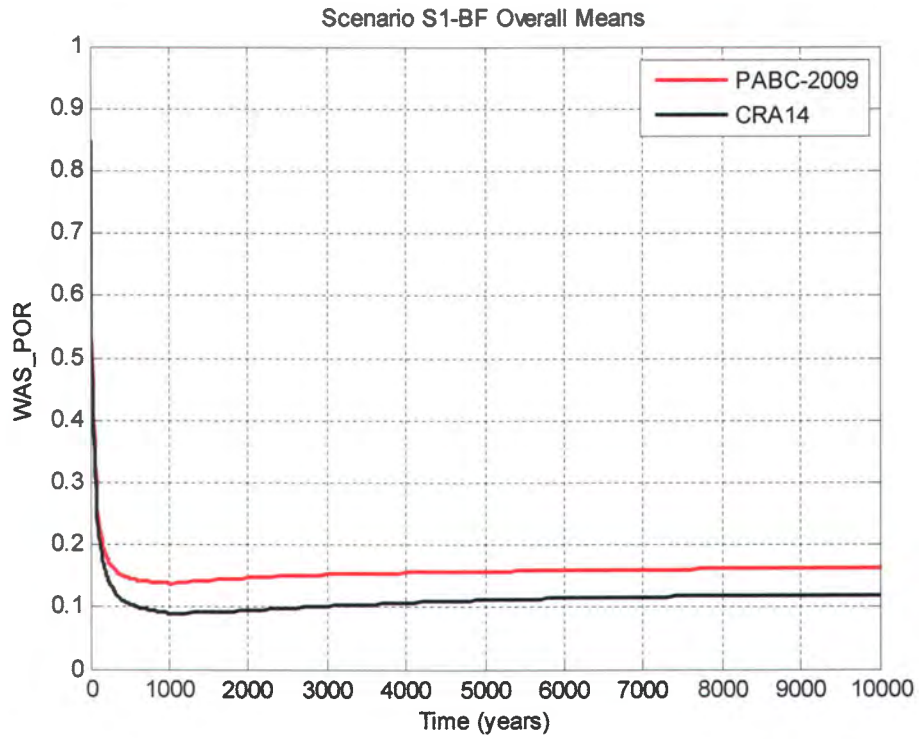


Figure 6-73: Overall Means of Waste Panel Porosity, Scenario S1-BF.

## 6.2 Results for an E1 Intrusion at 350 Years (Scenario S2-BF)

Results are now presented for disturbance scenario S2-BF. Results presented for this scenario are representative of those calculated for E1 intrusion scenarios (scenarios S2-BF and scenario S3-BF), with the only difference being the time of intrusion. In the results that follow, trends discussed for scenario S2-BF also apply to scenario S3-BF. Results presented in this section are limited to those calculated for the intruded waste panel. Quantities calculated for the SRoR, NRoR, and experimental repository regions in scenario S2-BF are very similar to those calculated and previously discussed for undisturbed conditions. As was done for the undisturbed case, results for each quantity calculated in scenario S2-BF are presented first for Case CRA14-BL, followed by their Case CRA14-0 counterpart.

### Pressure

The horsetail plot of volume-averaged waste panel pressure obtained in Case CRA14-BL is shown in Figure 6-74. The replicate 1 means of this quantity obtained in the PABC-2009, the PCS-2012 PA, and Case CRA14-BL are shown together in Figure 6-75. As seen in that figure, and discussed more fully in Camphouse (2012a), the “tighter” ROMPCS design results in a period of increased waste panel pressurization after the intrusion as compared to the PABC-2009 results. The inclusion of additional mined volume in the WIPP experimental area in Case CRA14-BL slightly reduces the mean waste panel pressure following the intrusion, with the mean waste panel pressure curve obtained in Case CRA14-BL eventually being slightly lower than the PABC-2009 result. The horsetail plot of waste panel pressure obtained for the 300 vector realizations of Case CRA14-0 is shown in Figure 6-76, with the three replicate means plotted together in Figure 6-77. As is evident in Figure 6-77, very good agreement is seen among the three replicate means. As discussed in the previous section, the mean waste panel porosity is reduced for undisturbed conditions as compared to the PABC-2009 when the refined water balance implementation and iron corrosion rate are included (Figure 6-73). As a result, the mean waste panel porosity is lower in Case CRA14-0 at 350 years when the E1 intrusion occurs, resulting in increased pressure in the waste panel after it is connected to highly pressurized Castile brine during the intrusion. The overall means of waste panel pressure obtained in the PABC-2009 and Case CRA14-0 are plotted together in Figure 6-78. As seen in that figure, the mean waste panel pressure obtained in Case CRA14-0 remains higher than that seen in the PABC-2009 for a period of time after the intrusion, but eventually falls below the PABC-2009 result at roughly 6200 years.

### Gas Generation

As was the case for the undisturbed results, the eventual reduction in mean waste panel pressure from Case CRA14-BL to Case CRA14-0 is largely due to the revised iron corrosion rate implemented in the latter case. The horsetail plot of molar gas generation in the intruded waste panel, quantity GASMOL\_W, obtained in Case CRA14-BL is shown in Figure 6-79. The replicate 1 mean of this quantity obtained in Case CRA14-BL is shown in Figure 6-80. Also seen in that figure are the mean curves of molar gas generation due to iron corrosion in the waste panel (quantity FEMOL\_W) and microbial degradation of cellulose in the waste panel (quantity CELMOL\_W). As is clear from that figure, the majority of gas generated in the intruded panel for Case CRA14-BL is due to iron corrosion. The horsetail plot of molar gas

generation in the waste panel for Case CRA14-0 is shown in Figure 6-81. Means of waste panel molar gas generation obtained in Case CRA14-0 are shown in Figure 6-82. (Figure 6-82 includes replicate 1 means as well as overall means to allow for direct comparison to results shown in Figure 6-80.) As is clear from Figure 6-82, gas generation due to iron corrosion is still the dominant gas production mechanism in Case CRA14-0. The abundance of available brine after the E1 intrusion yields nearly identical mean curves for gas generation due to CPR microbial degradation in Figure 6-80 and Figure 6-82. The impact of the revised iron corrosion rate, however, can be clearly seen. Mean molar gas production due to iron corrosion increases at a lower rate in the Case CRA14-0 results than in Case CRA14-BL. As the mean molar gas generation due to CPR microbial degradation is virtually unchanged from Case CRA14-BL to Case CRA14-0, the reduction (on average) in the rate of gas production due to iron corrosion yields a corresponding decrease in the rate of mean gas generation in the waste panel.

### Cumulative Brine Flow

The horsetail plot of cumulative brine inflow to the waste panel obtained for Case CRA14-BL is shown in Figure 6-83. Replicate 1 means of quantity BRNWASIC obtained in the PABC-2009, the PCS-2012 PA, and Case CRA14-BL are plotted together in Figure 6-84. Results obtained in the three calculations are quite similar. The horsetail plot of quantity BRNWASIC obtained in Case CRA14-0 is shown in Figure 6-85, with the three replicate means plotted together in Figure 6-86. Reasonable agreement is seen among the three replicate means. Mean waste panel pressure is significantly reduced in Case CRA14-0 as compared to the PABC-2009 for the undisturbed repository (Figure 6-5). The pressure reduction allows increased brine flow to the waste panel prior to the E1 intrusion at 350 years, as well as increased brine inflow to the panel at the time of intrusion. The result is an overall mean curve for quantity BRNWASIC in Case CRA14-0 that is greater than that obtained in the PABC-2009 (Figure 6-87).

Trends observed for the waste panel also hold for the repository overall. Increased brine inflow to the intruded panel yields an increase in brine inflow to the repository overall for scenario S2-BF. Results for cumulative brine inflow to the repository, quantity BRNREPIC, are shown in Figure 6-88 to Figure 6-92.

The horsetail plot of cumulative brine flow up the intrusion borehole, quantity BNBHUDRZ, obtained in Case CRA14-BL is shown in Figure 6-93. Replicate 1 means obtained for this quantity in the PABC-2009, the PCS-2012 PA, and Case CRA14-BL are plotted together in Figure 6-94. Results obtained in the three calculations are similar, with slightly increased results seen in the PCS-2012 PA. Results obtained for quantity BNBHUDRZ in Case CRA14-0 are shown in Figure 6-95 to Figure 6-97. The increased brine inflow to the waste panel in the CRA14-0 results, combined with the increase in mean waste panel pressure for a period of time after the intrusion, yields an increase in the overall mean obtained for quantity BNBHUDRZ in Case CRA14-0 as compared to the PABC-2009 (Figure 6-97).

### Brine Saturation

The increased brine inflow to the waste panel in the CRA14-0 results has a direct impact on waste panel brine saturation. The horsetail plot of quantity WAS\_SATB obtained in Case CRA14-BL is shown in Figure 6-98. Replicate 1 means obtained for this quantity in the PABC-2009, the PCS-2012 PA, and Case CRA14-BL are similar, and are shown in Figure 6-99. The

horsetail plot obtained for quantity WAS\_SATB in Case CRA14-0 is shown in Figure 6-100, with replicate means shown in Figure 6-101. The increased mean waste panel brine inflow seen in Case CRA14-0 as compared to the PABC-2009 (Figure 6-87), results in a corresponding increase in the Case CRA14-0 mean waste panel brine saturation following the E1 intrusion at 350 years (Figure 6-102).

Summary of Results for E1 Intrusion Scenarios

For E1 intrusion scenarios, results obtained for the SRoR, NRoR, and the repository experimental area do not change appreciably from those seen for the undisturbed repository. Changes included in the CRA-2014 PA yield an increase to the mean pressure in the intruded panel for a period of time after the intrusion as compared to results from the PABC-2009. The revised iron corrosion rate utilized in Case CRA14-0 results in slower gas production due to iron corrosion (on average), resulting in a mean waste panel pressure curve in Case CRA14-0 that eventually falls below that seen in the PABC-2009. Cumulative brine inflows to the intruded waste panel are greater (on average) in the CRA14-0 results as compared to the PABC-2009. This increased mean brine inflow yields a corresponding increase to the mean brine saturation of the intruded panel. The combination of increased mean pressure and brine saturation in the intruded panel translates to an increase in the mean cumulative brine flow up the intrusion borehole in the CRA14-0 results.

Summary statistics for BRAGFLO scenario S2-BF are shown in Table 6-2. Results presented in that table are calculated over all 300 vector realizations (and all times) of the PABC-2009 and Case CRA14-0 of the CRA-2014 PA.

Table 6-2: Summary Statistics for Scenario S2-BF

Quantity (units)	Description	Mean Value		Maximum Value	
		PABC-2009	CRA14-0	PABC-2009	CRA14-0
WAS_PRES (MPa)	Volume-averaged pressure in the waste panel.	7.39	7.36	15.63	16.15
GASMOL_W (x10 <sup>6</sup> moles)	Total moles of gas generated in the intruded panel.	54.75	36.66	149.00	92.54
BRNWASIC (x10 <sup>3</sup> m <sup>3</sup> )	Cumulative brine inflow to the waste panel.	14.03	16.11	182.15	187.90
BRNREPIC (x10 <sup>3</sup> m <sup>3</sup> )	Cumulative brine inflow to the entire repository.	30.26	35.25	204.98	213.42
WAS_SATB (none)	Brine saturation in the waste panel.	0.68	0.73	0.99	0.99
BNBHUDRZ (x10 <sup>3</sup> m <sup>3</sup> )	Cumulative brine flow up the intrusion borehole.	3.25	3.62	166.84	173.21

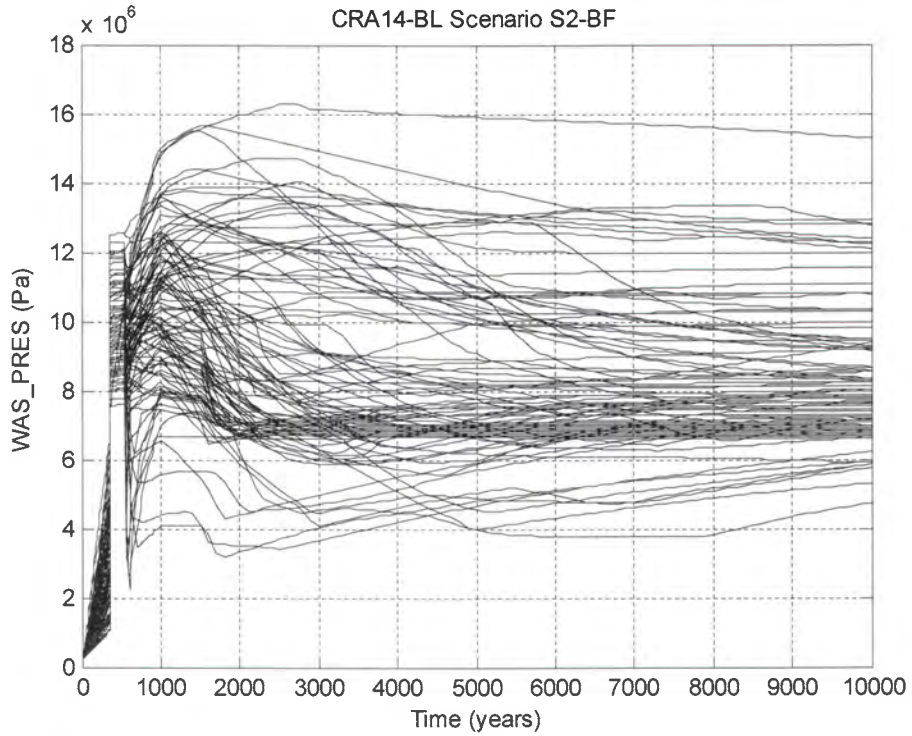


Figure 6-74: Horsetail Plot of Waste Panel Pressure for Case CRA14-BL, Scenario S2-BF

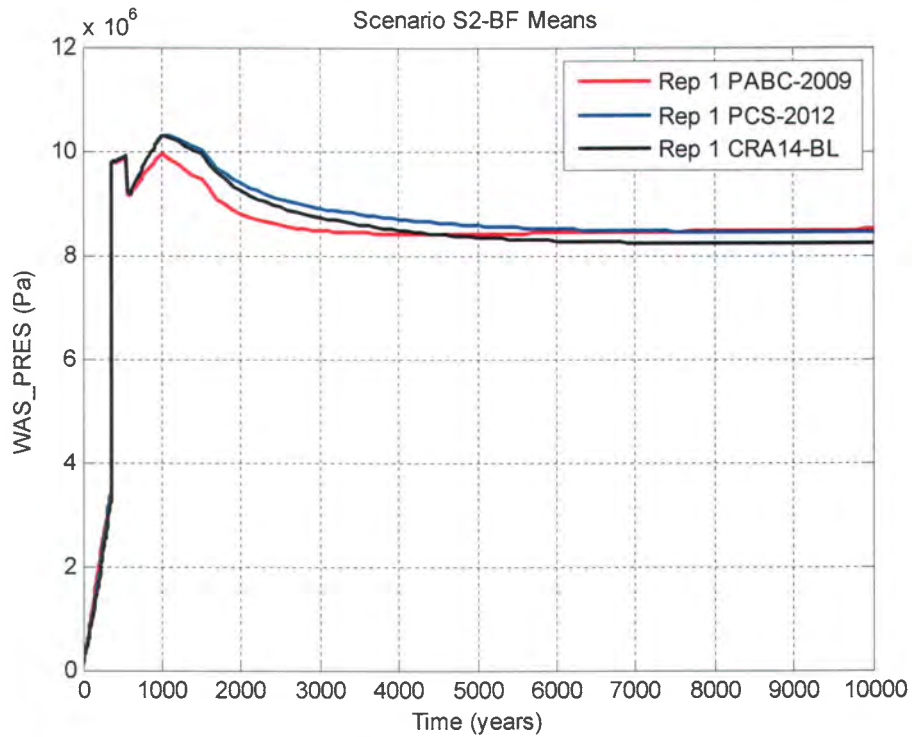


Figure 6-75: Replicate 1 Means of Waste Panel Pressure, Scenario S2-BF



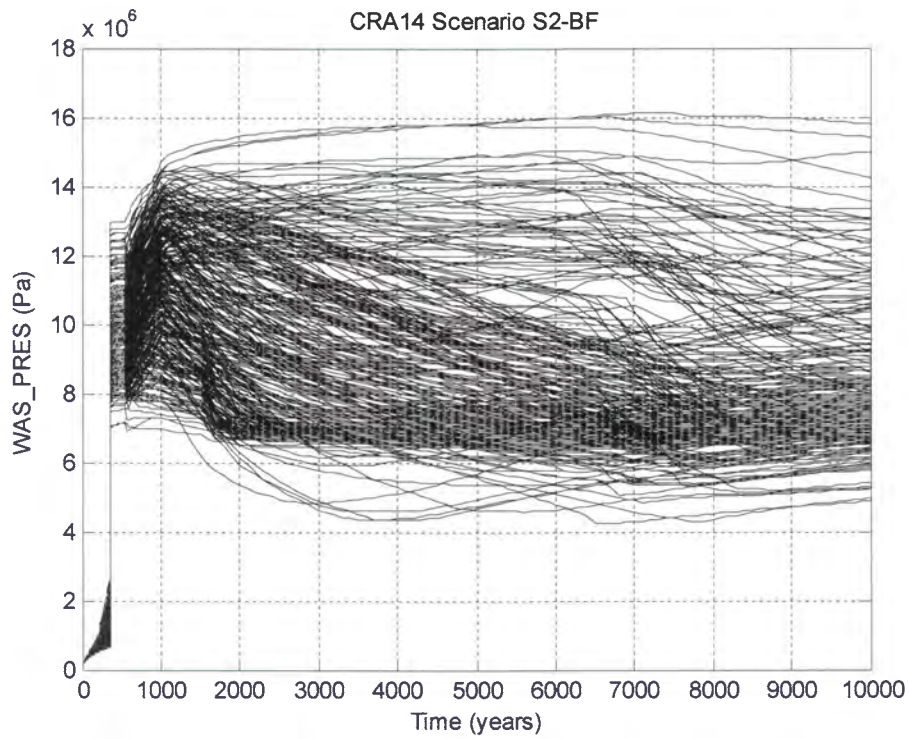


Figure 6-76: Horsetail Plot of Waste Panel Pressure for Case CRA14-0, Scenario S2-BF

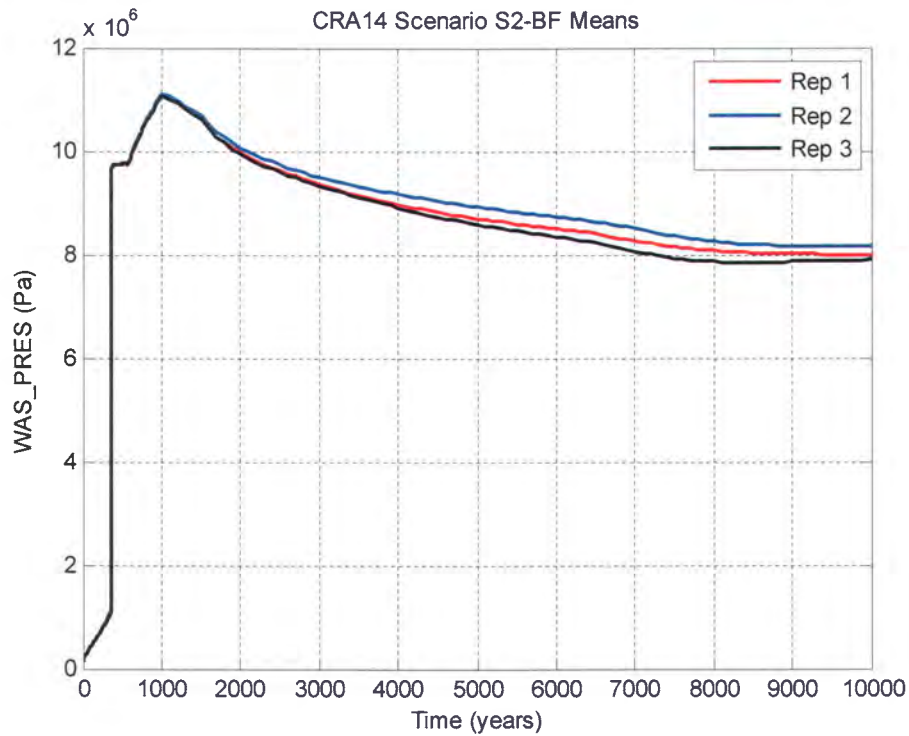


Figure 6-77: Replicate Means of Waste Panel Pressure for Case CRA14-0, Scenario S2-BF

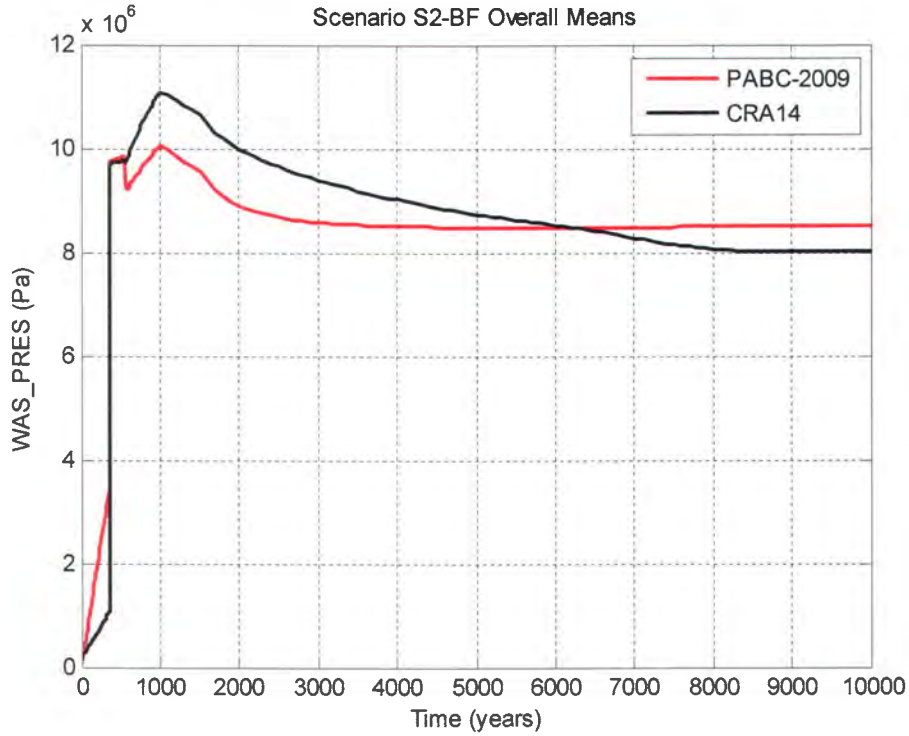


Figure 6-78: Overall Means of Waste Panel Pressure, Scenario S2-BF

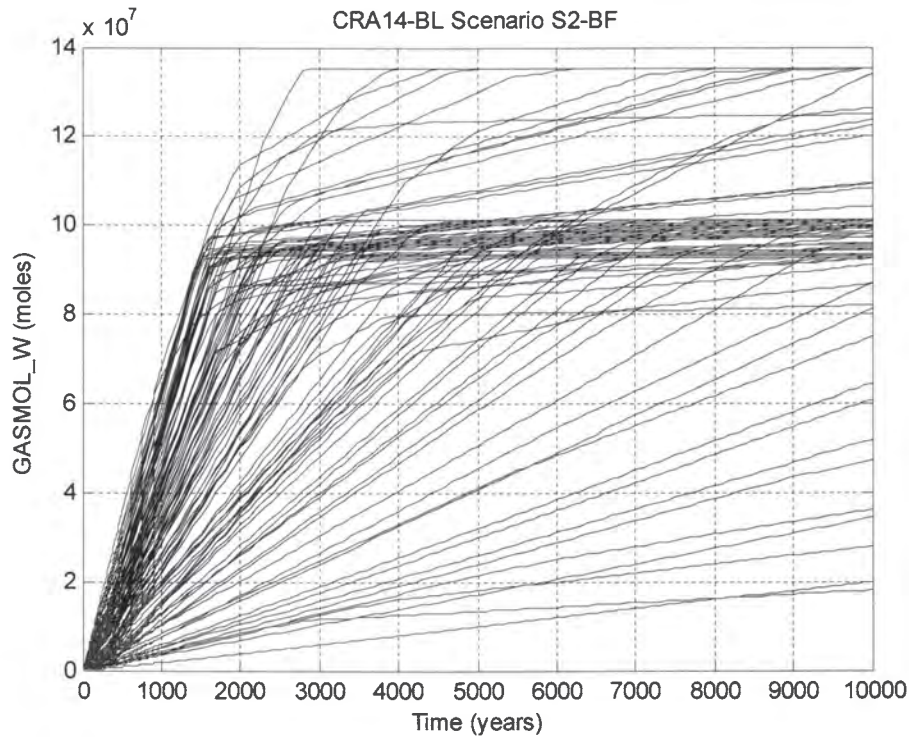


Figure 6-79: Horsetail Plot of Molar Waste Panel Gas Generation for Case CRA14-BL, Scenario S2-BF

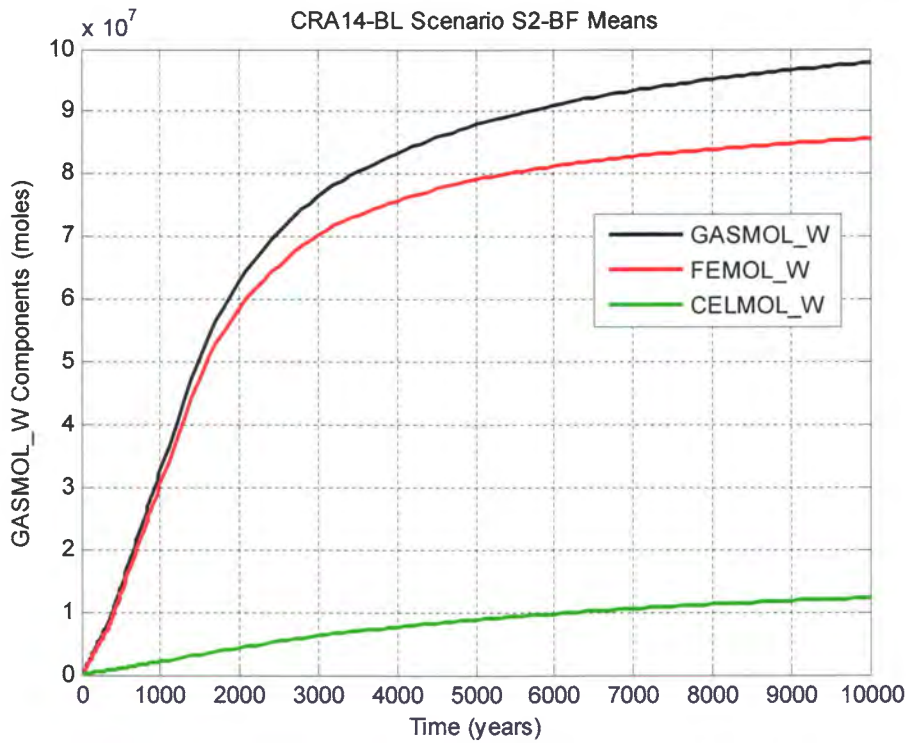


Figure 6-80: Replicate 1 Means of Molar Waste Panel Gas Generation for Case CRA14-BL, Scenario S2-BF

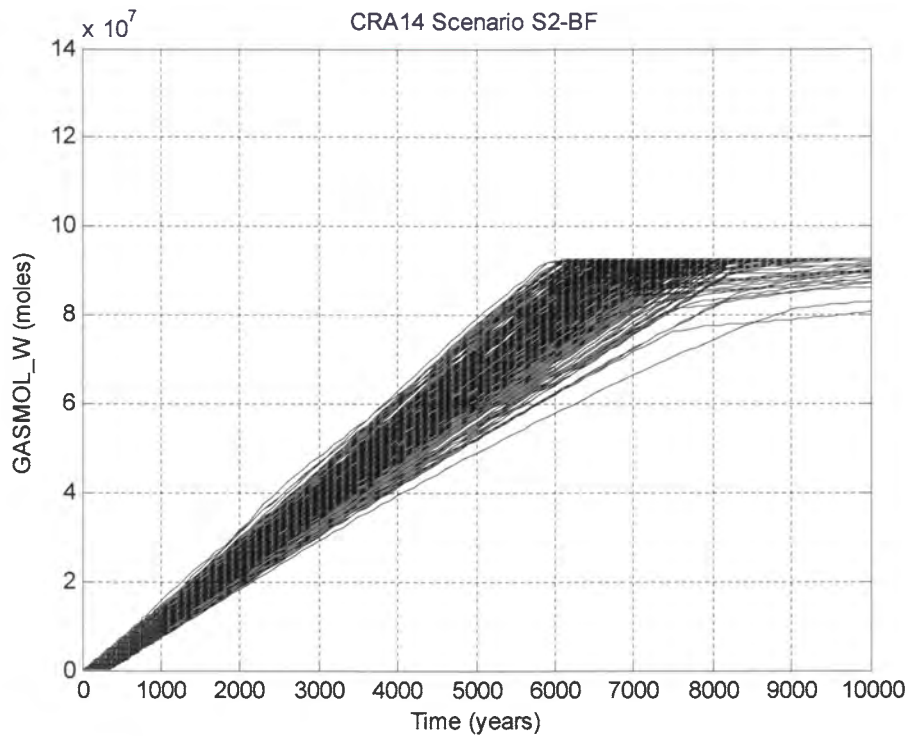


Figure 6-81: Horsetail Plot of Molar Waste Panel Gas Generation for Case CRA14-0, Scenario S2-BF

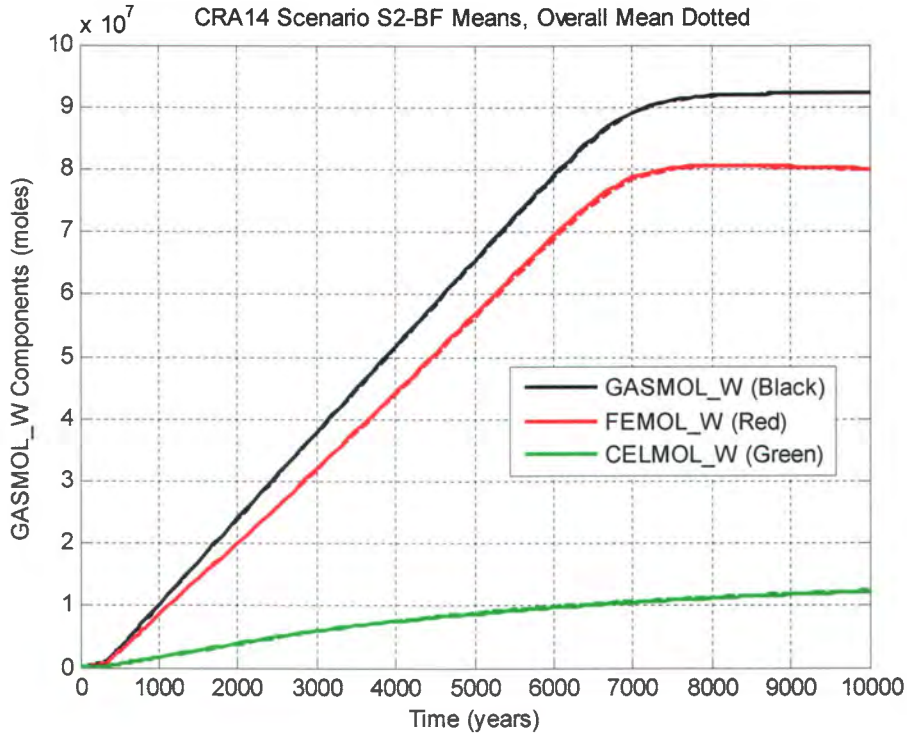


Figure 6-82: Means of Molar Waste Panel Gas Generation for Case CRA14-0, Scenario S2-BF (Replicate 1 Means – Solid, Overall Means – Dotted)

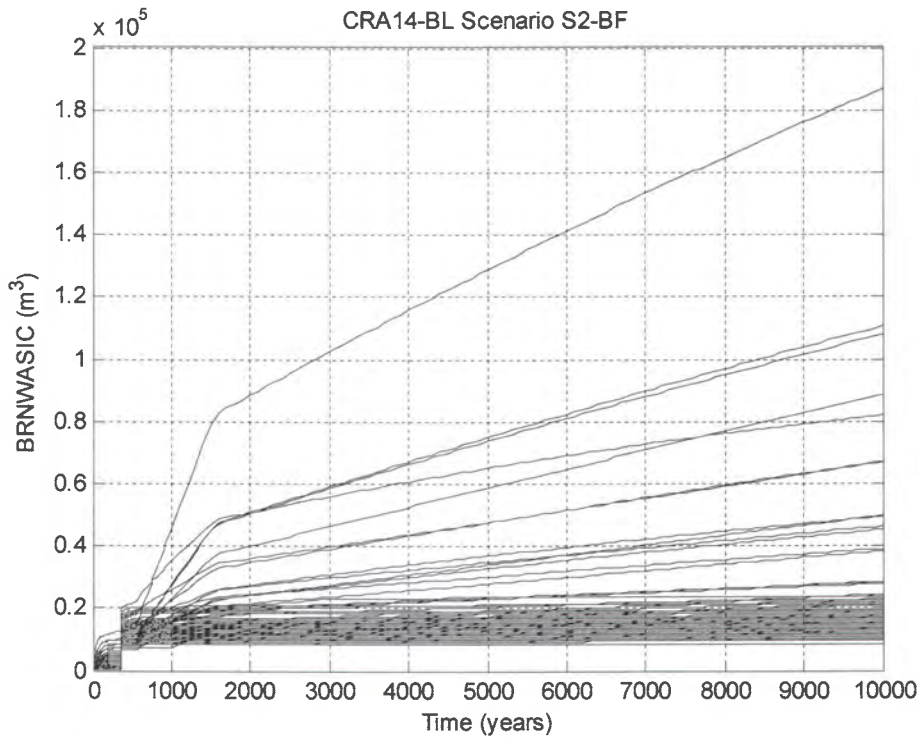


Figure 6-83: Horsetail Plot of Cumulative Brine Inflow to the Waste Panel, Case CRA14-BL, Scenario S2-BF.

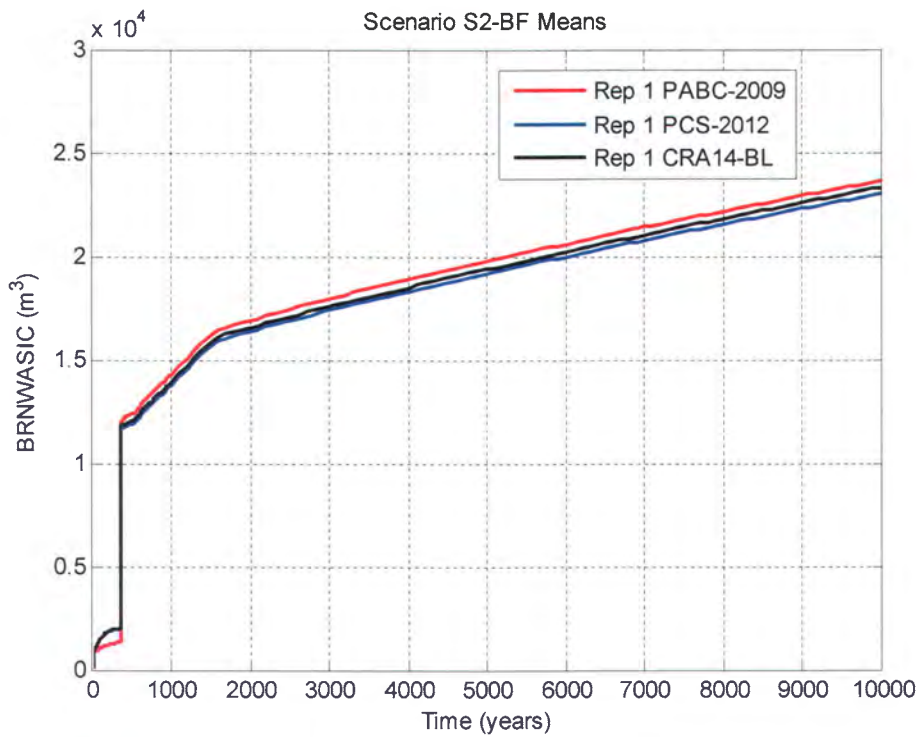


Figure 6-84: Replicate 1 Means of Cumulative Brine Inflow to the Waste Panel, Scenario S2-BF.

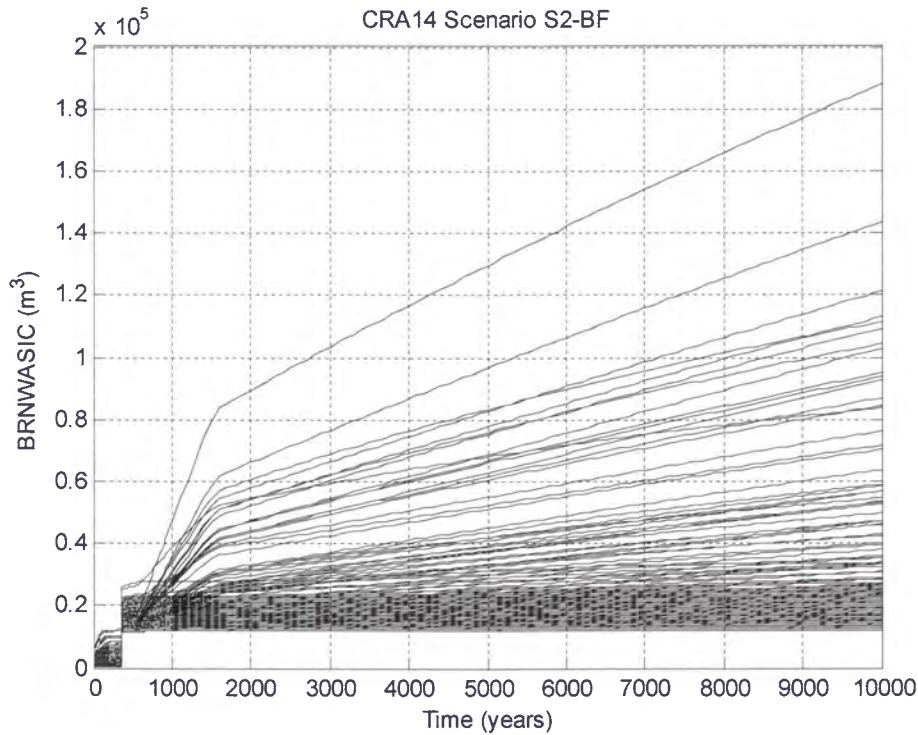


Figure 6-85: Horsetail Plot of Cumulative Brine Inflow to the Waste Panel, Case CRA14-0, Scenario S2-BF.

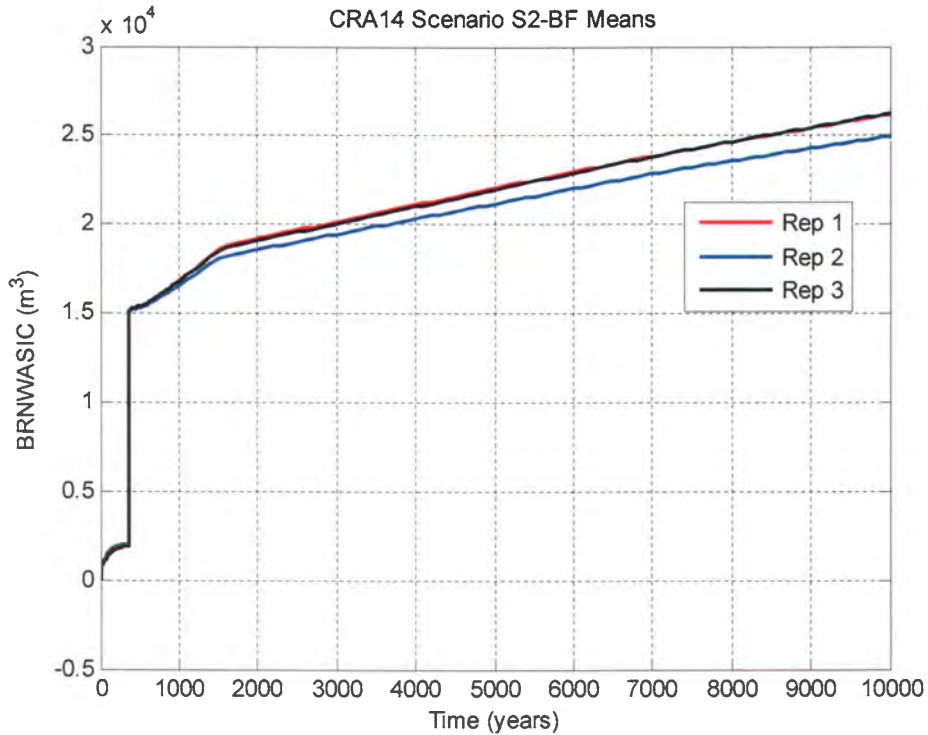


Figure 6-86: Replicate Means of Cumulative Brine Inflow to the Waste Panel, Case CRA14-0, Scenario S2-BF.

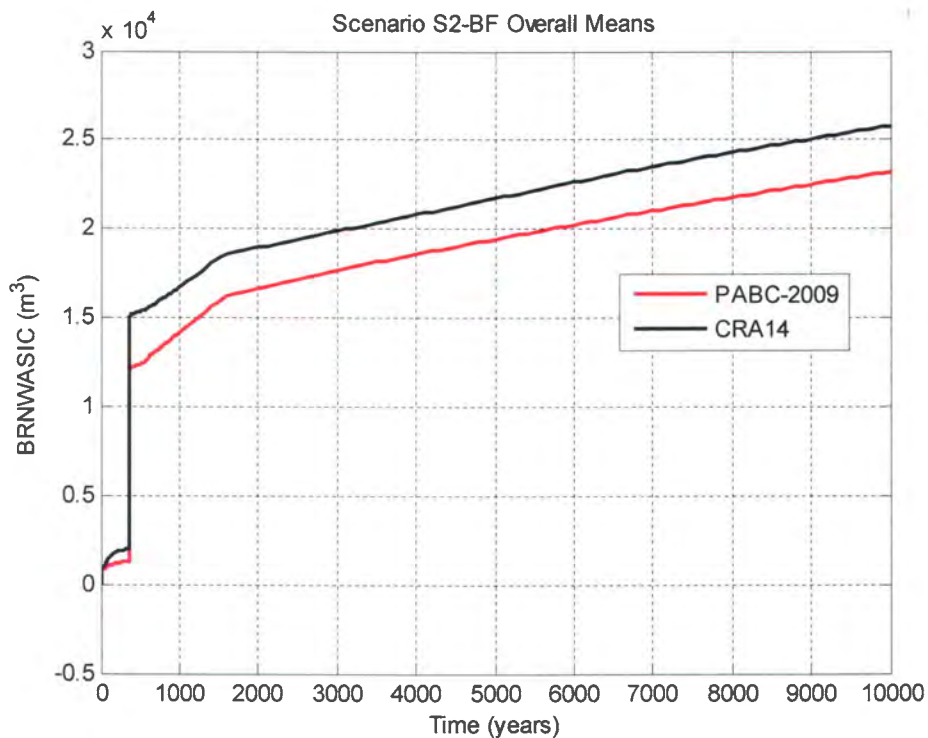


Figure 6-87: Overall Means of Cumulative Brine Inflow to the Waste Panel, Scenario S2-BF.

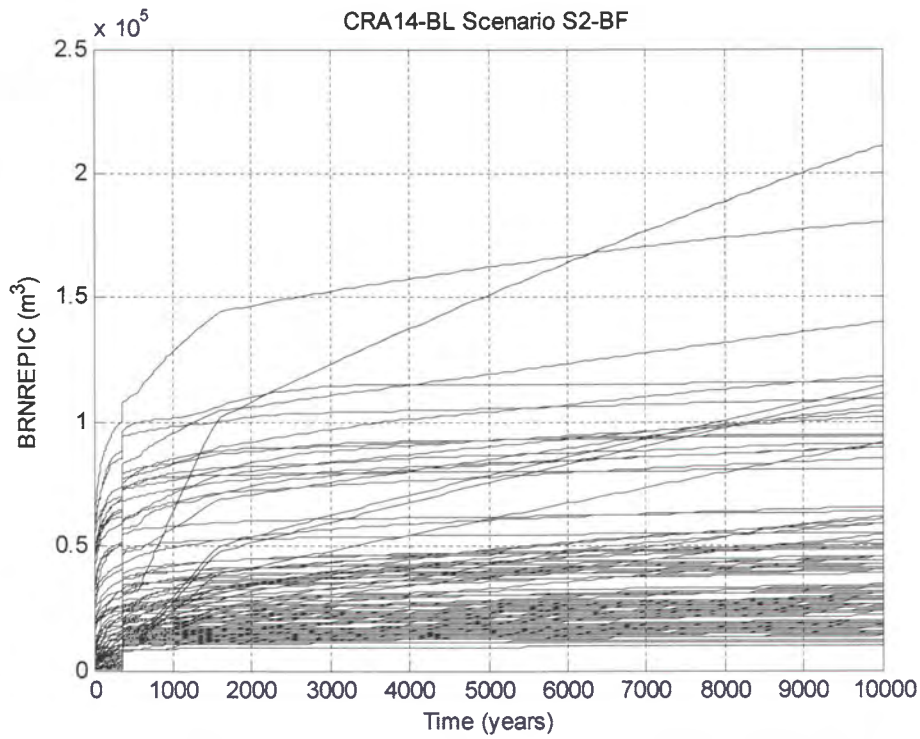


Figure 6-88: Horsetail Plot of Cumulative Brine Inflow to the Repository, Case CRA14-BL, Scenario S2-BF.

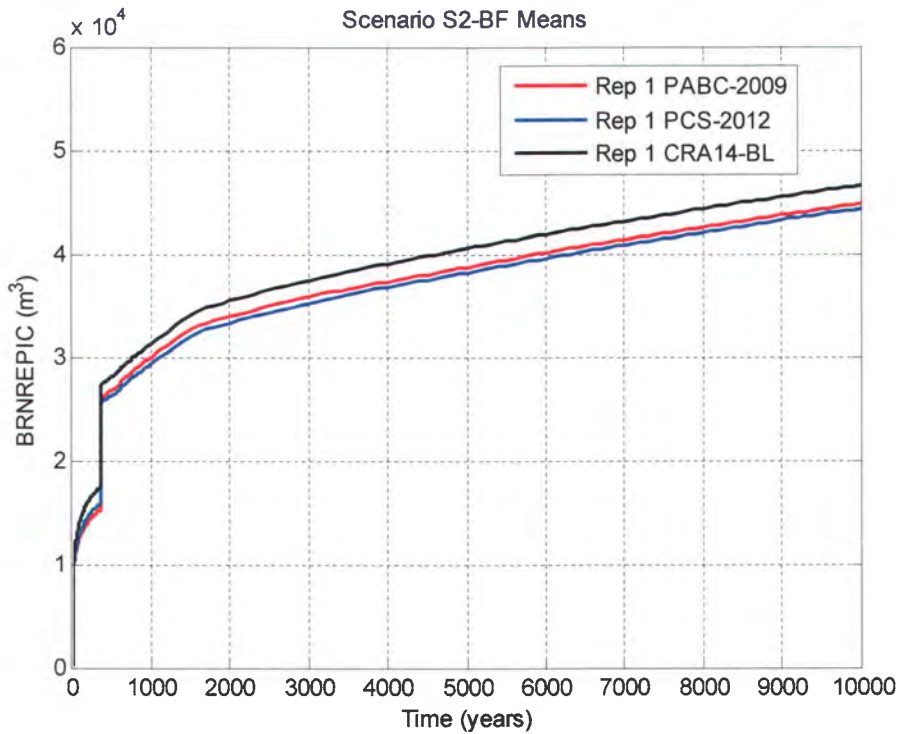


Figure 6-89: Replicate 1 Means of Cumulative Brine Inflow to the Repository, Scenario S2-BF.

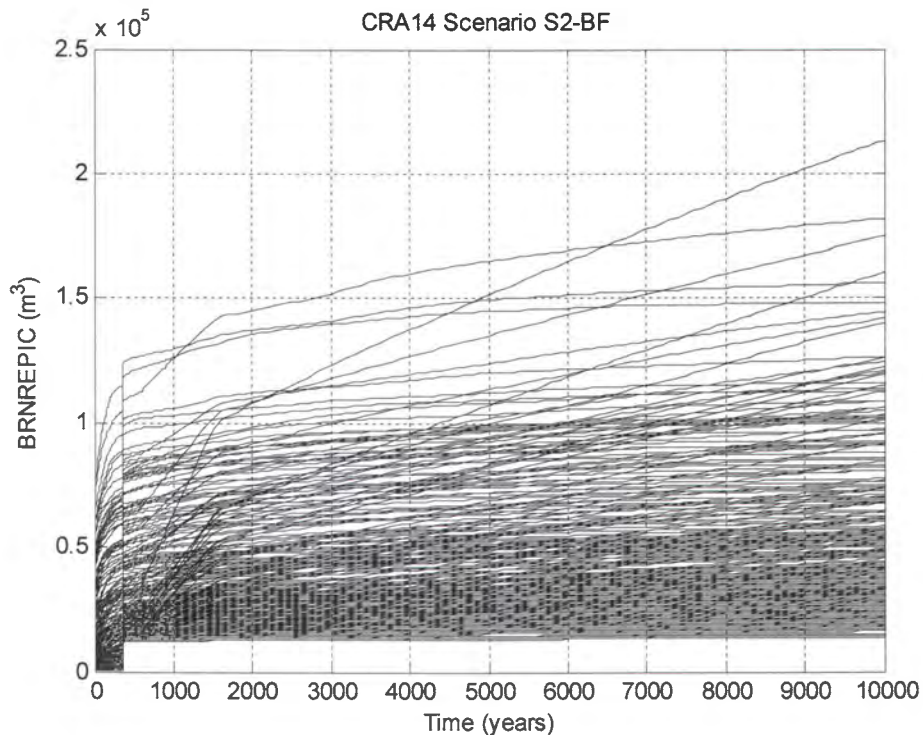


Figure 6-90: Horsetail Plot of Cumulative Brine Inflow to the Repository, Case CRA14-0, Scenario S2-BF.

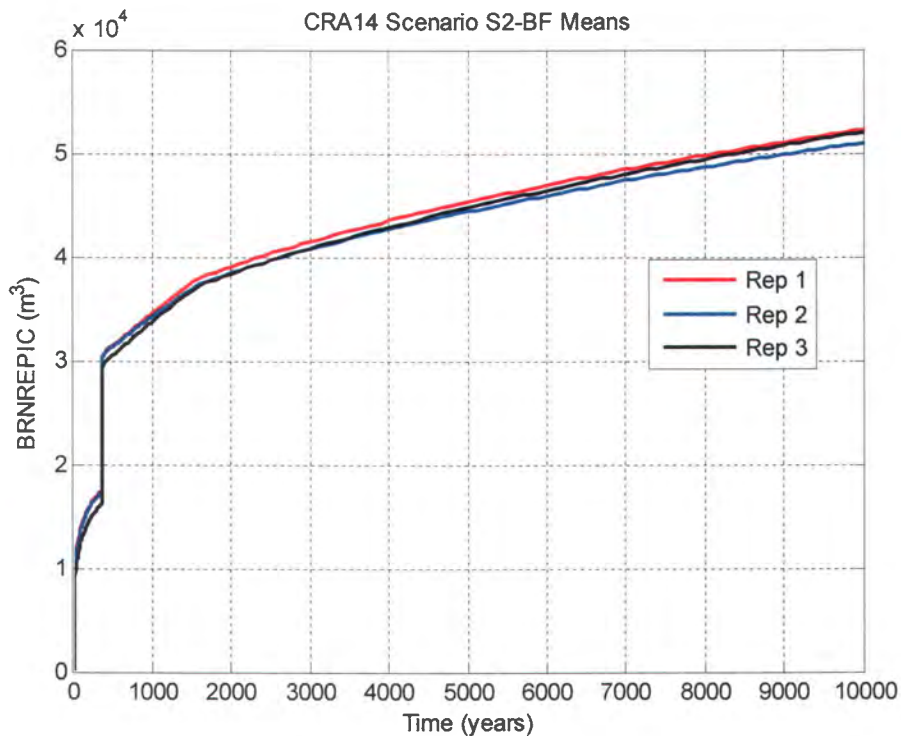


Figure 6-91: Replicate Means of Cumulative Brine Inflow to the Repository, Case CRA14-0, Scenario S2-BF.



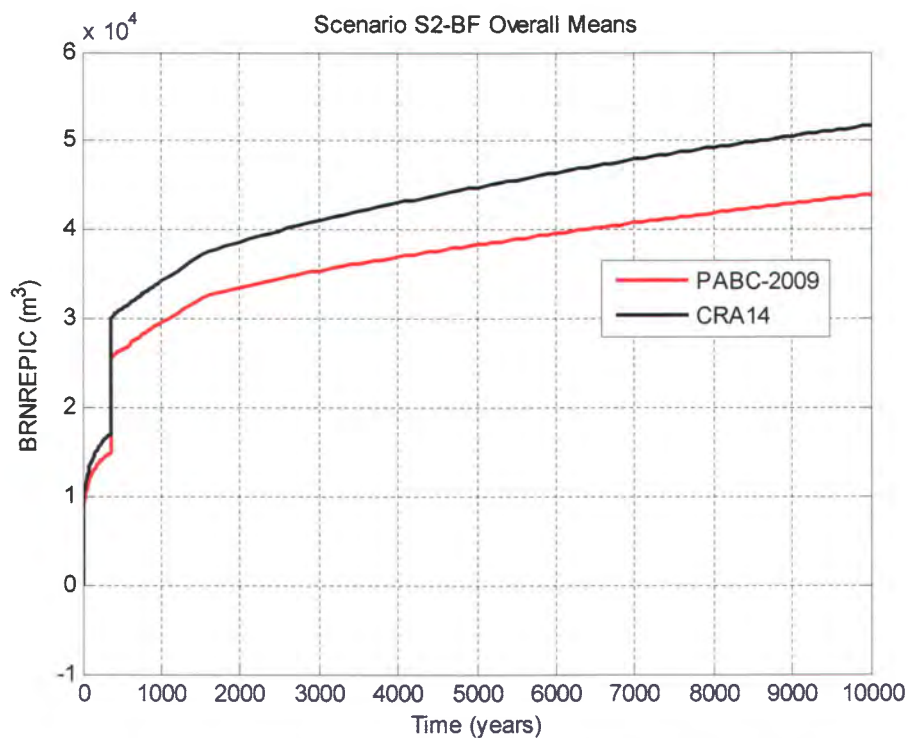


Figure 6-92: Overall Means of Cumulative Brine Inflow to the Repository, Scenario S2-BF.

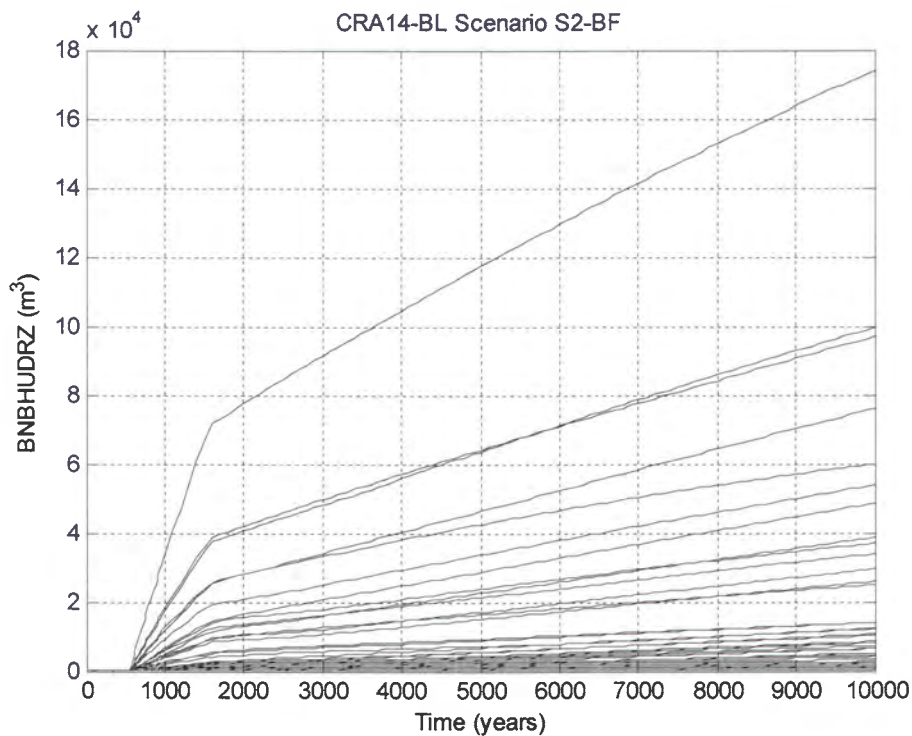


Figure 6-93: Horsetail Plot of Brine Flow up the Borehole, Case CRA14-BL, Scenario S2-BF.

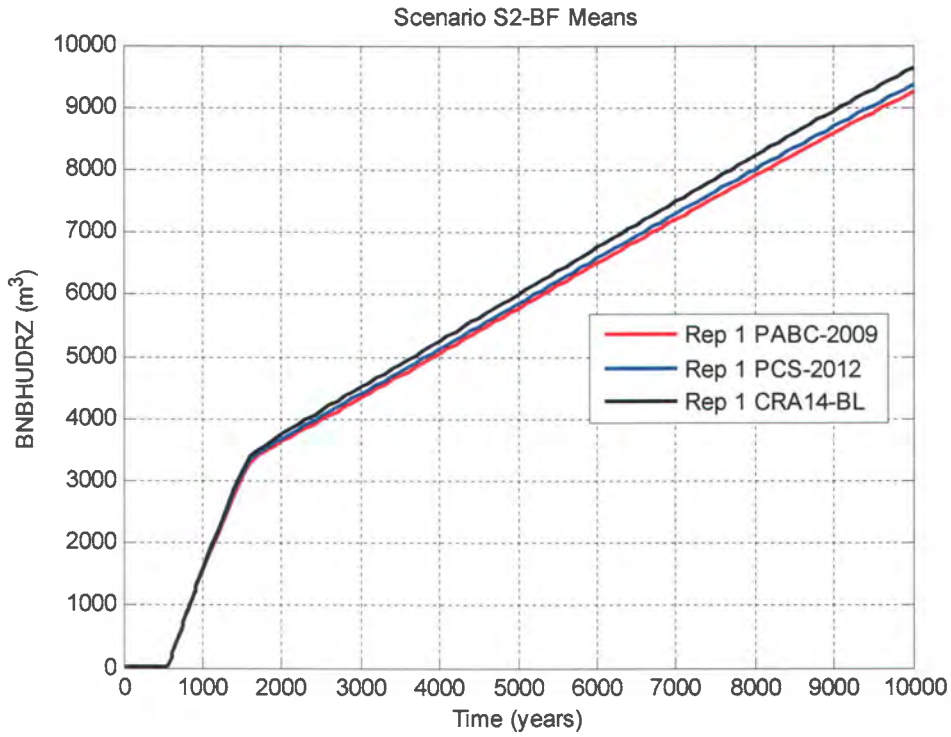


Figure 6-94: Replicate 1 Means of Brine Flow up the Borehole, Scenario S2-BF.

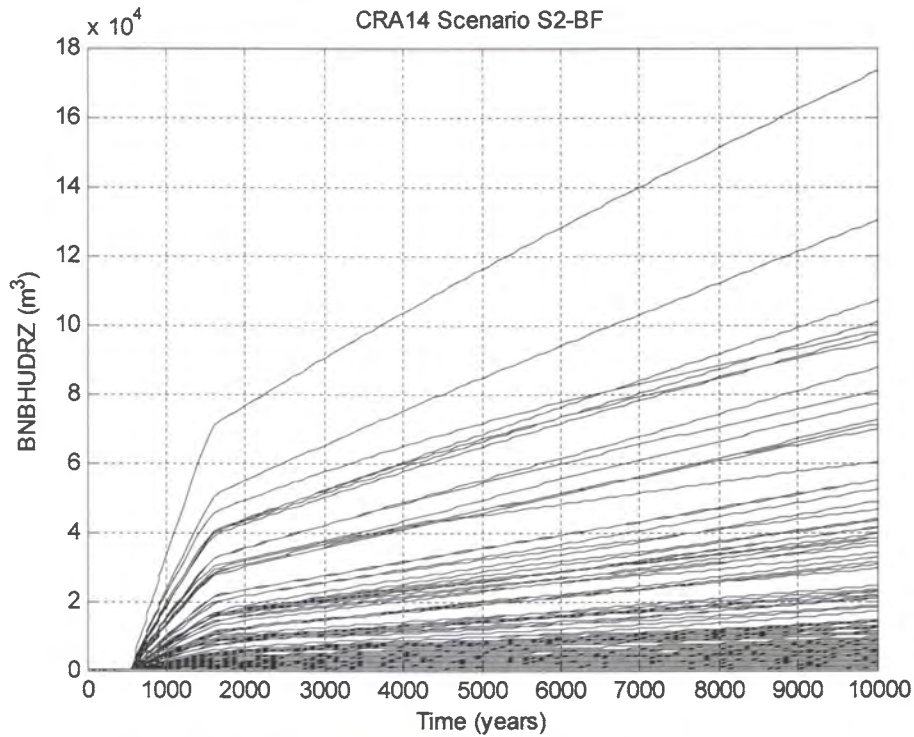


Figure 6-95: Horsetail Plot of Cumulative Brine Inflow to the Repository, Case CRA14-0, Scenario S2-BF.

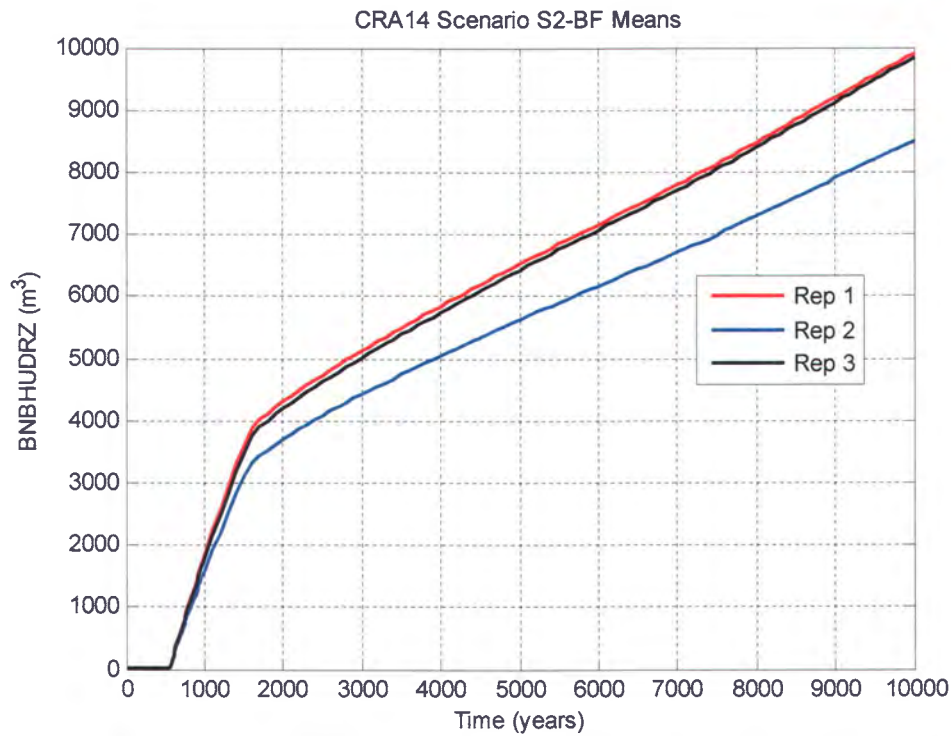


Figure 6-96: Replicate Means of Brine Flow up the Borehole, Case CRA14-0, Scenario S2-BF.

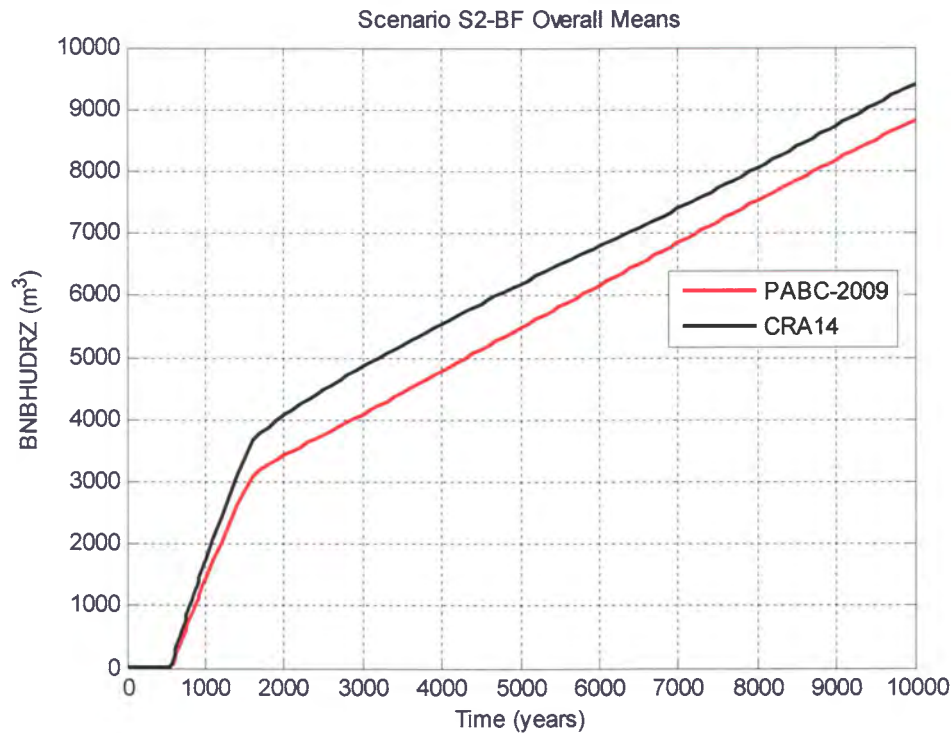


Figure 6-97: Overall Means of Brine Flow up the Borehole, Scenario S2-BF.

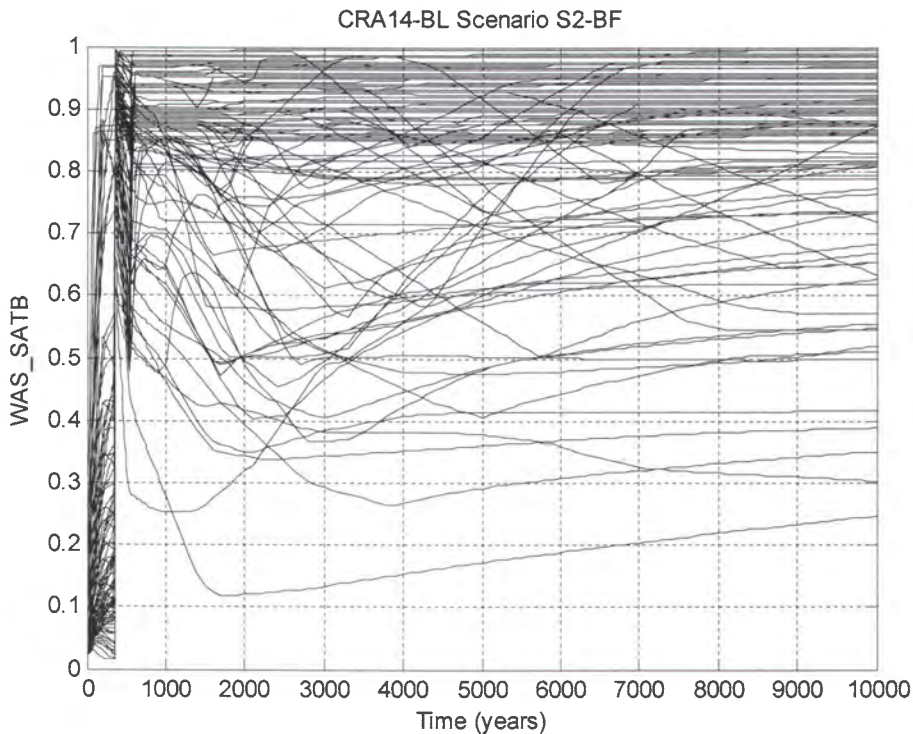


Figure 6-98: Horsetail Plot of Waste Panel Brine Saturation, Case CRA14-BL, Scenario S2-BF.

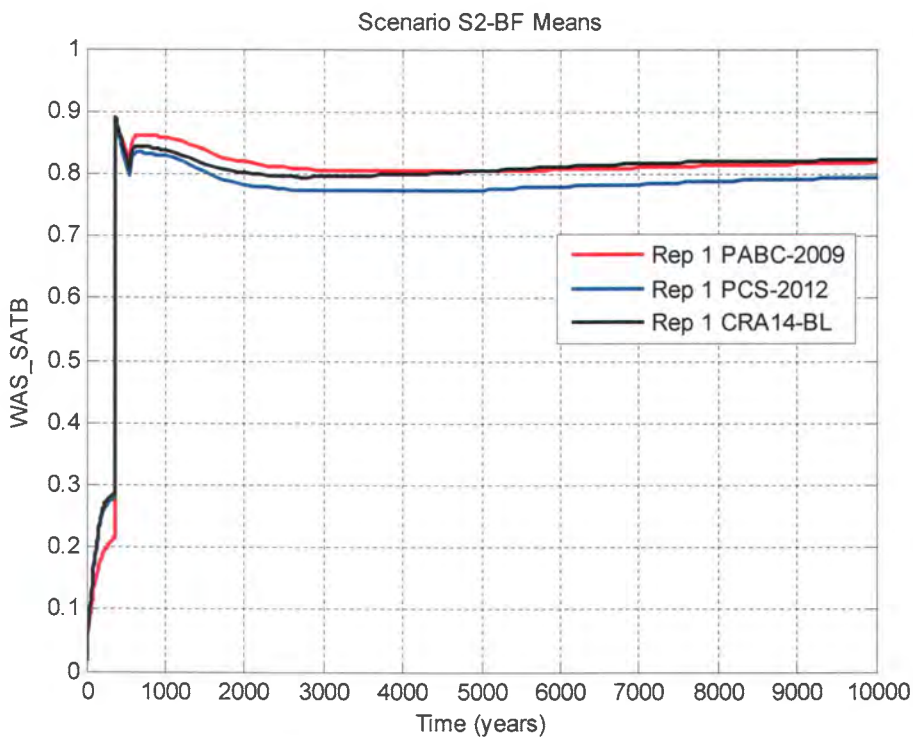


Figure 6-99: Replicate 1 Means of Waste Panel Brine Saturation, Scenario S2-BF.

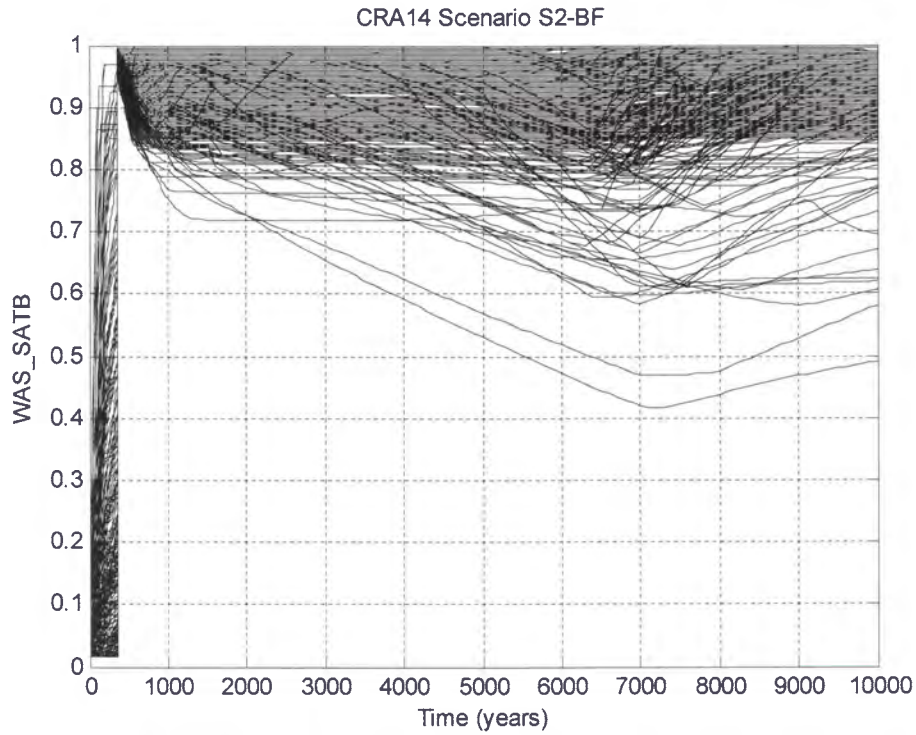


Figure 6-100: Horsetail Plot of Waste Panel Brine Saturation, Case CRA14-0, Scenario S2-BF.

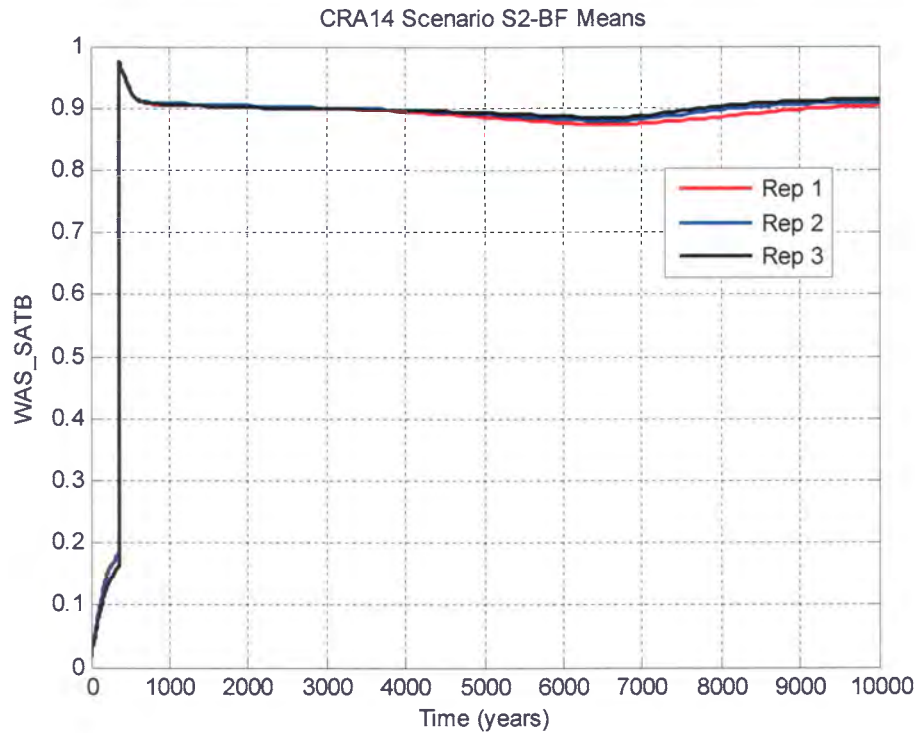


Figure 6-101: Replicate Means of Waste Panel Brine Saturation, Case CRA14-0, Scenario S2-BF.

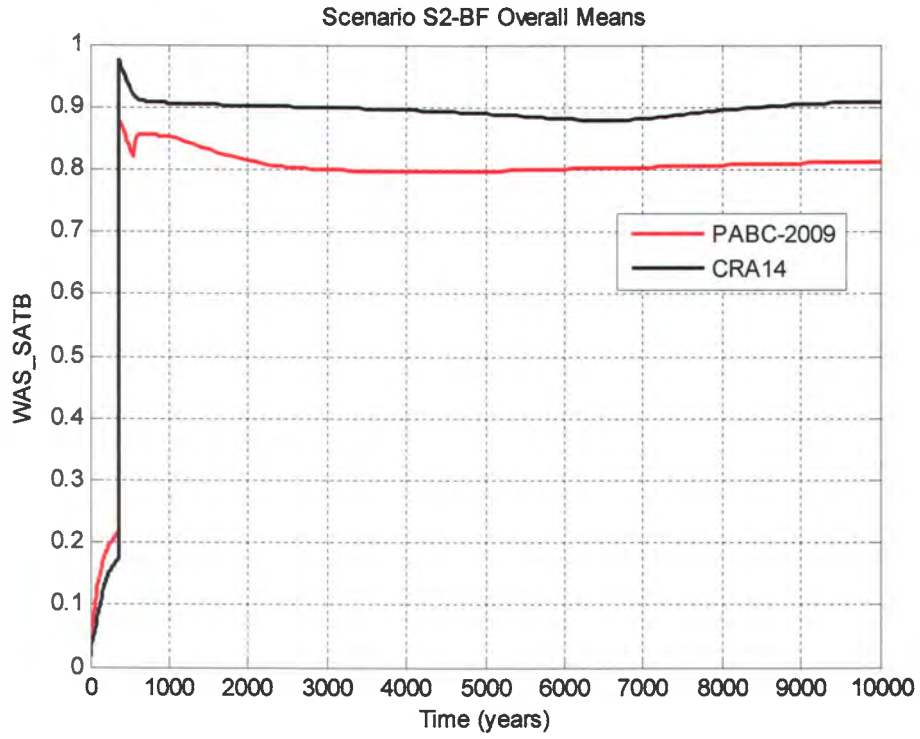


Figure 6-102: Overall Means of Waste Panel Brine Saturation, Scenario S2-BF.

### 6.3 Results for an E2 Intrusion at 350 Years (Scenario S4-BF)

Results are now presented for disturbance scenario S4-BF. Results presented for this scenario are representative of those calculated for E2 intrusion scenarios (scenarios S4-BF and scenario S5-BF), with the only difference being the time of intrusion. In the results that follow, trends discussed for scenario S4-BF also apply to scenario S5-BF. Results presented in this section are limited to those calculated for the intruded waste panel. Quantities calculated for the SRoR, NRoR, and experimental repository regions in scenario S4-BF are very similar to those calculated and previously discussed for undisturbed conditions. Results for each quantity calculated in scenario S4-BF are presented first for Case CRA14-BL, followed by their Case CRA14-0 counterpart.

#### Pressure

The horsetail plot of volume-averaged waste panel pressure obtained in Case CRA14-BL is shown in Figure 6-103. The replicate 1 means of this quantity obtained in the PABC-2009, the PCS-2012 PA, and Case CRA14-BL are shown together in Figure 6-104. As seen in that figure, and discussed more fully in Camphouse (2012a), the “tighter” ROMPCS design results in a slight increase in the mean waste panel pressure in the PCS-2012 PA result as compared to the PABC-2009. The inclusion of additional mined volume in the WIPP experimental area in Case CRA14-BL slightly reduces the mean waste panel pressure following the intrusion, resulting in a mean waste panel pressure curve for Case CRA14-BL that is generally lower than that obtained in the PABC-2009 for most of the regulatory time period. This waste panel pressure trend seen in Case CRA14-BL is consistent with that seen and discussed in Camphouse et al. (2011). The horsetail plot of waste panel pressure obtained for the 300 vector realizations of Case CRA14-0 is shown in Figure 6-105, with the three replicate means plotted together in Figure 6-106. The addition of the refined iron corrosion rate and water budget implementation utilized in Case CRA14-0 results in a reduction in the overall mean waste panel pressure as compared to the PABC-2009 for undisturbed conditions (Figure 6-5). Consequently, at the time of the E2 intrusion, the mean waste panel pressure is lower in the CRA14-0 result than in the PABC-2009, and is also lower 200 years later when the borehole plugs fail. The result is a lower scenario S4-BF mean pressure curve in Case CRA14-0 than in the PABC-2009 result. The overall means of waste panel pressure obtained in the PABC-2009 and Case CRA14-0 are plotted together in Figure 6-107.

#### Gas Generation

As was the case for the undisturbed results, the reduction in mean waste panel pressure from Case CRA14-BL to CRA14-0 is largely due to the revised iron corrosion rate implemented in the latter case. The horsetail plot of molar gas generation in the intruded waste panel obtained in Case CRA14-BL is shown in Figure 6-108. The replicate 1 mean of quantity GASMOL\_W obtained in Case CRA14-BL is shown in Figure 6-109. Also seen in that figure are the mean curves of molar gas generation due to iron corrosion and microbial degradation of cellulose in the waste panel. As is clear from Figure 6-109, the majority of gas generated in the intruded panel for Case CRA14-BL is due to iron corrosion. The horsetail plot of molar gas generation in the waste panel for Case CRA14-0 is shown in Figure 6-110. Means of waste panel molar gas generation obtained in Case CRA14-0 are shown in Figure 6-111. (Figure 6-111 includes

replicate 1 means as well as overall means to allow for direct comparison to results shown in Figure 6-109.) As is clear from Figure 6-111, gas generation due to iron corrosion is still the dominant gas production mechanism in Case CRA14-0. The influx of brine to the waste panel after the borehole plugs fail at 550 years results in nearly identical mean curves for gas generation due to CPR microbial degradation in Figure 6-109 and Figure 6-111. However, mean molar gas production due to iron corrosion increases at a lower rate in the Case CRA14-0 results than in Case CRA14-BL. As the mean molar gas generation due to CPR microbial degradation is virtually unchanged from Case CRA14-BL to Case CRA14-0, the reduction (on average) in the rate of gas production due to iron corrosion yields a corresponding decrease in the rate of mean gas generation in the waste panel.

### Cumulative Brine Flow

The horsetail plot of cumulative brine inflow to the waste panel obtained for Case CRA14-BL is shown in Figure 6-112. Replicate 1 means of quantity BRNWASIC obtained in the PABC-2009, the PCS-2012 PA, and Case CRA14-BL are plotted together in Figure 6-113. As discussed in Camphouse (2012a), the replacement of the Option D PCS with the ROMPCS results in an increase to the mean waste panel brine inflow for scenario S4-BF as compared to the PABC-2009. The added mined volume in the experimental region for Case CRA14-BL very slightly increases the overall mean of quantity BRNWASIC in Case CRA14-BL relative to the PCS-2012 PA result. The horsetail plot of quantity BRNWASIC obtained in Case CRA14-0 is shown in Figure 6-114, with the three replicate means plotted together in Figure 6-115. Good agreement is seen among the three replicate means. Mean waste panel pressure is significantly reduced in Case CRA14-0 as compared to the PABC-2009 for the undisturbed repository (Figure 6-5). This pressure reduction allows increased brine flow to the waste panel prior to the E2 intrusion at 350 years, as well as increased brine inflow to the panel after the borehole plugs fail at 550 years. The result is an overall mean curve for quantity BRNWASIC in Case CRA14-0 that is greater than that obtained in the PABC-2009 (Figure 6-116).

Trends observed for the waste panel also hold for the repository overall. Increased brine inflow to the intruded panel yields an increase to brine inflow to the repository overall for scenario S4-BF. Results for cumulative brine inflow to the repository, quantity BRNREPIC, are shown in Figure 6-117 to Figure 6-121.

The horsetail plot of cumulative brine flow up the intrusion borehole obtained in Case CRA14-BL is shown in Figure 6-122. Replicate 1 means obtained for quantity BNBHUDRZ in the PABC-2009, the PCS-2012 PA, and Case CRA14-BL are plotted together in Figure 6-123. As is clear from that figure, results obtained in Case CRA14-BL are nearly identical to those calculated in the PCS-2012 PA. Replicate 1 mean curves of quantity BNBHUDRZ obtained in Case CRA14-BL and the PCS-2012 PA are both greater than the corresponding replicate mean calculated in the PABC-2009. Results obtained for quantity BNBHUDRZ in Case CRA14-0 are shown in Figure 6-124 to Figure 6-126. The increased brine inflow to the waste panel in scenario S4-BF yields an increase in the overall mean obtained for quantity BNBHUDRZ in Case CRA14-0 as compared to the PABC-2009 (Figure 6-126).



### Brine Saturation

The increased brine inflow to the waste panel in the CRA14-0 results has a direct impact on waste panel brine saturation. The horsetail plot of quantity WAS\_SATB obtained in Case CRA14-BL is shown in Figure 6-127. Replicate 1 means obtained for this quantity in the PABC-2009, the PCS-2012 PA, and Case CRA14-BL are shown together in Figure 6-128, and generally follow the trends seen for quantity BRNWASIC in Figure 6-113. The horsetail plot obtained for quantity WAS\_SATB in Case CRA14-0 is shown in Figure 6-129, with replicate means shown in Figure 6-130. The increased mean waste panel brine inflow seen in Case CRA14-0 as compared to the PABC-2009 yields a corresponding increase in the Case CRA14-0 mean waste panel brine saturation following the failure of the borehole plugs at 550 years (Figure 6-131).

### Summary of Results for E2 Intrusion Scenarios

For E2 intrusion scenarios, results obtained for the SRoR, NRoR, and the repository experimental area do not change appreciably from those seen for the undisturbed repository. Changes included in the CRA-2014 PA yield a decrease to the mean pressure in the intruded panel as compared to results from the PABC-2009. The replacement of the Option D PCS with the ROMPCS results in reduced mean pressure in the waste panel prior to the E2 intrusion. The refined water balance implementation sequesters water, reducing the amount that is freely available for gas production processes prior to the intrusion. The revised iron corrosion rate utilized in Case CRA14-0 results in slower gas production due to iron corrosion (on average). As gas generation due to iron corrosion is the dominant gas production mechanism, the reduction (on average) in the rate of gas production due to iron corrosion yields a corresponding decrease in the rate of mean gas generation in the waste panel, further lowering waste panel mean pressure. Consequently, at the time of the E2 intrusion, the mean waste panel pressure is lower in the CRA14-0 result than in the PABC-2009, and is also lower 200 years later when the borehole plugs fail. Cumulative brine inflows to the intruded waste panel are greater (on average) in the CRA14-0 results as compared to the PABC-2009 due to the reduction in mean pressure. The increased mean brine inflow yields a corresponding increase to the mean brine saturation of the intruded panel for the Case CRA14-0 results. Cumulative brine flow up the borehole is increased (on average) in Case CRA14-0 as compared to the PABC-2009, but the increase is similar to that calculated in the PCS-2012 PA.

Summary statistics for BRAGFLO scenario S4-BF are shown in Table 6-3. Results presented in that table are calculated over all 300 vector realizations (and all times) of the PABC-2009 and Case CRA14-0 of the CRA-2014 PA.

Table 6-3: Summary Statistics for Scenario S4-BF

Quantity (units)	Description	Mean Value		Maximum Value	
		PABC-2009	CRA14-0	PABC-2009	CRA14-0
WAS_PRES (MPa)	Volume-averaged pressure in the waste panel.	4.64	2.86	14.92	14.85
GASMOL_W (x10 <sup>6</sup> moles)	Total moles of gas generated in the intruded panel.	36.40	21.58	149.00	92.54
BRNWASIC (x10 <sup>3</sup> m <sup>3</sup> )	Cumulative brine inflow to the waste panel.	2.73	3.81	23.81	21.04
BRNREPIC (x10 <sup>3</sup> m <sup>3</sup> )	Cumulative brine inflow to the entire repository.	19.11	22.79	117.40	139.90
WAS_SATB (none)	Brine saturation in the waste panel.	0.28	0.33	0.99	0.99
BNBHADRZ (m <sup>3</sup> )	Cumulative brine flow up the intrusion borehole.	34.76	52.36	4876.89	5390.83

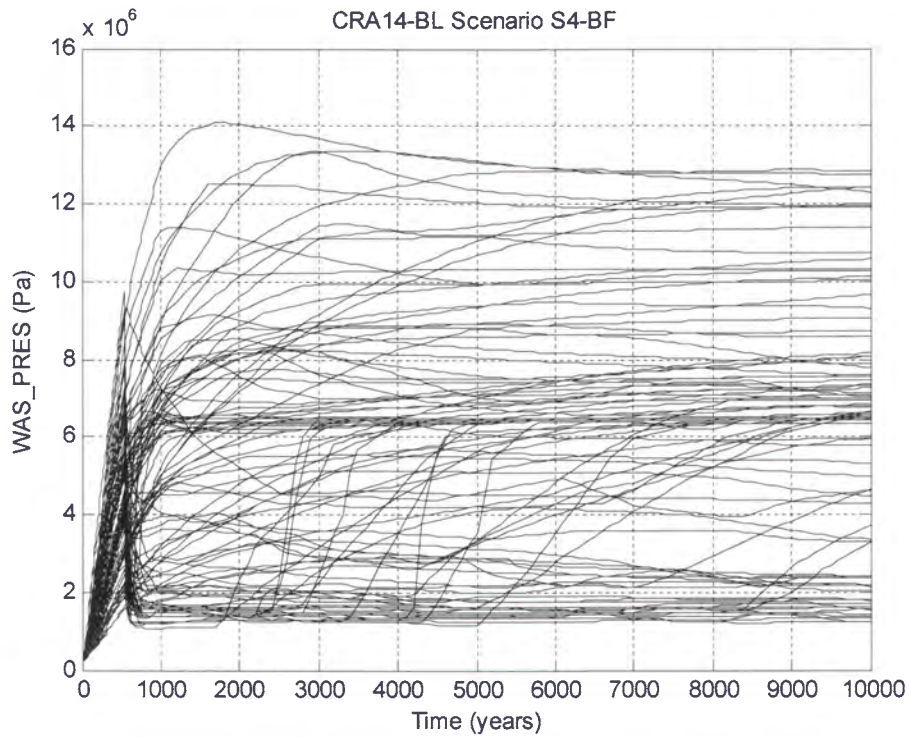


Figure 6-103: Horsetail Plot of Waste Panel Pressure for Case CRA14-BL, Scenario S4-BF

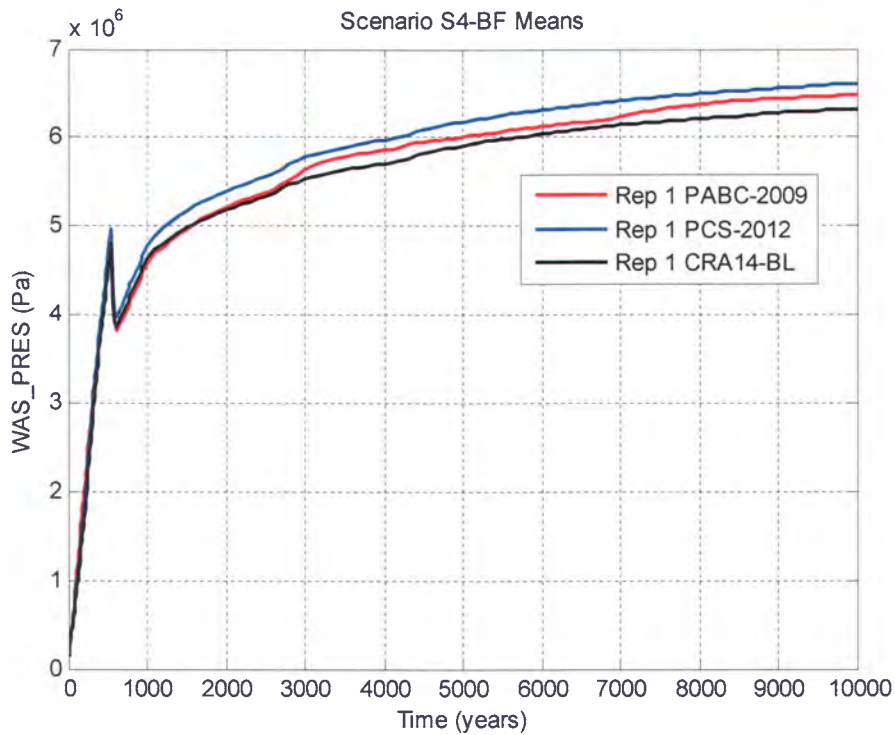


Figure 6-104: Replicate 1 Means of Waste Panel Pressure, Scenario S4-BF

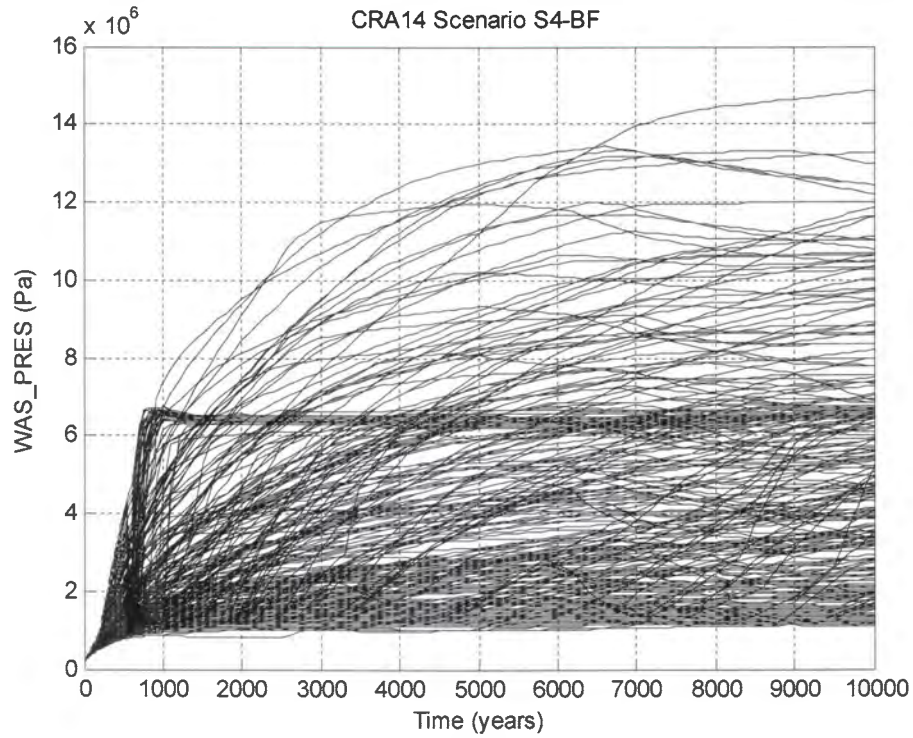


Figure 6-105: Horsetail Plot of Waste Panel Pressure for Case CRA14-0, Scenario S4-BF

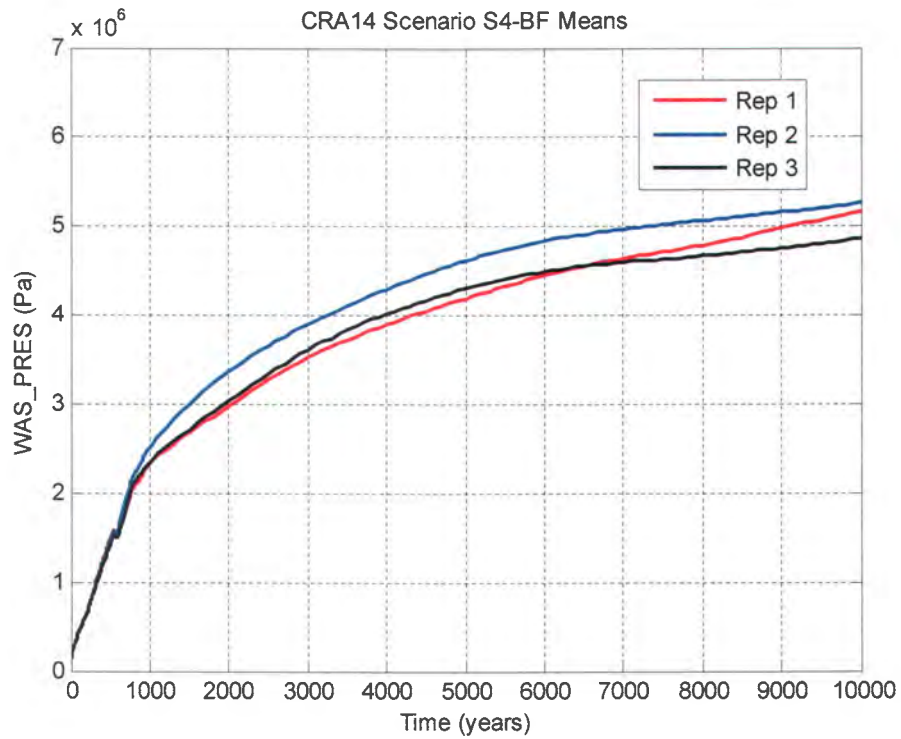


Figure 6-106: Replicate Means of Waste Panel Pressure for Case CRA14-0, Scenario S4-BF

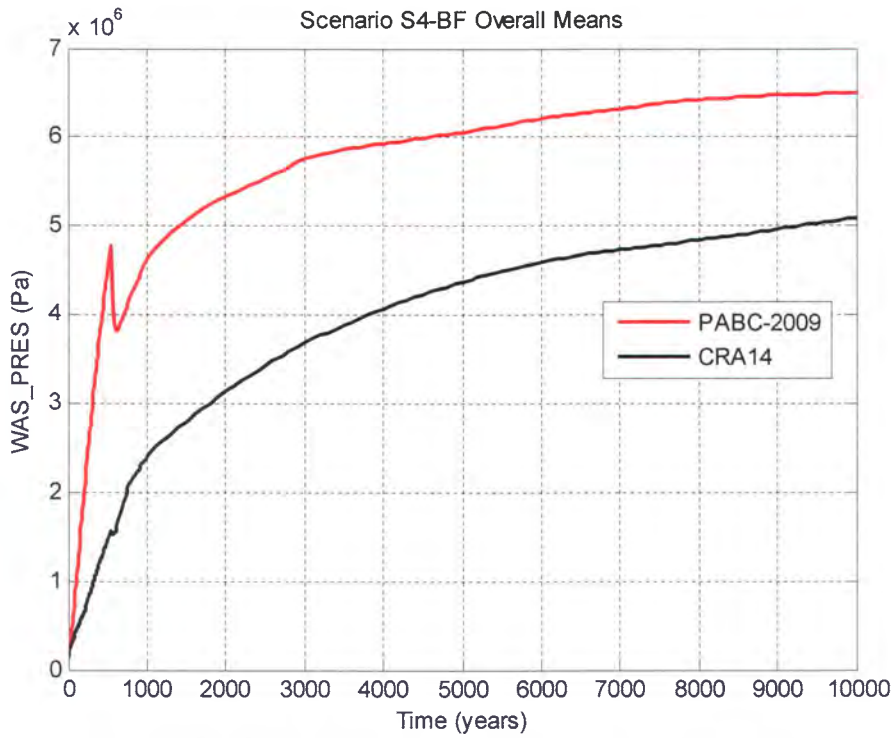


Figure 6-107: Overall Means of Waste Panel Pressure, Scenario S4-BF

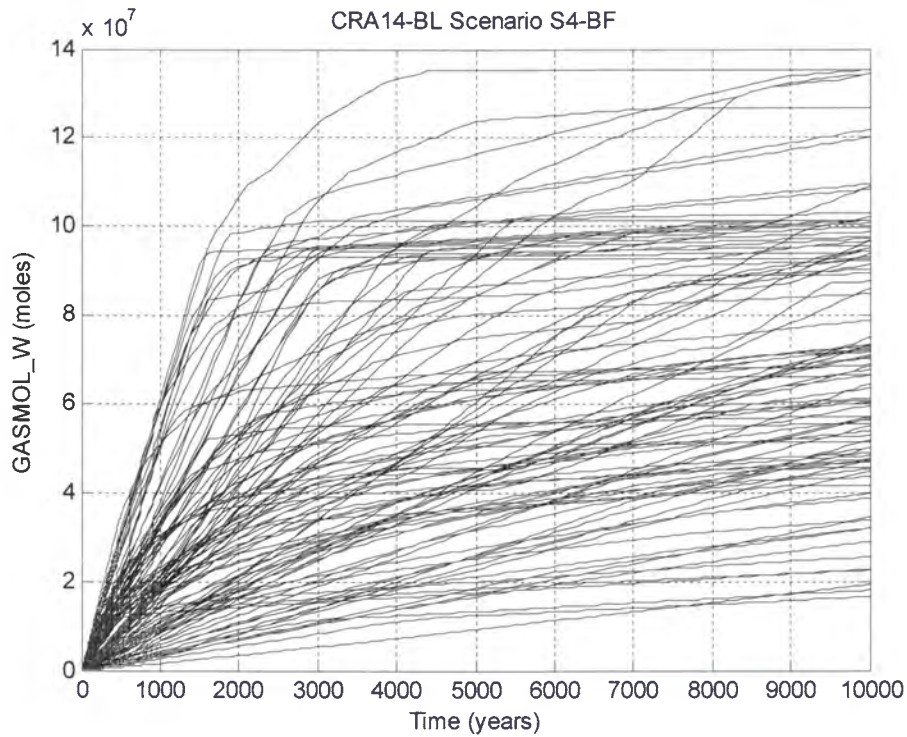


Figure 6-108: Horsetail Plot of Molar Waste Panel Gas Generation for Case CRA14-BL, Scenario S4-BF

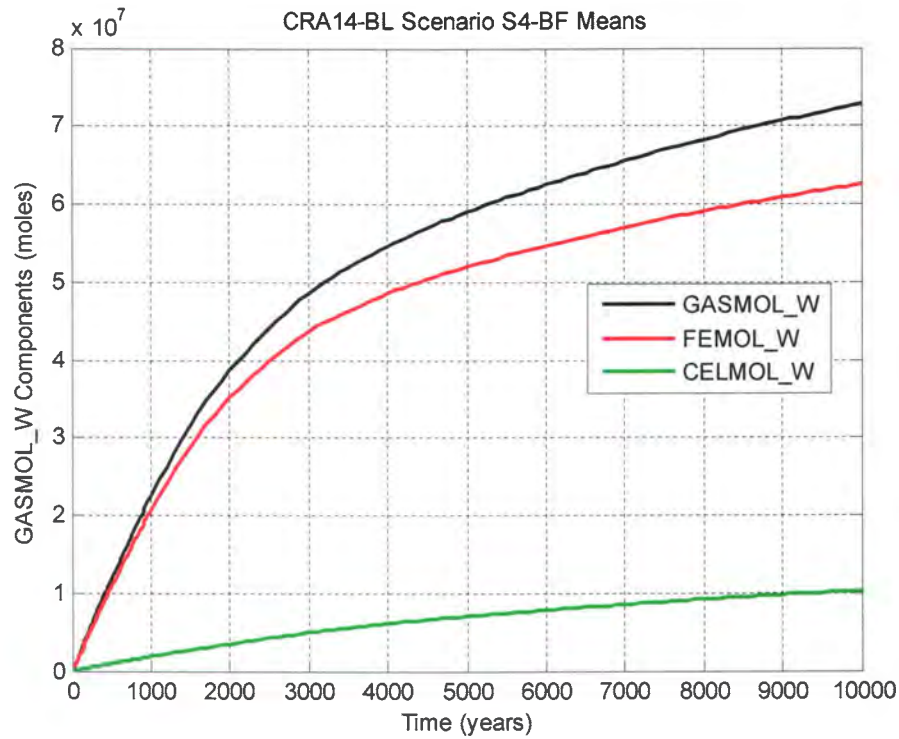


Figure 6-109: Replicate 1 Means of Molar Waste Panel Gas Generation for Case CRA14-BL, Scenario S4-BF

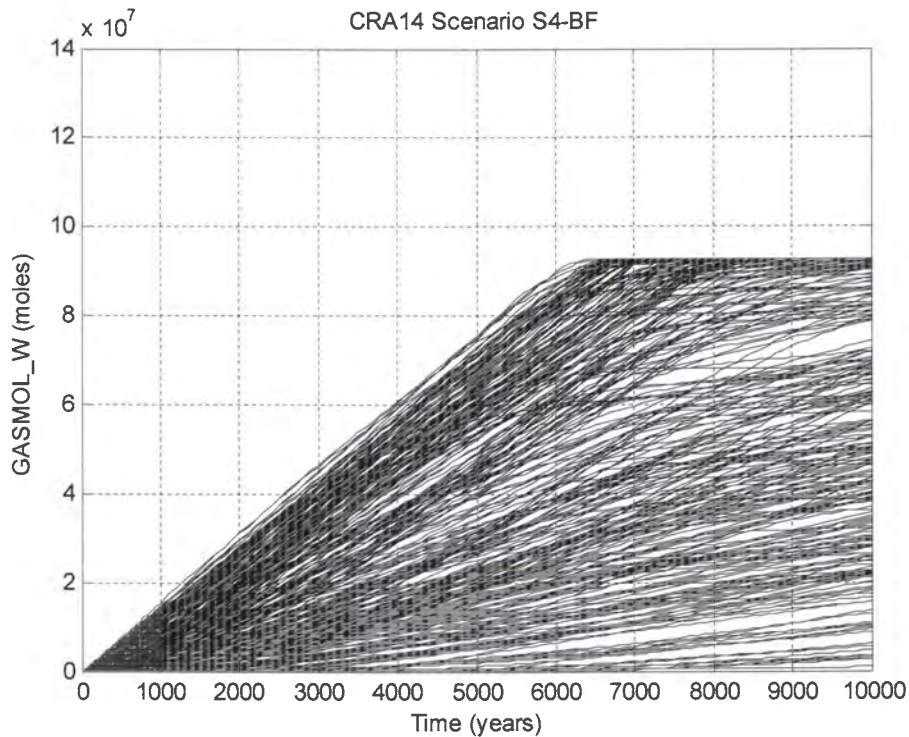


Figure 6-110: Horsetail Plot of Molar Waste Panel Gas Generation for Case CRA14-0, Scenario S4-BF

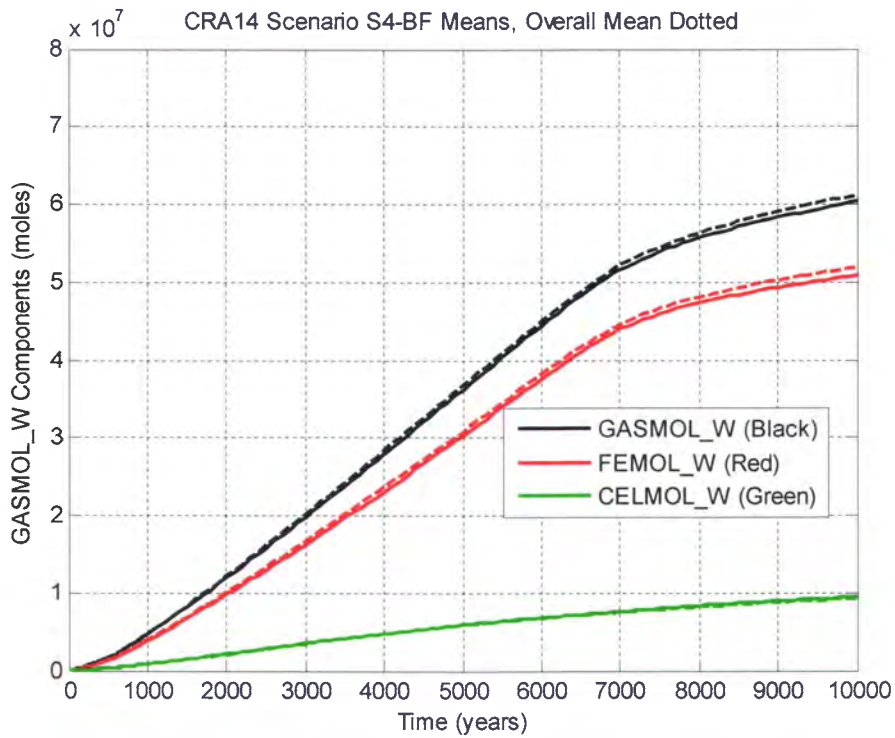


Figure 6-111: Means of Molar Waste Panel Gas Generation for Case CRA14-0, Scenario S4-BF (Replicate 1 Means – Solid, Overall Means – Dotted)

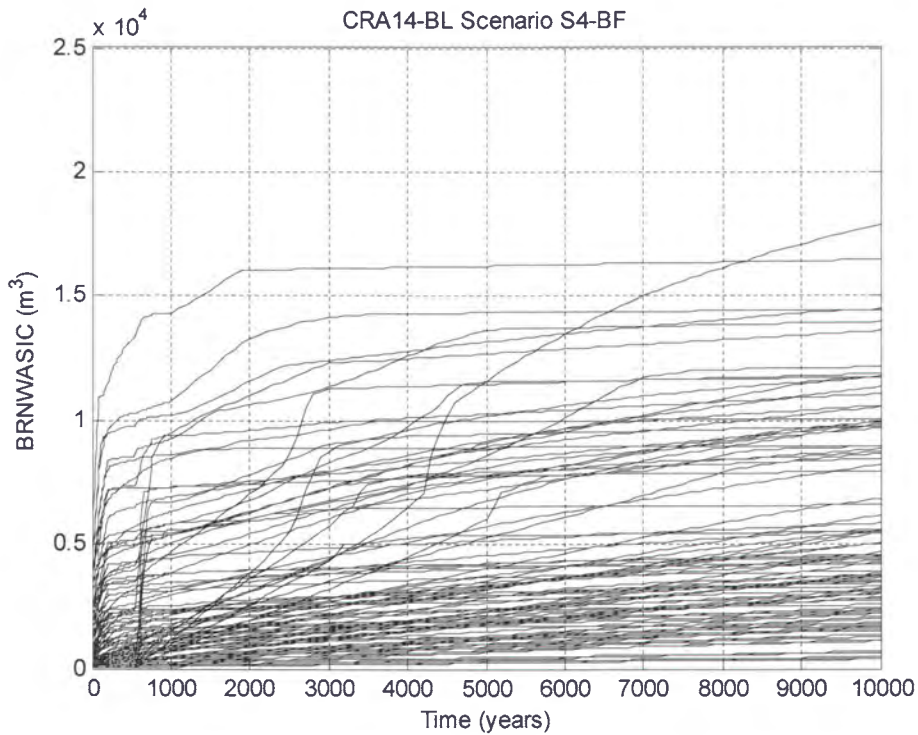


Figure 6-112: Horsetail Plot of Cumulative Brine Inflow to the Waste Panel, Case CRA14-BL, Scenario S4-BF.

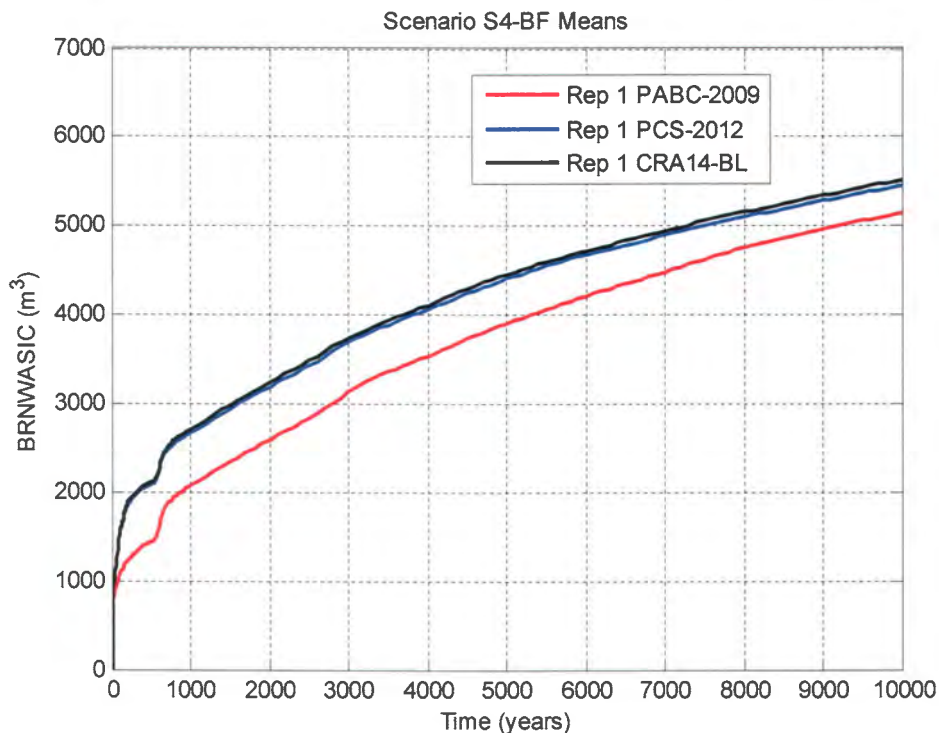


Figure 6-113: Replicate 1 Means of Cumulative Brine Inflow to the Waste Panel, Scenario S4-BF.

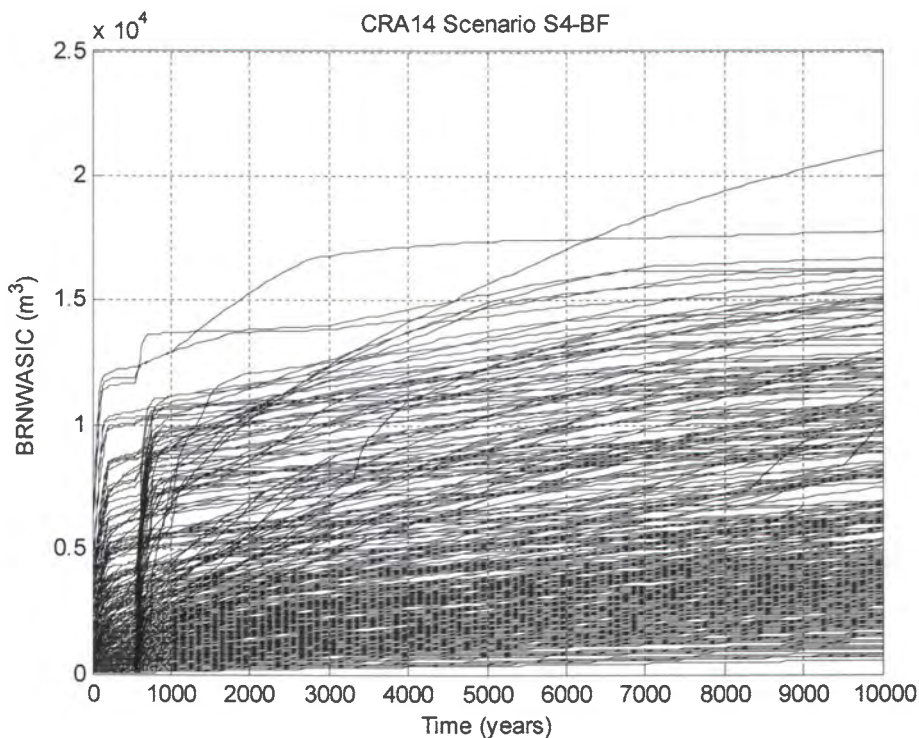


Figure 6-114: Horsetail Plot of Cumulative Brine Inflow to the Waste Panel, Case CRA14-0, Scenario S4-BF.



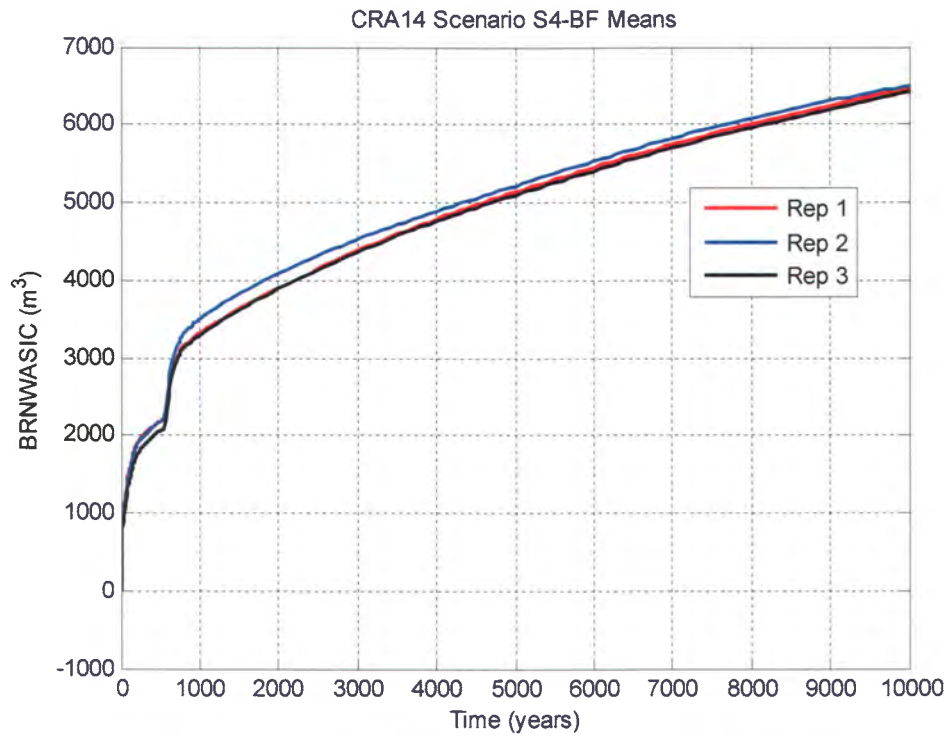


Figure 6-115: Replicate Means of Cumulative Brine Inflow to the Waste Panel, Case CRA14-0, Scenario S4-BF.

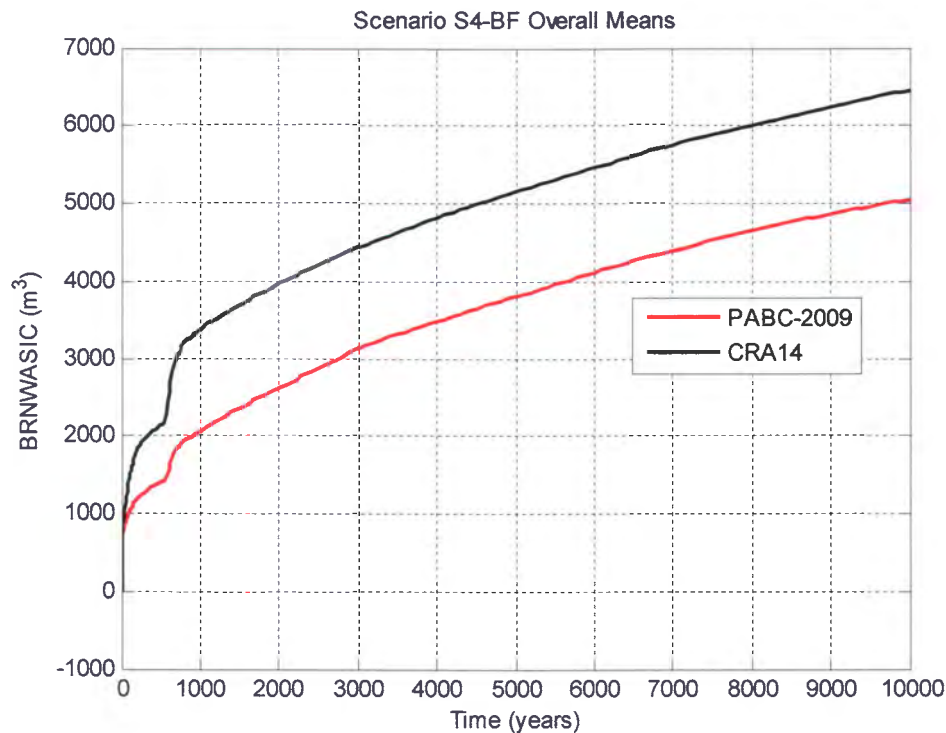


Figure 6-116: Overall Means of Cumulative Brine Inflow to the Waste Panel, Scenario S4-BF.

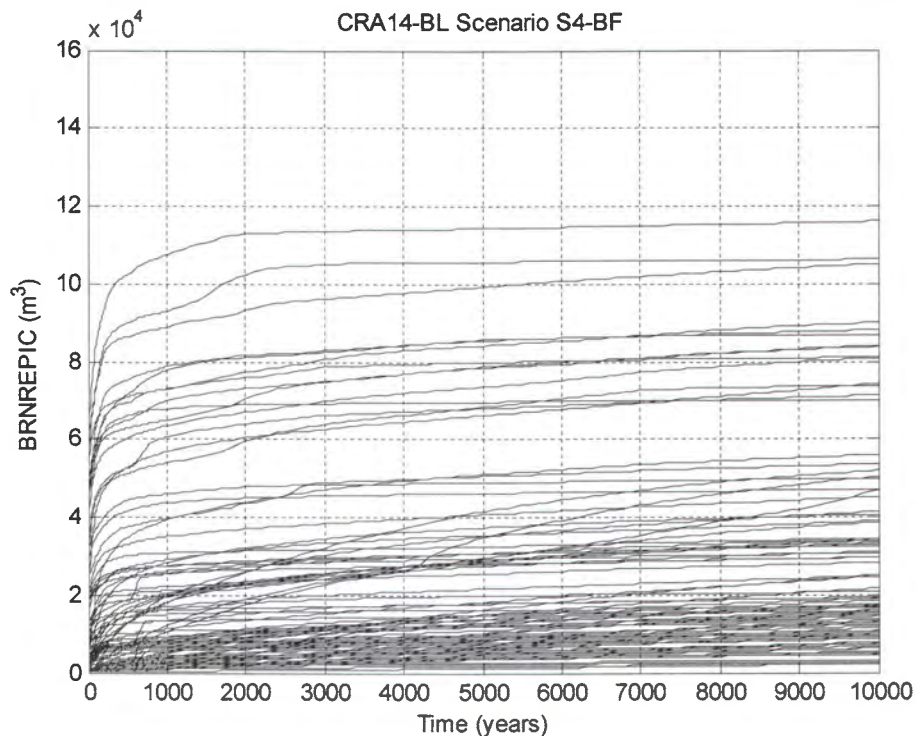


Figure 6-117: Horsetail Plot of Cumulative Brine Inflow to the Repository, Case CRA14-BL, Scenario S4-BF.

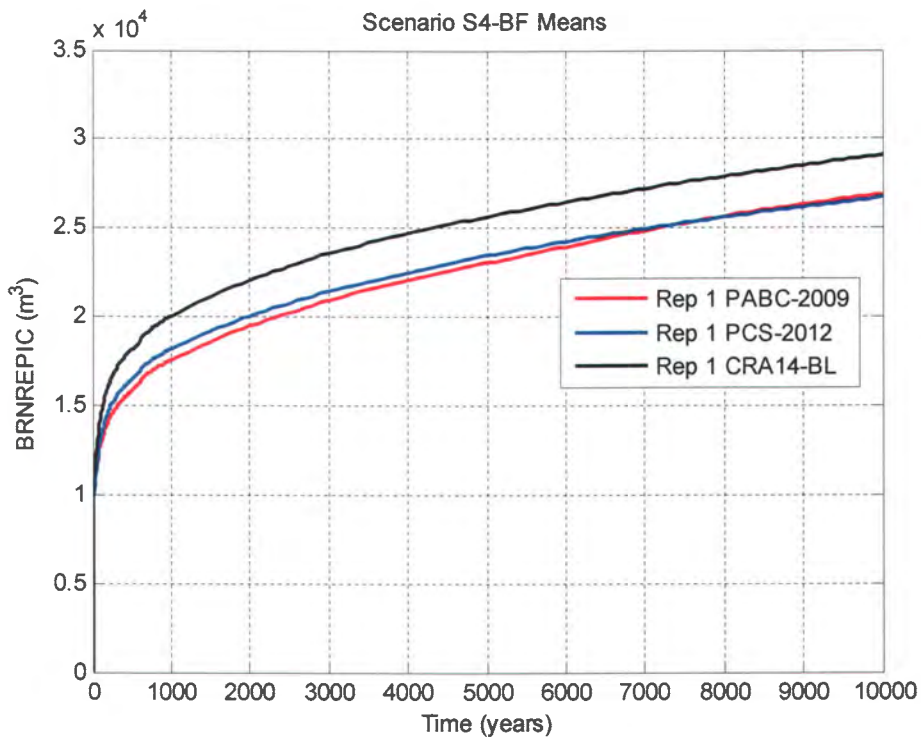


Figure 6-118: Replicate 1 Means of Cumulative Brine Inflow to the Repository, Scenario S4-BF.

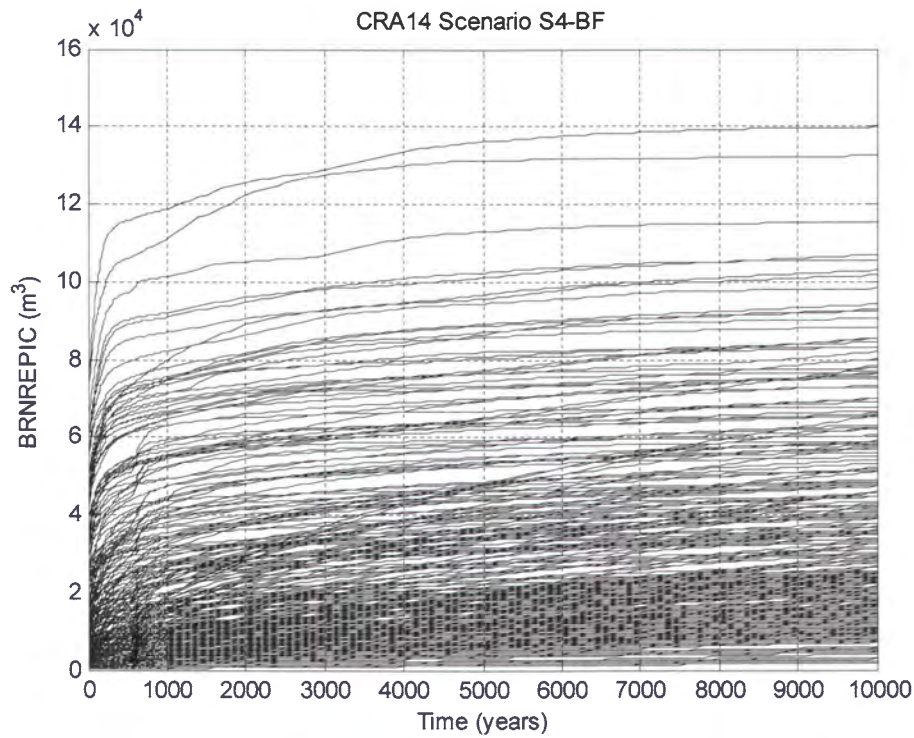


Figure 6-119: Horsetail Plot of Cumulative Brine Inflow to the Repository, Case CRA14-0, Scenario S4-BF.

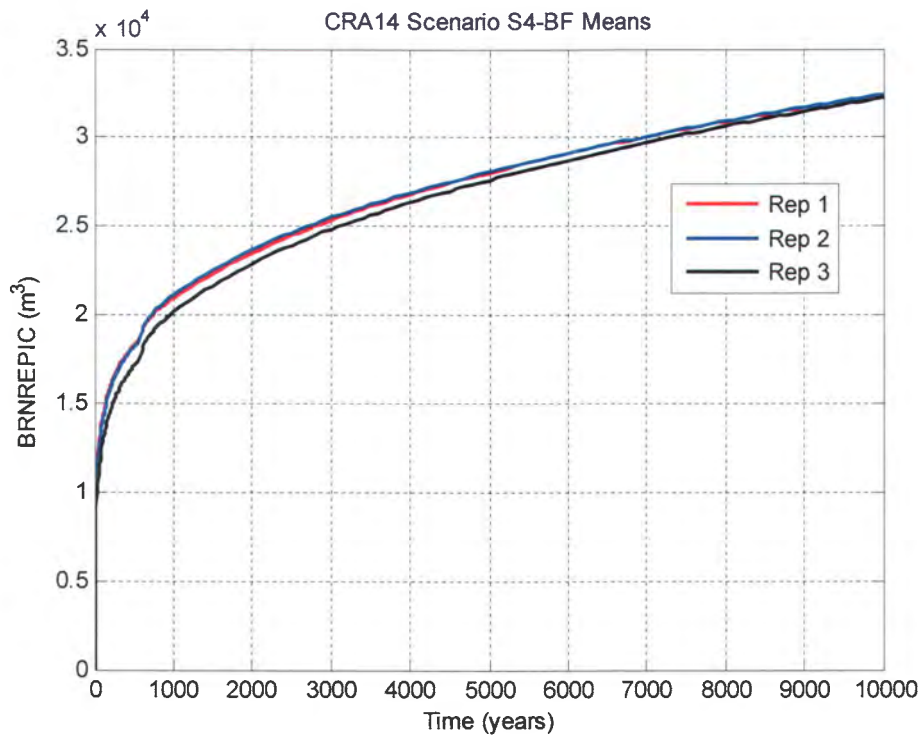


Figure 6-120: Replicate Means of Cumulative Brine Inflow to the Repository, Case CRA14-0, Scenario S4-BF.

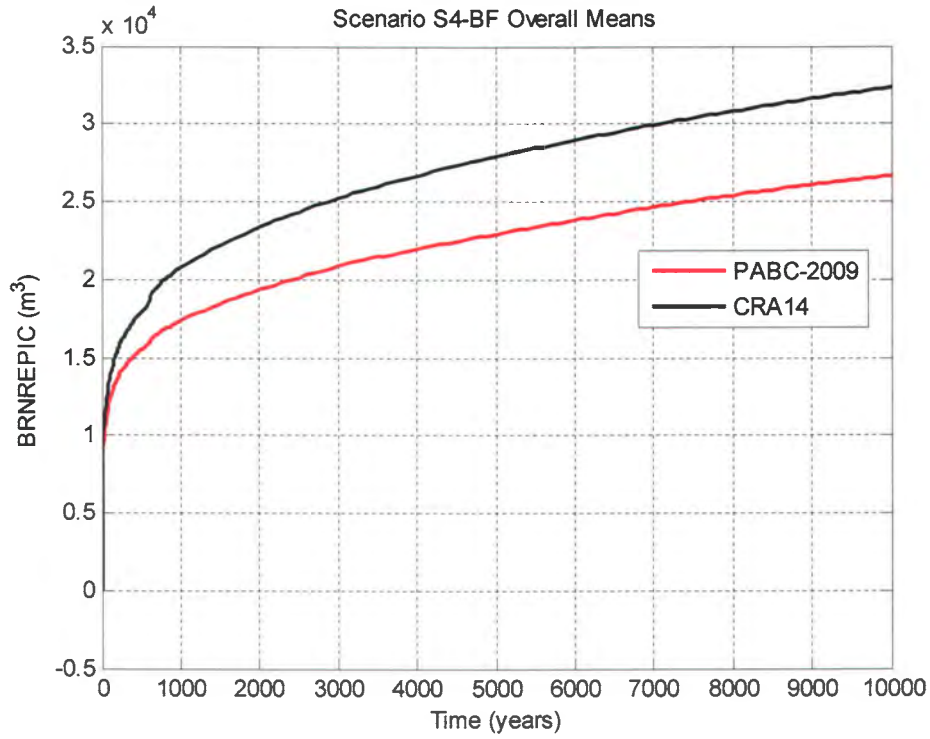


Figure 6-121: Overall Means of Cumulative Brine Inflow to the Repository, Scenario S4-BF.

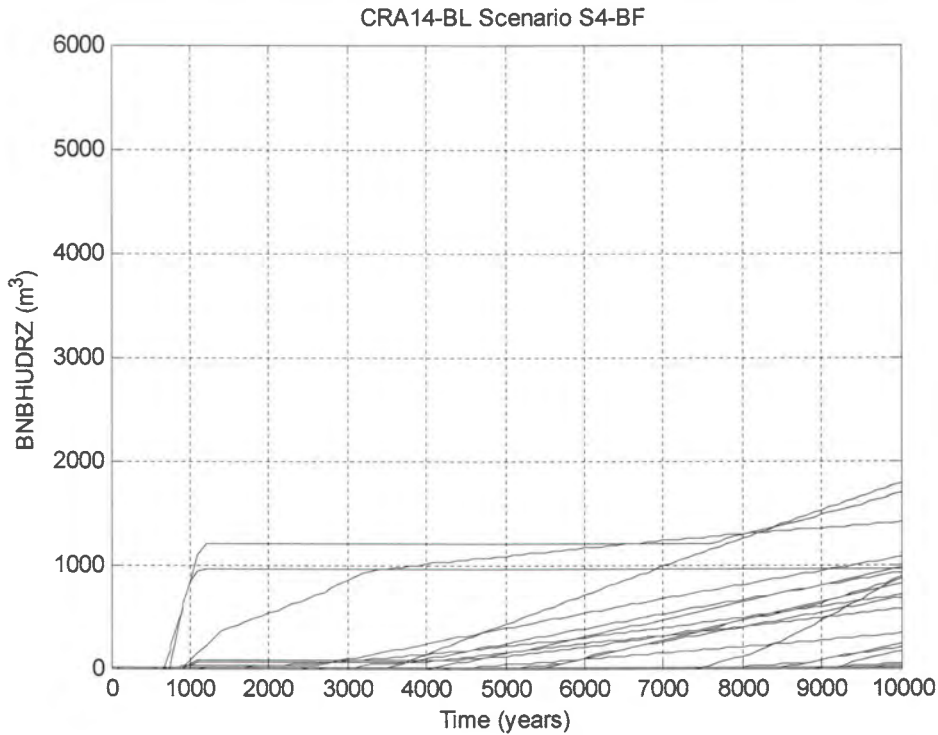


Figure 6-122: Horsetail Plot of Brine Flow up the Borehole, Case CRA14-BL, Scenario S4-BF.

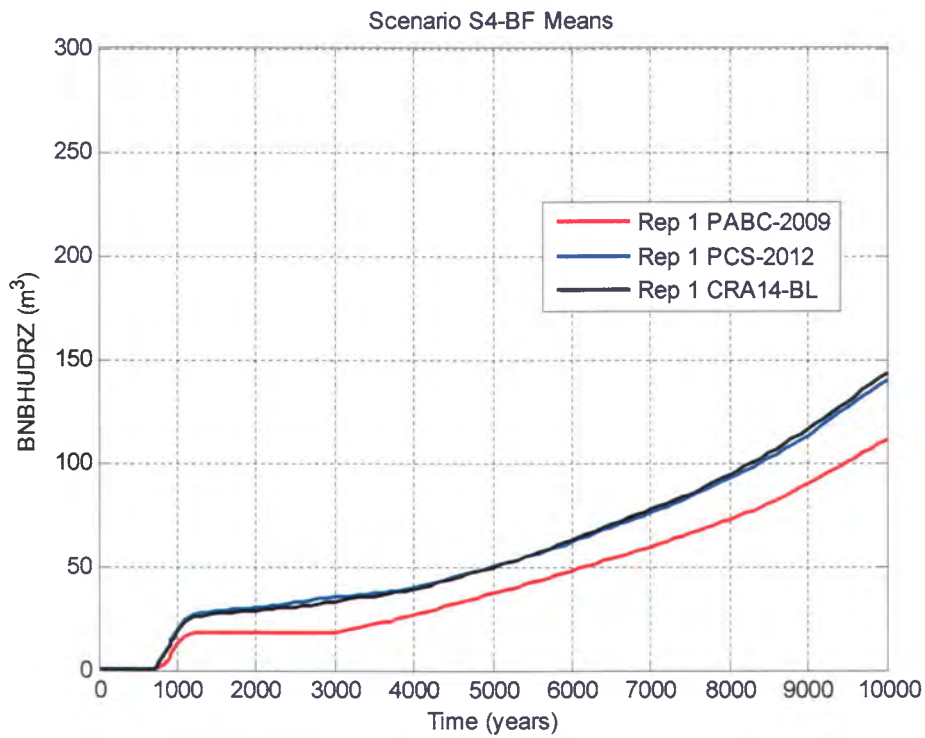


Figure 6-123: Replicate 1 Means of Brine Flow up the Borehole, Scenario S4-BF.

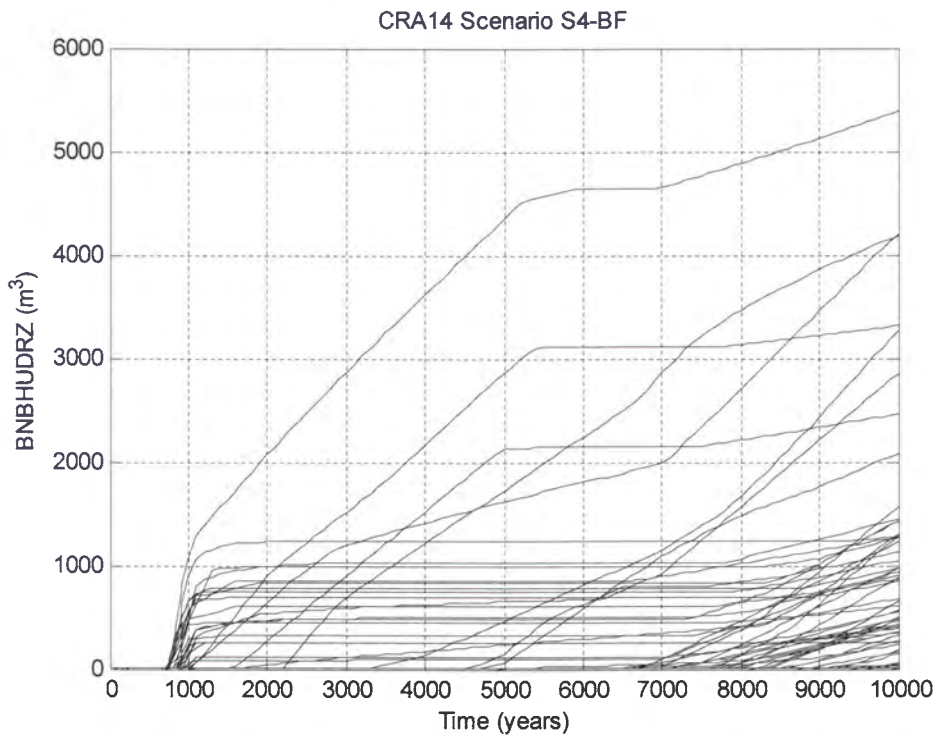


Figure 6-124: Horsetail Plot of Brine Flow up the Borehole, Case CRA14-0, Scenario S4-BF.

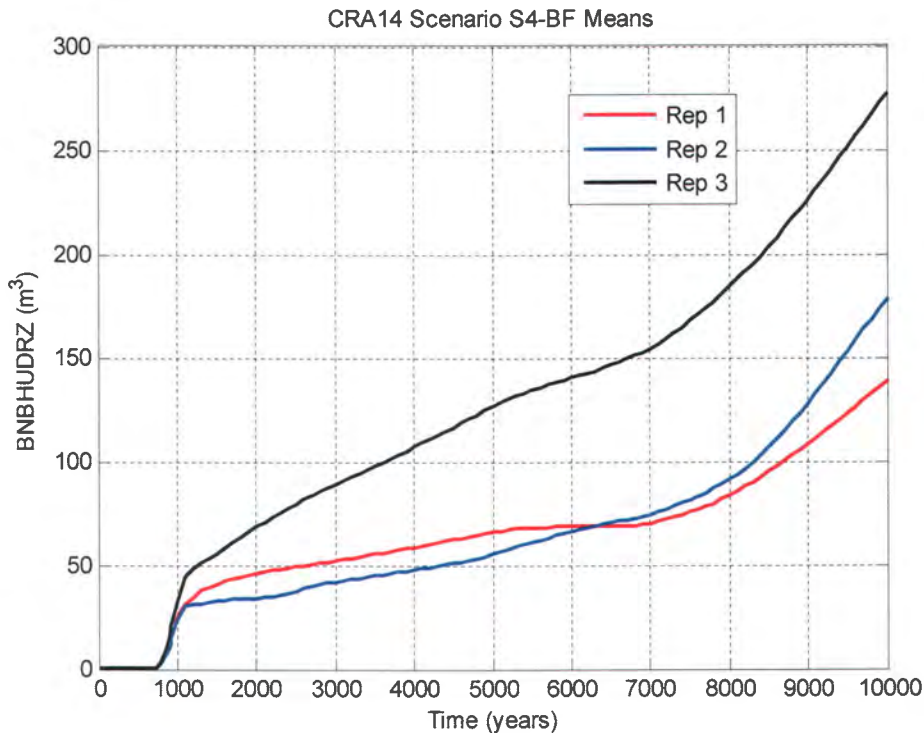


Figure 6-125: Replicate Means of Brine Flow up the Borehole, Case CRA14-0, Scenario S4-BF.

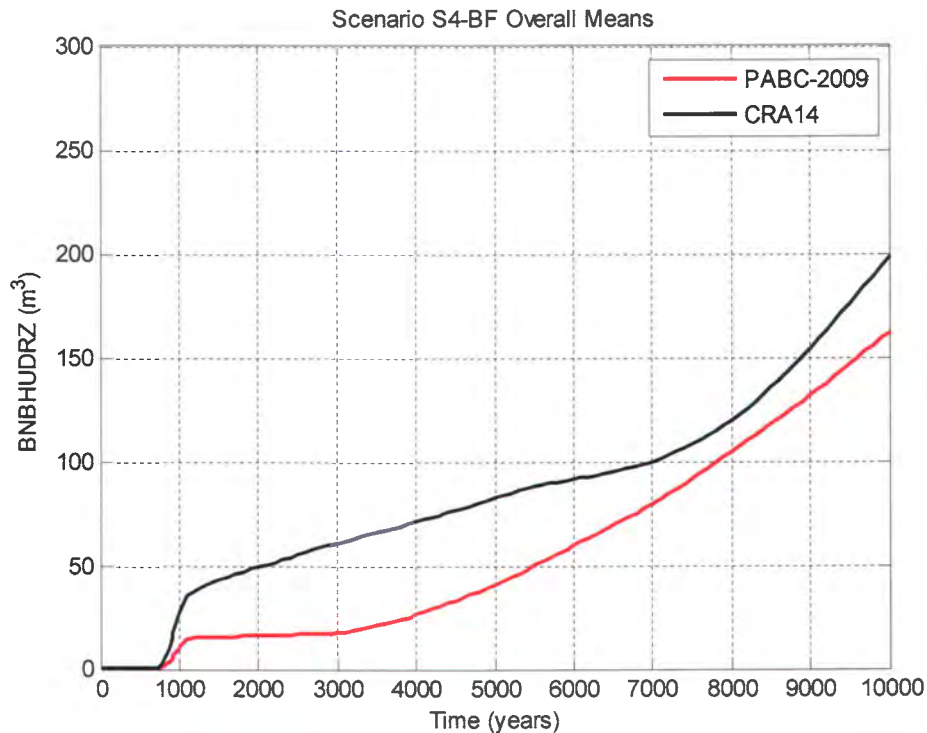


Figure 6-126: Overall Means of Brine Flow up the Borehole, Scenario S4-BF.

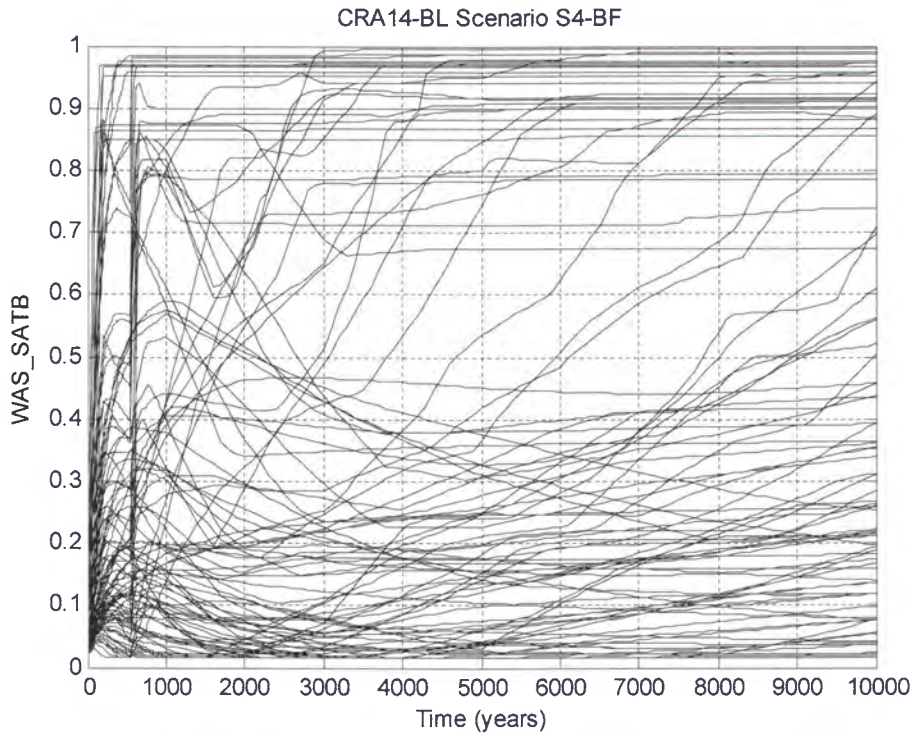


Figure 6-127: Horsetail Plot of Waste Panel Brine Saturation, Case CRA14-BL, Scenario S4-BF.

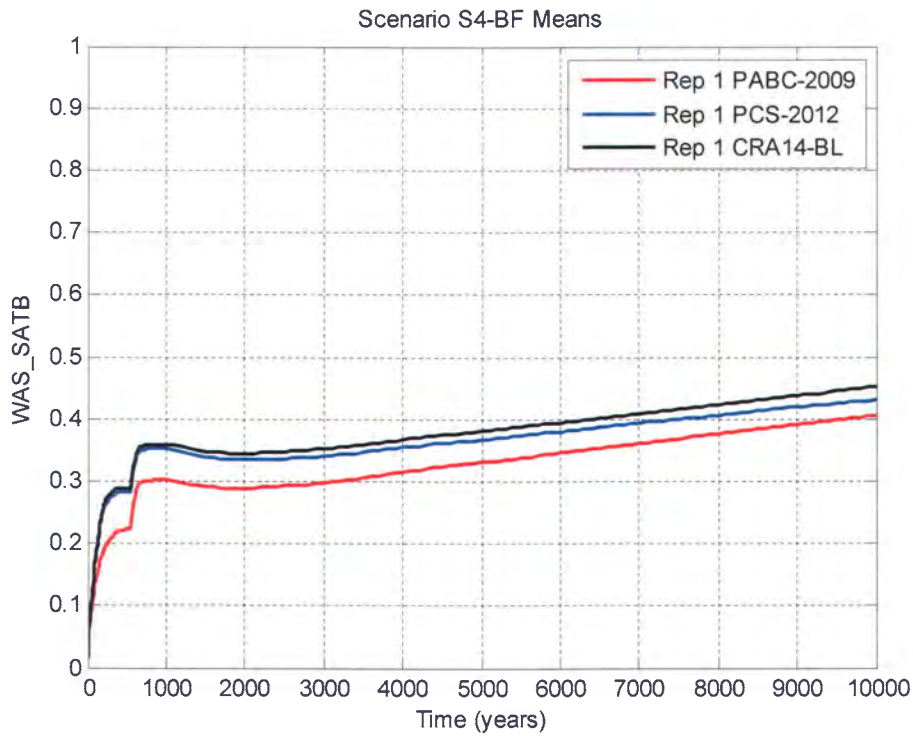


Figure 6-128: Replicate 1 Means of Waste Panel Brine Saturation, Scenario S4-BF.

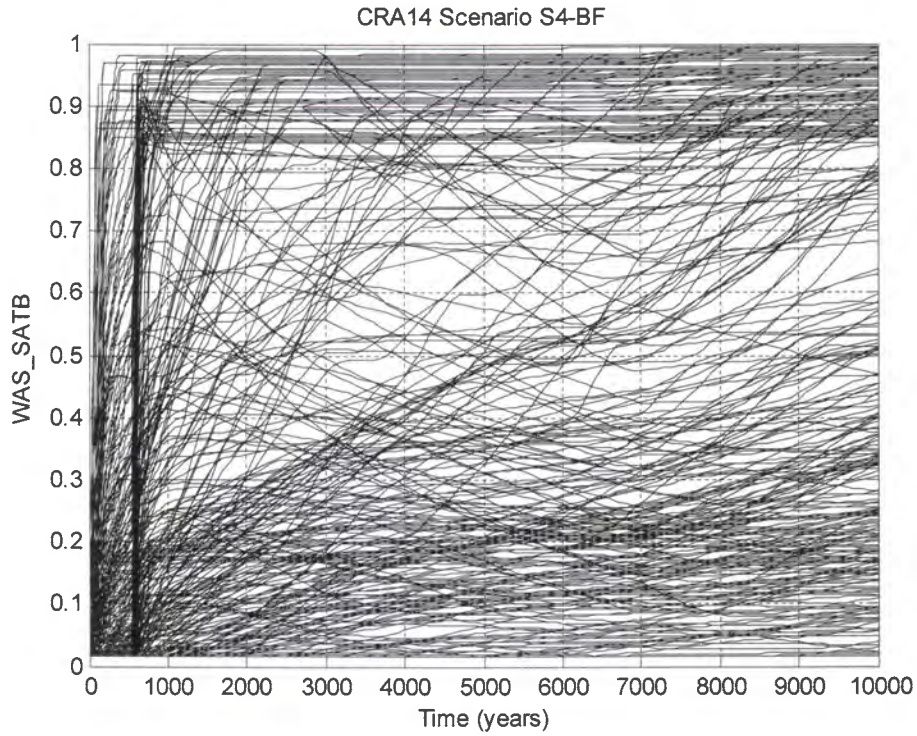


Figure 6-129: Horsetail Plot of Waste Panel Brine Saturation, Case CRA14-0, Scenario S4-BF.

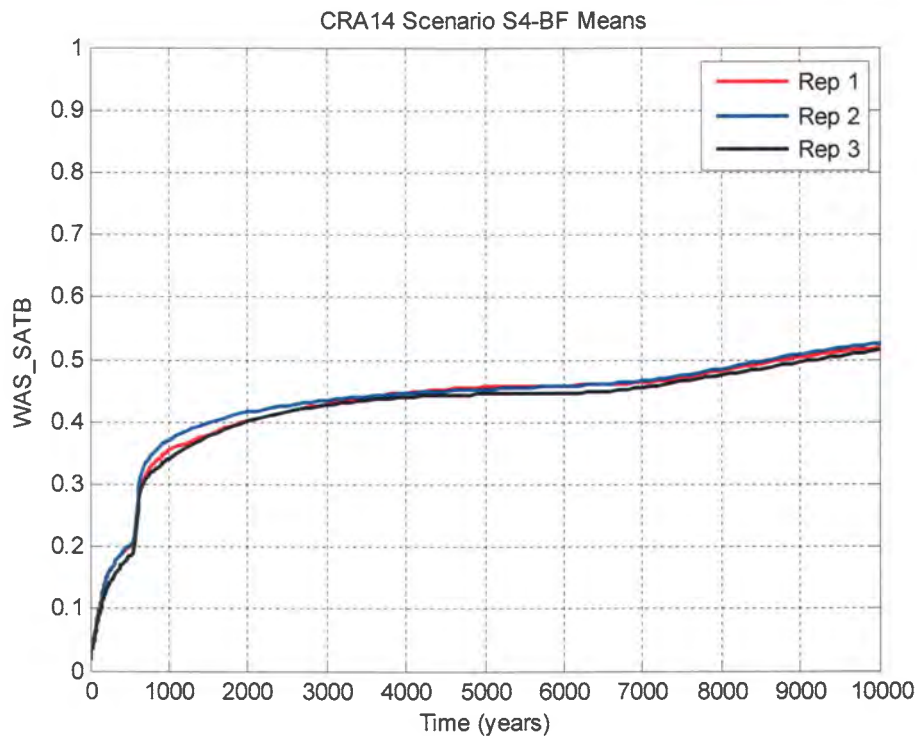


Figure 6-130: Replicate Means of Waste Panel Brine Saturation, Case CRA14-0, Scenario S4-BF.



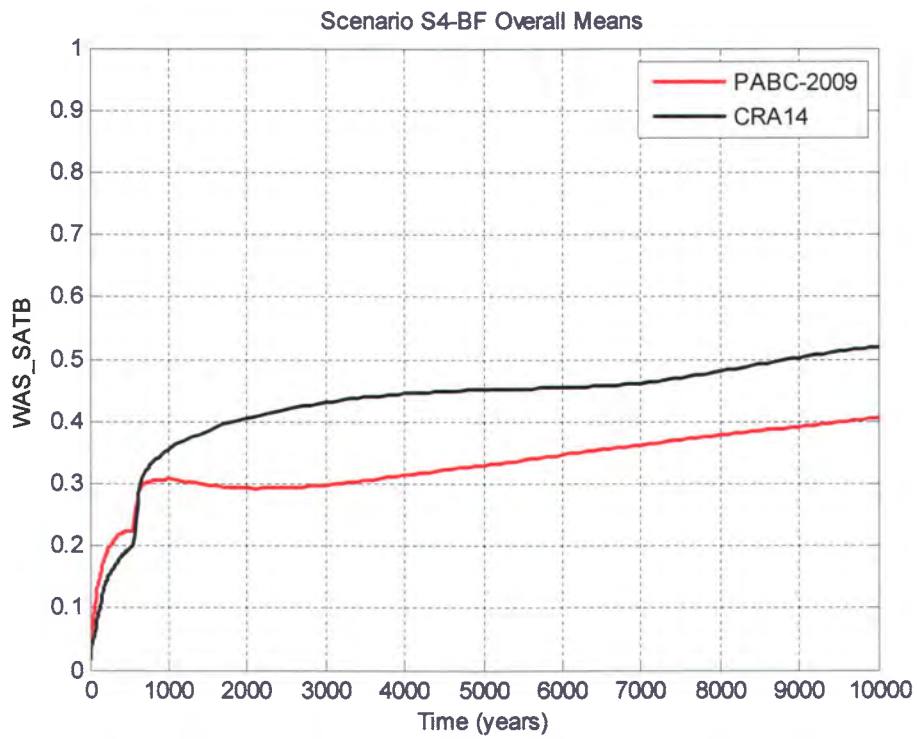


Figure 6-131: Overall Means of Waste Panel Brine Saturation, Scenario S4-BF.

#### 6.4 Results for an E2 Intrusion at 1000 Years Followed by a E1 Intrusion at 2000 Years (Scenario S6-BF)

BRAGFLO scenario S6-BF models an E2 intrusion occurring at 1000 years, followed by an E1 intrusion into the same panel at 2000 years. Calculated brine flows up the intrusion borehole obtained in scenario S6-BF are used in PA code PANEL to determine the radionuclide source term to the Culebra. Results from BRAGFLO scenario S6-BF are now briefly discussed in the context of brine flow up the intrusion borehole.

The horsetail plot of quantity BNBHADRZ obtained in Case CRA14-BL is shown in Figure 6-132. Replicate 1 means obtained for this quantity in the PABC-2009, the PCS-2012 PA, and Case CRA14-BL are plotted together in Figure 6-133. Results obtained for the replicate 1 means in the three calculations are similar. Results obtained for quantity BNBHADRZ in Case CRA14-0 are shown in Figure 6-134 to Figure 6-136. The overall mean of cumulative brine flow up the intrusion borehole is increased in Case CRA14-0 as compared to the PABC-2009 (Figure 6-136), with the increase similar to that seen for the E1 intrusion results (Figure 6-97).

Summary statistics for quantity BNBHADRZ obtained in scenario S6-BF are shown in Table 6-4. Results presented in that table are calculated over all 300 vector realizations (and all times) of the PABC-2009 and Case CRA14-0 of the CRA-2014 PA.

Table 6-4: Summary Statistics for Scenario S6-BF

Quantity (units)	Description	Mean Value		Maximum Value	
		PABC-2009	CRA14-0	PABC-2009	CRA14-0
BNBHADRZ (x 10 <sup>3</sup> m <sup>3</sup> )	Cumulative brine flow up the intrusion borehole.	2.92	3.10	169.03	173.36

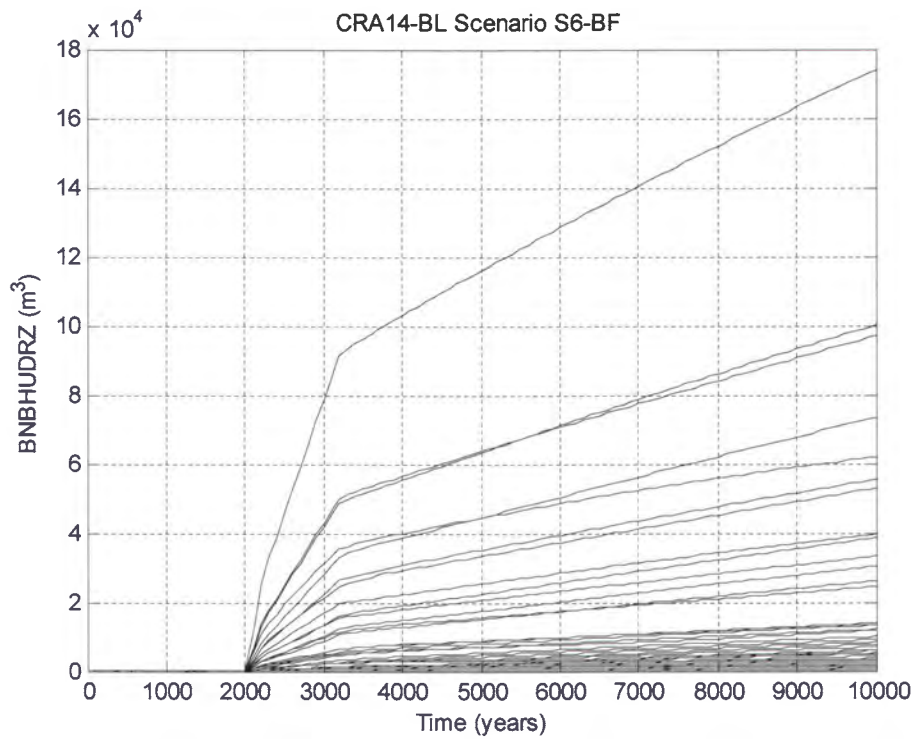


Figure 6-132: Horsetail Plot of Brine Flow up the Borehole, Case CRA14-BL, Scenario S6-BF.

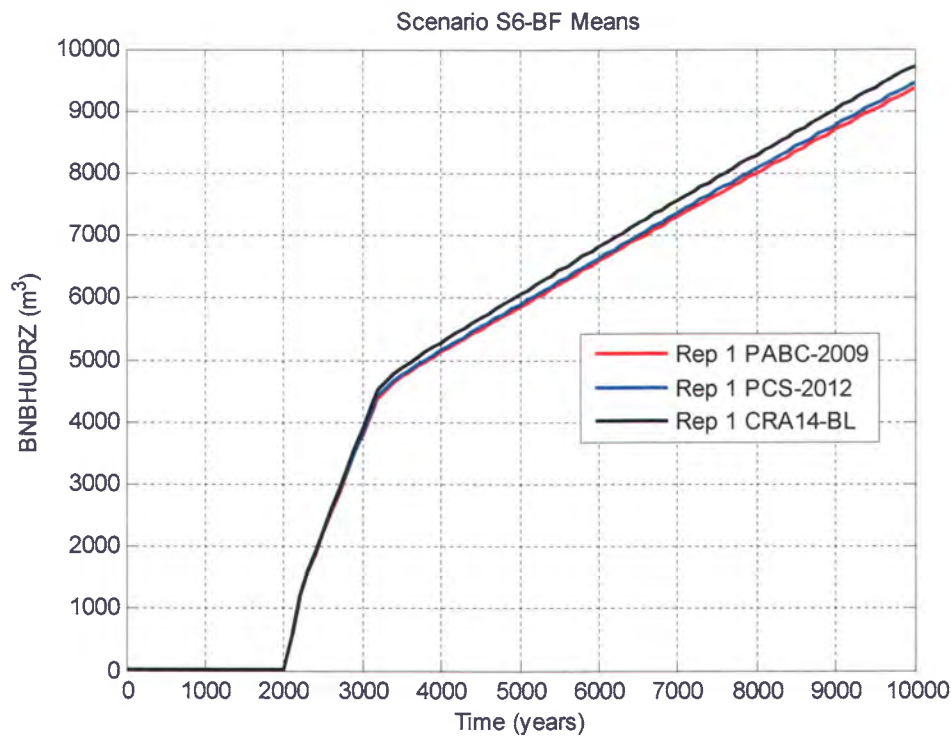


Figure 6-133: Replicate 1 Means of Brine Flow up the Borehole, Scenario S6-BF.

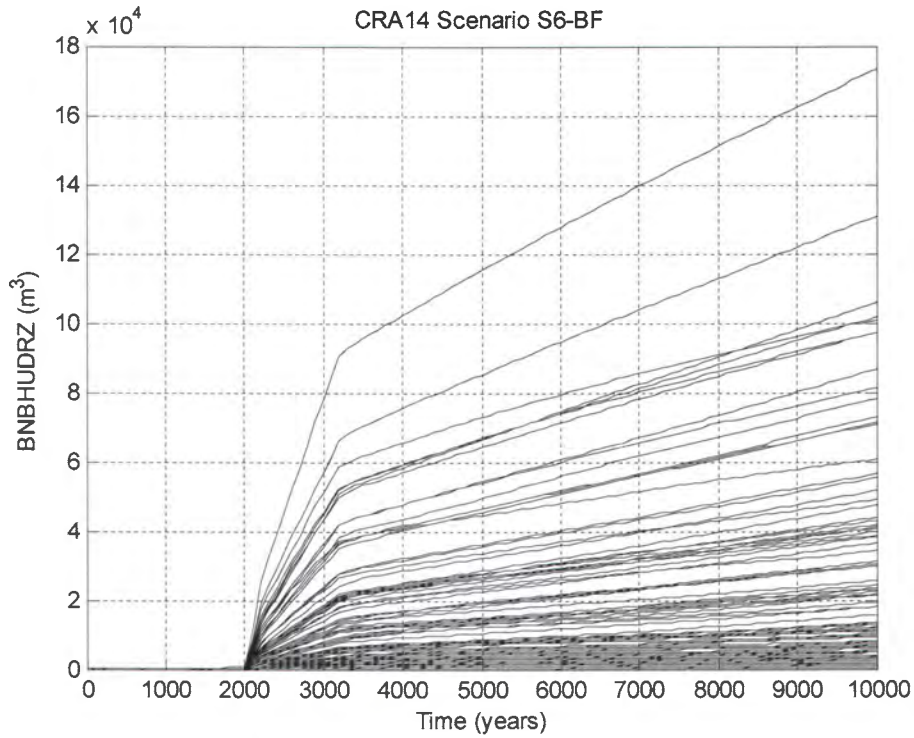


Figure 6-134: Horsetail Plot of Brine Flow up the Borehole, Case CRA14-0, Scenario S6-BF.

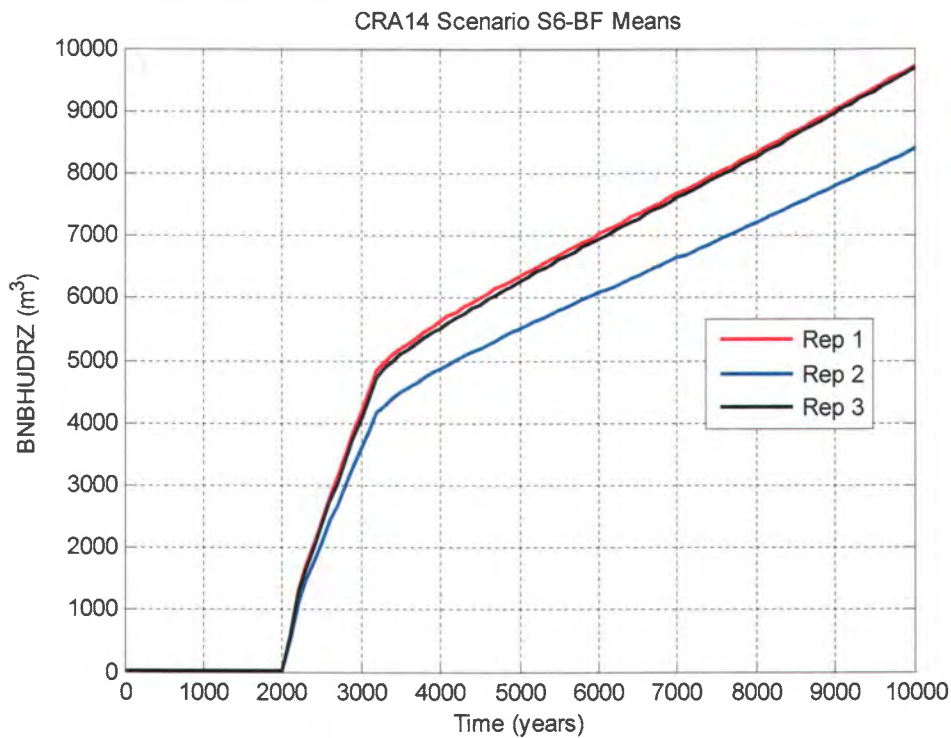


Figure 6-135: Replicate Means of Brine Flow up the Borehole, Case CRA14-0, Scenario S6-BF.

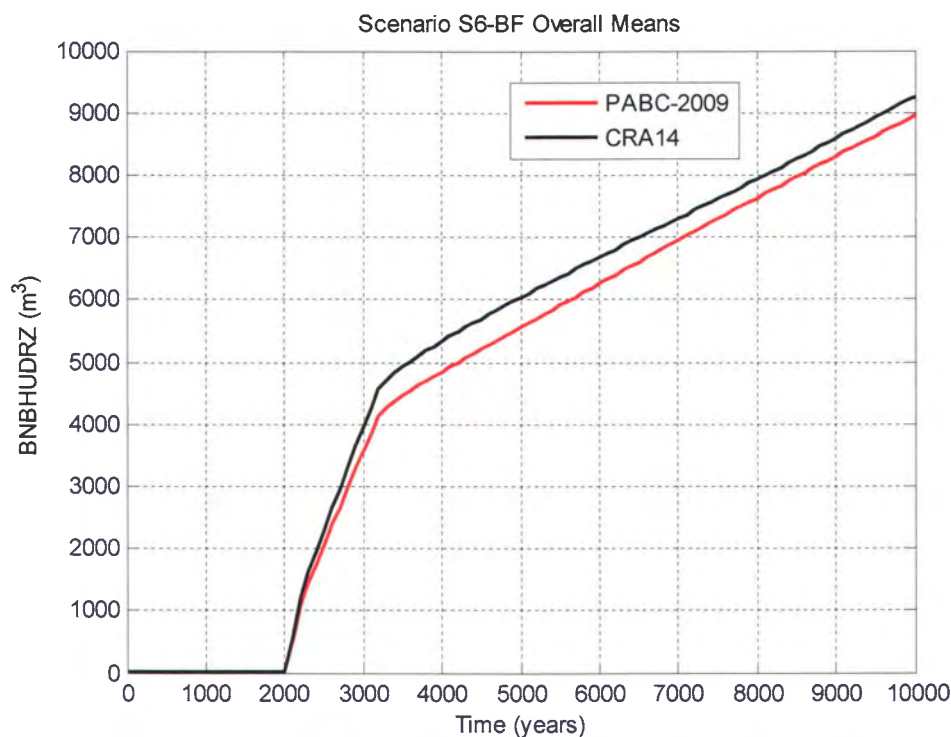


Figure 6-136: Overall Means of Brine Flow up the Borehole, Scenario S6-BF.

## 7 SUMMARY

Changes incorporated into the CRA-2014 PA include planned changes as well as parameter and implementation changes. Changes included in the CRA-2014 PA that potentially impact BRAGFLO results as compared to the PABC-2009 are:

- Replacement of the Option D PCS with the ROMPCS
- Additional excavation in the WIPP experimental area
- Updated waste inventory parameters
- Refinement to the iron corrosion rate parameter STEEL:CORRMC02
- Implementation of a water balance that includes MgO hydration

For undisturbed repository conditions, these changes yield a reduction in the mean pressure calculated for repository waste areas as compared to the PABC-2009. The expanded mined volume in the repository experimental area contributes somewhat to this reduction, but it is primarily due to reduced gas generation seen in the CRA-2014 PA results. The revised iron corrosion rate results in slower gas production due to iron corrosion (on average). The addition of MgO chemistry in the revised water balance implementation also reduces the amount of free water available for gas production by iron corrosion and microbial degradation of cellulose. The sequestration of free water further reduces gas production, and consequently pressure, in repository waste areas. Mean cumulative brine inflows to repository waste areas are increased in the CRA-2014 PA results (as compared to the PABC-2009), but these increases are more

pronounced for waste areas at lower elevation. Waste areas at higher elevation, such as the SRoR and the NRoR, have lower mean brine saturations in the CRA-2014 PA results as compared to the PABC-2009 due to water sequestration in the refined water balance implementation. Waste panels at lowest elevation, such as the separately modeled waste panel in BRAGFLO, have a lower mean brine saturation at early times as compared to the PABC-2009. However, the mean waste panel brine saturation gradually increases until it becomes greater than that seen in the PABC-2009. As the SRoR and NRoR together represent nine of the ten repository waste panels, the sequestration of brine in the refined water budget implementation yields a repository that tends to be drier overall for undisturbed conditions as compared to the PABC-2009.

For E1 intrusion scenarios, results obtained for the SRoR and NRoR do not change appreciably from those seen for the undisturbed repository. The ROMPCS effectively isolates impacts associated with borehole intrusion to the intruded panel. Changes included in the CRA-2014 PA yield an increase to the mean pressure in the intruded panel for a period of time after the intrusion as compared to results from the PABC-2009. The revised iron corrosion rate utilized in the CRA-2014 PA results in slower gas production due to iron corrosion (on average), resulting in a mean waste panel pressure curve that eventually falls below that seen in the PABC-2009. Cumulative brine inflows to the intruded waste panel are greater (on average) in the CRA-2014 PA results as compared to the PABC-2009. This increased mean brine inflow yields a corresponding increase to the mean brine saturation of the intruded panel.

For E2 intrusion scenarios, results obtained for the SRoR and NRoR do not change appreciably from those seen for the undisturbed repository. The ROMPCS effectively isolates impacts associated with borehole intrusion to the intruded panel. Changes included in the CRA-2014 PA yield a decrease to the mean pressure in the intruded panel as compared to results from the PABC-2009. The replacement of the Option D PCS with the ROMPCS results in reduced mean pressure in the waste panel prior to the E2 intrusion. The refined water balance implementation sequesters water, reducing the amount that is freely available for gas production processes prior to the intrusion. The revised iron corrosion rate results in slower gas production due to iron corrosion (on average). As gas generation due to iron corrosion is the dominant gas production mechanism, the reduction (on average) in the rate of gas production due to iron corrosion yields a corresponding decrease in the rate of mean gas generation in the waste panel, further lowering waste panel mean pressure. Consequently, at the time of the E2 intrusion, the mean waste panel pressure is lower in the CRA-2014 PA than in the PABC-2009, and is also lower 200 years later when the borehole plugs fail. Cumulative brine inflows to the intruded waste panel are greater (on average) in the CRA-2014 PA results as compared to the PABC-2009 due to the reduction in mean pressure. The increased mean brine inflow yields a corresponding increase to the mean brine saturation of the intruded panel for the CRA-2014 PA results.

Brine flows up the intrusion borehole that are used to calculate the radionuclide source term in WIPP PA are mildly altered by the set of changes included in the CRA-2014 PA. The mean of cumulative brine flow up the intrusion borehole for the E2E1 intrusion sequence of scenario S6-BF is increased in the CRA-2014 PA as compared to the PABC-2009, with an increase similar to that seen for E1 intrusion results.

## 8 REFERENCES

- Camphouse, R.C. 2012a. Analysis Package for Salado Flow Modeling Done in the AP-161 (PCS-2012) Performance Assessment. Sandia National Laboratories, Carlsbad, NM. ERMS 558204.
- Camphouse, R.C. 2012b. A summary of parameters to be implemented in the PCS-2012 PA. Memo to Janis Trone dated July 10, 2012. Sandia National Laboratories, Carlsbad, NM. ERMS 557721.
- Camphouse, R.C. 2012c. An overview of the BRAGFLO two-phase flow parameters used to model the run-of-mine salt panel closures implemented in the PCS-2012 PA. Memo to Paul Shoemaker dated June 7, 2012. Sandia National Laboratories, Carlsbad, NM. ERMS 557653.
- Camphouse, R.C. 2013. Analysis Plan for the 2014 WIPP Compliance Recertification Application Performance Assessment. Sandia National Laboratories, Carlsbad, NM. ERMS 559198.
- Camphouse, R.C., Kicker, D.C., Kirchner, T.B., Long, J.J., and Pasch, J.J. 2011. Impact Assessment of SDI Excavation on Long-Term WIPP Performance. Sandia National Laboratories, Carlsbad, NM. ERMS 555824.
- Camphouse, R.C., Gross, M., Herrick, C.G., Kicker, D.C., and Thompson, B. 2012a. Recommendations and Justifications of Parameter Values for the Run-of-Mine Salt Panel Closure System Design Modeled in the PCS-2012 PA. Memo to WIPP Records Center dated May 3, 2012. Sandia National Laboratories, Carlsbad, NM. ERMS 557396.
- Camphouse, R.C., Kicker, D.C., Kirchner, T.B., Long, J.J., Malama, B., and Zeitler, T.R. 2012b. Summary Report and Run Control for the 2012 WIPP Panel Closure System Performance Assessment. Sandia National Laboratories, Carlsbad, NM. ERMS 558365.
- Clayton, D.J. 2013. Justification of Chemistry Parameters for Use in BRAGFLO for AP-164, Revision 1. Sandia National Laboratories, Carlsbad, NM. ERMS 559198.
- Clayton, D.J., S. Dunagan, J.W. Garner, A.E. Ismail, T.B. Kirchner, G.R. Kirkes, M.B. Nemer. 2008. Summary Report of the 2009 Compliance Recertification Application Performance Assessment. Sandia National Laboratories, Carlsbad, NM. ERMS 548862.
- Clayton, D.J., R.C. Camphouse, J.W. Garner, A.E. Ismail, T.B. Kirchner, K.L. Kuhlman, M.B. Nemer. 2010. Summary Report of the CRA-2009 Performance Assessment Baseline Calculation. Sandia National Laboratories, Carlsbad, NM. ERMS 553039.

Cotsworth, E. 2005. EPA Letter on Conducting the Performance Assessment Baseline Change (PABC) Verification Test. U.S. EPA, Office of Radiation and Indoor Air, Washington, D.C. ERMS 538858.

Cotsworth, E. 2009. EPA Letter on CRA-2009 First Set of Completeness Comments. U.S. EPA, Office of Radiation and Indoor Air, Washington, D.C. ERMS 551444.

Fox, B., D. Clayton, T. Kirchner. 2009. Radionuclide Inventory Screening Analysis Report for the PABC-2009. Sandia National Laboratories, Carlsbad, NM. ERMS 551679.

Hansen, C. 2002. A Reconciliation of the CCA and PAVT Parameter Baselines, Revision 1. Sandia National Laboratories, Carlsbad, NM. ERMS 522337.

Ismail, A. 2007a. Revised Porosity Estimates for the DRZ. Sandia National Laboratories, Carlsbad, NM. ERMS 545755.

Ismail, A. 2007b. Update to DRZ\_PCS:POROSITY. Sandia National Laboratories, Carlsbad, NM. ERMS 547486.

Kicker, D. and T. Zeitler. 2013. Radionuclide Inventory Screening Analysis Report for the 2014 Compliance Recertification Application Performance Assessment. Sandia National Laboratories, Carlsbad, NM. ERMS 559257.

Leigh, C.D., J.F. Kanney, L.H. Brush, J.W. Garner, G.R. Kirkes, T. Lowry, M.B. Nemer, J.S. Stein, E.D. Vugrin, S. Wagner, and T.B. Kirchner. 2005. 2004 Compliance Recertification Application Performance Assessment Baseline Calculation, Revision 0. Sandia National Laboratories, Carlsbad, NM. ERMS 541521.

Long, J.J. 2013. Execution of Performance Assessment Codes for the CRA-2014 Performance Assessment. Sandia National Laboratories, Carlsbad, NM.

MacKinnon, R.J., and G. Freeze. 1997a. Summary of EPA-Mandated Performance Assessment Verification Test (Replicate 1) and Comparison With the Compliance Certification Application Calculations, Revision 1. Sandia National Laboratories, Carlsbad, NM. ERMS 422595.

MacKinnon, R.J., and G. Freeze. 1997b. Summary of Uncertainty and Sensitivity Analysis Results for the EPA-Mandated Performance Assessment Verification Test, Rev. 1. Sandia National Laboratories, Carlsbad, NM. ERMS 420669.

MacKinnon, R.J., and G. Freeze. 1997c. Supplemental Summary of EPA-Mandated Performance Assessment Verification Test (All Replicates) and Comparison With the Compliance



Certification Application Calculations, Revision 1. Sandia National Laboratories, Carlsbad, NM. ERMS 414880.

Nemer, M.B. 2010. Analysis Package for Salado Flow Modeling: CRA-2009 Performance Assessment Baseline Calculation. Sandia National Laboratories, Carlsbad, NM. ERMS 552956.

Nemer, M. B., J. S. Stein and W. Zelinski. 2005. Analysis Report for BRAGFLO Preliminary Modeling Results With New Gas Generation Rates Based Upon Recent Experimental Results. Sandia National Laboratories, Carlsbad, NM. ERMS 539437.

Roselle, G.T. 2013. Determination of Corrosion Rates from Iron/Lead Corrosion Experiments to be used for Gas Generation Calculations. Sandia National Laboratories, Carlsbad, NM. ERMS 559077.

Stein, J. 2002. Parameter Values for New Materials CONC\_PCS and DRZ\_PCS. Sandia National Laboratories, Carlsbad, NM. ERMS 520524.

U.S. Congress. 1992. WIPP Land Withdrawal Act, Public Law 102-579, 106 Stat. 4777, 1992; as amended by Public Law 104-201, 110 Stat. 2422, 1996.

U.S. Department of Energy (DOE) 1996. Title 40 CFR Part 191 Compliance Certification Application for the Waste Isolation Pilot. U.S. Department of Energy Waste Isolation Pilot Plant, Carlsbad Area Office, Carlsbad, NM. DOE/CAO-1996-2184.

U.S. Department of Energy (DOE) 2004. Title 40 CFR Part 191 Compliance Recertification Application for the Waste Isolation Pilot Plant, 10 vols., U.S. Department of Energy Waste Isolation Pilot Plant, Carlsbad Area Office, Carlsbad, NM. DOE/WIPP 2004-3231.

U.S. Department of Energy (DOE). 2007. "Transuranic Waste Acceptance Criteria for The Waste Isolation Pilot Plant, Revision 6.1." Carlsbad, NM: DOE/WIPP-02-3122.

U.S. Department of Energy (DOE), 2011a. Panel Closure System Design, Planned Change Request to the EPA 40 CFR Part 194 Certification of the Waste Isolation Pilot Plant. U.S. Department of Energy, Carlsbad Field Office. Carlsbad, New Mexico.

U.S. Department of Energy (DOE), 2011b. Notification of Intent to Begin the Salt Disposal Investigations. Letter from Edward Ziemianski to Jonathan Edwards dated August 11, 2011. U.S. Department of Energy, Carlsbad Field Office. Carlsbad, New Mexico.

U.S. Environmental Protection Agency (EPA). 1998. 40 CFR 194, Criteria for the Certification and Recertification of the Waste Isolation Pilot Plant's Compliance with the Disposal Regulations: Certification Decision: Final Rule, Federal Register. Vol. 63, 27354-27406.

U.S. Environmental Protection Agency (EPA). 2006. 40 CFR 194, Criteria for the Certification and Recertification of the Waste Isolation Pilot Plant's Compliance with the Disposal Regulations: Certification Decision: Final Rule, Federal Register. Vol. 71, 18010-18021.

U.S. Environmental Protection Agency (EPA). 2010a. 40 CFR Part 194 Criteria for the Certification and Recertification of the Waste Isolation Pilot Plant's Compliance With the Disposal Regulations: Recertification Decision, Federal Register No. 222, Vol. 75, pp. 70584-70595, November 18, 2010.

U.S. Environmental Protection Agency (EPA). 2010b. Technical Support Document for Section 194.24, Evaluation of the Compliance Recertification Actinide Source Term, Backfill Efficacy and Culebra Dolomite Distribution Coefficient Values (Revision 1), November 2010.

Van Soest, G.D. 2012. Performance Assessment Inventory Report – 2012. Los Alamos National Laboratory Carlsbad Operations. Carlsbad, NM. LA-UR-12-26643.

Vugrin, E.D. 2005. User's Manual for LHS Version 2.42 Document Version 2.42. Sandia National Laboratories. Carlsbad, NM. ERMS 538374.

Vaughn, P. 1996. WIPP Parameter Entry Form for SANTAROS: SAT\_IBRN. Sandia National Laboratories. Carlsbad, NM. WPO 33552.

Wall, N.A. and Enos, D. (2006) Iron and Lead Corrosion in WIPP-Relevant Conditions, TP 06-02, Rev 1. Sandia National Laboratories. Carlsbad, NM. ERMS 543238.